

Sunspaces for passive building heating

Calculation models and utilization of empirical data

Francesco Passerini



UNIVERSITÀ DEGLI STUDI DI TRENTO

Dipartimento di Ingegneria Civile
e Ambientale

2012

Doctoral thesis in **Environmental Engineering, 24° cycle**

Faculty of Engineering, **University of Trento**

Academic year **2010/2011**

Supervisor: **Prof. Antonio Frattari, University of Trento**

Dr. Eng. Rossano Albatici, University of Trento

Copyright: **Francesco Passerini** (text and images when not differently specified)

Cover photograph: **Rossano Albatici**

University of Trento

Trento, Italy

2012

Contents

List of Figures	III
List of Tables	X
Acknowledgements	XI
Summary	XIII
1. Passive solar systems	1
1.1 Overview to passive solar systems	1
1.2 Shape, solar gains and heating requirements	9
1.2.1 Compactness and exposure	10
1.2.2 Inclination of a glazed surface	10
1.3 Sunspaces	27
2. Literature overview	31
2.1 General considerations	31
2.2 Case studies	31
2.3 Calculation methods	34
2.4 Scale models	39
3. Calculation methods	43
3.1 Introduction to calculation methods	43
3.2 Quasi-steady-state methods	43
3.2.1 Method 5000	46
3.2.2 European technical standard EN ISO 13790:2008	53
3.2.3 Comparison between Method 5000 and EN ISO 13790:2008	56
3.2.4 Proposals to improve the technical standard	57
3.3 Dynamic methods	77
4. Scale models. An experimental case study in Trento (Italy)	81
4.1 Introduction to scale models	81
4.2 Monitoring	83
4.3 Modelling	94
4.4 Conclusions	105
5. Sunspaces to improve energy retrofitting in Freiburg (Germany)	107

5.1 Verandas as passive solar system	107
5.2 Analysis of a case study	109
5.2.1 The building	109
5.2.2 Monitoring	111
5.2.3 Data analysis	115
5.2.4 Modelling a solar air collector	121
5.3 Design proposals	131
5.3.1 Introduction to the design proposals	131
5.3.2 Introduction to calculations	131
5.3.3 Thermal properties of the considered elements	135
5.3.4 Outputs	136
5.3.5 Results	138
5.3.6 Conclusions	155
6. Guided procedure to the proper design of sunspaces	161
6.1 New construction	161
6.1.1 Clarifying the goals of bioclimatic design	161
6.1.2 Analysing the local climate	161
6.1.3 Defining position and shape of the sunspace	162
6.1.4 Defining the insulation levels	162
6.1.5 Providing thermal inertia	163
6.1.6 Defining ventilation strategies	163
6.1.7 Avoiding overheating during intermediate seasons and during summer	164
6.1.8 Dealing with a possible automation system	164
6.1.9 Calculations	164
6.2 Refurbishment	164
6.2.1 Clarifying the goals of bioclimatic design	164
6.2.2 Analysing the local climate	165
6.2.3 Defining insulation levels	165
6.2.4 Providing thermal inertia	165
6.2.5 Defining ventilation strategies	165
6.2.6 Avoiding overheating during intermediate seasons and during summer	166
6.2.7 Dealing with a possible automation system	166
6.2.8 Calculations	166
7. Conclusions	167
Appendix: Bioclimatic design of buildings considering heating requirements in Italian climatic conditions. A simplified approach	175

List of Figures

Figure 1.1 System with direct gain	2
Figure 1.2 System with indirect gain	3
Figure 1.3 On the horizontal axis: wavelength of the incident radiation. On the vertical axis: transparency coefficient of a glass pane for normal radiation. Source: Bonacina, C. et al. (1992).....	4
Figure 1.4 Incident angle of the solar radiation on a glazed surface (2-dimensional representation)	5
Figure 1.5 Three functions of the correction factor F_w . On the horizontal axis: angle between the radiation and the windowpane. On the vertical axis: the correction factor.....	6
Figure 1.6 Solar radiation incident in a completely sunny day on surfaces having different orientations, without shading, latitude 40°N $1 \text{ Btu/ft}^2 = 3,2 \text{ Wh/m}^2 = 1,1 \cdot 10^{-2} \text{ MJ/m}^2$ Source: Mazria, E. (1979).....	6
Figure 1.7 Monthly averages of daily solar radiation incident on surfaces having different orientations in Trento, Italy. Latitude 46°N Source of the data: UNI 10349:1994.....	7
Figure 1.8 Solar radiation incident in a completely sunny day on surfaces facing south but having different inclinations, without shading, latitude 40°N $1 \text{ Btu/ft}^2 = 3,2 \text{ Wh/m}^2 = 1,1 \cdot 10^{-2} \text{ MJ/m}^2$ Source: Mazria, E. (1979).....	8
Figure 1.9 Plotting the shading elements, which are represented on the sun chart. Source: Mazria, E. (1979)	9
Figure 1.10 Window having an inclination of i with respect to the vertical.....	16
Figure 1.11 Monthly radiation in Bolzano, Italy. Source of the data: Comitato Termotecnico Italiano	17
Figure 1.12 Maximum solar altitude on the 15 th of every month in Bolzano.....	17
Figure 1.13 Entering radiation in function of the inclination of the window for Bolzano, with an albedo of 0,2 and considering an isotropic model of the diffuse radiation, since January until April.	18
Figure 1.14 Entering radiation in function of the inclination of the window for Bolzano, with an albedo of 0,2 and considering an isotropic model of the diffuse radiation, since October until December	18
Figure 1.15 Entering radiation in function of the inclination of the window for Bolzano, with an albedo of 0,2 and considering an isotropic model of the diffuse radiation,	

during the heating period.....	19
Figure 1.16 Entering radiation in function of the inclination of the window for Bolzano, with an albedo of 0,6 and considering an isotropic model of the diffuse radiation, since January until April.....	19
Figure 1.17 Entering radiation in function of the inclination of the window for Bolzano, with an albedo of 0,6 and considering an isotropic model of the diffuse radiation, during the heating period.....	20
Figure 1.18 Mean monthly external temperatures in Cordova (Alaska, USA).....	20
Figure 1.19 Monthly radiation in Cordova (Alaska, USA). Source of the data: ASHRAE – TMY3	21
Figure 1.20 Maximum solar altitude on the 15 th of every month in Cordova (Alaska, USA).....	21
Figure 1.21 Entering radiation in function of the inclination of the window for Cordova, with an albedo of 0,2 and considering an isotropic model of the diffuse radiation, since January until April	22
Figure 1.22 Total entering radiation in function of the inclination of the window for Cordova, with an albedo of 0,2 and considering an isotropic model of the diffuse radiation during the coldest months (September – April)	22
Figure 1.23 Total entering radiation in function of the inclination of the window for Cordova, with an albedo of 0,2 and considering an isotropic model of the diffuse radiation, in the whole year	23
Figure 1.24 Entering radiation in function of the inclination of the window for Cordova, with an albedo of 0,6 and considering an isotropic model of the diffuse radiation, since January until April	23
Figure 1.25 Total entering radiation in function of the inclination of the window for Cordova, with an albedo of 0,6 and considering an isotropic model of the diffuse radiation, during the coldest months (September – April)	24
Figure 1.26 Total entering radiation in function of the inclination of the window for Cordova, with an albedo of 0,6 and considering an isotropic model of the diffuse radiation, in the whole year	24
Figure 1.27 Entering radiation in function of the inclination of the window for Cordova, with an albedo of 0,2 and considering the Perez model of the diffuse radiation, since January until April	25
Figure 1.28 Total entering radiation in function of the inclination of the window for Cordova, with an albedo of 0,2 and considering the Perez model of the diffuse radiation, during the coldest months (September – April)	25
Figure 1.29 Total entering radiation in function of the inclination of the window for	

Cordova, with an albedo of 0,2 and considering the Perez model of the diffuse radiation, in the whole year	26
Figure 1.30 Schematic representation of a sunspace	27
Figure 1.31 Thermal inertia on the wall	28
Figure 1.32 Thermal inertia as specific element within the sunspace	28
Figure 1.33 Thermal inertia on the floor slab	28
Figure 1.34 Schematic examples of additional insulation during the night	29
Figure 1.35 Cooling by ventilation during the summer nights. The internal temperature is higher than the external one and therefore the internal air is lighter than the external one. Hence the inlet for the air is on the lower part of the building and the outlet is on the upper part of the sunspace in order to increase the chimney effect. To evaluate the efficacy of such a solution, considering also the fluid-dynamic resistances, a Computational Fluid Dynamic calculation should be made.	30
Figure 2.1 On the horizontal axis: solar radiation. On the vertical axis: energy contribution of the active (mechanical) heating system and of the mechanical ventilation system to maintain the prefixed conditions divided by the temperature difference between internal and external environment and by the volume of the test cells. The points relative to the three solutions are fitted by three relative straight lines. Source: Meroni, I. et al. (1991).....	32
Figure 2.2 Temperature cumulative frequency in the external environment (n. 1), in the sunspace (n. 2) and in some adjacent internal environments during the winter 1986/1987 Source: Kunz, M. (1990).....	34
Figure 2.3 Model by Athienitis, A.K. and Santamouris, M. (2002). Unknown quantities are temperatures in the nodes 1, 2 and 3	35
Figure 2.4 Sunspace geometry and conductance network in TRNSYS 16	36
Figure 2.5 (a) Reflection to the outside (b) Transmission to other zones (c) Direct transmission to the outside Source: Voeltzel (2001)	37
Figure 2.6 Scale model of a storage wall. Source: Grimmer, D.P. et al. (1979).....	41
Figure 3.1 The logic of the calculation of the ANNEX E of EN ISO 13790:2008 and of the Method 5000.....	44
Figure 3.2 a. Part of the solar radiation enters directly the heated space; b. Part of the radiation is reflected to the external environment; c. Part of the radiation is absorbed by the opaque surfaces of the sunspace but it does not contribute to the increase of the sunspace temperature because it is conducted towards other environments.	45
Figure 3.3 Calculation scheme for the sunspace temperature	51
Figure 3.4 Calculation scheme of the gain due to solar radiation in the sunspace	

according to the ANNEX E of the European technical standard EN ISO 13790:2008 (the image was reviewed and modified by the author)	55
Figure 3.5 $F_{w,dir}$ trend for a winter period (hourly values).....	59
Figure 3.6 $F_{w,dir}$ trend for a summer period (hourly values).....	59
Figure 3.7 F_w trend throughout the year (monthly values).....	61
Figure 3.8 Schematic geometry of a sunspace	62
Figure 3.9 Shading angle of obstacles: A. frontal obstacle; B. horizontal obstacle; C. vertical obstacle.....	64
Figure 3.10 Calculation scheme of the shading. The angles relative to the shading factor of vertical obstacles are indicated	64
Figure 3.11 Total shading effect of two lateral vertical obstacles	65
Figure 3.12 Shading factors for the windows between the sunspace and the internal space	65
Figure 3.13 Radiation on a shaded window	66
Figure 3.14 Radiation on a shaded window behind another window.....	67
Figure 3.15 Solar gain through the opaque part and indirect heat gain.....	69
Figure 3.16 Solar gain through the opaque part	70
Figure 3.17 Solar indirect heat gain	71
Figure 3.18 The air is extracted from the sunspace by a mechanical system, in order to preheat the ventilation air of the heated space	73
Figure 3.19 Geometry to calculate the thermal transmittance through the ground with FEM software A. with insulation B. without insulation.....	75
Figure 3.20 Temperature increase due to solar radiation in the case of insulated floor slab and in the case of uninsulated floor slab.....	76
Figure 3.21 Scheme of the calculation of the solar radiation entering internal rooms in IDA-ICE.....	79
Figure 3.22 Convective exchange coefficients as function of the temperature difference between air and surface.....	79
Figure 4.1 The two sunspaces during the construction phase	81
Figure 4.2 The two sunspaces attached to the container and the measuring instruments	83
Figure 4.3 Position of the air temperature and relative humidity sensors.	84
Figure 4.4 Thermo-hygrometer DMA 527	85
Figure 4.5 Combined wind speed-direction sensor DNA 021.....	87
Figure 4.6 Thermo-hygrometer BSU 104	88
Figure 4.7 Inside the sunspaces the thermo-hygrometric conditions were measured at	

two different heights. The sensors were shaded in order to avoid the heating due to the incident solar radiation. Moreover, the air velocity and the surface temperatures of the glazed roof panel, of the floor and of the wall were monitored	88
Figure 4.8 Temperatures monitored in the big sunspace: 3 are surface temperatures, 2 are air temperatures	89
Figure 4.9 Temperatures monitored in the small sunspace: 3 are surface temperatures, 2 are air temperatures	89
Figure 4.10 Surface temperatures and air velocity within the small sunspace.....	90
Figure 4.11 Relationship between external wind velocity and air velocity in the sunspace.....	91
Figure 4.12 Influence of temperature difference between sunspace and external environment on the air velocity in the sunspace	91
Figure 4.13 Temperatures outside container and sunspaces	92
Figure 4.14 Temperatures of the floor inside sunspaces and outside them.	92
Figure 4.15 The temperatures on the inner side of the external tilted window for the two sunspaces. The time when the tank of water was moved is showed.	93
Figure 4.16 Temperatures on the floors of the two sunspace (2 sensors for every sunspace). The time when the tank of water was moved is showed.	94
Figure 4.17 Horizontal section of the results of the finite-element calculation.....	95
Figure 4.18 Vertical section of the results of the finite-element calculation. The floor of the container is insulated.	96
Figure 4.19 The modelled stratification of the coupling of concrete slab and ground	97
Figure 4.20 Comparison between the monitored temperatures of the container surface and the simulated temperatures with emissivity $\varepsilon = 0,85$ and solar absorptance $a = 0,3$	98
Figure 4.21 Simulated and monitored floor temperatures in February Left: big sunspace. Right: small sunspace.....	99
Figure 4.22 Simulated and monitored wall temperatures in February. Left: big sunspace. Right: small sunspace.....	99
Figure 4.23 Simulated and monitored window temperatures in February. Left: big sunspace. Right: small sunspace.....	99
Figure 4.24 Simulated and monitored floor temperatures in May. Left: big sunspace. Right: small sunspace.	100
Figure 4.25 Simulated and monitored wall temperatures in May. Left: big sunspace. Right: small sunspace.	100

Figure 4.26 Simulated and monitored window temperatures in May. Left: big sunspace. Right: small sunspace.....	100
Figure 4.27 On the horizontal axis: global solar radiation. On the vertical axis: floor temperature difference between the big sunspace and the small one in correspondence of daily peak values of sunspace temperature.....	102
Figure 4.28 On the horizontal axis: global solar radiation. On the vertical axis: floor temperature difference between the sunspace having linear dimensions which are two times the dimension of the big one and the big one in correspondence of daily peak values of sunspace temperature	103
Figure 4.29 On the horizontal axis: global solar radiation. On the vertical axis: floor temperature difference between the sunspace having linear dimensions which are two times the dimension of the big one and the small one in correspondence of daily peak values of sunspace temperature	104
Figure 5.1 Output of THERM. A. open veranda B. close veranda C. close veranda with external application of thermal insulation.....	108
Figure 5.2 The refurbished building which was analysed.	109
Figure 5.3 Plan of the apartment and ventilation scheme	110
Figure 5.4 Extractor chimneys and extractor fans on the flat roof.....	110
Figure 5.5 Weather station on the flat roof.....	111
Figure 5.6 Monitoring of the radiation on vertical surface facing south.....	112
Figure 5.7 Monitoring of internal conditions	113
Figure 5.8 Positions of the surface temperature sensors	114
Figure 5.9 Sensors which monitor the preheating of ventilation air and the openings through which the ventilation air has to pass	114
Figure 5.10 On the horizontal axis: air temperatures in the external environment. On the vertical axis: air temperatures in the veranda and in the internal room	115
Figure 5.11 On the horizontal axis: air temperatures in the external environment. On the vertical axis: air temperatures in the veranda. They are divided according to three ranges of solar radiation on the vertical surface facing south. The range corresponding to the lowest level of solar radiation was divided in two parts, in order to consider the part of the day (0.00-12.00 or 12.00-24.00).....	116
Figure 5.12 Air temperatures (external environment, supply air in the veranda, veranda) in relationship with the solar radiation on the vertical surface facing south.....	117
Figure 5.13 Monitored air temperatures in relationship with the wind velocity.....	117
Figure 5.14 Scheme for the estimation of the air change	118
Figure 5.15 On the horizontal axis: time in hours. On the vertical axis: variation of CO ₂	

concentration. For the fitting the considered time interval is 0-16 [fitting and graphs produced by the software R v.2.12.2 <www.r-project.org>]	119
Figure 5.16 On the horizontal axis: time in hours. On the vertical axis: variation of CO ₂ concentration. For the fitting the considered time interval is 1-11 [fitting and graphs produced by the software R v.2.12.2 <www.r-project.org>]	120
Figure 5.17 Schematic model of the solar air collector	121
Figure 5.18 Examples of combination between forced and natural convection.....	127
Figure 5.19 Comparison between the measured and the calculated supply air velocity. On 1 st March and on 3 rd March high supply air velocity peaks were measured but they were not due to a particularly high wind velocity. Probably the wind direction, which was not measured, influences strongly the supply air velocity.....	129
Figure 5.20 Comparison between the measured and the calculated supply air temperature	130
Figure 5.21 Comparison between the measured and the calculated supply air temperature for the period 8 th - 13 th February. On 10 th and 11 th February the wind velocity was, considering 30 minutes average values, even more than 6m/s.....	130
Figure 5.22 External facade of an apartment block of Weingarten West (Freiburg im Breisgau, Germany) which is going to be refurbished	134
Figure 5.23 An example of apartment of Weingarten West (Freiburg im Breisgau, Germany).....	134

List of Tables

Table 1.1 The considered localities.....	12
Table 1.2 Coefficients for the calculation of the circumsolar and horizontal brightness according to Perez (1990)	15
Table 1.3 Ranges of inclination angles which maximize the entering solar radiation	26
Table 3.1 Values of the coefficients a_1 and a_2 . Source of the data: Zappone, C. (2009)	50
Table 3.2 Monthly correction factors according to IDA-ICE and to linear regression proposed by Oliveti, G. (2009).....	61
Table 3.3 Shading factors F_{sh} for different surfaces inside the sunspace, during the heating season. Weather data of Bolzano (Italy)	63
Table 4.1 Relationships between geometrical dimensions and physical quantities.....	82
Table 4.2 Results of calculation of the thermal bridges between the sunspace and the external environment.....	101
Table 4.3 Distribution of the points in relationship with the ranges of Figure 4.27	102
Table 4.4 Distribution of the points in relationship with the ranges of Figure 4.28	103
Table 4.5 Distribution of the points in relationship with the ranges of Figure 4.29.....	105

Acknowledgements

Firstly, I acknowledge the support of my supervisors, Prof. Antonio Frattari and Dr. Rossano Albatici, who allowed me to work with them and to develop an important research experience.

My sincere gratitude is also conveyed to all people who work in the Building Design group of the University of Trento, in particular to Paolo Bottura, who worked for the project of the sunspace prototype and of the scale model, and to Dr. Michela Chiogna, who, as researcher and as former PhD Student in this Doctoral School, has given me good advice.

The two sunspaces (the prototype and the scale model) have been constructed within the courses for apprentices organized in Trento by the *Agenzia del Lavoro* under the supervision of Roberto Mattarei and Tullio Polo, two master craftsmen. The work was coordinated by the professional school ENAIP Villazzano (Referent of the sector for apprentices: Paolo Arrigo - Tutor for the timber sector: Carlo De Godenz).

With pleasure, I acknowledge the people who allow the life of the Doctoral School. Particularly, the extremely competent secretary, Laura Martuscelli. I remember also the “colleagues” PhD candidates, in particular Alessandro Prada, always helpful to convey his knowledge, and Maria Cristina Grillo, who helped me in this work, and the professors of the Doctoral School, in particular Prof. Paolo Baggio, who helped me understand better some aspects of my work.

Thank you to Eleonora Pellizzaro, librarian at the University of Trento, for the help for my researches.

Thank you to Prof. Werner Lang of the Technical University Munich, the external reviewer of my thesis, whom I met in Munich and who provided me some very useful advice for the final developments of my work.

Thank you to Dr. Francesco Frontini: meeting him allowed me to work in a big research body, an international experience which I consider a great enriching.

Thank you to Fraunhofer ISE of Freiburg, in particular to the Department Thermal Systems and Buildings and to the group *Solarbau*. Dr. Jens Pfafferott and Florian Kagerer guided my work there. From Dr. Tobias Zitzmann I had the possibility to learn a lot.

Thank you for the help and for the friendship to Satya Gopisetty, to Felix Ohr, and to Andreas Hasenohr.

I thank also two professors of the University of Lund, who, although I had never met them personally, made me a present of their works, useful reading for the following development of my work: Prof. Maria Wall and Prof. Bertil Fredlund.

I thank also the students of the course *Architecture and Techniques for sustainable building* because with them I understood better how future designers approach the bioclimatic design and what advice they need in order to improve the results of their work.

Summary

The present thesis is the main result of a doctoral work at the Doctoral School of Environmental Engineering of the University of Trento.

Solar systems exploit solar radiation in order to decrease the use of non-renewable energy sources. Therefore their importance is both environmental and economic. According to “The passive solar energy books” (1979) of Edward Mazria the difference between “active systems” and “passive systems” is that in the latter the heat flows happen without mechanical equipment. Passive solar systems have direct practical applications but they need to be better investigated, particularly because they could be used in “*nearly zero-energy buildings*”, which according to the European Directive 2010/31/EU will become the standard in the next few decades. Among the passive solar systems, the sunspaces have a particular architectural value. They are unheated spaces having a largely glazed external surface, exposed to solar radiation, and placed adjacent to heated rooms. One of the reasons why architects design them is the creation of particular and pleasant environments which are integrated in the building. Present research focuses on the other reason, i.e. the reduction of winter energy requirements, without forgetting that the value of the sunspaces concerns not only energy savings. The research has analysed what the causes are of those savings and how they can be maximized, also through integration with the ventilation system and with attention to the constructive details.

After an intensive literature review whose main results are reported in Chapter 2 (“Literature overview”), the goals of the research were established: a deep comprehension of the phenomena involved and developments of the now available tools to design sunspaces and to optimize them from the point of view of energy requirements and thermal comfort.

Chapter 1 (“Passive solar systems”) is an introduction to the main concepts regarding passive solar systems. It highlights their importance, it classifies them and it illustrates how they work. In the passive design, which can reduce the energy requirements decreasing the thermal losses and maximizing the exploitation of solar radiation, the building shape plays an important role. Because of this, some aspects concerning the relationships between building shape and reduction of heating requirements are analysed. Finally, the first chapter presents the sunspaces, which are the main subject of this thesis.

Generally building designers calculate energy requirements through quasi-steady-state methods. The European technical standard EN ISO 13790:2008 “Energy performance of buildings - Calculation of energy use for space heating and cooling” in the ANNEX E presents also a quasi-steady-state method in order to consider the presence of the sunspace. Chapter 3 (“Calculation methods”) critically analyses calculation methods, identifies their

problematic aspects and provides some indications to improve the method of the technical standard.

As well as by the theoretical part, in the research a fundamental role is played by experimental campaigns. In fact, it is possible to understand completely construction problems, qualities and limitations of a technological system only through the experience with concrete examples. Moreover, the simplifications adopted in modelling can bring to conclusions which are too far from physical reality and so, in order to avoid that risk, the analysis of empirical data and their comparison with the results of the modelling is fundamental. With this aim, empirical data have been collected in relation both to existing sunspaces and to sunspaces which were specifically constructed for the research. Two sunspaces, one having the dimensions of a small room and the other one which is its scale model, with halved dimensions, were created and were the object of an experimental campaign (see Chapter 4, "Scale models - An experimental case study in Trento (Italy)"). This experimental study has allowed us to observe how the physical behaviour of sunspaces changes by changing their dimensions and to achieve a deep comprehension of sunspaces through quantitative analyses of involved physical quantities. A virtual model of the sunspaces was created and validated.

Because of the long renovation cycle for buildings, the improvement of the energy performance of existing buildings is fundamental. That is the reason why part of the research concerns the refurbishments of verandas which are closed with elements having a large glazed surface (Chapter 5, "Sunspaces to improve energy retrofitting in Freiburg (Germany)"). This part was developed at the Fraunhofer Institut - Institut für Solare Energiesysteme (ISE) of Freiburg (Germany). The concept is the same as for the sunspaces: the presence of an adjacent not heated space which works as "solar collector" can decrease the heating requirements. An existing building which between 1997 and 1999 was renovated (among other things, by closing the veranda with windows, improving the insulation, and adding a solar air collector for the supply air entering the veranda and a mechanical air extraction system) was monitored and the data were analysed critically. Considering the experience with the past renovation, design proposals for future refurbishments have been considered. The energy performances of different possibilities were calculated and compared among them. Attention was paid to thermal insulation, to exploitation of the solar radiation and to ventilation strategies (also mechanical and integrated with heat recovery systems).

Chapter 6 ("Guided procedure for the proper design of sunspaces") presents guided steps for a proper design of sunspaces, considering both new constructions and refurbishments. European countries can achieve the goal of "nearly zero-energy buildings" only if the building designers will have at their disposal more information.

Chapter 7 ("Conclusions") summarizes the main conclusions of the work. It also provides some indications for the development of future works about the treated subjects.

In writing this thesis, the hope is that the results can actually be useful for designers. Hopefully, the utilization of passive solar systems will become ever more widespread and designers will gain greater technical awareness of these subjects.

1. Passive solar systems

1.1 Overview to passive solar systems

The reasons for energy saving are numerous (economical, geopolitical, environmental...) and in the last years legislation and market are paying more and more attention to the energy saving in buildings. This attention is well justified by the fact that “*Buildings account for 40 % of total energy consumption in the Union*”, as the Directive 2010/31/EU of the European Parliament and of the Council notices¹. ANNEX I of the same directive, “Common general framework for the calculation of energy performance of buildings”, provides that in calculating the building energy performance the “passive solar systems” must be taken into consideration. The 32th preamble of the Directive 2009/28/EC of the European Parliament and of the Council on the promotion of the use of energy from renewable sources states that “*Passive energy systems use building design to harness energy*”, meaning that concepts relative to energy efficiency and to renewable energy exploitation are integrated in the architectural design. According to Mazria, E. (1979), in buildings we can consider separately active solar systems and passive solar systems: “*In general, active systems employ hardware and mechanical equipment to collect and transport heat. (...) Passive systems, on the other hand, collect and transport heat by non-mechanical means*” (p. 28).

Often passive systems are close to inner rooms which they contribute to heat. They can be even part of the built environment. According to Zappone, C. (2005), within a passive solar system it is possible to identify the following functions:

- collection of the solar radiation;
- heat storage and heat release;
- heat distribution within the inhabited spaces;
- control of the system.

A single element can carry out more than one function.

¹ The same directive provides:

Member States shall ensure that:

(a) by 31 December 2020, all new buildings are nearly zero- energy buildings; and

(b) after 31 December 2018, new buildings occupied and owned by public authorities are nearly zero-energy buildings.

where

“nearly zero-energy building” means a building that has a very high energy performance, as determined in accordance with Annex I. The nearly zero or very low amount of energy required should be covered to a very significant extent by energy from renewable sources

The Annex I specifies what must be considered in the calculation of the energy performance. It is foreseeable that the future impact of that directive on the building construction will be very important.

Mazria, E. (1979) divides passive solar systems in three categories:

- Systems with direct gain (Figure 1.1): the actual living space is directly heated by the solar radiation. The collection of the solar radiation happens through the windows. The heat storage and the heat release are provided directly by internal elements of the heated room. Therefore the exploitation of the solar radiation depends also on the geometry and on the thermal inertia of the actual living space, as well as on the solar absorptance of its surfaces. There is no heat distribution and the system can be controlled through shading elements or, more drastically, opening the windows. A proper design takes into consideration the heat dispersions, the dimensions and the properties of the glazed parts and the thermal inertia. An examination of the exploitation of direct gains is presented in paragraph 1.2.1 “Compactness and exposure” of the present thesis.

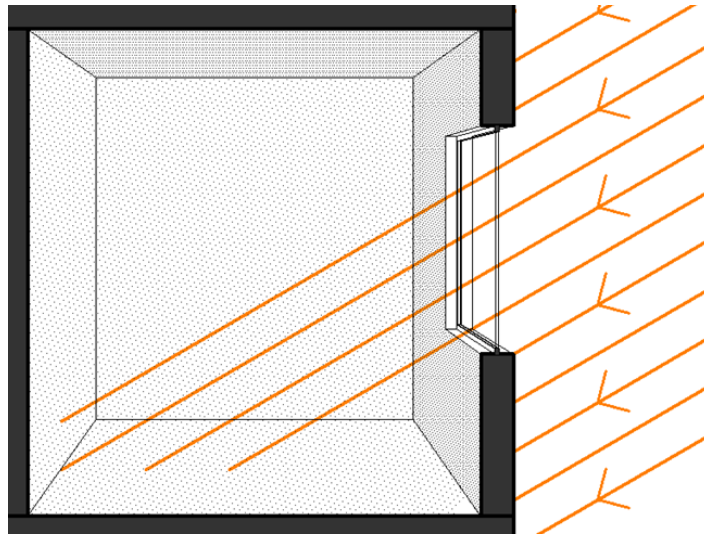


Figure 1.1 System with direct gain

- Systems with indirect heat gain (Figure 1.2): solar radiation first strikes a thermal mass which is located between the sun and the living space (heat collection). Then the absorbed heat is transmitted through conduction or ventilation towards the internal rooms. The wall carries out both the function of heat storage and heat release and the function of heat distribution.

In Figure 1.2 we can see an air cavity between a window and a wall. In the wall there are adjustable openings. Those openings are at different heights in order to increase the ventilation flow when they are open. Obviously if the temperatures of the two sides of the wall are different there is always heat flow between them (with flux delays and flux attenuations due to the thermal inertia of the wall), while the ventilation flow can be stopped.

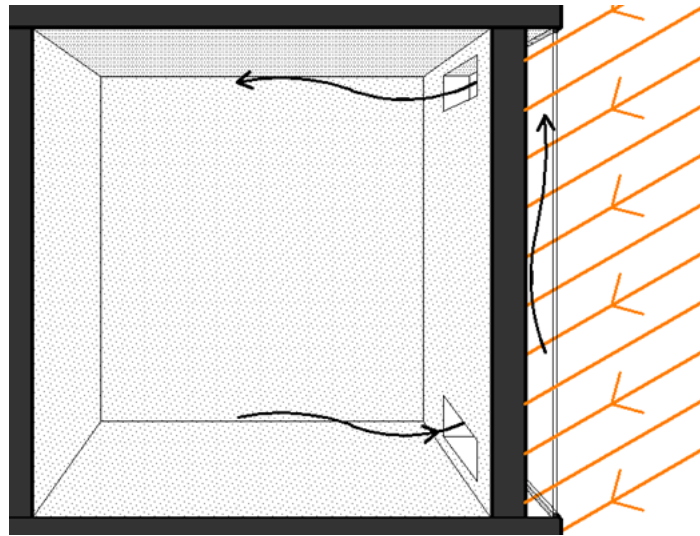


Figure 1.2 System with indirect gain

During the heating season, stopping it is useful when the temperature in the air cavity is lower than the temperature in the heated space (it is extremely probable during the night or also with a low solar radiation). Therefore the openings carry out the functions of heat distribution and of system control.

- Systems with isolated gain: solar collection is completely separated from the living space. The distribution system is in that case particularly important. An application of this concept is the natural convective loop. Generally the heat is distributed by air or water.

Generally the passive solar systems are based on the greenhouse effect. The collection of energy happens with the passage of solar radiation through a glazed element. The solar radiation enters collector element (e.g. a panel, or an air cavity, or a room...) and strikes its surfaces, whose temperatures thus increase. The visible spectrum is radiation with wavelength in the range $0,4\div 0,7 \mu\text{m}$ and the peak of the solar radiation corresponds to a wavelength of about $0,5 \mu\text{m}$. For the wavelengths corresponding to visible light the transparency of the glass is very high. For every temperature T of the body which emits radiation, the monochromatic emission² has a maximum value, which corresponds to a certain wavelength, called λ_{max} .

² The monochromatic emission is defined as $e_{\lambda} = \lim_{\Delta A, \Delta \lambda} \frac{q_{\lambda A}}{\Delta A \cdot \Delta \lambda} = \frac{\partial^2}{\partial A \partial \lambda} q_{\lambda A}$ where $q_{\lambda A}$ is the radiative flow emitted by the surface ΔA of the considered body in an interval of wavelengths having amplitude $\Delta \lambda$

The Wien's law states that:

$$\lambda_{\max} T = 2898 \mu\text{m}\cdot\text{K} \quad (1.1)$$

Therefore for the temperatures of the bodies which are inside buildings and passive solar systems λ_{\max} is between $8\mu\text{m}$ and $12\mu\text{m}$. Hence the monochromatic emission of those bodies is maximum for wavelengths to which the glass transparency is very low (see Figure 1.3. for normal radiation). Glass is much more transparent to short-wave radiation than to long wavelength therefore the greatest part of the radiation emitted by the internal surfaces remains inside. At the same time the internal surfaces release heat to the air (or to the used fluid, e.g. water) through convection and the heated air cannot exit to the external environment because of the envelope of the collector element. In presence of solar radiation, because of those phenomena, within the collector the air temperature is higher than the external temperature (it can be much higher).

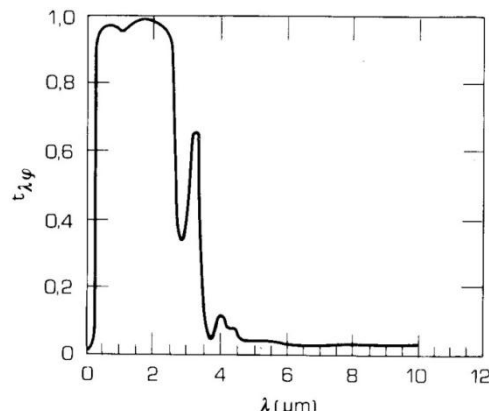


Figure 1.3 On the horizontal axis: wavelength of the incident radiation. On the vertical axis: transparency coefficient of a glass pane for normal radiation. Source: Bonacina, C. et al. (1992)

The transparency coefficient of a glass depends also on the incident angle of the solar radiation on the glazed surface (see Figure 1.4).

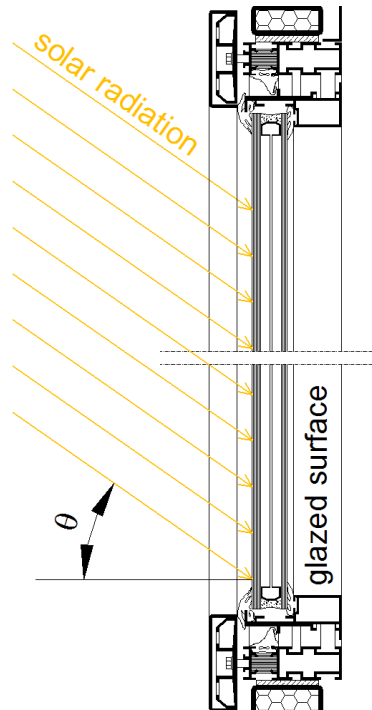


Figure 1.4 Incident angle of the solar radiation on a glazed surface (2-dimensional representation)

If τ_n is the transparency coefficient for a normal radiation, the transparency coefficient for any other inclination of the radiation can be considered

$$\tau = F_{w,dir}(\theta) \cdot \tau_n \quad (1.2)$$

In literature there are different models of the function $F_{w,dir}$, which is called correction factor. As example, in Figure 1.5, the model which is present in software for the dynamic simulations IDA – Indoor Climate and Energy³ and the models presented in J. Karlsson and A. Roos (2000) for a window having a Ag+ coating layer and for a window having a SnO₂ coating layer are illustrated. There is no big difference among those models. It is possible to observe that the derivative of F_w is always negative: up to about 40° the slope of the curve is small, then it becomes much bigger and F_w is equal to 0 for radiation normal to the windowpane.

The inclination angle between the radiation and a surface is important also because of a purely geometric question: considering constant the direct radiation which is present in the environment, the direct radiation striking the surface, per unit of surface, is maximum if the surface is normal to the surface.

The issue of the influence of the inclination of a glazed surface on the entering energy is analysed in paragraph 1.2.2 “Inclination of the glazed surface”.

³ <www.equa.se/eng.ice.html>

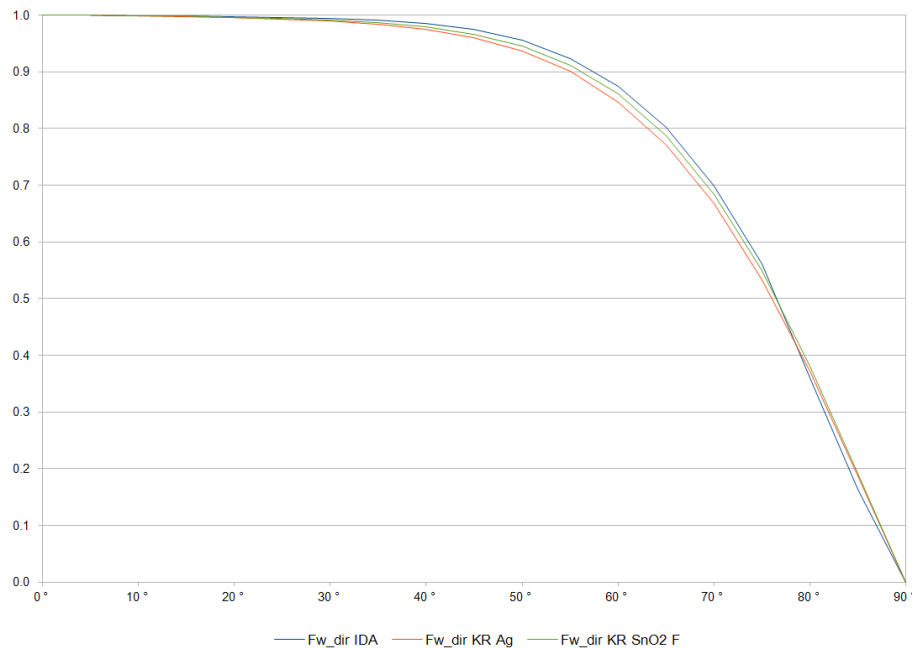


Figure 1.5 Three functions of the correction factor F_w . On the horizontal axis: angle between the radiation and the windowpane. On the vertical axis: the correction factor

The design of passive solar systems has to consider how much and when the solar radiation is available in the considered locality. In Figure 1.6 the radiation available in a completely sunny day on surfaces located at a latitude of 41°N and having different orientations is showed.

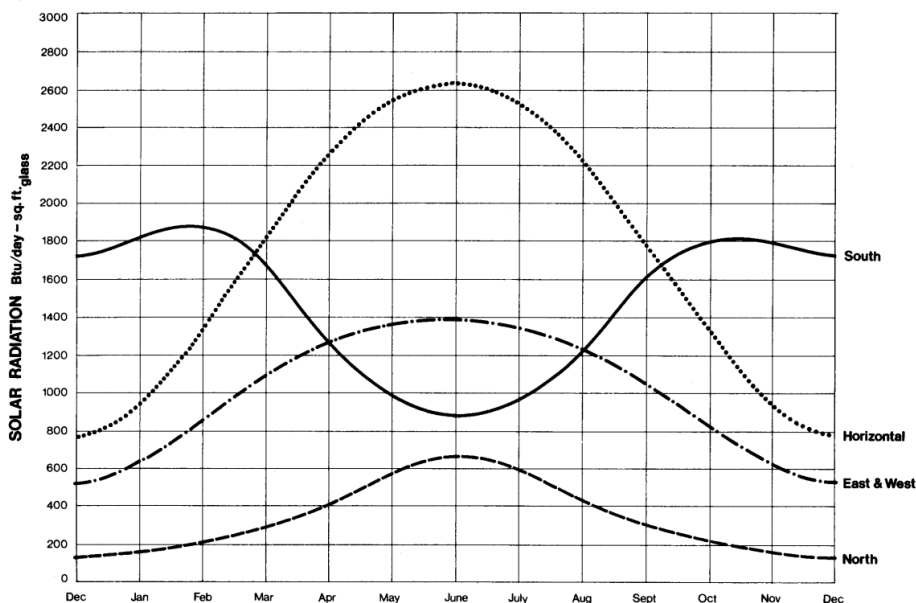


Figure 1.6 Solar radiation incident in a completely sunny day on surfaces having different orientations, without shading, latitude 40°N

$1 \text{ Btu/ft}^2 = 3,2 \text{ Wh/m}^2 = 1,1 \cdot 10^{-2} \text{ MJ/m}^2$ Source: Mazria, E. (1979)

Apart from the issue of the local shades, generally in the northern hemisphere the best solution

is the orientation of the solar collector towards south: during the winter months the solar radiation is maximum for the surfaces facing south (and that is the most important aspect for passive solar systems) and during the summer the solar radiation for surfaces facing south is less than for surfaces having other orientations (horizontal, or towards east or west).

If the sky is perfectly clear the solar radiation for surfaces facing south is even higher during winter than during summer. Considering real conditions of the sky, the situation can be different, or at least more irregular. In Figure 1.7 monthly mean values for Trento (Italy) taken from the Italian technical standard UNI 10349:1994 *Riscaldamento e raffrescamento degli edifici. Dati climatici* are represented. Hence for the design choices considering the characteristics of the local climate is important.

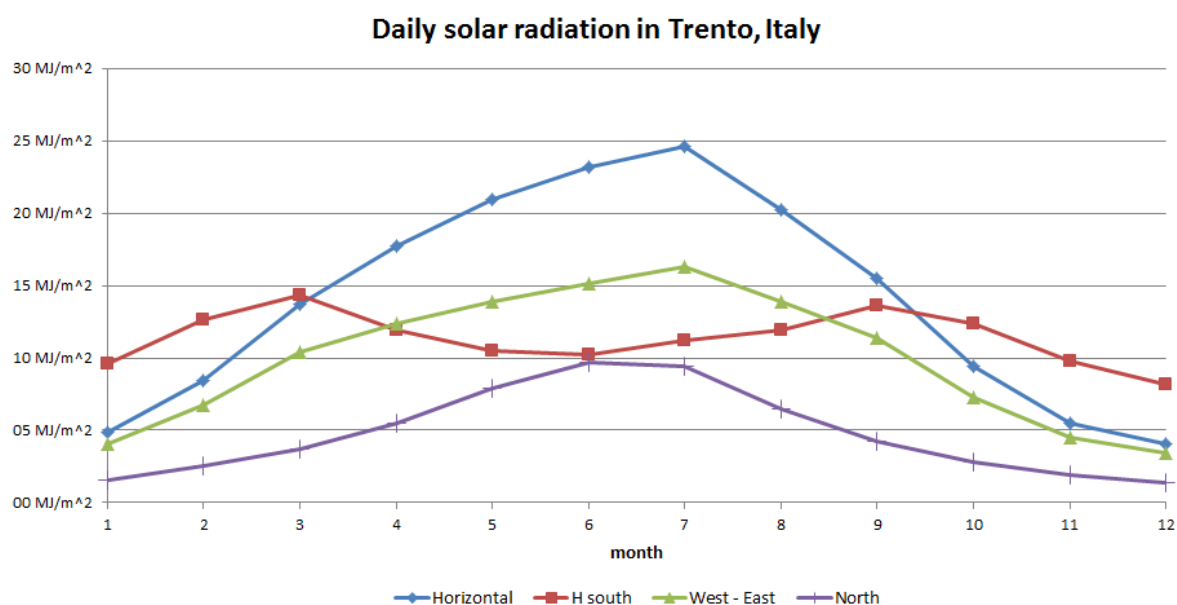


Figure 1.7 Monthly averages of daily solar radiation incident on surfaces having different orientations in Trento, Italy. Latitude 46°N Source of the data: UNI 10349:1994

Considering that in the day/night cycle the minimum temperatures are in the early morning, a solution could be the orientation of the solar collector not exactly towards the south but a little inclination towards the east. In fact, in the early morning the exploitation of the solar radiation could be particularly useful. However, the specific habits of the building inhabitants should be considered.

For the orientation towards the south the Figure 1.8 considers also surfaces which are tilted with different inclinations from the vertical one and the horizontal one. It supposes a perfectly clear sky.

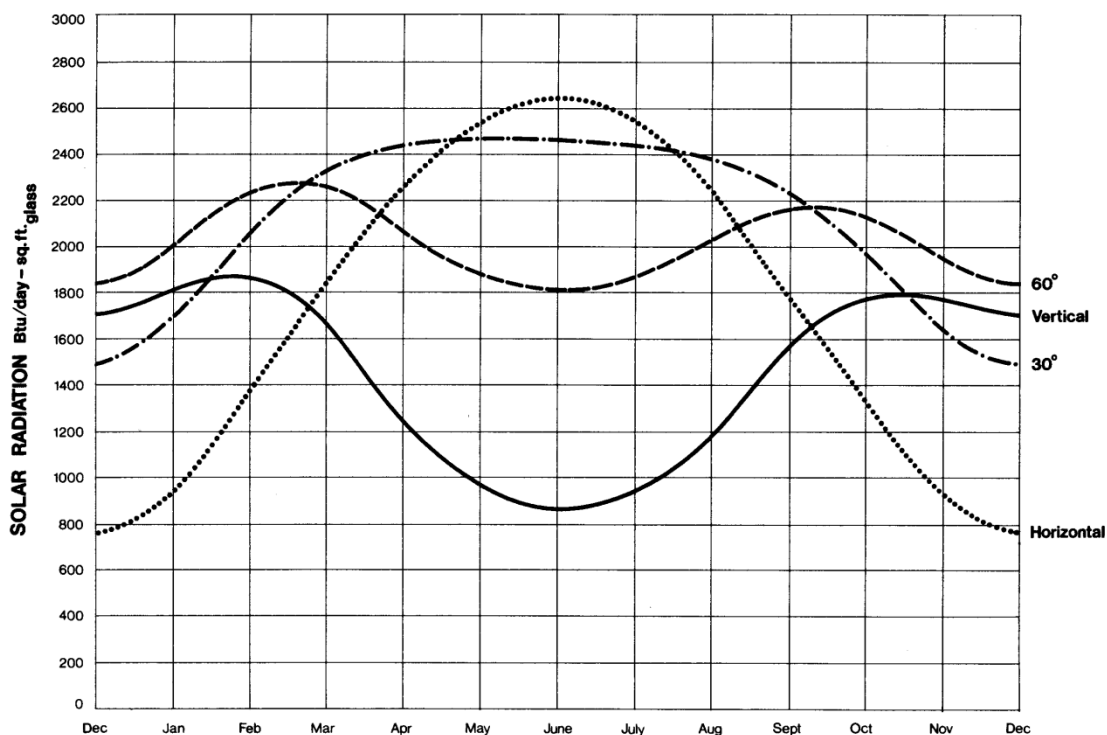


Figure 1.8 Solar radiation incident in a completely sunny day on surfaces facing south but having different inclinations, without shading, latitude 40°N
 $1 \text{ Btu/ft}^2 = 3,2 \text{ Wh/m}^2 = 1,1 \cdot 10^{-2} \text{ MJ/m}^2$ Source: Mazria, E. (1979)

During the winter the higher values of the solar radiation are on a surface tilted by 60° with respect to the horizontal. Such a surface is struck by more radiation than the vertical surface also during the rest of the year and this can be counter-predictive.

The horizontal surface and the surface tilted by 30° respect to the horizontal are worse than the vertical one throughout the year: during the winter season they are struck by less solar radiation and during the summer season they are struck by more solar radiation.

The inclination of tilted glazed surfaces is dealt with by paragraph 1.2.2 “Inclination of the glazed surface”.

In order to know the position of the sun in the sky at a specific time, it is possible to examine the so-called sun chart. A different chart exists for each latitude. The designer has also to consider the local shadings, particularly in mountain areas. The angles of the obstacles could be reported in the sun chart, highlighting what is permanent and what is not permanent (see Figure 1.9).

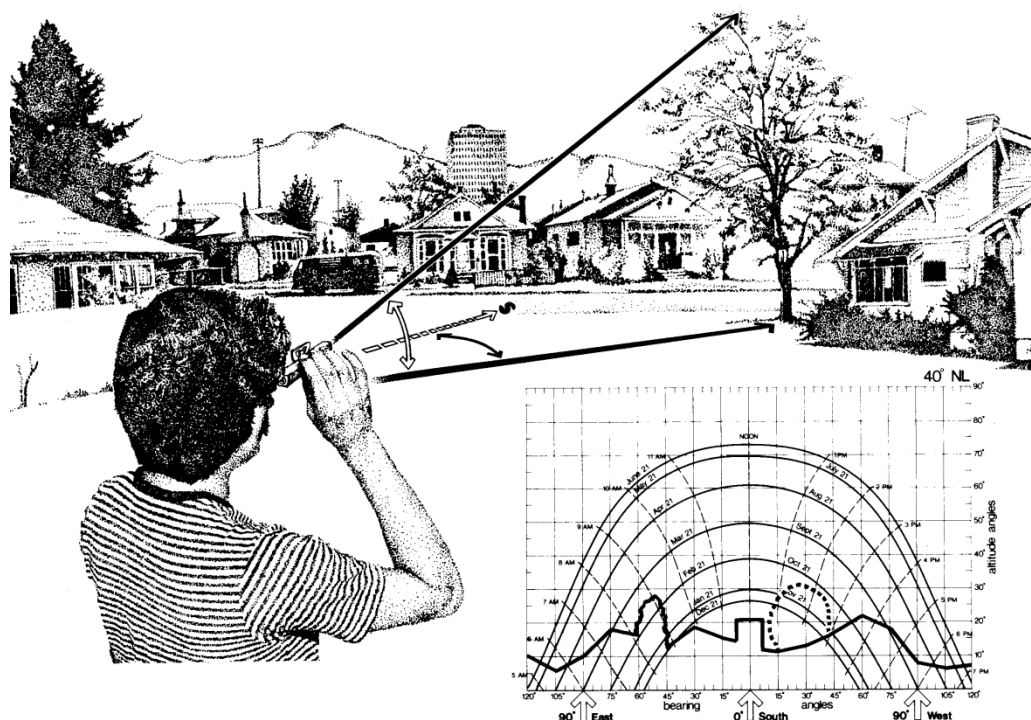


Figure 1.9 Plotting the shading elements, which are represented on the sun chart. Source: Mazria, E. (1979)

1.2 Shape, solar gains and heating requirements

The present paragraph deals with some concepts concerning not only sunspaces, but, more in general, the optimization of the bioclimatic design. The present study started from two considerations:

1. The bioclimatic design has to minimize heat losses and to maximize exploitation of solar gains.
2. Important aspects of the shape of a building are its compactness and the orientation of its surfaces; in particular, the ability of the geometry to capture the solar radiation has a fundamental role.

Paragraph 1.2.1 “Compactness and exposure” presents a research which clarifies how much in the Italian context the decrease of compactness can be balanced by the increase of exposure to solar radiation, in order to minimize the heating requirements.

Paragraph 1.2.2 “Inclination of the glazed surface” deals with the issue of the best inclination with respect to the vertical of a south facing window to maximize the entering solar radiation during the heating season.

The relationship between shape and energetic performance during the summer season would be an interesting subject also, but it was not dealt in the present thesis because the energetic advantages of sunspaces regard the cold season.

1.2.1 Compactness and exposure

Often in discussions concerning the relationship between building shape and energy performance, the only parameter which is considered is the compactness, in particular the shape coefficient, defined as the ratio between the envelope surface of the building S and the inner volume of the building V :

$$C_f = S / V \quad (1.3)$$

Depecker, P. et al. (2001) found a strong correlation between energy consumption and shape coefficient in Paris, but in Carpentras, a milder French locality, they did not. So they gave no specific indications for building design in mild climates. For climatic conditions similar to those of Carpentras they asserted:

“A link between the energy consumption of a building and its shape can no longer be stated. As a consequence, that leaves architects to choose any shape”.

The matter is particularly important in Italy and in countries with similar geographic conditions. Therefore a study which considers the heating requirements of different shapes in Italian localities was developed. The results were published in Albatici, R. and Passerini, F. (2011), which is available in Appendix (with permission from Elsevier). The Figures 1.6, 1.7 and 1.8 show the importance of the solar radiation on surface facing south in the coldest months (in the northern hemisphere). A new parameter was introduced, namely south exposure coefficient C_{fs} , which is the ratio of the area of south walls to the volume of the building:

$$C_{fs} = S_{\text{south}}/V \quad (1.4)$$

The results of the calculation show that an appropriate increase of the south exposure coefficient can balance, in term of heating requirements, an increase of the shape coefficient (for every faces fixed ratio between the glazed surfaces and the opaque surfaces was considered). The compactness is therefore not the only parameter to take into account, but at the same time the exposure to solar radiation must be considered.

Moreover, in a specific paragraph the article deals with the ratios between glazed surface and total surface of facades having different orientations which minimize the heating requirements. Different orientations and different properties of the windows have been considered.

More details are available in Appendix.

1.2.2 Inclination of a glazed surface

The solar radiation which enters through a window depends on the window orientation. In fact, more in general, the amount of radiation which hits a tilted surface depends on the surface orientation. Moreover, the optical properties of a window depend on the inclination between the window and the incoming solar radiation (see Figure 1.4 and Figure 1.5).

Generally the total short-wave radiation on a tilted surface is considered as the sum of three contributions: direct radiation, diffuse radiation from the sky and diffuse radiation coming from the ground. In the calculation of the solar radiation which enters through a tilted window we can identify the following steps:

- Measurement and utilization of meteorological data (in particular concerning the solar radiation). The measurement can be made specifically for the design or the data can be obtained from an existing database. A “test reference year” is a series of hourly data having a statistical value for the considered locality.
- If only the global radiation was measured, a subdivision in diffuse radiation and direct radiation has to be done. In order to achieve that goal in literature different kinds of system exist.
- A model of the diffuse radiation has to be considered. The diffuse radiation is not completely isotropic, at least because the radiation coming from the sky is different from the radiation coming from the ground. More complex models consider typically also the circumsolar radiation and the horizon brightening.
- The albedo of the surrounding environment, in particular of the ground, has to be evaluated or estimated.
- The optical properties of the windows have to be determinate. In particular, a model of the correction factor of the window transparency for non-normal incidence has to be considered. The model has to be chosen considering the kind of utilized window.

For every step some uncertainties and errors exist.

The present paragraph considers south facing windows and its goals is to give some indications about the better inclination to maximize the exploitation of the entering solar radiation. Some mentions about the influence of the locality, of the ground albedo and of the diffuse radiation model are presented.

The results concerning two different localities, having very different latitudes, are here reported. They are Bolzano (Italy) and Cordova (Alaska, USA).

Table 1.1 The considered localities

Locality	Latitude	Longitude	Database
Bolzano, Italy	46°29' N	11°20' E	Comitato Termotecnico Italiano ⁴
Cordova, Alaska, USA	60°30' N	145°83' W	ASHRAE – TMY3 ⁵

The utilized data are part of Test Reference Years therefore they have statistical value. For Bolzano the direct radiation and the diffuse radiation were not available, because the data of the Comitato Termotecnico Italiano provide only the global radiation on the horizontal surface.

A method provided by Reindl, D.T. et al. (1990) was used to estimate the diffuse radiation and the direct radiation from the global one. The method was validated for 5 localities in America and in Europe with very different climates (latitudes from 28.4°N to 59.56°N). The used piecewise correlation is:

interval: $0 \leq k_t \leq 0,3$ constraint: $I_d/I \leq 1,0$

$$I_d/I = 1,020 - 0,245 k_t + 0,0123 \text{ sen}\alpha$$

interval: $0,3 \leq k_t \leq 0,78$ constraint: $I_d/I \geq 0,1$

$$I_d/I = 1,400 - 1,749 k_t + 0,177 \text{ sen}\alpha$$

(1.5)

interval: $k_t \geq 0,78$ constraint: $I_d/I \geq 0,1$

$$I_d/I = 0,486 k_t - 0,182 \text{ sen}\alpha$$

where

k_t is the hourly clearness index, i.e. the ratio of hourly global horizontal to hourly extraterrestrial radiation $k_t = I / I_{on}$

I_d is the hourly diffuse radiation on a horizontal plane

I is the hourly global radiation on a horizontal plane

α is the solar altitude

The extraterrestrial radiation can be calculated with the following equation, which considers the variation of the distance between the Earth and the Sun (see for example Spitters, C.J.T. et al. (1990)):

$$I_{on} = S_{cs} \cdot [1 + 0,033 \cos(360t_d/365)] \cdot \text{sen}\alpha$$

(1.6)

where

S_{cs} is the solar constant $1370 \text{ Jm}^{-2}\text{s}^{-1}$

⁴ <www.cti2000.it>

⁵ National Renewable Energy Laboratory <www.nrel.gov>

t_d is the number of the day, starting since 1st January

It is possible to observe that if the hourly clearness increases, diffuse fraction decreases.

For tilted surfaces ASHRAE (1997) states that:

"The incident beam radiation is just the normal beam radiation multiplied by the cosine of the incidence angle" .

Therefore if the direct beam radiation is known, calculating the beam radiation on a tilted surface is a purely geometric question.

$$I_{dir,w} = I_{dir,norm} \cos\theta \quad (1.7)$$

If $\cos\theta$ is less than 0, the direct radiation was set to 0.

$I_{dir,w}$ is the beam radiation on the considered window [W/m^2]

$I_{dir,norm}$ is the normal beam radiation [W/m^2]

The following equation can be written:

$$\cos \theta = \cos \alpha \cdot \cos \gamma \cdot \sin \Sigma + \sin \beta \cdot \cos \Sigma \quad (1.8)$$

where

θ is the incident angle

γ is the surface-solar azimuth (in this case it is equal to solar azimuth because the window is facing south)

Σ is the slope of the surface. It is equal to 0° if the surface is horizontal facing the sky and to 180° if the surface is horizontal facing the ground

α is the solar altitude

Two models of the diffuse radiation were used to observe how they influence the results: the isotropic model and the Perez model. In all cases, it is supposed that there are no obstacles and that the ground surface is perfectly horizontal.

The isotropic model is used, for example, in the ASHRAE (1997) and in Gueymard, C.A. (2009) and it calculates the diffuse solar radiation from the sky on a surface through the equation:

$$I_{Diff,w} = I_{DiffHor} \cdot F_{ss} \quad (1.9)$$

$I_{Diff,w}$ is the diffuse solar radiation on the considered window [W/m^2]

$I_{DiffHor}$ is the diffuse solar radiation on the horizontal surface [W/m^2]

F_{ss} is the view factor between the sky and the surface. It is considered

$$F_{ss} = (1 + \cos \Sigma) / 2 \quad (1.10)$$

Hence F_{ss} is equal to 1 if the surface is horizontal facing the sky and to 0 if the surface is horizontal facing the ground.

The diffuse reflected radiation from the ground on the considered window can be calculated with the equation

$$I_{gr,w} = \rho F_{sg} \cdot (I_{DiffHor} + I_{dirHor}) \quad (1.11)$$

where

$I_{gr,w}$ is the diffuse radiation on the considered window coming from the ground [W/m^2]

ρ is the reflectivity of the ground, i.e. if the albedo is called "a" $\rho = 1 - a$

F_{sg} is the view factor between the ground and the surface. It is considered:

$$F_{sg} = (1 - \cos \Sigma) / 2 \quad (1.12)$$

I_{dirHor} is the beam radiation on the horizontal surface [W/m^2]

The model of Perez (1990) is more complex. It considers the circumsolar and horizontal brightness. The solar irradiation on a tilted surface is calculated through the following equation:

$$I_{Diff,w} = I_{DiffHor} \cdot \left[(1 - F_1) \frac{1 + \cos \Sigma}{2} + F_1 \frac{a}{b} + F_2 \sin \Sigma \right] \quad (1.13)$$

where

$a = \max(0, \cos \theta)$ θ is angle of incidence

$b = \max(0,087, \cos \gamma)$ γ is zenith angle

F_1 is the circumsolar brightness coefficient

F_2 is the horizontal brightness coefficient

Coefficients F_1 and F_2 are calculated by the equations

$$\begin{aligned} F_1 &= f_{11} + f_{12}\Delta + f_{13} \gamma \\ F_2 &= f_{21} + f_{22}\Delta + f_{23} \gamma \end{aligned} \quad (1.14)$$

Δ is the brightness index

f_{xx} are coefficients whose values are presented in Table 1.2.

Table 1.2 Coefficients for the calculation of the circumsolar and horizontal brightness according to Perez (1990)

ϵ	f_{11}	f_{12}	f_{13}	f_{21}	f_{22}	f_{23}
0.000 – 1.065	-0.008	0.588	-0.062	-0.060	0.072	-0.022
1.065 – 1.230	0.130	0.683	-0.151	-0.019	0.066	-0.029
1.230 – 1.500	0.330	0.487	-0.221	0.055	-0.064	-0.026
1.500 – 1.950	0.568	0.187	-0.295	0.109	-0.152	-0.014
1.950 – 2.800	0.873	-0.392	-0.362	0.226	-0.462	0.001
2.800 – 4.500	1.132	-1.237	-0.412	0.288	-0.823	0.056
4.500 – 6.200	1.060	-1.600	-0.359	0.264	-1.127	0.131
6.200 -	0.678	-0.327	-0.250	0.156	-1.377	0.251

The brightness index Δ is calculated from the equation:

$$\Delta = m \frac{I_{\text{DiffHor}}}{I_{\text{on}}} \quad (1.15)$$

where

m is air mass

I_{DiffHor} is diffuse radiation on the horizontal plane

I_{on} is the normal-incidence extraterrestrial irradiance

The sky clearness, which is required by the Table 1.2, is calculated by the equation

$$\epsilon = \frac{\frac{I_{\text{DiffHor}} + I_{\text{dir, norm}}}{I_{\text{DiffHor}}} + 1,1041\gamma^3}{1 + 1,1041\gamma^3} \quad (1.16)$$

After having calculated the short-wave radiation incident on the external side of the windows it is possible to calculate the short-wave radiation which enters through the window. The model used is proposed by IDA-ICE.

The angle dependence of $F_{w, \text{dir}}$ is handled by using different trigonometric functions for different angle intervals (see Figure 1.5):

$$F_{w, \text{dir}} = 1,267 \cdot \begin{cases} 1,48 \cdot \cos\theta & \text{if } \theta > 85^\circ \\ 1,8 \cdot \cos\theta - 0,028 & \text{if } 75^\circ < \theta \leq 85^\circ \\ -0,105 + \cos\theta \cdot [2,821 + \cos\theta \cdot (-2,998 + \cos\theta \cdot 1,071)] & \text{if } 0 < \theta \leq 75^\circ \end{cases} \quad (1.17)$$

where θ is the angle of incidence.

For the diffuse radiation the reduction factor of the entering short-wave radiation is considered equal to 0,85 which derives from the average of $F_{w, \text{dir}}$ over the hemisphere.

The albedo of the ground depends on the material of the surface, on its colour and surface finish, on its condition at the considered time, on the inclination of the solar radiation (therefore during a day it changes)...

For the present work the calculations were made with two different values of the albedo: 0,2 or 0,6, considered as constant. According to Thevenard, D. and Haddad, K. (2006) the dry bare ground has an albedo of 0,2. 0,2 is the most commonly used value for the albedo of the ground. Thevenard, D. and Haddad, K. (2006) states:

“As noted by many authors, ground reflectivity increases dramatically in the presence of snow. Fresh snow has a very high reflectivity (listed, depending on the sources, between 0,75 and 0,95). The reflectivity then diminishes with time, to values between 0,7 and 0,5 or less”.

Therefore 0,6 can be a value relative to a situation with snow or to a light artificial surface.

For different inclinations of the window respect to vertical (Figure 1.10), the radiation entering through window having an unitary area was calculated for every month of the heating season. The window was always considered facing south.

A normal double glazing with $g_{gl,n} = 0,75$ was considered (see Italian technical standard UNI/TS 11300-1:2008). The total solar energy transmittance considers also the heat which has been adsorbed by the glazing and it is transmitted by convection and IR-radiation to the inner space (“secondary heat transfer”; see EN 410:2011).

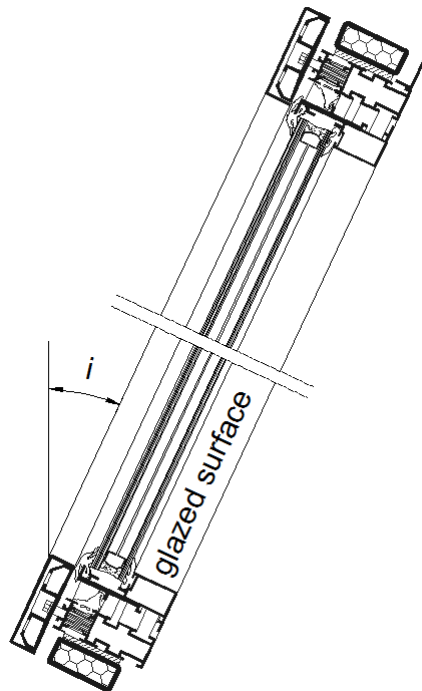


Figure 1.10 Window having an inclination of i with respect to the vertical

In Figure 1.11 the monthly radiations of Bolzano are plotted.

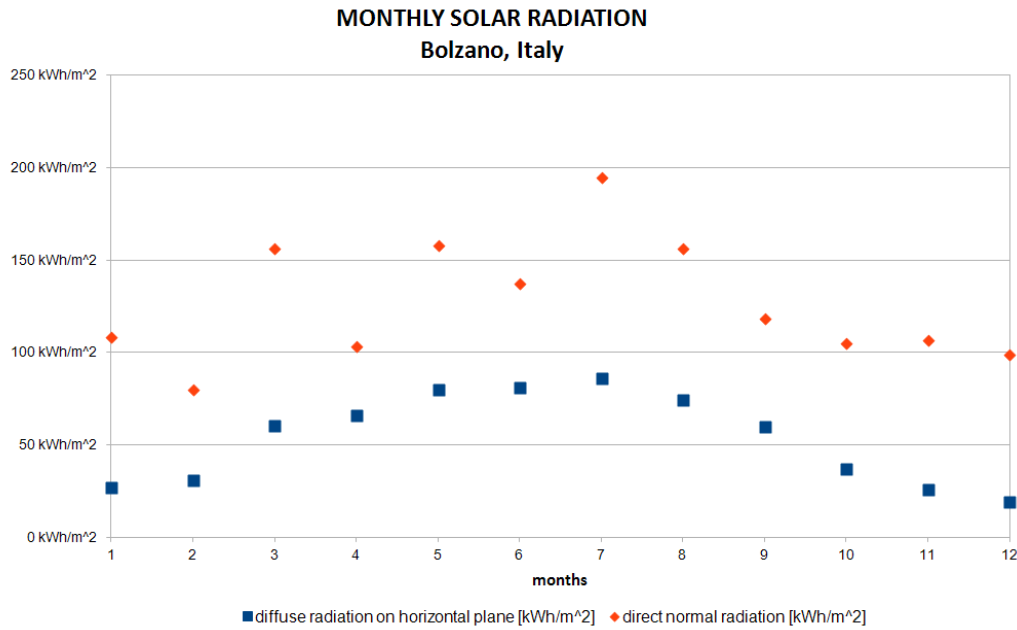


Figure 1.11 Monthly radiation in Bolzano, Italy. Source of the data: Comitato Termotecnico Italiano

In the Figure 1.12 the maximum solar altitude in Bolzano on the 15th of every month is plotted.

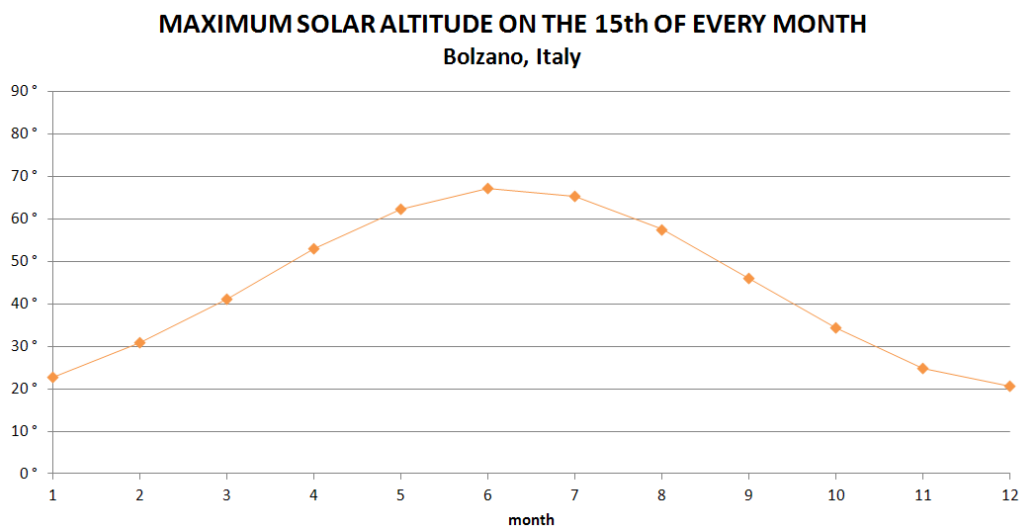


Figure 1.12 Maximum solar altitude on the 15th of every month in Bolzano.

In the Figures 1.13, 1.14 and 1.15. the variations of the entering radiation in function of the inclination of the window for Bolzano, with an albedo of 0,2 and considering an isotropic model of the diffuse radiation, are shown (0° is relative to a vertical surface).

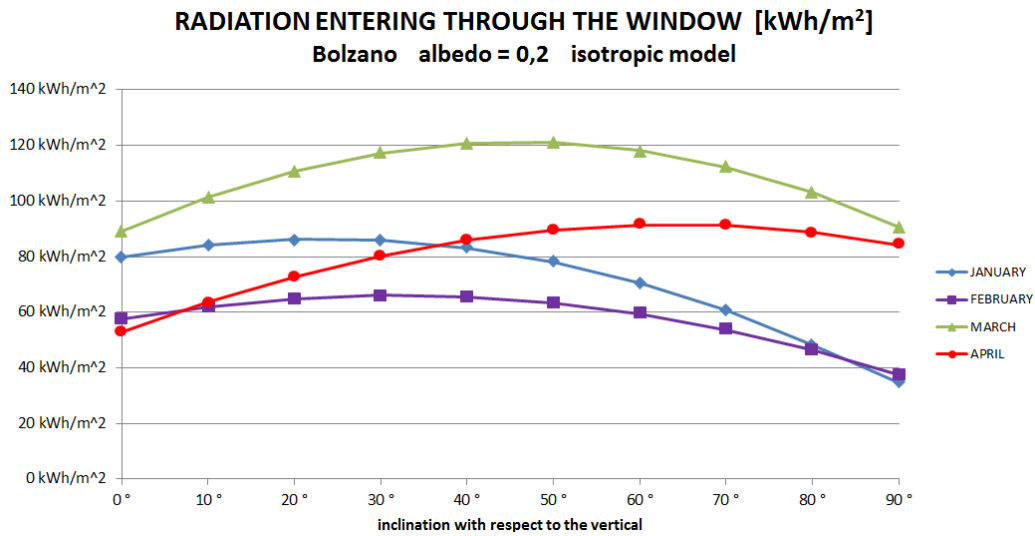


Figure 1.13 Entering radiation in function of the inclination of the window for Bolzano, with an albedo of 0,2 and considering an isotropic model of the diffuse radiation, since January until April.

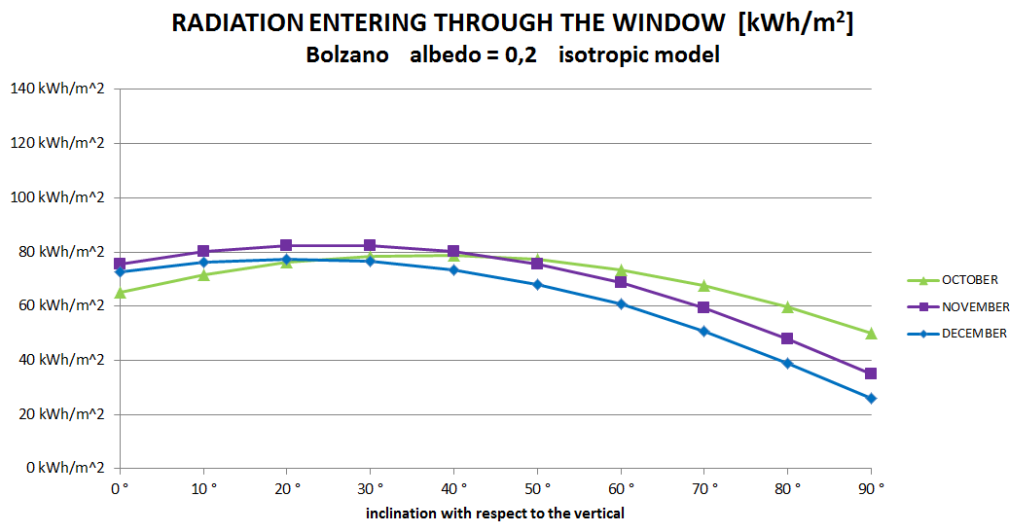


Figure 1.14 Entering radiation in function of the inclination of the window for Bolzano, with an albedo of 0,2 and considering an isotropic model of the diffuse radiation, since October until December

It is possible to observe that for every month the best solution is an inclination with respect to the vertical close to the maximum solar altitude on the 15th of that month (e.g. Figure 1.13 shows that in January the best inclination is between 20° and 30°, and Figure 1.12 shows that the maximum solar altitude on 15th January is about 22°).

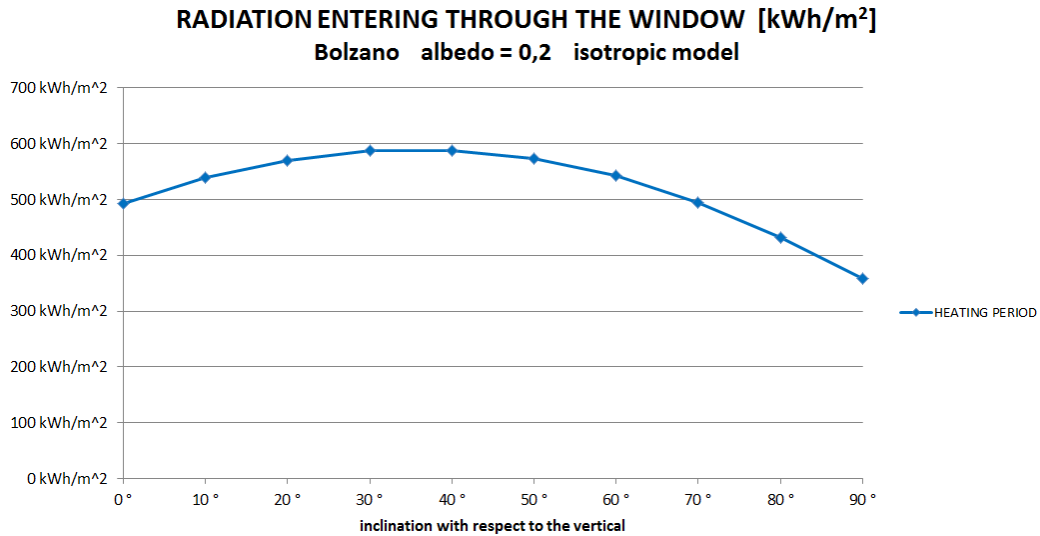


Figure 1.15 Entering radiation in function of the inclination of the window for Bolzano, with an albedo of 0,2 and considering an isotropic model of the diffuse radiation, during the heating period

Only the heating months, according to the Italian legislation, are considered. Obviously exploiting the solar radiation is more important in the coldest periods.

The inclination which maximizes the sum of the solar radiation during the heating period is between 30° and 40° (see Figure 1.15). An inclination of 30° can be preferable from the point of view of the coldest months.

The same calculation was made changing the albedo to 0,6 (Figures 1.16 and 1.17).

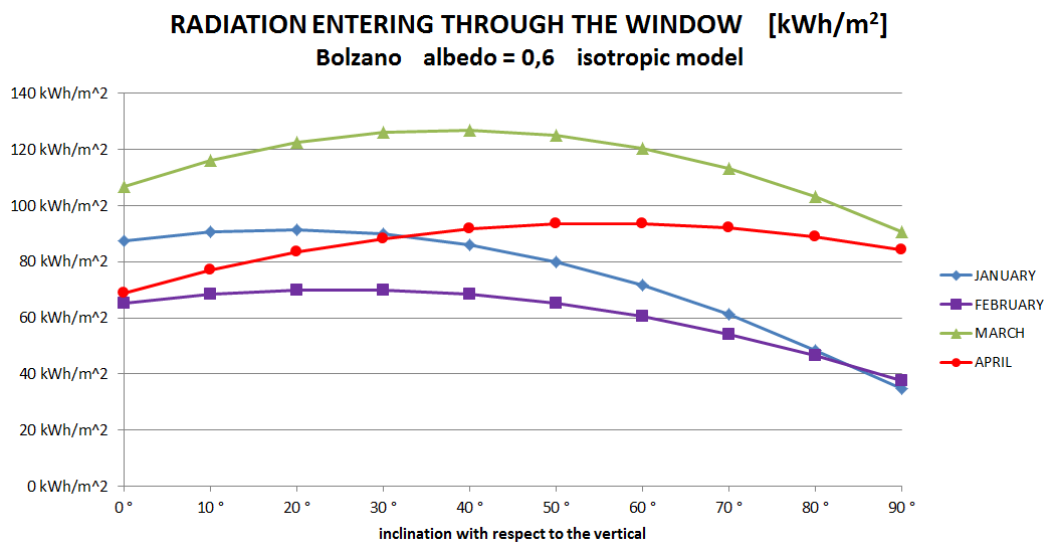


Figure 1.16 Entering radiation in function of the inclination of the window for Bolzano, with an albedo of 0,6 and considering an isotropic model of the diffuse radiation, since January until April

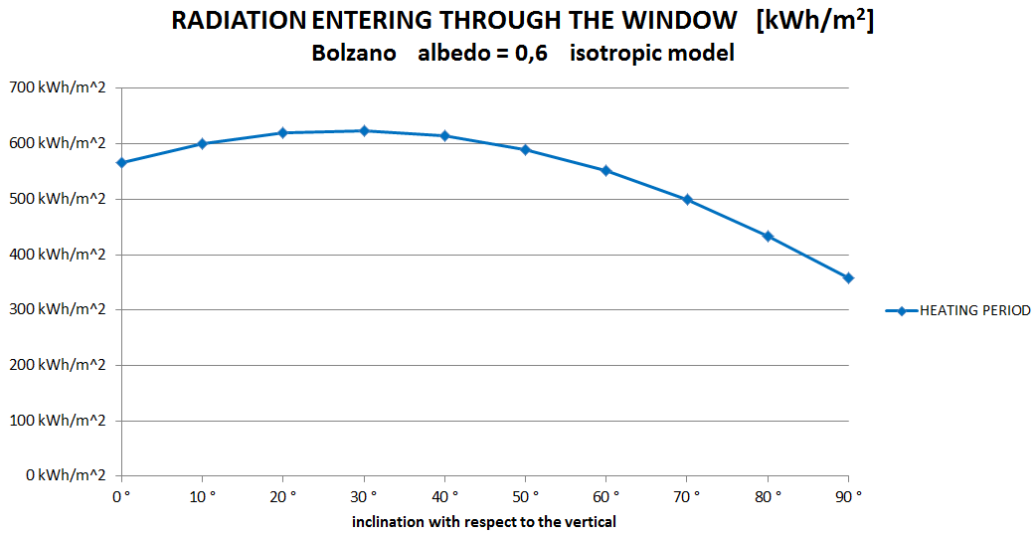


Figure 1.17 Entering radiation in function of the inclination of the window for Bolzano, with an albedo of 0,6 and considering an isotropic model of the diffuse radiation, during the heating period

Increasing the albedo the entering solar radiation increases for all inclinations except for the horizontal one (inclination 90°) which has a view factor with the ground equal to 0. The greatest increase happens for the inclinations closest to the vertical. In the case of albedo equal to 0,6 the best solution can be again an inclination of 30° or of 20°.

Now the results relative to Cordova (Alaska, USA) are presented.

The main characteristics of the locality are showed in Figures 1.18, 1.19 and 1.20. It is possible to observe that because of the low temperatures we can consider the heating period to last throughout the year.

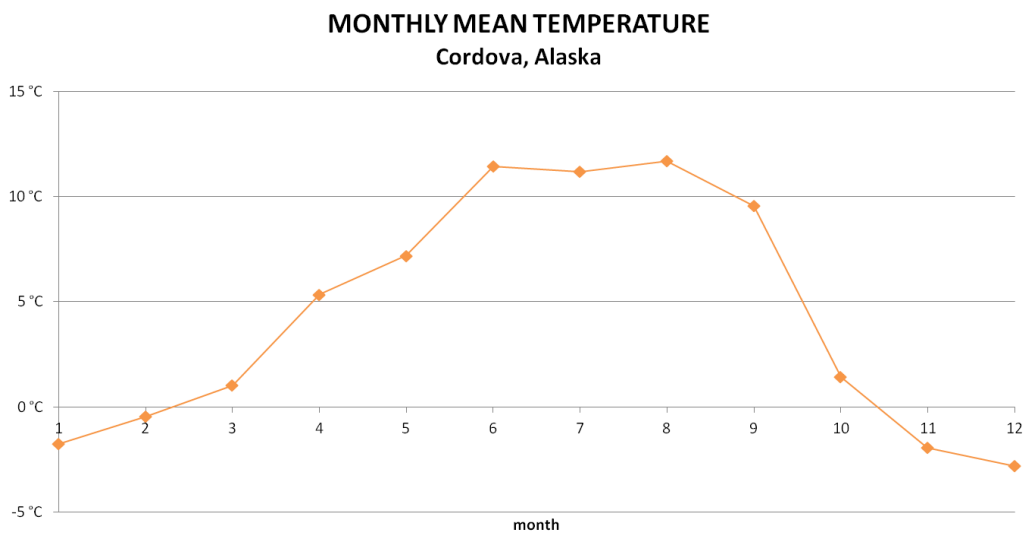


Figure 1.18 Mean monthly external temperatures in Cordova (Alaska, USA)

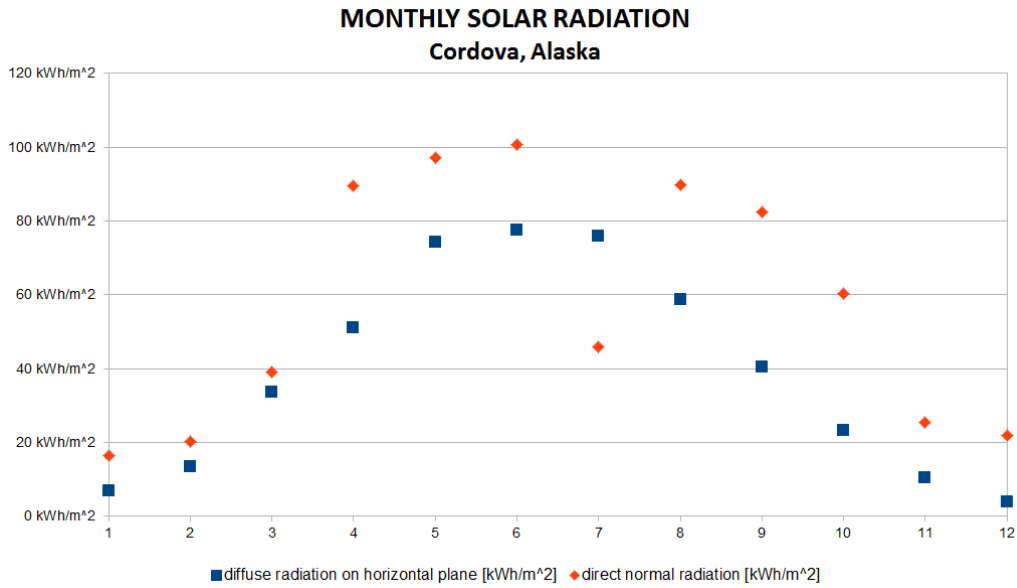


Figure 1.19 Monthly radiation in Cordova (Alaska, USA). Source of the data: ASHRAE – TMY3

In such a northern locality the values of the diffuse radiation are similar to the values of the direct normal radiation, therefore the used model of the diffuse radiation is more important than in Bolzano.

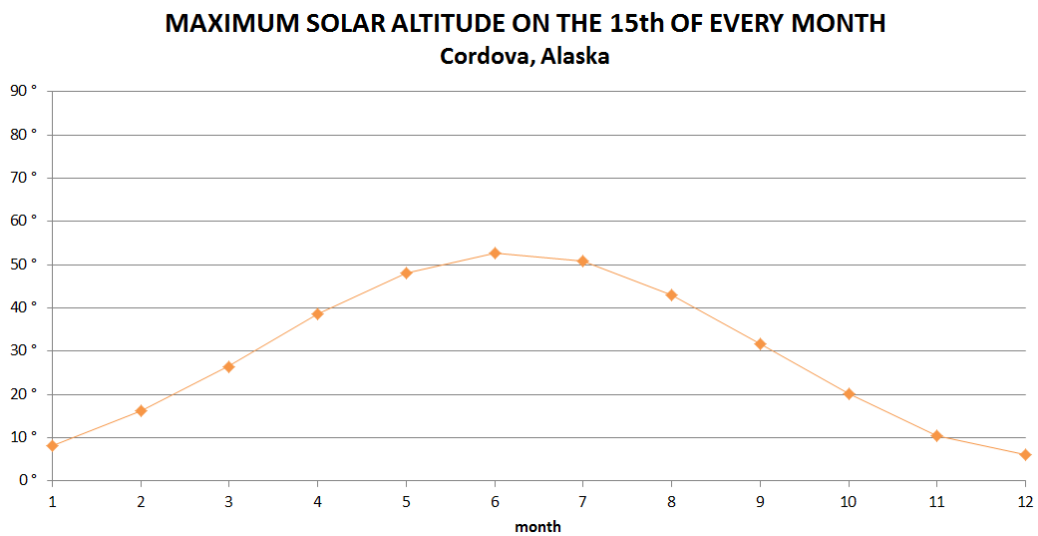


Figure 1.20 Maximum solar altitude on the 15th of every month in Cordova (Alaska, USA).

The following figures show the results of the calculations.

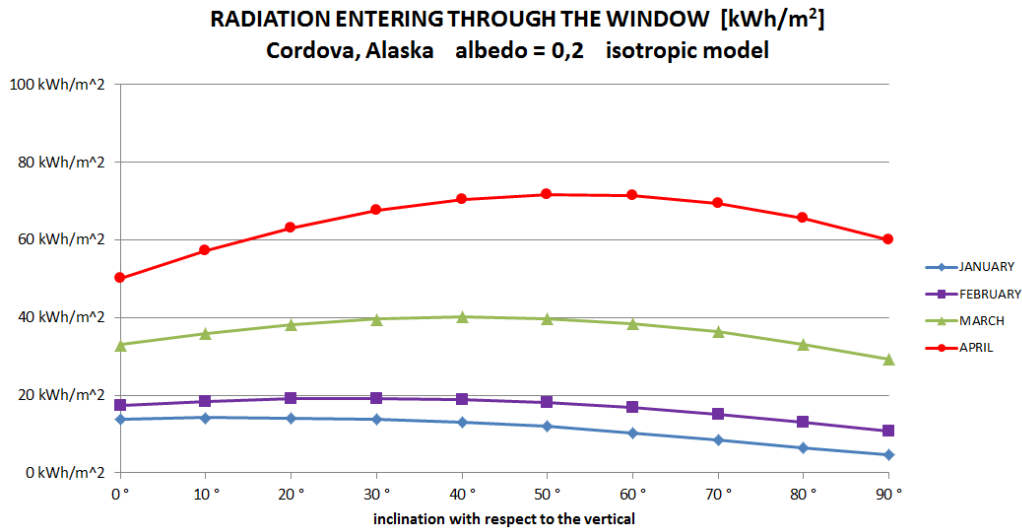


Figure 1.21 Entering radiation in function of the inclination of the window for Cordova, with an albedo of 0,2 and considering an isotropic model of the diffuse radiation, since January until April

In Cordova the angles which maximize the entering solar radiation are a little greater than the mean daily maximum solar altitudes, because the diffuse radiation is more important, in comparison with the global radiation, than in Bolzano and the diffuse radiation is present throughout the sky (Figure 1.21).

The advisable angles increase further if we consider that the external temperatures impose the heating for the whole year (in Figure 1.22, relative to the coldest months, the maximum corresponds to 30°, while in Figure 1.23, relative to the whole year, it corresponds to 50°).

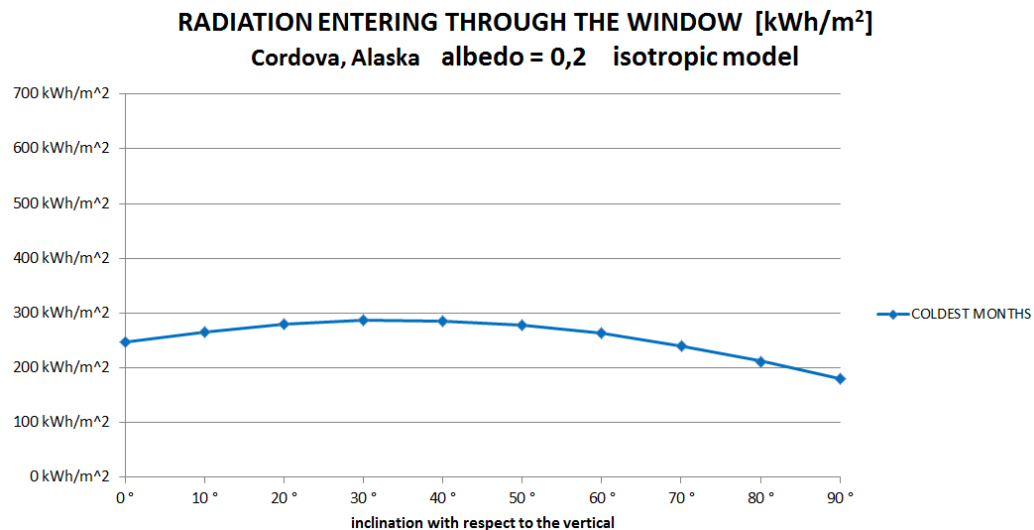


Figure 1.22 Total entering radiation in function of the inclination of the window for Cordova, with an albedo of 0,2 and considering an isotropic model of the diffuse radiation during the coldest months (September – April)

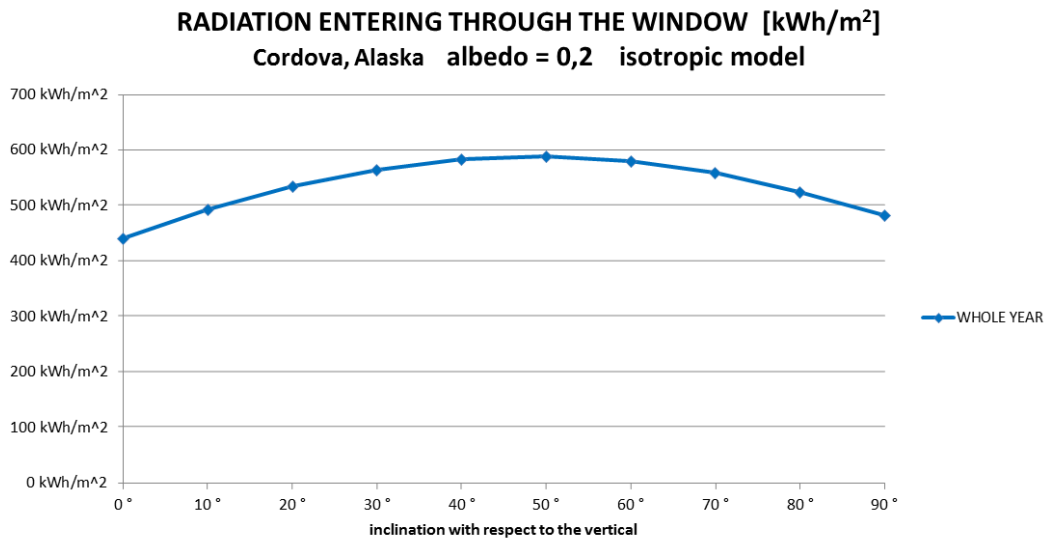


Figure 1.23 Total entering radiation in function of the inclination of the window for Cordova, with an albedo of 0,2 and considering an isotropic model of the diffuse radiation, in the whole year

Because of the presence of snow, it is probably that in Cordova the natural ground has higher albedo values than in Bolzano. In the following figures the calculations obtained with an albedo of 0,6 are shown.

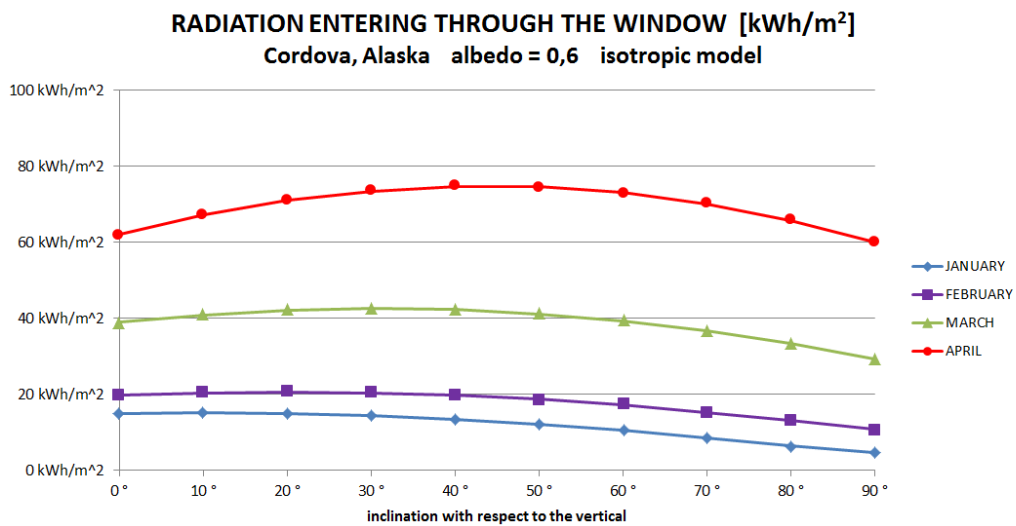


Figure 1.24 Entering radiation in function of the inclination of the window for Cordova, with an albedo of 0,6 and considering an isotropic model of the diffuse radiation, since January until April

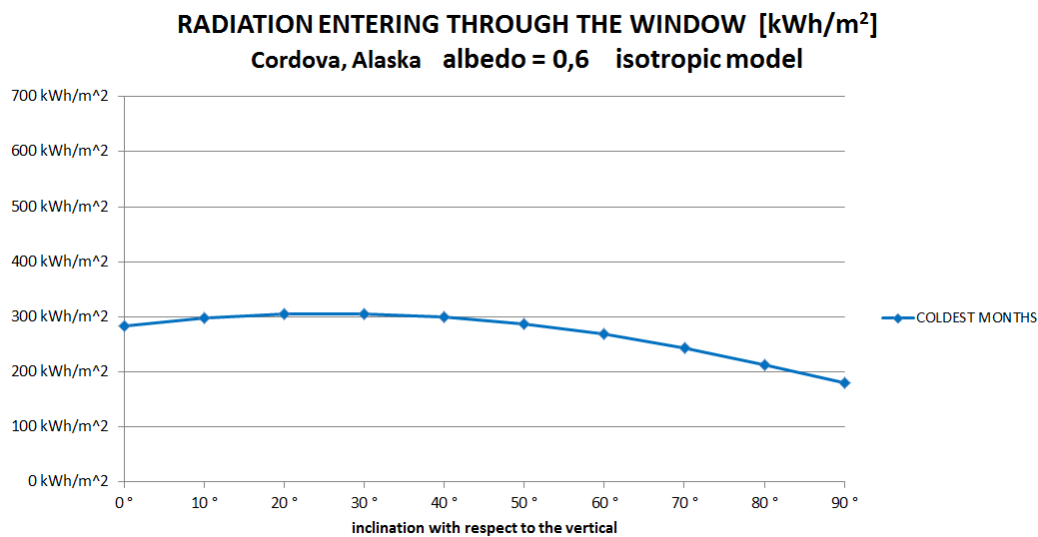


Figure 1.25 Total entering radiation in function of the inclination of the window for Cordova, with an albedo of 0,6 and considering an isotropic model of the diffuse radiation, during the coldest months (September – April)

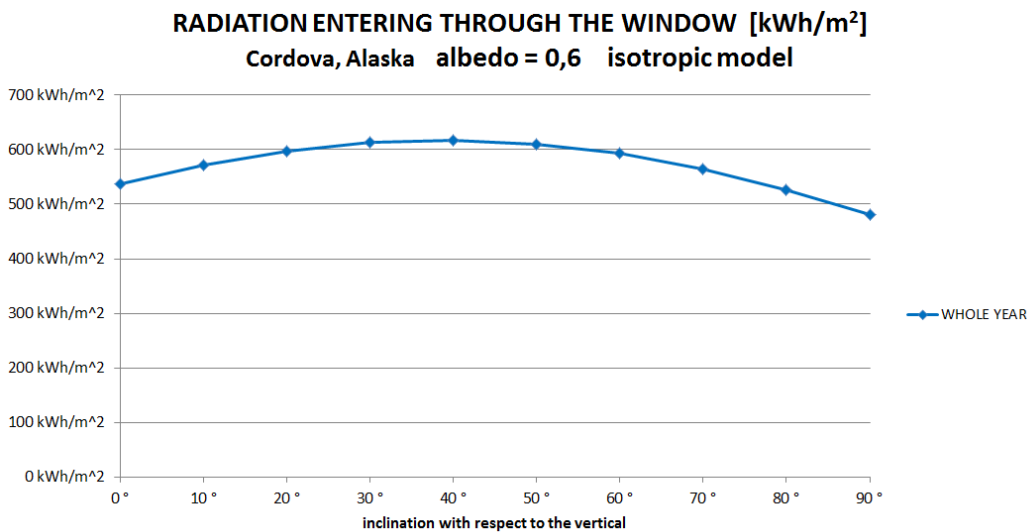


Figure 1.26 Total entering radiation in function of the inclination of the window for Cordova, with an albedo of 0,6 and considering an isotropic model of the diffuse radiation, in the whole year

With higher albedo values the convenience of the lowest angles increase. Obviously the albedo of the ground has no importance for the horizontal windows facing the sky, because for them the view factor ground-window is considered equal to 0.

Because of the importance of the diffuse radiation in Cordova, calculations were made also with the use of the Perez model. The obtained results are presented in the following figures.

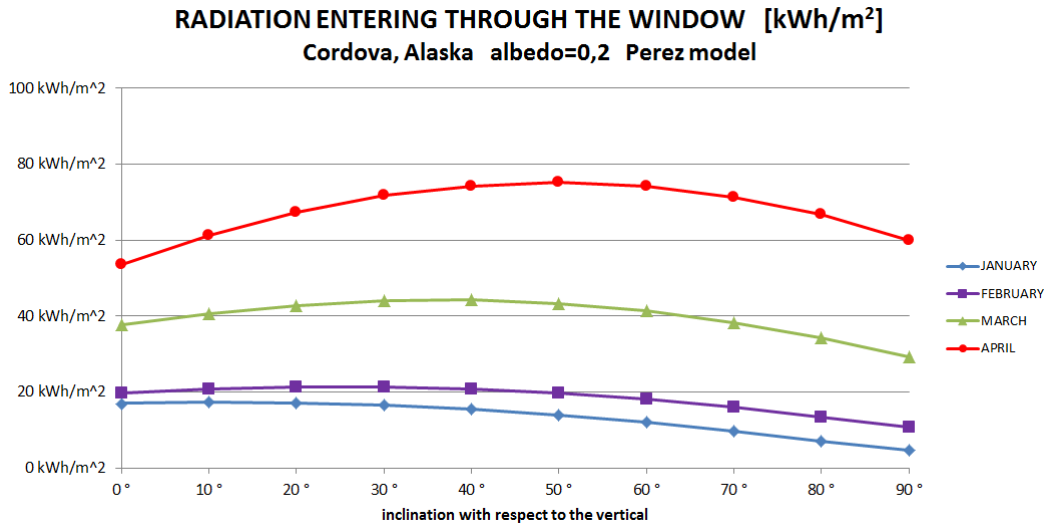


Figure 1.27 Entering radiation in function of the inclination of the window for Cordova, with an albedo of 0,2 and considering the Perez model of the diffuse radiation, since January until April

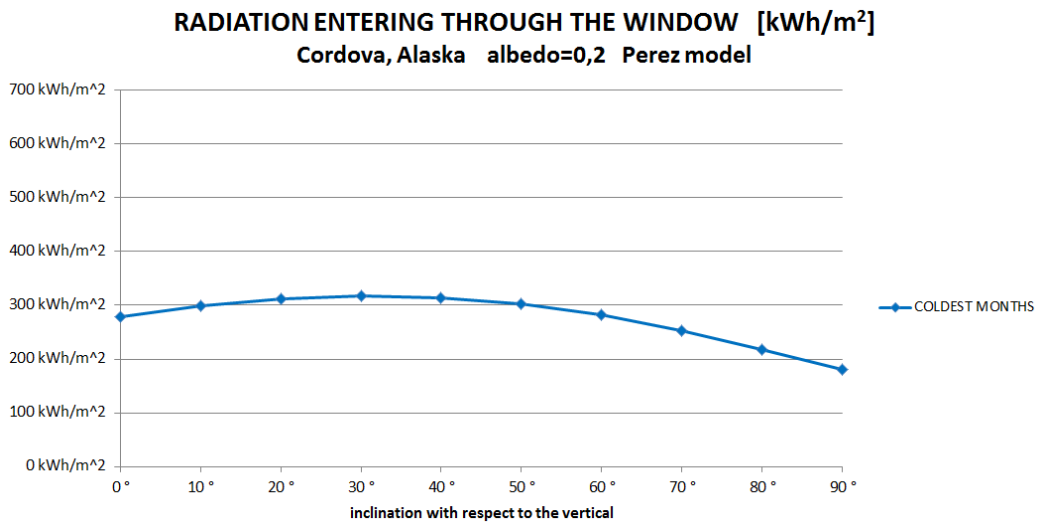


Figure 1.28 Total entering radiation in function of the inclination of the window for Cordova, with an albedo of 0,2 and considering the Perez model of the diffuse radiation, during the coldest months (September – April)

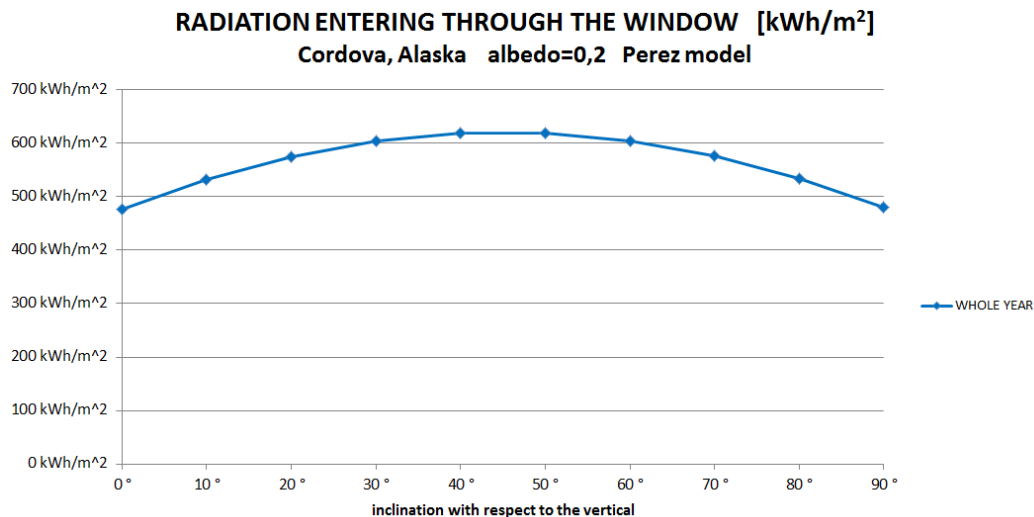


Figure 1.29 Total entering radiation in function of the inclination of the window for Cordova, with an albedo of 0,2 and considering the Perez model of the diffuse radiation, in the whole year

With the Perez model the solar radiation values are higher⁶, particularly for the lowest inclinations with respect to the vertical, but the curves are similar, also for a geographical location where the diffuse radiation is very important. The peaks are a little more in correspondence of low angles, but for an albedo of 0,2 both with the isotropic model and with the Perez model the maximum entering radiation is for an inclination of 30° considering the coldest months and for an inclination of 50° considering the whole year.

The Table 1.3 summarizes what ranges of the inclination angles are advisable.

Table 1.3 Ranges of inclination angles which maximize the entering solar radiation

Locality	Latitude	Advisable inclination angles	
		albedo 0,2	albedo 0,6
Bolzano, Italy	46°29' N	30°÷40°	20°÷30°
Cordova, Alaska, USA	60°30' N	30°÷50°	20°÷40°

⁶ Gueymard, C.A. (2009) states: “The results (...) clearly indicate that the isotropic approximation underestimates systematically” the measured radiations on tilted surfaces.

1.3 Sunspaces

Sunspaces (also known as “bioclimatic greenhouses” or “conservatories”) are a particular passive solar system. If it is an actual living room it can be considered as a system with direct gain. If it is not used commonly by the building inhabitants it can be considered as a system with indirect gain. Generally the sunspaces are used by the building inhabitants but because of their particular characteristics they are used in different ways than normal rooms. They can be considered as systems with “semi-direct gain”.

Sunspaces are not heated and therefore a physic division, which can be permanent or removable, from the mechanically heated spaces is advisable.

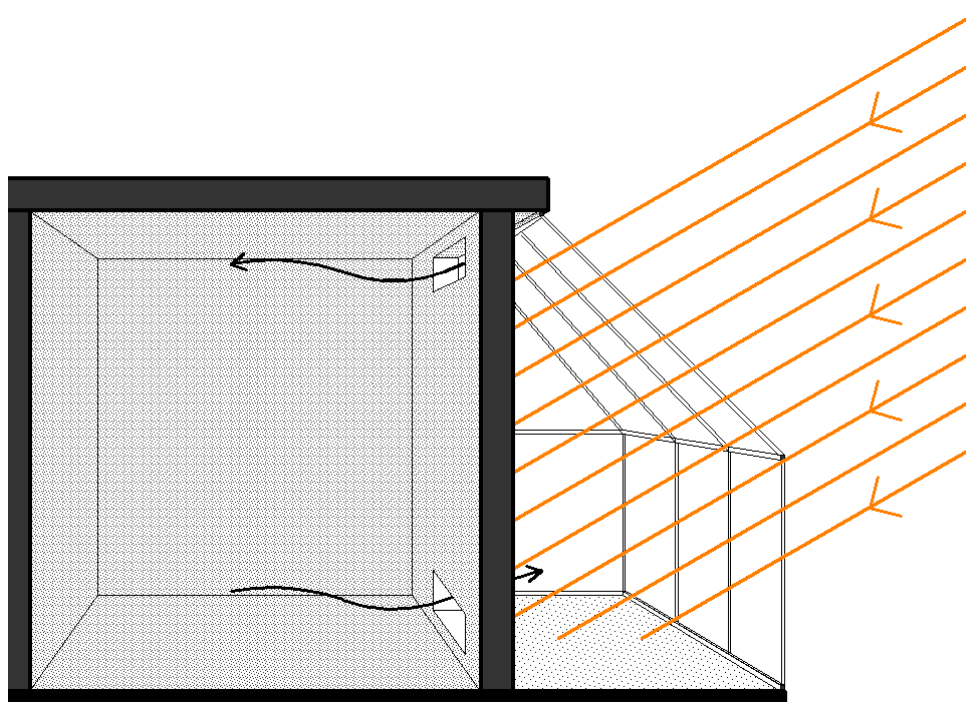


Figure 1.30 Schematic representation of a sunspace

Design of a sunspace consists of making proper choices concerning different aspects: shape, dimensions, relationship between sunspace and building, properties of glazed elements (e.g. thermal transmittance and optical properties), properties of opaque elements (e.g. thermal transmittance and thermal inertia), position and openings area, and so on. A more detailed overview of the main aspects of the bioclimatic design of sunspaces is presented in Chapter 6 “Guided procedure to the proper design of sunspaces”.

Management of a sunspace consists of positioning shading devices, of controlling air flows (opening and closing windows between external environment and sunspace and between sunspace and inner rooms/areas, opening/closing ventilation pipes) and of moving the night insulation, if it is present (in order to decrease losses in absence of solar radiation or with a too low solar radiation).

Both design and management of sunspaces must consider the relationship among studied

building (geometry, thermal properties of the structures, equipment...), occupants' habits (occupation schedules of rooms, internal gains, management of devices...), and external environment (weather data and exposure).

In a sunspace the function of heat storage can be carried out by three different elements (they can have that function together, at the same time):

- By the wall which separates the sunspace from the internal environments.

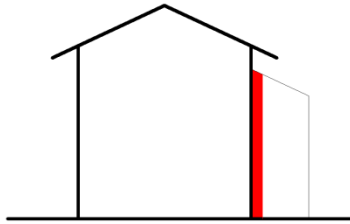


Figure 1.31 Thermal inertia on the wall

- By a specific element which is placed within the sunspace. Water tanks can be particularly effective because of their thermal inertia.

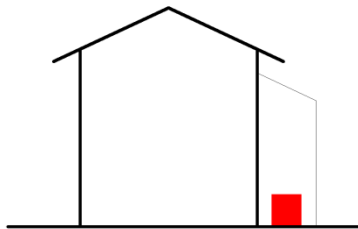


Figure 1.32 Thermal inertia as specific element within the sunspace

- By the floor slab. The behaviour of such an element depends on the position of the insulating materials and of the materials which provide thermal inertia.

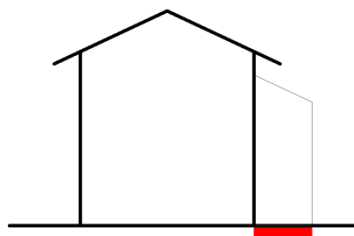


Figure 1.33 Thermal inertia on the floor slab

Thermal masses which are not directly exposed to solar radiation begin to absorb heat only after the air of the sunspace increases its temperature and they are called “secondary”.

In the study of the behaviour of the elements which provide thermal inertia the designer has to consider extents of the involved surfaces, depths and thermal properties (thermal conductivity, density, specific heat) of their layers, colours and surface finishes, exposure to solar radiation (when and how much are they exposed?), and so on. The design of elements having thermal inertia must have as goal the obtainment of attenuation of the temperature oscillations in order to optimize the system from the point of view of energy saving and thermal comfort. To evaluate in a precise way their behaviour a dynamic calculation is advisable.

During the winter nights an additional insulation is opportune. In fact, when there is no more solar radiation the temperature of the sunspace decreases and the losses from the internal environment increase (supposing that the internal environment is at the set-point temperature). The heat dispersions towards the external environment, which happen to the air through convection and to the sky and to the external surfaces through long-wave radiation, can be reduced by a movable insulation. In Figure 1.34 two solutions are presented: in the solution A during the night additional insulation is on the wall between the sunspace and the internal environment, in the solution B on the external envelope of the sunspace.



Figure 1.34 Schematic examples of additional insulation during the night

Generally the solution A is preferable from the point of view of heating requirements, while the solution B is preferable if a higher temperature within the sunspace is desired. The solution B can be better also from the energy point of view if there is often the risk of formation of frost on the sunspace window. In fact, if there is frost on the window in the morning the solar radiation does not enter the sunspace, but it becomes latent heat for the frost.

The usefulness of a sunspace is particularly evident during the winter season. During the warm season the presence of a sunspace, if it is not properly shaded and ventilated, can be counterproductive because it can cause overheating. Nevertheless, a proper design can exploit sunspace within a natural ventilation system also during the summer season. From the point of view of energy requirements, increasing the night ventilation during the summer can be very useful and the sunspace can be used as wind tower or to obtain the chimney effect.

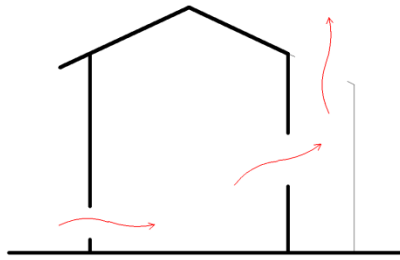


Figure 1.35 Cooling by ventilation during the summer nights. The internal temperature is higher than the external one and therefore the internal air is lighter than the external one. Hence the inlet for the air is on the lower part of the building and the outlet is on the upper part of the sunspace in order to increase the chimney effect. To evaluate the efficacy of such a solution, considering also the fluid-dynamic resistances, a Computational Fluid Dynamic calculation should be made.

During the summer the shading is necessary when there is solar radiation. It is more efficient if it is placed on the external side. Nevertheless during the night removing it is advisable, because thus the radiative exchange with the sky increases.

During the intermediate months the values of the solar radiation on surfaces can be particularly high. Therefore unwanted overheating can take place in those periods, when there are moments when heating is necessary and other moments when it is not necessary. The paragraph 1.1 “Overview to passive solar systems” explained that among the elements of a passive system there is the control. It is plain that in the context of a proper management the conditions of shading systems and of openings have to change on the basis of the requirements of the inhabitants and of the conditions in the internal rooms and in the external environment (weather conditions, seasonal cycle, night/day cycle, and so on). Because of the complexity of the problem, an automation system (also known as “domotic system”) can be useful (devices are managed by actuators, connected into a network where also sensors are present). For a sunspace the sensors could monitor the presence of people (in case of presence, strategies to improve the comfort level would be activated), the solar radiation, temperatures in the sunspace, in the internal rooms and in the external environment. The actuators could control shading systems and openings, both between the sunspace and the external environment and between the sunspace and the internal environment.

2. Literature overview

2.1 General considerations

In a research work the overview of the state of the art is necessary to understand what was already studied, what conclusions the previous researches reached, what tools they used, what subjects need to be further investigated, and so on.

The passive solar systems are subject of research for more than 30 years. In fact, for example, a general presentation of the passive solar systems is available in Mazria, E. (1979). In the introduction of the Italian edition the architect Sergio Loss defined the Mazria's book "*the first completely dedicated to the design of passive buildings handbook which systematically deals with all the problems concerning the construction of that kind of buildings*". It illustrates the main concepts at the basis of passive solar systems and it divides the passive systems in different types, amongst which are sunspaces. An important part of the book concerns "design patterns", which are forms presenting the different phases of the design of passive solar systems. They contain empirical rules which could be useful for the designers in choosing general building characteristics, type of passive systems, details of different types of passive systems, strategies about their management.

Steven Winter Associates (1998) presents functioning principles of sunspaces, rules of thumb for dimensioning, different solutions for the design and for the control strategies, constructive details.

Hestnes, A.G. et al. (2003) highlight an important concept:

"Because higher temperatures are acceptable in sunspaces, more solar energy can be collected than comfort or glare would allow in a sunlit living space."

Additionally, they present the energetic reasons of the construction of sunspaces when they illustrate three ways sunspaces can be used as part of an energy design:

"as a sun-tempered buffer space to passively reduce heat losses of the building envelope, (...) as a pre-heated air supply for ventilation of a house, (...) as a heat source for a heat pump."

The influence of design parameters and management strategies on the energy requirements (considering both heating and cooling) in Jordanian conditions was analysed through dynamic simulations by K.M. Bataineh and N. Fayez (2011).

2.2 Case studies

After having presented different technologies, both passive systems and active systems, Hestnes, A.G. et al. (2003) present buildings which implement those technologies and which have a high energetic performance. In particular, they propose examples for every way sunspaces can be used.

Meroni, I. et al. (1991) constructed 3 test cells measuring 2.80m x 2.80m x 5m. On the three walls facing south three different systems were applied: a hollow brick wall with an insulated air gap, a double glazing, and a system consisting of a similar window with an attached sunspace. They defined precise management rules. For the ventilation between the sunspace and the test cell they considered both passive and mechanical solutions. After a monitoring campaign they compared temperatures and heating requirements relative to the three solutions. The results highlight the importance of the weather conditions on the performance (obviously the sunspace is the solution which is more influenced by the weather, see Figure 2.1).

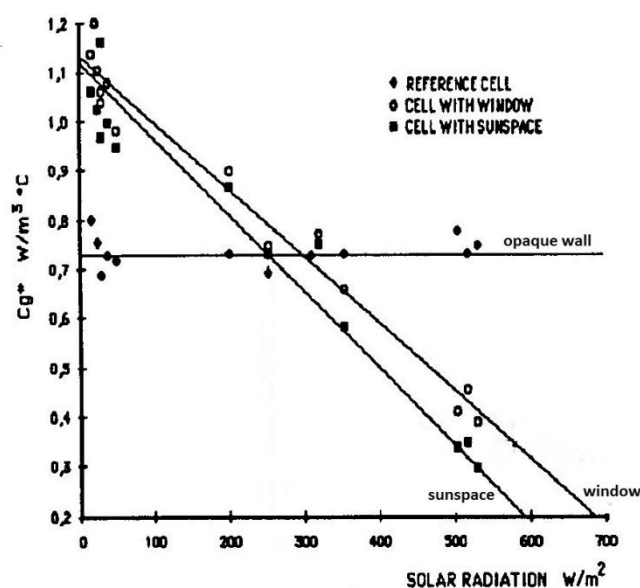


Figure 2.1 On the horizontal axis: solar radiation. On the vertical axis: energy contribution of the active (mechanical) heating system and of the mechanical ventilation system to maintain the prefixed conditions divided by the temperature difference between internal and external environment and by the volume of the test cells. The points relative to the three solutions are fitted by three relative straight lines. Source: Meroni, I. et al. (1991)

The two publications Fredlund, B. (1989) and Wall, M. (1996) are results of research works at the Department of Building Science of the University of Lund (Sweden). Fredlund presents the results of a monitoring campaign and of calculations concerning blocks of flats in a Swedish locality. The analysed buildings have two storeys and glazed sunspaces are present on their south facades. The measurements and the calculations concern both temperatures and heating requirements. The calculations were developed both through semi-stationary (the semi-stationary methods can be called also “quasi-steady-state methods”) and dynamic models, created through BKL and DEROB respectively. The functioning of DEROB, which has been created by that research group, is illustrated in the report. A comparison between calculation results and monitoring data is presented. Wall, M. (1996) deals very deeply with different aspects relative to glazed spaces: examples from the architecture history, design tools,

evaluation of different design possibilities, monitoring and analysis of a big variety of real cases situated in Sweden. In particular, possibilities and limitations of design software available at that time were analysed and a stationary method for the calculation of temperature mean values in sunspaces and of energy requirements is proposed as preliminary tool for the choice among different solutions. For the glazed space Wall, M. (1996) defines the “solar collection property S”, which is the ratio between the solar gain which contributes to glazed space temperature increase and the total solar gain entering glazed space (of the transmitted radiation through the glazed envelope some will exit directly, some will be reflected outwards, some will pass into the surrounding built environments and some will be absorbed inside the glazed space increasing its temperature). Because calculating S is not easy, particularly in the context of a stationary method, Wall, M. (1996) calculated its dependence on different parameters through the dynamic software DEROB-LTH, *“which requires a geometrical description of the building and makes use of this for an accurate calculation of solar radiation. The calculations demonstrate that the type of glazed space, the transmission properties of the glazing and the absorptivity of the surfaces inside the glazed space have a great significance for the proportion of the transmitted solar radiation which is retained inside the glazed space. On the other hand, the geographical position, orientation and time of the year are of less importance”* (p. 106). The obtained relationships between S and the considered input parameters can be considered within the simplified stationary method.

Using both stationary and dynamic calculations Wall, M. (1996) studied the influence of design on internal climate (comfort analysis) and energy requirements. Among other aspects, the possibility of using the glazed space as part of the ventilation system, considering different ventilation schemes, was analysed.

Wall, M. (1996) concludes that:

“The results of the case studies show that the energy contribution from the glazed spaces is rather small when they are used as buffer zones or to preheat the supply air to the buildings. This reduction in energy for space heating in adjacent building has been less than 10%. The main reason for this is that solar gain can be significantly reduced if air leakage is high. A high air leakage will reduce the temperature level and also increase heating requirements.” (p. 385)

However, considering the results of the researches of the University of Lund, which were developed in Sweden, we have to consider that they are not directly transferable to central or south European conditions, because of the very important difference among the relative climates.

Kunz, M. (1990) presents two cases of Swiss houses having passive solar systems. One has also a sunspace. The air of the sunspace is distributed in internal spaces through a mechanical system, therefore Kunz highlights that it cannot be considered a completely passive system, but rather a “hybrid system”. Closing the openings the ventilation can be stopped. The fans for the air distribution are controlled by a system which considers the temperature difference between

the sunspace and the internal rooms. The building was object of a measurement campaign. The Figure 2.2 shows that the temperature in the sunspace is more variable than in other adjacent internal environments.

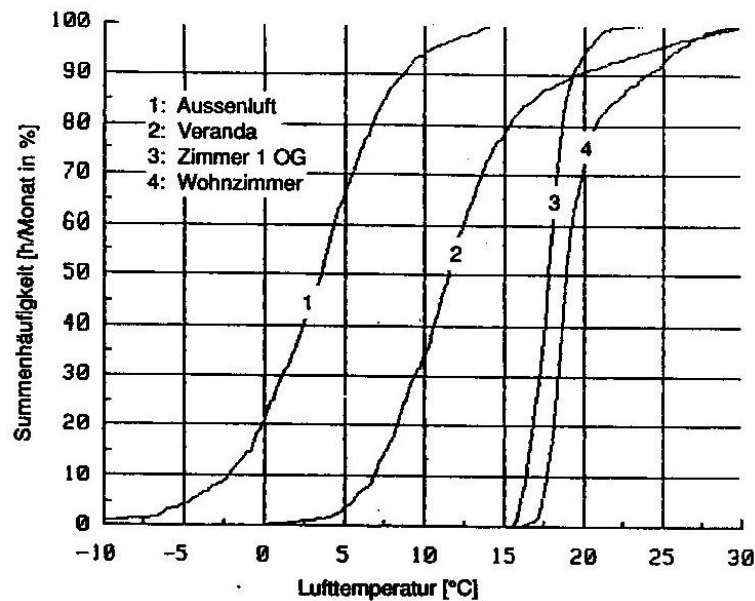


Figure 2.2 Temperature cumulative frequency in the external environment (n. 1), in the sunspace (n. 2) and in some adjacent internal environments during the winter 1986/1987
Source: Kunz, M. (1990)

Through the calculation method NUTZENERGIE Kunz, M. (1990) has calculated an energy saving due to the presence of the sunspace of the 34%.

2.3 Calculation methods

The calculation of sunspace performance is a subject that has been studied during the present research (see Chapter 3 “Calculation methods”). The Chapter 6 of Sodha, M.S. et al. (1986) deals with calculation methods for passive solar systems and it divides them in three categories (p. 193):

1. *approximate methods*: “they are used to find out the average energy requirements of a building for heating or cooling purposes, and are helpful during the planning stage of the project. The methods like the degree day and steady state methods are the examples of this kind”. Examples of quasi-stationary methods (“quasi” means that there is a “utilization factor” in order to estimate the effect of the dynamic phenomena) are the unutilizability method, which is illustrated in Duffie, J. A. and Beckman, W.A. (1980), the Method 5000, which was invented for Mediterranean bioclimatic buildings and it is illustrated in Colombo, R. et al. (1994) and the ANNEX E “Heat transfer and solar heat gains of special elements” of the European technical standard EN ISO 13790:2008 “Energy performance of buildings - Calculation of energy use for space heating and

cooling”. They estimate how much the solar energy contributes to the energy requirement;

2. *correlation methods*: the relationship between the different characteristics and the energy performance is expressed in terms of correlation coefficients. Often “*the correlations are derived using data developed from hour by hour computer simulation*”;
3. *analytical methods*: they are based “*on the solution of heat conduction equation with appropriate boundary conditions*”. Despite the name “analytical” Sodha, M.S. et al. (1986) considers also the numerical methods as part of that category.

Sodha, M.S. et al. (1986) illustrates some methods particularly deeply, from the mathematical point of view as well.

A lot of aspects of passive solar buildings are presented by Athienitis, A.K. and Santamouris, M. (2002), with particular attention to calculation methods. To model sunspaces they propose an equivalent network constituted by nodes, thermal resistances and thermal capacities (lumped parameter model). It is a non-stationary model in which thermal inertia of the wall separating inner environment and sunspace is considered (Figure 2.3).

An approximation of the temporal derivative by finite differences method is proposed and energetic balances of nodes whose temperatures are unknown are inserted in a system. Knowing the external conditions and the relevant thermal properties, after having imposed the initial temperatures it is possible to calculate the temperatures relative to the following time steps.

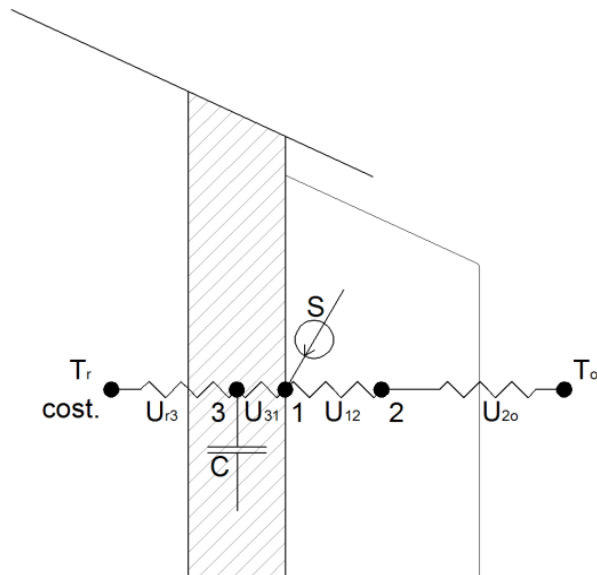


Figure 2.3 Model by Athienitis, A.K. and Santamouris, M. (2002). Unknown quantities are temperatures in the nodes 1, 2 and 3

The work of Duffie, J. A. and Beckman, W.A. (1980) is divided in three parts: the first one is

theoretic and deals with the physic laws of thermal radiation, giving particular attention to transmission, absorption, reflection and storage of solar radiation in different contexts, the second part regards the applications, both passive applications and active ones, both for heating and for cooling, the third part regards the design methods, with calculation examples. A chapter illustrates how we can evaluate the solar systems from the economic point of view.

Duffie and Beckman were part of the research group of the University of Wisconsin-Madison which created TRNSYS. TRNSYS 16 models attached sunspace with the “Type 37” (the TRNSYS module modelling sunspace has had during the time different versions). Thermal conductances are calculated from user supplied geometry, thermal properties and heat transfer coefficients.

“The calculation of the sunspace interior infrared conductance uses net exchange factors. This involves using the view factors between the various nodes. (...) The glazing and air nodes are assumed to have negligible thermal capacity” (Figure 2.4).

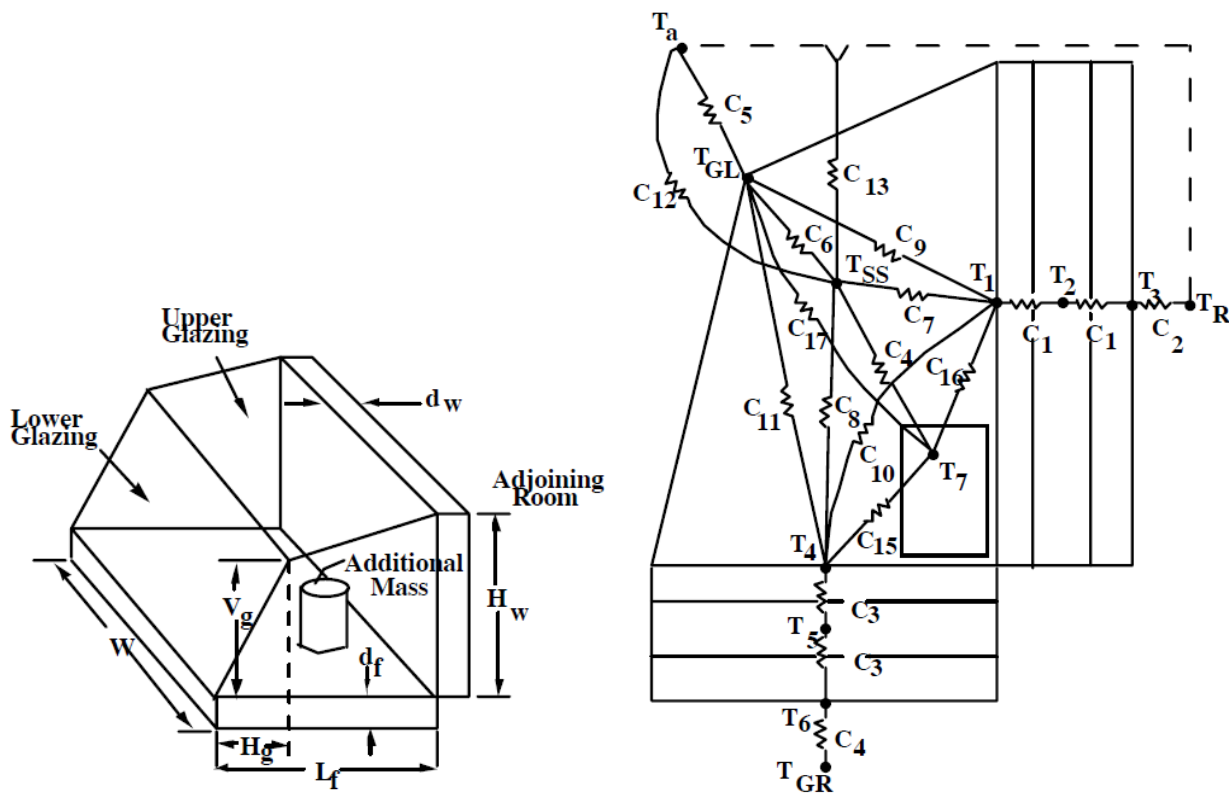


Figure 2.4 Sunspace geometry and conductance network in TRNSYS 16

Voeltzel, A. et al. (2001) explains that in simulating highly-glazed spaces “erroneous results can be explained by the poor modelling of some physical phenomena that is usually sufficient in conventional buildings. (Note that these building simulation codes were originally developed to study buildings with ordinary window sizes and volume)”.

“This is, namely, that there are a number of simplifying assumptions regarding shortwave (SW) and longwave (LW) radiation heat transfer that cannot be applied to highly-glazed spaces. A significant fraction of the solar radiation entering a large highly-glazed room can be lost by direct transmission to the outside, direct transmission to other zones of the building, or diffuse retransmission to the outside.” (Figure 2.5). Actually, the reflection to the outside is not necessary a perfect diffuse radiation, but it is generally modeled so (otherwise adopting a more realistic model would be really complicated).

Moreover, “standard thermal building simulation codes generally assume that a room can be treated as a single zone with homogeneous air temperature. Clearly, this does not apply to large highly-glazed spaces”.

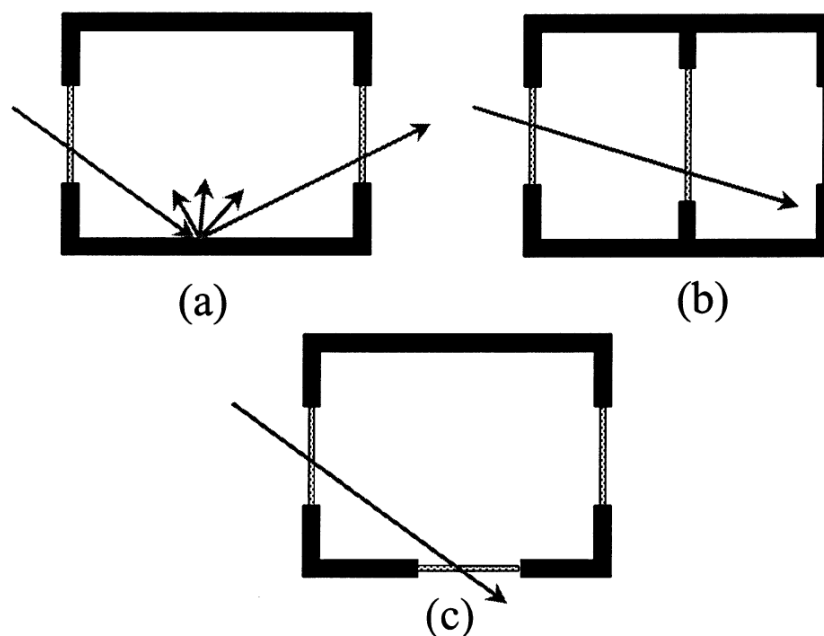


Figure 2.5 (a) Reflection to the outside (b) Transmission to other zones (c) Direct transmission to the outside Source: Voeltzel (2001)

The authors present AIRGLAZE, a simulation code which they developed expressly for large highly-glazed spaces. AIRGLAZE considers air temperature diversification within a single zone through a model which, unlike the majority of Computational Fluid Dynamic software, is not based on Navier-Stokes equations and it is suitable for dynamic simulations. AIRGLAZE takes the multiple reflections, direct retransmission, reflection to the outside and transmission to other zones into account. It assumes that the reflection on the interior surfaces of the building is diffuse. Longwave radiation is considered as well. The validation of two models with empirical data is presented.

Another detailed model is presented by Mottard, J.M. and Fissore, A. (2007). The internal

radiation is accurately considered through a surface discretization. In order to save calculation time, for the air temperature only one node is considered. The model was validated through comparison with empirical data from an opportunely constructed full-scale sunspace with adjacent room. Air and surface temperatures and heat fluxes were considered. The new model was used for a sensitivity analysis which *has shown that the solar absorptance and the convective heat coefficient of the wall* (the wall between the sunspace and the internal room) *have a strong influence on the results*. Heat capacity has less influence.

Professor Giuseppe Oliveti and his research group, at the University of Calabria, developed some research works in order to provide more accurate calculation tools for the solar gains, for the semi-stationary methods as well. Oliveti, G. (2011) states that:

“In simplified models, entering solar radiation through glazed surfaces is commonly held to be completely absorbed by the cavity surfaces (black body cavity hypothesis). This formulation overlooks the solar irradiation fraction which is reflected outside by the internal surfaces.”

We have to precise that for sunspaces also the technical standard EN ISO 13790:2008 considers that not all entering radiation contributes to sunspace temperature increase. In fact, the equation (E.3) of ANNEX E to calculate the solar radiation absorbed by the sunspace does not consider the solar radiation entering through the external envelope, but the sum of solar radiation contributions absorbed by every internal surface. However, the calculation presents some difficulties, e.g. because calculation of shading factors for every internal surface is often complicated. The technical standard assumes, as approximation, that *“the absorbing surfaces are all shaded in the same proportion by external obstacles and by the outer envelope of the sunspace”*. From the point of view of the calculation of the absorbed radiation, the works of professor Oliveti are important investigations. Oliveti, G. et al. (2008) calculated with the dynamic simulation software DEROB-LTH the solar energy absorbed by a parallelepiped environment, with different hypotheses of glazed surfaces. The solutions with the largest glazed surfaces reproduce sunspaces. DEROB-LTH calculates the solar radiation transmission coefficient of the glazed surfaces by the application of the Fresnel equations and of the Snell laws. Every surface is discretized to determine the area directly hit by solar radiation. As approximation, the direct solar radiation reflected by the internal surfaces is considered as diffuse radiation. Through dynamic simulations the authors have calculated the monthly absorption coefficients of the sunspace, which are defined as the ratio $\frac{Q_{ab}}{Q_{tg}}$ of the solar energy absorbed by the internal surfaces of the room Q_{ab} and the solar energy entering through the glazed surfaces Q_{tg} that separate it from the outside. The absorption factors have been calculated for different possibilities of latitude, exposure, month, percentage and orientation of the glazed surface. On the basis of the results of dynamic simulations, exponential interpolations in no-dimensional forms which regard the main involved physical quantities were obtained.

In Oliveti, G. et al. (2011) a similar work is presented for windows.

According to EN ISO 13790:2008 (paragraph 11.4.2), for transparent surfaces the total solar energy transmittance g_{gl} can be considered as

$$g_{gl} = F_w \cdot g_{gl,n} \quad (2.1)$$

where $g_{gl,n}$ is the solar energy transmittance for the glazing and it shall be calculated in accordance with the relevant standard on optical properties of multiple glazing (EN 410:2011) and F_w is a correction factor for non-scattering glazing. The European standard states that in the absence of national values, the value for the correction factor is equal to 0,9. The Italian and the German standards do not add anything else concerning F_w , but the calculation of F_w is extremely important if the solar gains are relevant (and for sunspaces they are fundamental). Oliveti, G. et al. (2009) calculated more precise monthly values of F_w for Italian localities considering a double glazing with defined characteristics. The calculation was developed with the Type 56 of TRNSYS. The greatest deviations from the 0,9 which is indicated by the technical standard are for the south exposure, both for the warmest months (values between 0,75 and 0,80) and for the coldest months (values between 0,97 and 0,99). For the coldest months because of the imprecision of the technical standard for south surfaces there is a monthly underestimation of the solar gains of the order of $15 \div 30 \text{ MJ/m}^2$ and for horizontal surfaces an overestimation to the order of $10 \div 20 \text{ MJ/m}^2$. For every month and every exposure the F_w values have been interpolated linearly as function of the latitude, with a good precision. The PhD thesis Pfrommer, P. (1995) presents an analysis of the solar transmission through different kinds of windows and of the distribution of solar radiation within the relative room, proposing a new calculation method. The new method is used in order to give design indications, with particular attention to energy requirements and thermal comfort. The Pfrommer's work deals with a lot of design aspects (geometry, ventilation, windows' dimensions, properties..) comparing the conclusions available in literature with the results of the new calculations. For example, considering a heated room modelled with the new calculation method, in absence of ventilation between the sunspace and the internal environment: *"The attachment of the base-case conservatory to south window yielded the same reduction of the energy demand (13.5%) in Sheffield (UK) and North-Württemberg (Germany). (..) For Denver (USA) the energy saving was predicted to be 16% (..). The time-of-usability ($T > 15^\circ\text{C}$) of the conservatory in North-Württemberg was 58.4% of the annual occupied hours. It was only slightly in Sheffield (61.6%). However, it was significantly higher in Denver (78.6%)."*

2.4 Scale models

Prototypes (or scale models) can be useful when there is not good precision, or there is not enough confidence, in the modelling. In the case of sunspaces the problems in modelling regard

particularly three-dimensional effects and interaction between thermal and fluid-dynamic phenomena. Turns, S.R. (2006) introduces the subject very clearly:

“For many devices, particularly those of large scale, construction and testing of full-size prototypes as a part of the design process is not practical. In such cases, small-models, geometrically similar models are used to provide the information needed to improve and evaluate the design.” (p. 588)

Chapter 8 of that book focuses on subjects which are important in order to deal with scale models: the concept of similarity, dimensionless parameters and equations, the Buckingham Pi Theorem.

Simpson, J.R. and McPherson, E.G. (1997) present the utilization of a scale model for the evaluation of the thermal behaviour of buildings in real weather conditions. The study deals with temperatures and air-conditioning electrical use in warm conditions. Comparisons among three different 1/4-scale models having different roof properties were developed. Some arrangements have the goal to be as close as possible to the thermal similarity among scale models and full-sized buildings:

“inside thermal mass was scaled down in proportion to the ratio of model/house surface area $(1/4)^2$ instead of volume $(1/4)^3$. (...) Interior thermal mass added to each building compensated for effects of increased surface area to volume ratio of scale model compared to full-sized buildings (...) 1:1 ratio of wall thickness allowed conductivity and heat capacity to be the same. (...) Identical air-conditioning units (...) were used.”

The authors have not considered the impact of heat transfer through thermal bridges, which varies with the linear length or, for punctual thermal bridges, is theoretically independent on geometrical dimensions. After a monitoring campaign and data analysis Simpson, J.R. and McPherson, E.G. (1997) concluded that:

“Comparison of these results with a previous simulation study showed good agreement, confirming the measured results and the scaling procedure used to ensure thermodynamic similarity between the models and full-sized buildings. This indicates that results from scale models can be successfully extrapolated to the full-size scale, at least for the current set of experimental conditions. Giving the non-linear dependence of heat gain on atmospheric temperature and wind structure, additional research will be necessary to completely establish the range of relationships between scale model and full-sized buildings, their environment, and cooling and heating load.”

Unfortunately, except these statements the article does not examine the issue of the variation of the thermal-energetic quantities due to the scale variation.

Grimmer, D.P. (1979) and Grimmer, D.P. et al. (1979), on the basis of modeling of passive solar systems as networks of thermal resistances and thermal capacities, assert the importance of the normalization of thermal capacities and thermal resistances to the glazing area of the passive systems. The first article deals with theoretical considerations, the latter deals with data analysis.

“Distorted models that present real-scale values for data collected” were used, i.e. the results, in particular the temperatures, are not expressed in non-dimensional form, but they should be directly transferred to the full-scale cases. Grimmer, D.P. (1979) considers also the ventilation between the Trombe wall cavity and the internal environment, the air infiltration, the thermal bridges and the shading, but without experimental validations (“rather simplistic arguments have been used, and experimental confirmations are necessary”). While data analysis is present in Grimmer, D.P. et al. (1979), which analyses the case of a storage wall placed between the window and the internal environment (see Figure 2.6).

No ventilation between the environments was possible (not even between the internal environment and the air cavity between the wall and the glass). A much greater insulation level was put on the lateral walls than on the other ones, in order to have through them a negligible flow. Those assumptions were made in order to have a case which is particularly easy to study and to model.

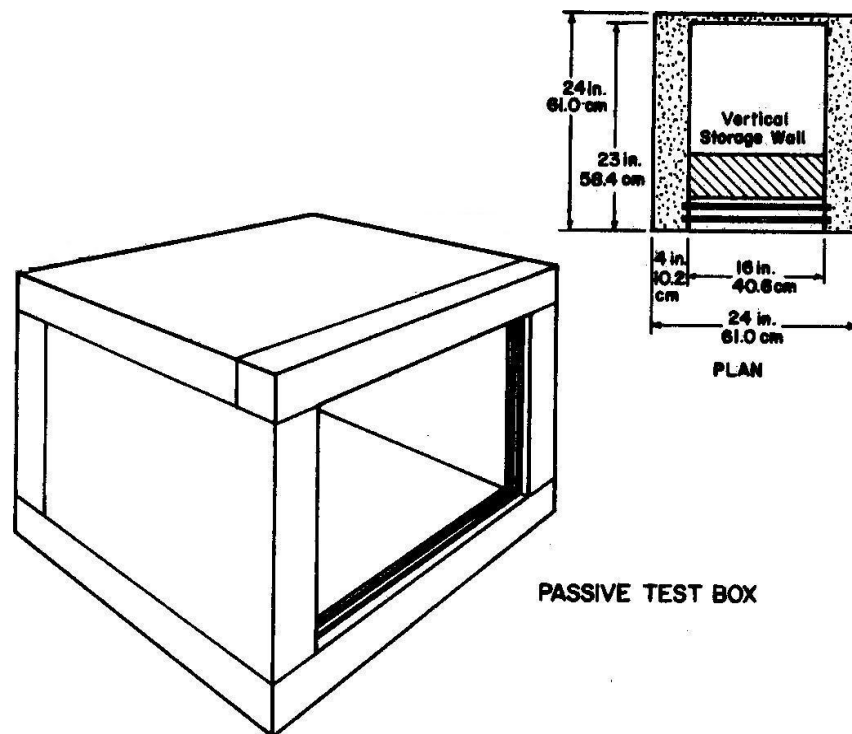


Figure 2.6 Scale model of a storage wall. Source: Grimmer, D.P. et al. (1979)

Dynamic computer models were validated by the authors. A comparison between a full-scale computer model and a real test box with smaller dimensions was made. In the two cases the normalized wall heat capacity and the normalized thermal conductance through the wall were the same and “The correlation between the test box and a modified test room simulation is encouraging”. The energy requirements were not considered (the experiment was in “free running” conditions) but the authors state that “The electrical energy produced by the heater could be monitored (e.g. in a scale model) and normalized to area of glazing” (in order to

translate the results to a full-scale case). Considering the other types of passive systems the article states:

“With the possible exception of roof-pond storage designs, the modeling with small test boxes is expected to be more difficult for these designs than for a simple storage wall behind vertical glass”.

3. Calculation methods

3.1 Introduction to calculation methods

The calculation methods for the energy performance of buildings and of their parts can be divided in two big categories (see the European technical standard EN ISO 13790:2008, pp. 15-16):

- *Quasi-steady-state methods* (or “semi-stationary methods”), *calculating the heat balance over a sufficiently long time (typically one month or a whole season), take dynamic effects into account by an empirically determined gain and/or loss utilization factor (...)* For heating, a utilization factor for the internal and solar heat gains takes into account of the fact that only part of the internal and solar heat gains is utilized to decrease the energy need for heating, the rest leading to an undesired increase of the internal temperature above the set-point. (...) The European Standard EN ISO 13790:2008 specifies in the category of quasi-steady-state methods a monthly and seasonal method for heating and cooling.
- *Dynamic methods, calculating the heat balance with short times steps (typically one hour) taking into account the heat stored in, and released from, the mass of the building.*

Obviously the dynamic methods can model in a more realistic way the real phenomena involved in the physical behaviour of buildings and HVAC plants and they provide more output data. There are, however, reasons because of which the quasi-steady-state methods are still used. In fact the quasi-steady-state methods require less input data, their utilization is easier, less time is needed to learn an appropriate utilization of them. Therefore they are typically employed by the building designers and generally they are what the local legislations require, e.g. to obtain the Energy performance certificate (for Italy, see Technical standard UNI/TS 11300:2008).

A reasonable approach to the calculation is the utilization of the quasi-steady-state methods in the early stage of the design, in order to have an idea about the quality of the first design hypotheses and to reject the worst ones, and the utilization of the dynamic methods in the definition of the final details, in order to produce an aware and accurate design. In particular, the dynamic methods can be useful in analysing the aspects in which the quasi-steady-state methods have not given adequate answers (e.g. for aspects concerning the thermal inertia).

3.2 Quasi-steady-state methods

The Method 5000 and the method presented in the ANNEX E of UNI EN ISO 13790:2008 are based on quasi-steady-state models (losses obtained by a stationary calculation and solar and

internal heat gains are reduced by a utilization factor that considers thermal inertia of building). The utilized equation is of the kind:

$$Q_{h,nd} = Q_{h,ht} - \eta_{h,gn} Q_{h,gn} \quad (3.1)$$

where

$Q_{h,nd}$ is the heating need

$Q_{h,ht}$ is the heat transfer from inside to outside (losses)

$\eta_{h,gn}$ is the gain utilization factor

$Q_{h,gn}$ is the total heat gain (typically solar radiation and internal gains)

Generally the quasi-steady-state methods are used with monthly calculations.

In the next paragraph only the calculations regarding sunspaces are showed. The logic of the calculation is presented in Figure 3.1. The losses through the sunspace are calculated considering the sunspace as common unheated space, i.e. like an adjacent space which is unheated but whose temperature is higher than the external one because of buffer effect. While the solar heat gains due to the presence of a sunspace have to be calculated in a different way than for common unheated spaces. The reasons are explained in the following. Those gains, like all solar gains, must be multiplied by the utilization factor.

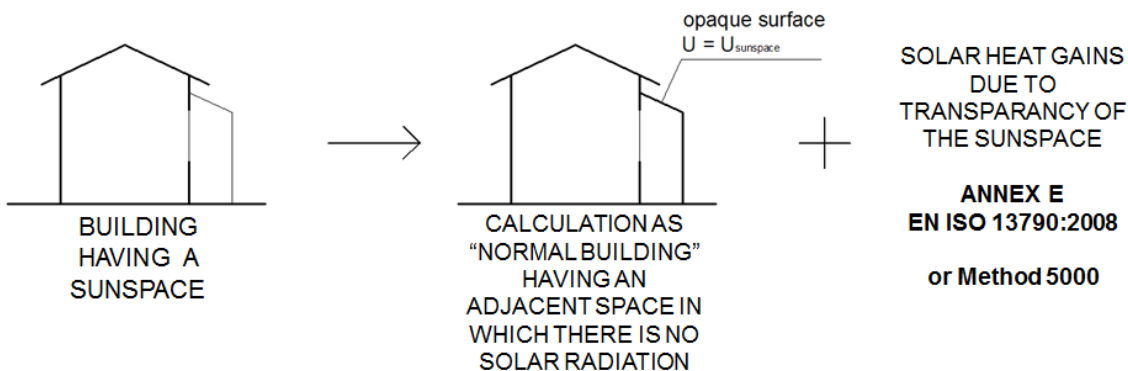


Figure 3.1 The logic of the calculation of the ANNEX E of EN ISO 13790:2008 and of the Method 5000

One goal of the present work is the improvement of the quasi-steady-state methods, also considering the results of the dynamic ones. The importance of this goal is highlighted considering that a lot of building designers utilize only the quasi-steady-state methods, in particular in a context, like the Italian one, in which the design offices have generally small dimensions.

From the point of view of the heat transmission the European technical standard EN ISO 13790:2008 considers sunspaces as general unheated adjacent spaces (paragraph “8.3.2.4 Heat transmission to adjacent unconditioned space”): we have to consider the decrease of the heat losses from the heated environment to the external one due to a buffer space having a

higher temperature than the external environment. From the point of view of the passive gain the behaviours of general unheated spaces and sunspaces are considered in different ways. Physically, we can consider a “general unheated adjacent space” as a close space which is adjacent to the heated space and whose windows towards the external environment are so small that the part of solar radiation which exits from it can be neglected. While the sunspace has a highly glazed external envelope and therefore “*The effective collecting area of a sunspace, which has in most cases several collecting areas, cannot be calculated in a simple way*” (EN ISO 13790:2008, paragraph 11.3.6). In fact part of the entered solar radiation does not contribute to the increase of the sunspace temperature, because of two possibilities:

1. it exits, directly or after reflections, from the sunspace to other environments (if it enters the heated space it is considered directly as a solar gain of the heated space, see Figure 3.2 a.; if it goes back to the external environment the solar radiation does not contribute to the building energy performance, see Figure 3.2 b.);
2. part of the heat absorbed by the opaque parts is not released to the sunspace air but it is conducted towards other environments (if the heat is conducted to the heated space it is considered directly as a solar gain of the heated space, see Figure 3.2 c.).

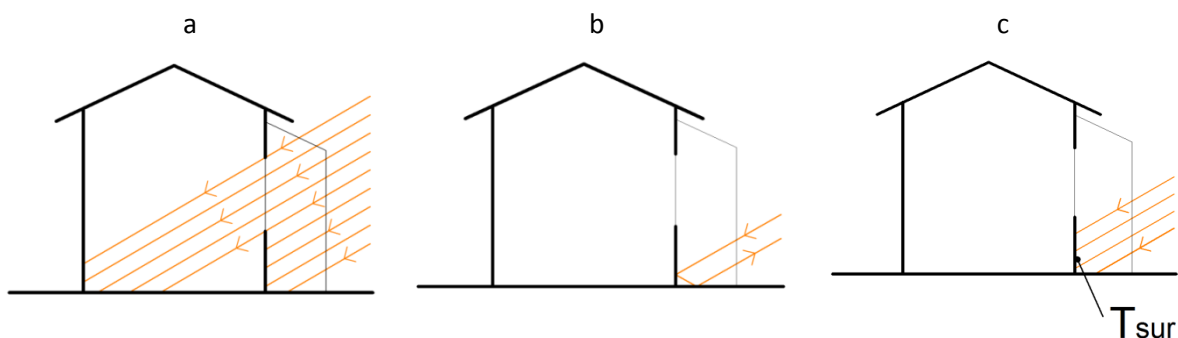


Figure 3.2 a. Part of the solar radiation enters directly the heated space; b. Part of the radiation is reflected to the external environment; c. Part of the radiation is absorbed by the opaque surfaces of the sunspace but it does not contribute to the increase of the sunspace temperature because it is conducted towards other environments.

Actually, those phenomena exist also for general unheated adjacent spaces, but they are neglected by the technical standard, because in that case the solar gains are not so relevant like for the sunspaces and because it is less probable that the solar radiation enters directly the adjacent spaces or exit after reflections.

Oliveti, G. et al. (2011) presents a study concerning the evaluation of the amount of solar radiation which is absorbed by an internal space, heating it. The paper defines the effective absorption coefficient of the indoor environment α_{cav} as the ratio between absorbed solar energy and entering solar energy

$$\alpha_{cav} = \frac{Q_{sol,in} - Q_{sol,out}}{Q_{sol,in}} \quad (3.2)$$

where the absorbed energy is calculated as the difference between the solar energy entering through the glazed surfaces $Q_{sol,in}$ and that reflected out of the cavity $Q_{sol,out}$.

The glazed fraction of the internal space is calculated as the ratio between the total glazed area $\sum_j A_{gl,j}$ and the total opaque area of the cavity $\sum_i A_i$

$$\psi = \frac{\sum_j A_{gl,j}}{\sum_i A_i} \quad (3.3)$$

Through dynamic simulations with the software TRNSYS they obtained graphs in which α_{cav} is function of ψ and of the absorption coefficient of the internal surfaces α_m . α_{cav} decreases if ψ increases and it increases if α_m increases. For a specific geometry and specific weather conditions, Oliveti, G. et al. (2011) states that if $\psi = 0,7$ then for absorption coefficient of the surfaces equal to 0,8 the absorption coefficient of the indoor environment is equal to 0,7 while for absorption coefficient of the surfaces equal to 0,2 the absorption coefficient of the indoor environment is equal to 0,45. That means that an important amount of the entered solar radiation exits back.

In conclusion, as the next paragraphs illustrate in a more exhaustive way, since the sunspaces need a more accurate calculation of the solar gains than normal unheated adjacent spaces, the technical standard EN ISO 13790:2008 dedicates them a specific part, the ANNEX E.

3.2.1 Method 5000

The documentation concerning the Method 5000 which was consulted is available in Zappone, C. (2009) and in Chapter 2 of VV.AA. (1992-1995) *Manuale di progettazione edilizia – Fondamenti, strumenti, norme*, vol. 2.

The method regards not only the sunspaces, but has versions also for other passive solar systems. The calculation of the utilization factor is very simplified, because it considers only the total mass of the elements which constitute the built environment (from the insulation towards the internal side), without considering, for example, their heat capacities. Like the technical standard EN ISO 13790:2008, it considers a constant set-point temperature throughout the cold period, both during the day and during the night.

As weather input it requires the global solar radiations on the glazed surfaces and the mean external temperatures.

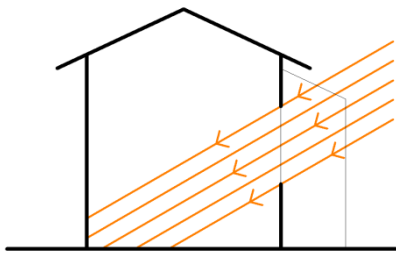
The method calculates the solar gain relative to the presence of the sunspace as the sum of four parts:

- A. solar radiation which enters heated space directly, passing through the glazed surfaces;
- B. solar radiation which is absorbed by the wall which divides the sunspace from the internal space causing an increase of the wall temperature;

- C. increase of the buffer effect due to the increase of the sunspace temperature because of solar radiation;
- D. reduction of ventilation losses, from the point of view of the heated environment, due to the increase of the sunspace temperature because of solar radiation.

The single contributions are calculated as following.

A. Solar radiation through the glazed surfaces Φ_{sdg}



The proposed equation is

$$\Phi_{sdg} = A \cdot m \cdot \tau \cdot m_s \cdot \tau_s \cdot E_i \cdot S_f \quad [\text{kWh/day}] \quad (3.4)$$

where

A = area of the window between the sunspace and the heated space [m^2]

m = ratio between the glazed area and the total area of the window between the sunspace and the heated space. According to EN ISO 10077-1:2007 the total window area, A_w , is the sum of the frame area, A_f , and of the glazed area, A_g

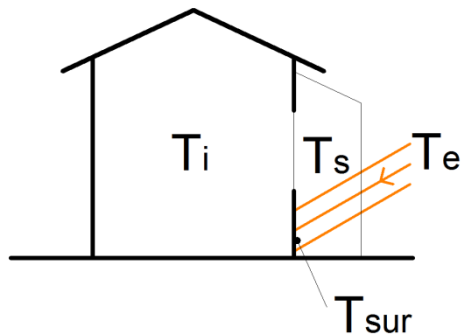
τ = solar transmission factor of the window between the sunspace and the heated space

m_s = ratio between the glazed area and the total area of the external envelope of the sunspace

τ_s = solar transmission factor of the external glazed parts of the sunspace

E_i = energy on the glazed surface between the sunspace and the internal environment in conditions of absence of obstacles (shadings, windows or others) [$\text{kWh}/(\text{m}^2\text{day})$]

S_f = shading factor

B. Solar gain due to heat absorption by the wall Φ_{smv} 

The Method 5000 proposes the following equation:

$$\Phi_{smv} = 0,11 \cdot U \cdot \alpha \cdot m_s \cdot \tau_s \cdot A \cdot E_i \cdot S_f \quad [\text{kWh/day}] \quad (3.5)$$

where

U is the thermal transmittance of the opaque wall between the sunspace and the heated space [$\text{W}/(\text{m}^2\text{K})$]

α is the solar absorptance of the opaque wall between the sunspace and the heated space (surface toward the sunspace)

E_i is the energy on the opaque surface between the sunspace and the internal environment in conditions of absence of obstacles (shadings, windows or others) [$\text{kWh}/(\text{m}^2\text{day})$]

m_s is the ratio between the glazed area and the total area of the external envelope of the sunspace

τ_s is the solar transmission factor of the external glazed parts of the sunspace

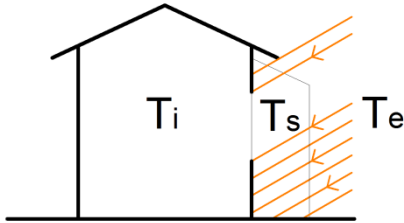
S_f is the shading factor

Heat conductivity and density of the materials are not considered, because the phenomenon is considered as stationary. That is obviously a simplification. It would be interesting to know how the coefficient 0,11 was obtained. Probably it is valid only for certain insulation levels of the sunspace envelope.

C. Increase of the buffer effect due to the increase of the sunspace temperature Φ_{sb}

and

D. Reduction of ventilation losses due to the increase of the sunspace temperature Φ_{sa}



Part of the solar energy entering sunspace causes the increase of the sunspace temperature. Because of this phenomenon, there is a decrease of heat losses from the heated environment. These heat losses regard both the conduction (point C.) and the ventilation (point D.).

As first step, the solar radiation entering sunspace is calculated:

$$E_s = E \cdot S_f \cdot A \cdot m_s \cdot \tau_s \quad [\text{kWh/day}] \quad (3.6)$$

where

E_i is the solar energy on the glazed envelope of the sunspace in conditions of absence of obstacles [$\text{kWh}/(\text{m}^2\text{day})$]

S_f is the shading factor

A is the total area of the sunspace envelope [m^2]

m_s is the ratio between the glazed area and the total area of the external envelope of the sunspace

τ_s is the solar transmission factor of the external glazed parts of the sunspace, see point 1.

The second step consists of calculating the part F_s of entered radiation which contributes to sunspace temperature increase. The equation proposed by the Method 5000 is the following:

$$F_s = (a1 \cdot E_s) - (a2 \cdot \Phi_{sdg}) - \Phi_{smv} \quad [\text{kWh/day}] \quad (3.7)$$

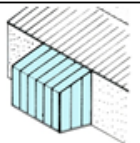
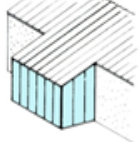
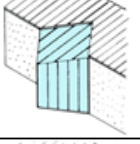
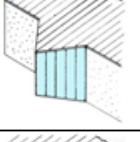
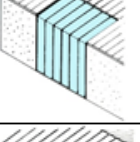
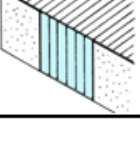
where

E_s is the solar radiation entering sunspace which has been calculated as the first step [kWh/day]

$a1$ and $a2$ are dimensionless coefficients which regard reflections of radiation and dispersions towards the external environment which do not contribute to the temperature increase of the sunspace. The Table 3.1 reports the values presented by Zappone, C. (2009). They depend on the relationship between sunspace and building, on the number of capturing surfaces, on the type of window (single glazing or double glazing), on the presence or absence of insulation

between the floor and the ground (there is no reference to thermal transmittance and the issue is not treated in quantitative terms), on the solar absorbance of the floor (Method 5000 considers the floor the surface which absorbs more solar radiation). For higher values of a_1 the part of the entered radiation which contributes to increase the sunspace temperature is higher. Φ_{sdg} is the solar radiation which enters heated space passing through the sunspace, see point A. Φ_{smv} is the solar gain due to heat absorption by the wall, see point B.

Table 3.1 Values of the coefficients a_1 and a_2 . Source of the data: Zappone, C. (2009)

	sunspace shape	uninsulated floor		insulated floor			
		single glazing	double glazing	light colour ($\alpha < 0,3$)		dark colour ($\alpha > 0,3$)	
				single glazing	double glazing	single glazing	double glazing
A	 4 capturing surfaces	$a_1=0,65$ $a_2=0,85$	$a_1=0,69$ $a_2=0,87$	$a_1=0,63$ $a_2=0,85$	$a_1=0,67$ $a_2=0,87$	$a_1=0,59$ $a_2=0,85$	$a_1=0,63$ $a_2=0,87$
B	 3 capturing surfaces: 3 vertical windows	$a_1=0,70$ $a_2=0,89$	$a_1=0,74$ $a_2=0,91$	$a_1=0,68$ $a_2=0,89$	$a_1=0,71$ $a_2=0,91$	$a_1=0,65$ $a_2=0,89$	$a_1=0,68$ $a_2=0,91$
C	 3 capturing surfaces: roof + 2 vertical windows	$a_1=0,67$ $a_2=0,86$	$a_1=0,71$ $a_2=0,89$	$a_1=0,66$ $a_2=0,86$	$a_1=0,70$ $a_2=0,89$	$a_1=0,62$ $a_2=0,86$	$a_1=0,66$ $a_2=0,89$
D	 2 capturing surfaces: 2 vertical windows	$a_1=0,64$ $a_2=0,91$	$a_1=0,67$ $a_2=0,92$	$a_1=0,62$ $a_2=0,91$	$a_1=0,66$ $a_2=0,92$	$a_1=0,59$ $a_2=0,91$	$a_1=0,63$ $a_2=0,92$
E	 2 capturing surfaces: wall + vertical window	$a_1=0,87$ $a_2=0,87$	$a_1=0,90$ $a_2=0,90$	$a_1=0,84$ $a_2=0,87$	$a_1=0,87$ $a_2=0,90$	$a_1=0,80$ $a_2=0,87$	$a_1=0,82$ $a_2=0,90$
F	 one vertical capturing surface	$a_1=0,92$ $a_2=0,92$	$a_1=0,94$ $a_2=0,94$	$a_1=0,90$ $a_2=0,92$	$a_1=0,91$ $a_2=0,94$	$a_1=0,85$ $a_2=0,92$	$a_1=0,87$ $a_2=0,94$

It would be interesting to know how the presented values were obtained (empirically or in a computational way? If empirically, in which conditions? If in a computational way, with what calculation methods and calculation hypotheses?).

As third step, the temperature in the sunspace is calculated.

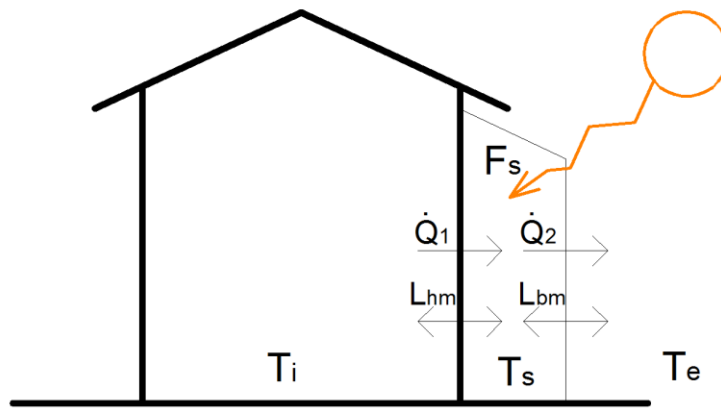


Figure 3.3 Calculation scheme for the sunspace temperature

According to Figure 3.3, the following symbol definitions are used:

T_e is the mean external temperature

T_i is the set-point temperature of the heated space

T_s is the sunspace temperature

L_{hm} is the heat transfer coefficient between the heated space and the sunspace [W/K]

L_{bm} is the heat transfer coefficient between the heated space and the external environment [W/K]

In the previous step F_s was calculated as [kWh/day]. To convert from [kWh/day] to [W] a conversion factor must be introduced:

$$1 \frac{\text{kWh}}{\text{day}} = 10^3 \frac{\text{Wh}}{\text{day}} = 10^3/24 \text{ W} = \frac{1}{0,024} \text{ W} \quad (3.8)$$

The equations relative to the heat balance in the sunspace and to heat transmission among the different environments are:

$$\begin{cases} \dot{Q}_2 = \dot{Q}_1 + \frac{F_s}{0,024} & [\text{W}] \\ \dot{Q}_1 = L_{hm} \cdot (T_i - T_s) & [\text{W}] \\ \dot{Q}_2 = L_{bm} \cdot (T_s - T_e) & [\text{W}] \end{cases} \quad (3.9)$$

Therefore

by substituting the first equation in the third one

$$L_{bm} \cdot (T_s - T_e) = \dot{Q}_1 + F_s/0,024$$

considering also the second one

$$L_{bm} \cdot (T_s - T_e) = L_{hm} \cdot (T_i - T_s) + F_s/0,024$$

solving for T_s

$$T_s \cdot (L_{bm} + L_{hm}) = L_{hm} \cdot T_i + L_{bm} \cdot T_e + F_s/0,024$$

$$T_s = \frac{L_{hm} \cdot T_i + L_{bm} \cdot T_e}{L_{hm} + L_{bm}} + \frac{Fs/0.024}{L_{hm} + L_{bm}} \quad (3.10)$$

In theoretical conditions of absence of solar gain the sunspace temperature would be

$$T_{sng} = \frac{L_{hm} \cdot T_i + L_{bm} \cdot T_e}{L_{hm} + L_{bm}} \quad (3.11)$$

The temperature in the sunspace would be the weighted average of the temperatures in the internal environment and in the external one.

The gain due to the increase of the buffer effect because of solar radiation is the decrease of losses from the heated space to the sunspace because of solar radiation:

$$\Phi_{sb} = L_{hm} \cdot (T_s - T_{sng}) \cdot 0,024 = L_{hm} \cdot \frac{Fs}{L_{hm} + L_{bm}} \quad [\text{kWh/day}] \quad (3.12)$$

The gain relative to the preheating of the entering air is:

$$\Phi_{sa} = \dot{m}c_a \cdot (T_s - T_{sng}) \cdot 0,024 = \rho \dot{V}c_a \cdot \frac{Fs}{L_{hm} + L_{bm}} \quad [\text{kWh/day}] \quad (3.13)$$

where

\dot{m} is the mass flow of air which is preheated in the sunspace [kg/s]

\dot{V} is the volume flow of air which is preheated in the sunspace [m^3/s]

ρ is the air density [kg/m^3]

c_a is the specific heat of the air [$\text{J}/(\text{kg} \cdot \text{K})$]

Total heat gain

The total heat gain due to the presence of solar radiation in the sunspace is the sum of the 4 contributions:

$$\Phi = \Phi_{sdg} + \Phi_{smv} + \Phi_{sb} + \Phi_{sa} \quad [\text{kWh/day}] \quad (3.14)$$

The Method 5000 has a particular procedure for the estimation of the utilization factor, which depends of the involved masses per floor area of the building and on the temperature difference between the set-point temperature and the building temperature in conditions of absence of heating system.

3.2.2 European technical standard EN ISO 13790:2008

Within the European technical standard EN ISO 13790:2008 “Energy performance of buildings - Calculation of energy use for space heating and cooling” the annex E deals with “*Heat transfer and solar heat gains of special elements*” and the paragraph E.2 with unconditioned sunspaces:

“The following applies to unconditioned sunspaces adjacent to a conditioned space, such as conservatories and attached greenhouses separated by a partition wall from the conditioned space.

If the sunspace is heated, or if there is a permanent opening between the conditioned space and the sunspace, it shall be considered as part of the conditioned space”.

The solar gain which the sunspace provides to the heated space Q_{ss} is considered as the sum of the direct gain Q_{sd} through the wall which divides the heated space from the sunspace (both transparent and opaque parts) and the indirect gain Q_{si} relative to the temperature increase of the sunspace (Q_{si} is the increase of the buffer effect because of solar radiation).

$$Q_{ss} = Q_{sd} + Q_{si} \quad (3.15)$$

Required data

The following data are the required inputs. The subscript “w” is relative to the transparent part between the sunspace and the heated space, the subscript “e” is relative to the transparent part between the sunspace and the external environment.

F_F is the frame area fraction, i.e. the frame area to total surface ratio

The paragraph of the technical standard “11.4.5 Frame area fraction” states that:

“For each window the frame area fraction shall be determined in accordance with ISO 10077-1.

As an alternative it may be decided nationally to use a fixed frame area fraction for all windows in the building. (...) For instance, in the case of heating-dominated climates, use 0,20 or 0,30, whichever gives the higher thermal transmittance value of the window (see 8.3.1), or a fixed value of 0,30; for cooling-dominated climates use a fixed value of 0,20”.

F_{Sh} is the shading correction factor

The paragraph of the technical standard “11.4.4 External shading reduction factors” states that: *“The shading by different obstacles can coincide, partly or as a whole. Consequently, adding the shading reduction factors can significantly overestimate the shading”* and that the direct solar radiation, the sky-reflected and the ground-reflected radiations are obstructed by the obstacles in different ways. Therefore the calculation of shading factors without using

dynamic three-dimensional software is often strongly approximated.

g is the effective total solar energy transmittance of glazing. It “*is the time-averaged ratio of energy passing through the transparent element to that incident upon it*”. More details are presented in paragraph 3.2.4.1 “Calculation of the solar heat entering the veranda through the external window”.

A_w is the area of windows and glazed doors in partition wall.

A_e is the area of sunspace envelope.

A_j is the area of each surface j , absorbing the solar radiation in the sunspace (floor, opaque walls; among them the opaque part of the partition wall, which has subscript p).

α_j is the average solar absorption factor of absorbing surface j in the sunspace.

I_i is the solar irradiance on surface i during the calculation step(s).

$H_{p,tot}$ is the heat transfer coefficient by transmission from the internal environment, through the opaque part of the partition wall and the sunspace, to the external environment (see paragraphs 8 and 9 of EN ISO 13790:2008 and Figure 3.4).

$H_{p,e}$ is the heat transfer coefficient by transmission from the absorbing surface of this wall, via the sunspace, to the external environment (see paragraphs 8 and 9 of EN ISO 13790:2008 and Figure 3.4).

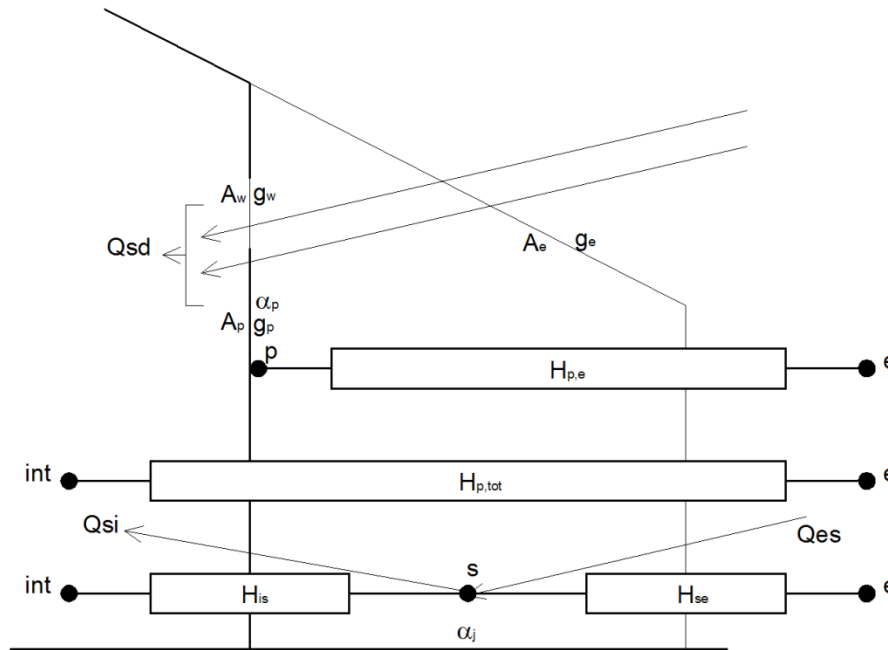


Figure 3.4 Calculation scheme of the gain due to solar radiation in the sunspace according to the ANNEX E of the European technical standard EN ISO 13790:2008 (the image was reviewed and modified by the author)

“It is assumed, in a first approximation, that the absorbing surfaces are all shaded in the same proportion by external obstacles and by the outer envelope of the sunspace”.

This approximation is discussed in paragraph 3.2.4 “Proposed improvements to the technical standard”.

The direct solar heat gains, Q_{sd} , expressed in megajoules, are the sum of heat gains through the transparent (subscript w) and opaque (subscript p) parts of the partition wall.

Equation (E.2) in EN ISO 13790:2008:

$$Q_{sd} = F_{sh}(1 - F_{F,e})g_e \left[(1 - F_{F,w})g_w A_w + \alpha_p A_p \frac{H_{p,tot}}{H_{p,e}} \right] I_p t \quad (3.16)$$

The indirect heat gains are calculated by summing the solar heat gains of each absorbing area, j , in the sunspace, but deducting the direct heat gains through the opaque part of the partition wall. In fact, the gain through the opaque partition was already calculated by the previous equation.

Equation (E.3) in EN ISO 13790:2008:

$$Q_{si} = (1 - b_{tr}) \cdot F_{sh,e}(1 - F_{F,e})g_e \sum_j (I_j \alpha_j A_j) - F_{sh,e}(1 - F_{F,e})g_e \alpha_p A_p \frac{H_{p,tot}}{H_{p,e}} I_p t \quad (3.17)$$

where the weighting factor $(1 - b_{tr})$ is that part of the solar heat gains to the sunspace which contributes to the decrease of the heating requirements. b_{tr} is defined in the technical standard EN ISO 13789:

$$b_{tr} = \frac{H_{ue}}{H_{iu} + H_{ue}} \quad (3.18)$$

H_{ue} is the heat transfer coefficient between the unconditioned space and the external environment, in W/K.

H_{iu} is the direct heat transfer coefficient between the conditioned space and the unconditioned space (...) in W/K.

It is possible to observe that the equation (E.3) of the ANNEX E is not dimensionally consistent, because the time t multiplies only the subtrahend. The calculation of Q_{si} is redeveloped in paragraph 3.2.4.3.

It is supposed that the radiation entering heated space through the glazed part does not exit (in the physical reality a non-negligible part can exit back if the glazed part is big in relation to the dimensions of the room and the average solar absorption factor of the internal surfaces is low). Moreover, it is supposed that the solar heat which heats the sunspace coincides with the radiation which is absorbed by its internal surfaces.

The solar radiation which contributes to heat the sunspace can be called Φ

$$\Phi = F_{sh,e}(1 - F_{F,e})g_e \sum_j (I_j \alpha_j A_j) - F_{sh,e}(1 - F_{F,e})g_e \alpha_p A_p \frac{H_{p,tot}}{H_{p,e}} I_p \quad (3.19)$$

Therefore the mean air temperature T_u in the sunspace in the considered period can be calculated as

$$T_u = \frac{\Phi + H_{is}T_i + H_{se}T_e}{H_{is} + H_{se}} \quad (3.20)$$

where

θ_i is the mean temperature in the heated space (generally it is supposed equal to the set-point temperature)

θ_e is the mean temperature in the external environment.

3.2.3 Comparison between Method 5000 and EN ISO 13790:2008

Method 5000 and EN ISO 13790:2008 consider a constant temperature in the heated space. In practice, both systems consider the heat gain due to solar radiation in the sunspace as the sum of three contributions: solar radiation which enters heated space, solar radiation which heats the partition wall between the sunspace and the heated space, solar radiation which heats

the sunspace causing a decrease of the heat losses for the heated space (the losses are both through conduction and through ventilation).

The Method 5000 refers explicitly also to the preheating of the ventilation air.

With regard to direct gain through the glazed parts there is no difference.

With regard to direct gain through the opaque parts the calculation according to EN ISO 13790:2008 considers the heat transfer coefficients and therefore the thermal resistance of the sunspace while the method 5000 considers only the thermal transmittance of the wall, without paying attention to the insulation level of the sunspace. In fact, according to EN ISO 13790:2008 the heat which is absorbed by the wall surface is multiplied by $\frac{H_{p,tot}}{H_e}$ while according to Method 5000 it is multiplied by $0,11 \cdot U$. From this point of view the calculation according to EN ISO 13790:2008 is surely more correct.

With regard to solar gain relative to the increase of the buffer effect the approaches of the two methods are different. The first step of Method 5000 consists in calculating solar radiation entering from the external glazed parts of the sunspace, while EN ISO 13790:2008 calculates the solar radiation which is directly absorbed by the internal surfaces of the sunspace. In the following step Method 5000 calculates the heat which contributes to increase the sunspace temperature by subtracting from the entered solar radiation the direct gains (both through glazed parts and through opaque parts) and by multiplying the entered solar radiation by a factor between 0 and 1, which considers the heat originated by the solar radiation which is lost towards the external environment (by reflection of solar radiation and because of losses through the envelope elements toward the external environment). The method of EN ISO 13790:2008 supposes that *the absorbing surfaces are all shaded in the same proportion by external obstacles* but surfaces with different orientations and different positions are surely shaded in different ways.

The utilization factor is calculated by the two methods in different ways, but it is not among the subjects of this work.

3.2.4 Proposals to improve the technical standard

In the previous paragraphs the calculation method proposed by ANNEX E of the technical standard EN ISO 13790:2008 was critically analysed and compared with Method 5000. In the present paragraph some proposals to improve it are presented. The improving proposals regard only the method of technical standard because it is an official document and about Method 5000 the available documentation is too poor. Results of calculations based on the technical standard and on the new proposals were compared among them and with dynamic

simulations (for dynamic simulations see paragraph 3.3). Nevertheless, the proposals are not immediately applicable but they should be further studied and tested. The validations should consider a representative variety of situations (from the point of view of geometry, properties, climatic context...).

For the climatic context, hourly data relative to a test reference year of Bolzano (Italy) were considered. The data are from the database of the Comitato Termotecnico Italiano and they are available online⁷.

The model created in IDA-ICE was created like the paragraph 4.3 explains. In that paragraph the results of the validation of a model created in IDA-ICE with empirical data are presented.

3.2.4.1 Calculation of the solar heat entering the veranda through the external windows

The calculation of the heat entering the veranda through the external windows is fundamental both for the direct heat gains and for indirect heat gains.

In the technical standard for the quasi-steady-state calculation the total solar energy transmittance of the transparent part g_{gl} of a window is

$$g_{gl} = F_w \cdot g_{gl,n} \quad (3.21)$$

where

$g_{gl,n}$ is the value for the radiation having a direction normal to the window surface

F_w is a correction factor which was introduced in order to consider that “the time-averaged total solar energy transmittance is somewhat lower than g_n ” (see eq. (47) in EN ISO 13790:2008). It must be observed that in equation (1.2) $F_{w,dir}(\theta)$ refers to a specific angle, while in this equation it is a mean value throughout the period considered.

In the absence of national values, the value for the correction factor F_w is 0,9. Neither the European technical standard, nor the Italian one (UNI/TS 11300-1:2008), nor the German one (DIN 18599-2:2007) consider differences among different months. Improving the precision of that calculation is particularly important in the calculation of sunspaces, where the entering solar radiation has a fundamental importance (for a vertical glass the calculation of the solar energy incident on the floor of the sunspace is particularly tricky, because when the solar radiation incident on an external horizontal plane is particularly high the angle between direct solar radiation and the window normal direction is particularly great and therefore there is a big difference between the effective g-factor and the normal g-factor).

As Chapter 1 (“Passive solar systems”) already explained, in literature there are different models of the function which establishes a connection between the incident angle of the solar radiation and the solar transmittance. As example, in Figure 1.5, the model which is present in

⁷ < www.cti2000.it >

software IDA-ICE (see equation (1.17)) and the models presented in Karlsson, J. and Roos, A. (2000) for a window having a Ag+ coating layer and for a window having a SnO₂ coating layer are illustrated. Starting from the model of IDA-ICE, the F_w factors for a vertical south facing window located in Bolzano were calculated. Considering only the direct radiation, in Figure 3.5 $F_{w,dir}(\theta)$ hourly values relative to a winter period are represented and in Figure 3.6 hourly values relative to a summer period. If the solar altitude is negative or if the incidence angle is greater than 90° $F_{w,dir}$ is equal to 0. Obviously the peaks of the correction factor are higher during winter.

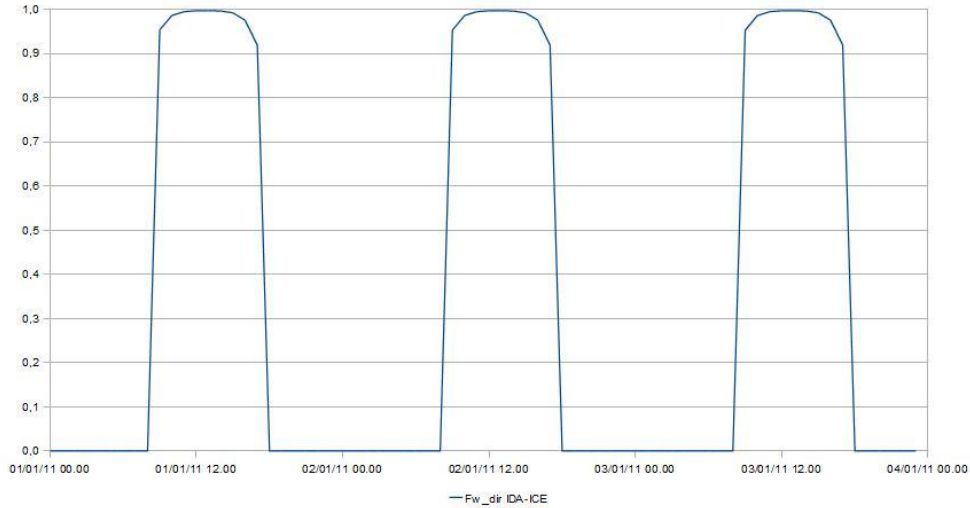


Figure 3.5 $F_{w,dir}$ trend for a winter period (hourly values)

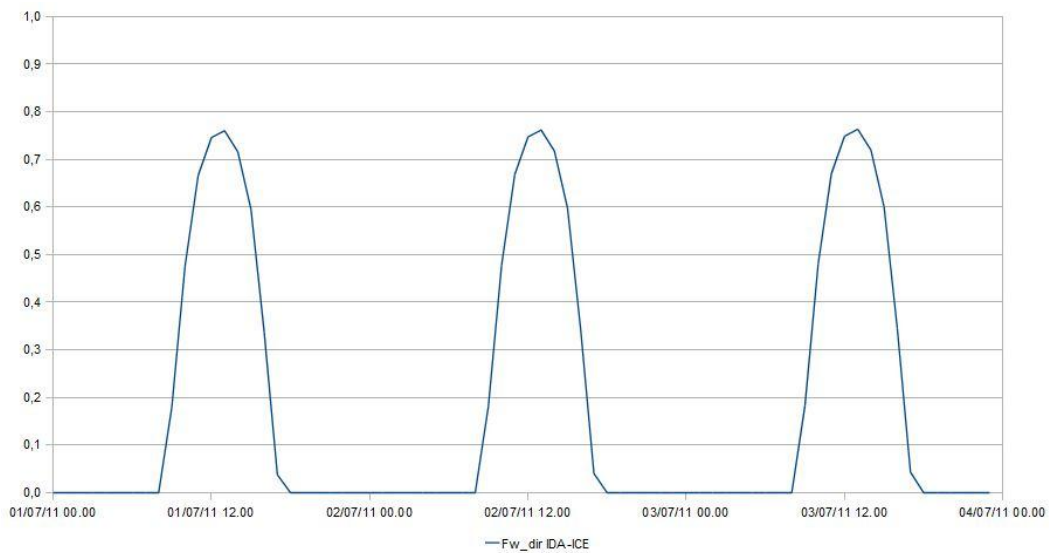


Figure 3.6 $F_{w,dir}$ trend for a summer period (hourly values)

According to Oliveti, G. et al. (2009), the coefficient F_w relative to the time period Δt can be expressed as

$$F_w = \frac{\sum \left[\frac{g_b}{g_{gl,n}} I_b + \frac{g_d}{g_{gl,n}} I_d + \frac{g_r}{g_{gl,n}} I_r \right] \Delta t}{\sum [I_b + I_d + I_r] \Delta t} \quad (3.22)$$

where

I_b is the direct radiation on the external side of the window

I_d is the diffuse radiation from the sky on the external side of the window

I_r is the diffuse radiation coming from the ground on the external side of the window

g_b the total solar energy transmittance considering only the direct radiation

g_d the total solar energy transmittance considering only the diffuse radiation from the sky

g_r the total solar energy transmittance considering only the diffuse radiation coming from the ground

Considering a vertical window and supposing that the sky view factor and the ground view factor are both 0,5 we can consider for them the same correction factor $F_{w,dif}$ and therefore we can express F_w as

$$F_w = \frac{\sum [F_{w,dir} I_b + F_{w,dif} I_d + F_{w,dif} I_r] \Delta t}{\sum [I_b + I_d + I_r] \Delta t} \quad (3.23)$$

Calling I_{dif} the sum of the diffuse radiation from the sky I_d and the diffuse radiation from the ground I_r

$$F_w = \frac{\sum [F_{w,dir} I_b + F_{w,dif} I_{dif}] \Delta t}{\sum [I_b + I_{dif}] \Delta t} \quad (3.24)$$

Considering this equation, the monthly average values using the IDA-ICE model were calculated. They are presented in Figure 3.7 and in Tab. 3.2 where also the results of the linear regression presented by Oliveti, G. (2009) are indicated. In fact, Oliveti, G. (2009) proposed the following linear regression in order to estimate the correction factor as a linear function of the latitude:

$$F_w = a_1 L + a_2 \quad (3.25)$$

where

L is the latitude of the considered locality

a_1 and a_2 are parameters which depend on the month and on the orientation of the surface.

In the calculations an albedo value equal to 0,2 was supposed.

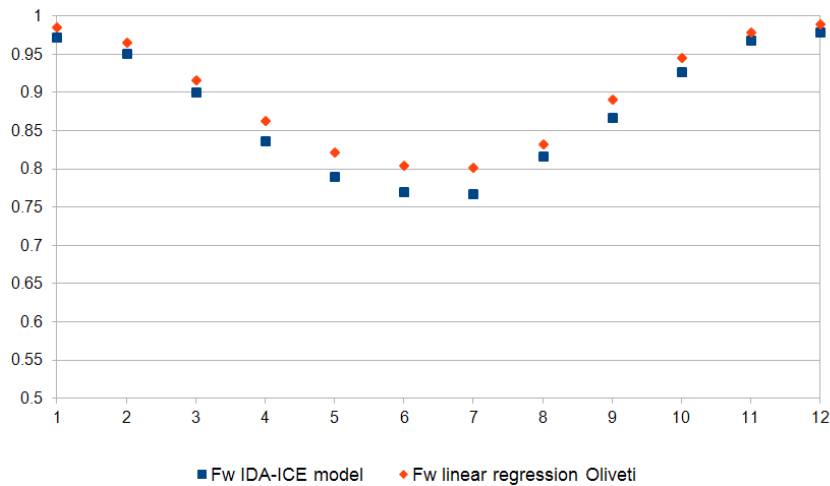


Figure 3.7 F_w trend throughout the year (monthly values)

It is also possible to observe that the linear regression proposed by Oliveti, G. (2009) and the results obtained with IDA-ICE are quite similar, but the Oliveti’s values are always greater, particularly during the warmest months.

Table 3.2 Monthly correction factors according to IDA-ICE and to linear regression proposed by Oliveti, G. (2009)

	Jan	Feb	Mar	Apr	May	Jun	Jul	Aug	Sep	Oct	Nov	Dec
F _w IDA-ICE model	0,97	0,95	0,90	0,84	0,79	0,77	0,77	0,82	0,87	0,93	0,97	0,98
F _w linear regression Oliveti, G. (2009)	0,98	0,96	0,92	0,86	0,82	0,80	0,80	0,83	0,89	0,95	0,98	0,99

It is possible to observe that during the heating season, i.e. when the sunspace has to be exploited energetically, the monthly correction factor is greater than 0,9, the value proposed by technical standards (except in April, when heating requirements are low). A next version of the technical standard could provide linear regressions like Oliveti, G. (2009). The calculation would be surely more precise than assuming the correction factor equal to 0,9 throughout the year.

The reduction of the solar transmission is more important for surfaces which are perpendicular to the external window than for surfaces which are parallel to it because for a surface which is perpendicular the F_w for the direct radiation is particularly low when the radiation is close to the normal direction of the surface. The amount of the impact of the radiation reduction on a specific internal surface depends on the geometry and on the sun position in such an important way that for a determined surface a really precise calculation is possible only with a three-dimensional model which considers short time steps (e.g. one hour).

3.2.4.2 Direct heat gain

In ANNEX E the equation (E.2) is relative to the direct heat gain, i.e. to the solar radiation directly entering the heated space, considering both the transparent parts and the opaque parts.

$$Q_{sd} = F_{sh,e} \cdot (1 - F_{F,e})g_e \cdot \left[\underbrace{(1 - F_{F,w})g_w A_w}_{\text{relative to the transparent part}} + \underbrace{\alpha_p A_p \frac{H_{p,tot}}{H_{p,e}}}_{\text{relative to the opaque part}} \right] I_p t \quad (3.26)$$

Considering the solar radiation and the shading correction factor F_{sh} , which does not depend only on the external envelope, separately for every surface the equation can be written in a new form:

$$Q_{sd} = \underbrace{(1 - F_{F,e})g_e}_{\text{reduction factor relative to sunspace envelope}} \cdot \left[\sum_j (F_{sh,w} \cdot (1 - F_{F,w})g_w A_w I_{w,j}) + \sum_k \left(F_{sh,p} \cdot \alpha_p A_p I_p \frac{H_{p,tot}}{H_{p,e}} \right)_k \right] t \quad (3.27)$$

The geometry which is presented in Figure 3.8 was considered to obtain some quantitative results (both dynamic and stationary). The windows are facing south.

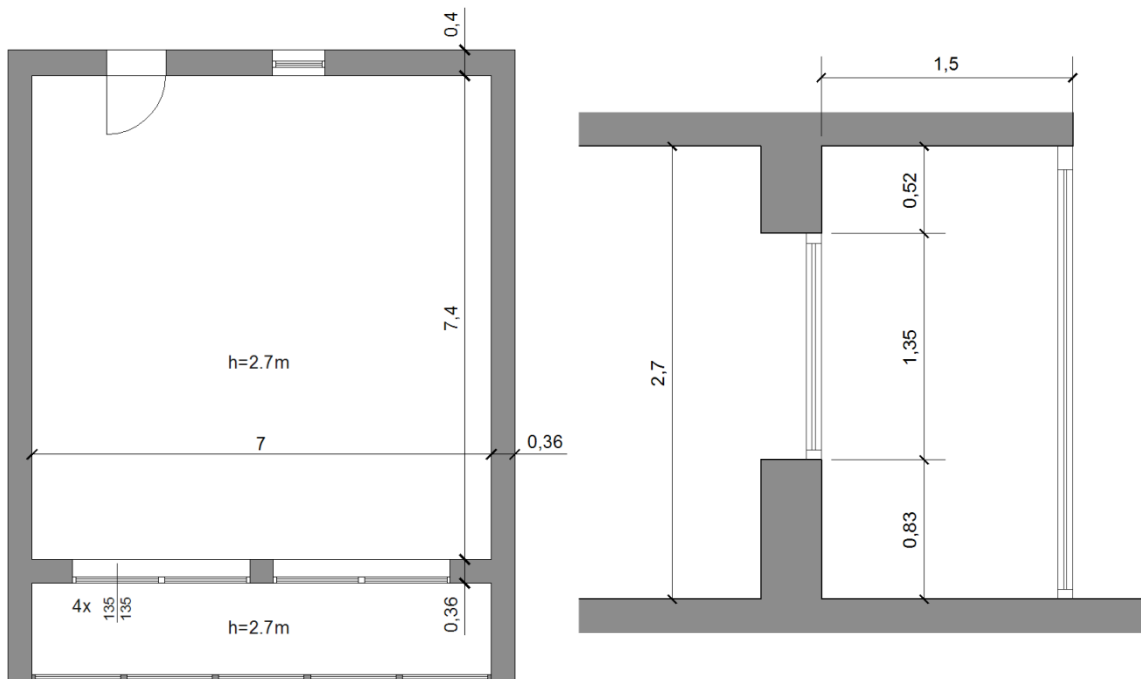


Figure 3.8 Schematic geometry of a sunspace

The shading factors have been calculated with dynamic calculations in IDA-ICE. From this point of view, the outputs of the dynamic calculations have been used also in the stationary calculations, because the proposals of improvement of the technical standard do not regard the way in which the shading factors are calculated. However, different shading factors for different surfaces should be used. For the calculation of shading factors the Italian technical legislation refers to the paragraph 14.4 of UNI/TS 11300-1:2008, while the German legislation to ANNEX A of DIN V 18599-2:2007.

To estimate the shading factors a three-dimensional model, in which the external windows of the sunspace were removed, was created. The shading factors were calculated with the following equation:

$$F_{sh} = \frac{\text{radiation on a surface within the sunspace}}{\text{radiation on a surface having the same orientation, without shading}} \quad (3.28)$$

The Table 3.3 presents the obtained results.

Table 3.3 Shading factors F_{sh} for different surfaces inside the sunspace, during the heating season. Weather data of Bolzano (Italy)

	JAN	FEB	MAR	APR	OCT	NOV	DEC
FLOOR	0,31	0,29	0,34	0,24	0,44	0,47	0,47
WALL opaque partition sunspace- internal environment	0,43	0,34	0,27	0,22	0,32	0,41	0,47
WINDOW 1 sunspace- internal environment	0,70	0,61	0,40	0,25	0,61	0,68	0,71
WINDOW 2 sunspace- internal environment	0,74	0,65	0,45	0,28	0,64	0,73	0,77
WINDOW 3 sunspace- internal environment	0,74	0,65	0,43	0,28	0,62	0,73	0,77
WINDOW 4 sunspace- internal environment	0,67	0,55	0,37	0,25	0,48	0,65	0,72
LATERAL WALL 1 facing west	0,53	0,45	0,45	0,38	0,41	0,54	0,53
LATERAL WALL 2 facing east	0,50	0,50	0,48	0,32	0,56	0,53	0,52

Considering the wall and the windows between the sunspace and the internal environment, the shading factors are lower, i.e. the shading effect is more important, in March and in April, when the sun's altitude is higher and the opaque roof of the sunspace projects a bigger shadow. The differences between the shading factors of the two lateral walls are not due to the geometry (they have the same geometry and they are symmetrical with respect of the axis north-south), but only to asymmetry in the data of the solar radiation.

The shading factors obtained with IDA-ICE have been compared with a calculation made

according to UNI/TS 11300-1:2008. The technical standard divides the obstacles in three categories:

- frontal obstacles (shading factor F_{hor});
- horizontal obstacles (shading factor F_{ov});
- vertical obstacles (shading factor F_{fin}).

The standard states that the global shading factor can be calculated by multiplying the shading factors relative to the three kinds of obstacle.

The shading factors can be obtained from tables in which the required inputs are: kind of obstacle, latitude of the location, shading angle (see Figure 3.9), orientation (of the normal to the surface of the building element), and month.

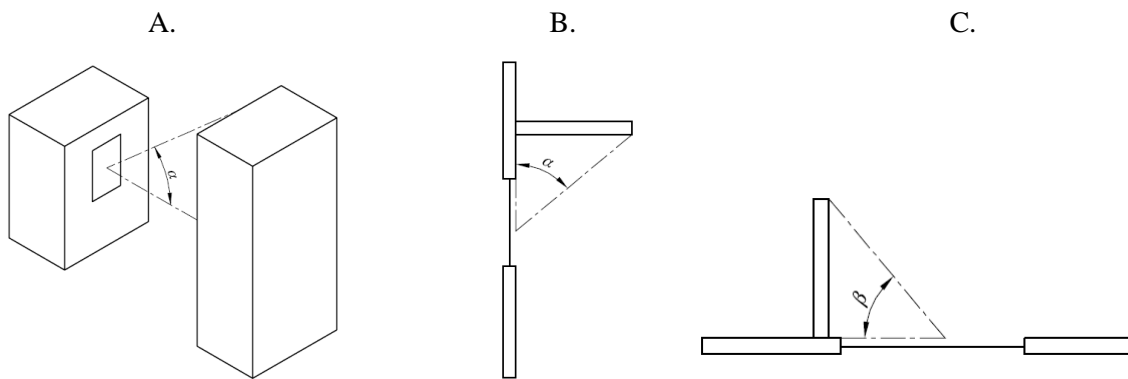


Figure 3.9 Shading angle of obstacles: A. frontal obstacle; B. horizontal obstacle; C. vertical obstacle

In the considered case there is no frontal obstacle. According to UNI/TS 11300-1:2008 the shading factors of the windows were calculated considering two pairs of windows (see Figure 3.10).

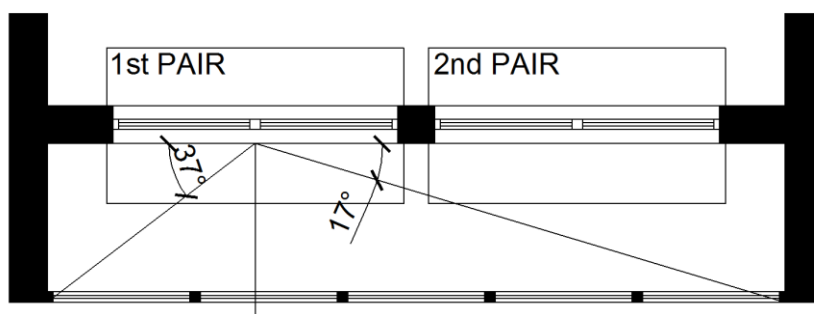


Figure 3.10 Calculation scheme of the shading. The angles relative to the shading factor of vertical obstacles are indicated

The shadows of the two lateral obstacles are considered independent. The total shading factor of the two lateral obstacles is calculated as (Figure 3.11):

$$F_{sh} = F_{sh1} - (1 - F_{sh2}) = F_{sh1} + F_{sh2} - 1 \quad (3.29)$$

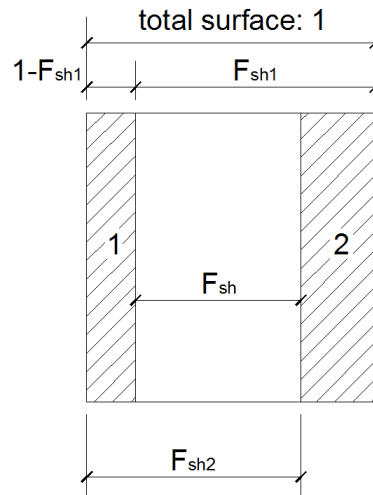


Figure 3.11 Total shading effect of two lateral vertical obstacles

The agreement with the shading factors calculated with IDA-ICE is quite good (see Figure 3.12). We have to consider that the values of the technical standard consider the latitude, but they do not consider the specific climatic conditions of Bolzano.

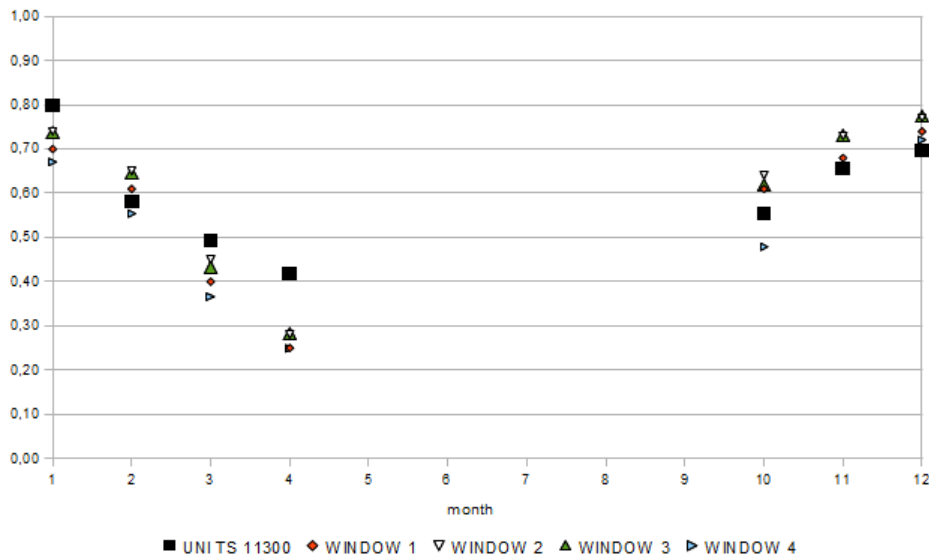


Figure 3.12 Shading factors for the windows between the sunspace and the internal space

Unfortunately UNI/TS 11300:2008-1 does not provide indications for horizontal surfaces (i.e. for the floor), while they are available in DIN V 18599-2, but only as seasonal mean values.

Some considerations concerning the distribution of solar radiation in the sunspace, in particular the radiation striking the window between the sunspace and the internal environment can be made.

As first case, an external space with an opaque roof but without any vertical element which separates it from the external space is considered. A unitary depth is considered.

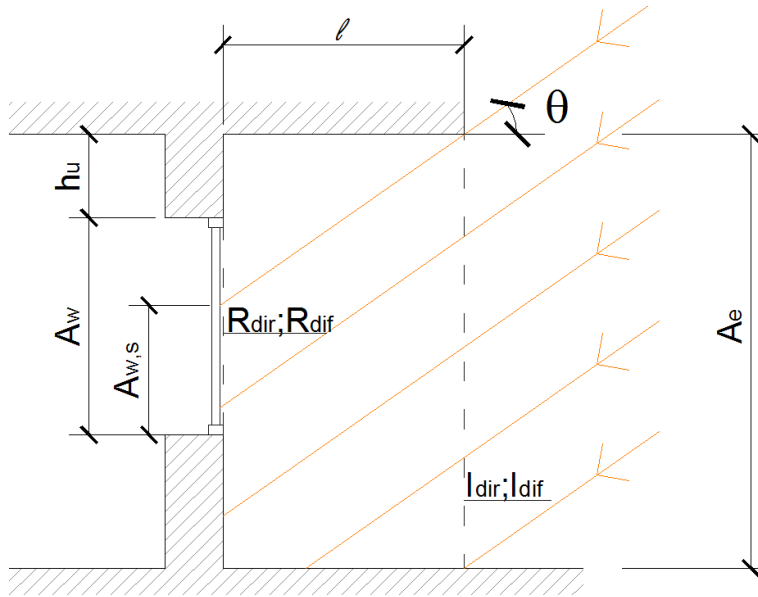


Figure 3.13 Radiation on a shaded window

I_{dir} is the direct radiation on the vertical surface, without obstacles, having the same orientation of the considered window

I_{dif} is the diffuse radiation on the vertical surface, without obstacles, having the same orientation of the considered window

R_{dir} is the direct radiation on the considered window

R_{dif} is the diffuse radiation on the considered window

h_u is the distance between the upper side of the window and the ceiling

A_w is the total area of the window

$A_{w,s}$ is the area of the window which the direct radiation strikes

$F_{sh,dir}$ is the shading factor for the direct radiation

As approximation, it is supposed that the diffuse radiation is distributed from the aperture according to the view factors

$$R_{dir} = F_{sh,dir} I_{dir} \quad (3.30)$$

$$R_{dif} A_w = I_{dif} A_e F_{e-w} \quad (3.31)$$

Therefore

$$R_{dif} = I_{dif} \frac{A_e}{A_w} F_{e-w} \quad (3.32)$$

Because of geometrical reasons:

$$A_{w,s} = A_w - (l \cdot \operatorname{tg}\theta - h_u) \quad (3.33)$$

On the outer side of the internal window:

$$R_{\text{dir}} = \frac{I_{\text{dir}} \cdot A_{w,s}}{A_w} = I_{\text{dir}} \cdot \left(1 - \frac{l \cdot \operatorname{tg}\theta - h_u}{A_w}\right) \quad (3.34)$$

therefore

$$\frac{R_{\text{dif}}}{R_{\text{dir}}} = \frac{I_{\text{dif}}}{I_{\text{dir}}} \cdot \frac{A_e F_{e-w}}{A_w - l \cdot \operatorname{tg}\theta - h_u} \quad (3.35)$$

The instantaneous shading factor is

$$F_{\text{sh}} = \frac{R_{\text{dir}} + R_{\text{dif}}}{I_{\text{dir}} + I_{\text{dif}}} = \frac{I_{\text{dif}} A_e F_{e-w} + I_{\text{dir}} \cdot (A_w - l \cdot \operatorname{tg}\theta - h_u)}{A_w \cdot (I_{\text{dir}} + I_{\text{dif}})} \quad (3.36)$$

Now a situation with the presence of an external window having, theoretically, the frame factor F_F equal to 1, is considered.

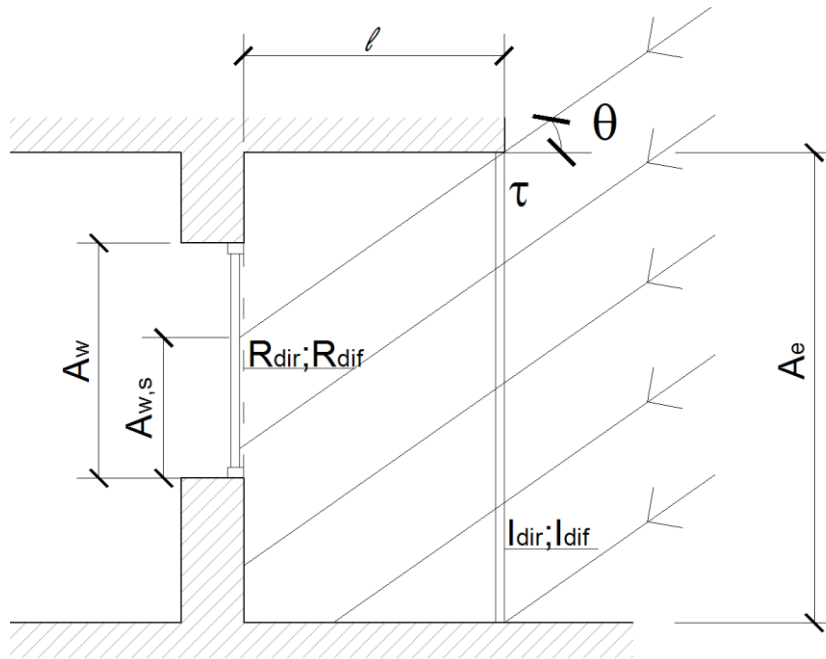


Figure 3.14 Radiation on a shaded window behind another window

$$R_{\text{dif}} = (I_{\text{dif}} \tau F_{w,\text{dif}}) \cdot \frac{A_e}{A_w} \cdot F_{e-w} \quad (3.37)$$

where $F_{w,\text{dif}}$ is the average value of the correction factor on the external semi-space delimited by the window. It can be considered, for a typical commercial window, about 0,85. The global correction factor F_w can be expressed through equation (3.22).

$$R_{dir} = I_{dir} \tau F_{w,dir}(\theta) \cdot \left(1 - \frac{l \cdot \text{tg}\theta - h_u}{A_w}\right) \quad (3.38)$$

In the case with a window the instantaneous shading factor is

$$F_{sh} = \frac{R_{dir} + R_{dif}}{F_w \tau \cdot (I_{dir} + I_{dif})} = \frac{I_{dif} F_{w,dif} A_e F_{e-w} + I_{dir} F_{w,dir}(\theta) \cdot (A_w - l \cdot \text{tg}\theta - h_u)}{F_w A_w \cdot (I_{dir} + I_{dif})} \quad (3.39)$$

and it is different from that one calculated in absence of window (see equation (3.36)).

Therefore the so-called F_{sh} depends on the geometry, on the presence of a window, on the rates of direct radiation and diffuse radiation. Therefore its estimation cannot be really detailed in a semi-stationary method.

3.2.4.3 Solar gain through the opaque part and indirect heat gain

The indirect heat gain is the decrease of heat dispersion from the heated space through the sunspace (considering ventilation as well) due to the increase of the temperature caused by solar radiation. ANNEX E of EN ISO 13790:2008 considers it in the equation (E.3):

$$Q_{si} = \underbrace{(1 - b_{tr})}_{\substack{\text{factor to consider the} \\ \text{heat gain for the} \\ \text{internal environment}}} F_{sh,e} \cdot \underbrace{(1 - F_{F,e})}_{\substack{\text{solar heat absorbed by} \\ \text{the internal surfaces of} \\ \text{the sunspace}}} g_e \sum_j (I_j \alpha_j A_j) - \underbrace{F_{sh,e} \cdot (1 - F_{F,e})}_{\substack{\text{solar heat entering heated space} \\ \text{through the opaque part} \\ \text{(considered among direct gains)}}} g_e \alpha_p A_p \frac{H_{p,tot}}{H_{p,e}} I_p t \quad (3.40)$$

where (see equation (3.18)):

$$b_{tr} = \frac{H_{ue}}{H_{iu} + H_{ue}} \quad (3.41)$$

and therefore

$$1 - b_{tr} = \frac{H_{iu}}{H_{iu} + H_{ue}} \quad (3.42)$$

It was already observed that equation (3.40) is not consistent, because the time multiplies only the subtrahend.

In the following pages the calculation of solar gain through the opaque part and indirect heat gain is redeveloped. A situation in which the heat transmission between the mechanically heated space and the sunspace occurs only through conduction is considered (i.e. a condition of absence of ventilation from the sunspace and to the sunspace; the ventilation is considered in paragraph 3.2.4.4).

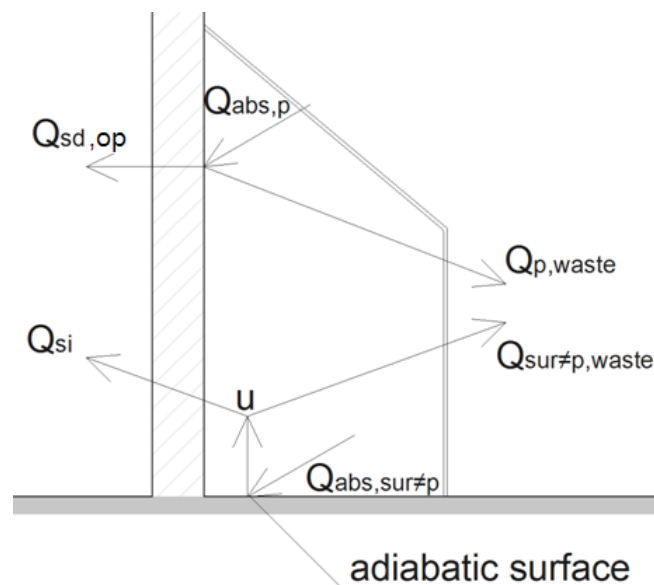


Figure 3.15 Solar gain through the opaque part and indirect heat gain

Both the solar radiation which strikes the wall and the solar radiation which strikes the other surfaces (see Figure 3.15) cause an increase of the temperature of the wall surface: the radiation which strikes the surface of the wall heats the wall directly; that one which strikes the other surfaces, e.g. the floor, causes an increase of the sunspace air temperature and, as a consequence, an increase of the temperature of the wall surface. This temperature increase causes a decrease of heat transmission from the heated space. Actually, also the part of radiation which is absorbed by the wall surface but does not “enter” the heated space, $Q_{p,waste}$, contributes to heat the sunspace air. In absence of ventilation, this effect cannot be considered, because the effect of $Q_{abs,p}$ on the heat conduction between heated space and sunspace has been already considered with $Q_{sd,op}$, the solar gain through the opaque part. In this paragraph the floor slab is considered as adiabatic, because implicitly the technical standard considers it as such when it calculates the solar gain (but obviously it considers the heat losses through the floor when it calculates H_{u-e} , the heat transfer coefficients between the sunspace and the external environment). The issue of the heat losses through the ground is dealt with by paragraph 3.2.4.5 “Solar heat dispersion through opaque surfaces”.

According to Figure 3.15, in the following heat balances $Q_{abs,sur}$ indicates the solar radiation which is absorbed by all the surfaces inside the sunspace, $Q_{abs,p}$ indicates the solar radiation which is absorbed by the partition wall, $Q_{abs,sur\neq p}$ indicates the solar radiation which is absorbed by the surfaces inside the sunspace except the partition wall. The technical standard does not consider the radiation which is absorbed after reflections.

$$Q_{\text{abs,sur}} = Q_{\text{abs,p}} + Q_{\text{abs,sur}\neq\text{p}} \quad (3.43)$$

$$Q_{\text{abs,p}} = Q_{\text{sd,op}} + Q_{\text{p,waste}} \quad (3.44)$$

$$Q_{\text{abs,sur}\neq\text{p}} = Q_{\text{si}} + Q_{\text{sur}\neq\text{p,waste}} \quad (3.45)$$

$$Q_{\text{abs,sur}} = (1 - F_{\text{F,e}}) \cdot g_e \cdot \sum_j (F_{\text{sh},j} I_j \alpha_j A_j) t \quad (3.46)$$

$$Q_{\text{abs,sur}\neq\text{p}} = (1 - F_{\text{F,e}}) \cdot g_e \cdot \sum_{j \neq \text{p}} (F_{\text{sh},j} I_j \alpha_j A_j) t \quad (3.47)$$

$$Q_{\text{abs,p}} = (1 - F_{\text{F,e}}) \cdot g_e \cdot F_{\text{sh,p}} I_p \alpha_p A_p t \quad (3.48)$$

The calculated Q_{abs} are not exactly the heat absorbed by the internal surfaces, because g_e considers also heat which enters the sunspace by convection from the windowpane⁸.

In the following step the solar gain through the opaque part $Q_{\text{sd,op}}$ is calculated.

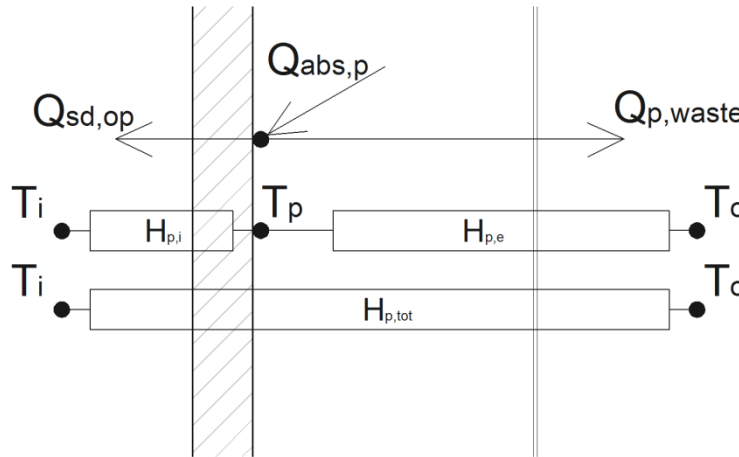


Figure 3.16 Solar gain through the opaque part

If we express heat quantities in [Wh], heat transfer coefficients H in [W] and the time step t in [hours], the mean value of the surface temperature is

$$T_p = \frac{Q_{\text{abs,p}}/t + H_{\text{p,e}} T_o + H_{\text{p,i}} T_i}{H_{\text{p,e}} + H_{\text{p,i}}} \quad (3.49)$$

Therefore the temperature increase due to the solar radiation is

⁸ see EN 410:2011: “The total solar energy transmittance g is calculated as the sum of the solar direct transmittance τ_e and the secondary heat factor q_i of the glazing towards the inside (..), the latter resulting from heat transfer by convection and longwave IR-radiation of that part of the incident solar radiation which has been absorbed by the glazing: $g = \tau_e + q_i$ ”

$$(\Delta T_p)_{\text{sol}} = \frac{Q_{\text{abs,p}}/t}{H_{\text{p,e}} + H_{\text{p,i}}} \quad (3.50)$$

The effect on the heat transmission through the wall is

$$Q_{\text{sd,op}} = H_{\text{p,i}} \cdot (\Delta T_p)_{\text{sol}} t = \frac{H_{\text{p,i}}}{H_{\text{p,e}} + H_{\text{p,i}}} \cdot Q_{\text{abs,p}} \quad (3.51)$$

where

$$\frac{H_{\text{p,i}}}{H_{\text{p,e}} + H_{\text{p,i}}} = \frac{1/R_{\text{p,i}}}{\frac{1}{R_{\text{p,e}}} + \frac{1}{R_{\text{p,i}}}} = \frac{1/R_{\text{p,i}}}{\frac{R_{\text{p,i}} + R_{\text{p,e}}}{R_{\text{p,i}}R_{\text{p,e}}}} = \frac{R_{\text{p,e}}}{R_{\text{p,i}} + R_{\text{p,e}}} = \frac{R_{\text{p,e}}}{R_{\text{p,tot}}} = \frac{H_{\text{p,tot}}}{H_{\text{p,e}}} \quad (3.52)$$

Therefore, considering also equation (3.48)

$$Q_{\text{sd,op}} = F_{\text{sh,p}} \cdot (1 - F_{\text{F,e}}) \cdot g_e \alpha_p A_p \frac{H_{\text{p,tot}}}{H_{\text{p,e}}} I_p t \quad (3.53)$$

which corresponds to the second part of equation (E.2) of the technical standard (see eq. (3.40)).

In the following step the solar indirect heat gain Q_{si} is calculated

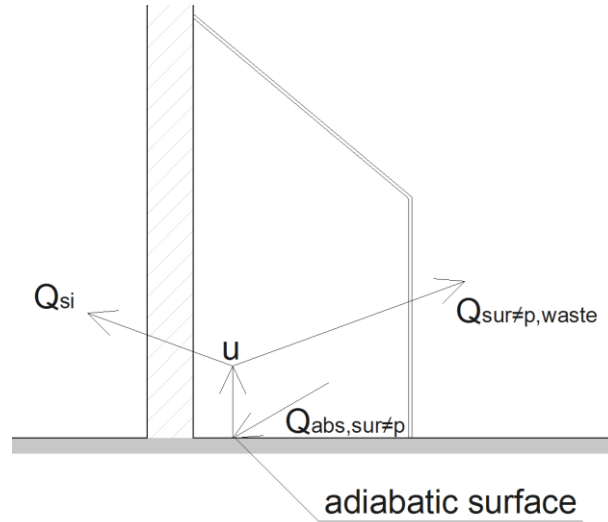


Figure 3.17 Solar indirect heat gain

Like the technical standard, here we suppose that the heat absorbed by the floor slab and by every surface which delimits the sunspace contributes to the indirect gain. The partition with the heated space is not considered here because the contribution of the solar heat absorbed by the partition $Q_{\text{abs,p}}$ to the decrease of heat conduction is already considered in $Q_{\text{sd,op}}$, equation

(3.53). The part of heat absorbed by the internal surfaces of the sunspace, with the exception of the elements which separate the sunspace from the internal space, is expressed by the equation (3.47).

The increase of the sunspace temperature due to solar radiation absorbed by the internal surfaces, expect the partition, is:

$$(\Delta T_u)_{sol} = \frac{Q_{abs,sur \neq p}/t}{H_{iu} + H_{ue}} \quad (3.54)$$

The effect on the heat transmission through the wall is

$$Q_{si} = H_{iu} \cdot (\Delta T_u)_{sol} \cdot t = H_{iu} \cdot \frac{Q_{abs,sur \neq p}}{H_{iu} + H_{ue}} = \frac{H_{iu}}{H_{iu} + H_{ue}} \cdot Q_{abs,sur \neq p} \quad (3.55)$$

The decrease of heat transmission from the heated space is the so-called indirect solar gain:

$$Q_{si} = \frac{H_{iu}}{H_{iu} + H_{ue}} \cdot (1 - F_{F,e}) \cdot g_e \cdot \sum_{j \neq p} (F_{sh,j} I_j \alpha_j A_j) \cdot t \quad (3.56)$$

Since b_{tr} is defined equal to $\frac{H_{ue}}{H_{iu} + H_{ue}}$, in conditions without ventilation the indirect heat gain

can be expressed as

$$Q_{si} = (1 - b_{tr}) \cdot (1 - F_{F,e}) \cdot g_e \cdot \sum_{j \neq p} (F_{sh,j} I_j \alpha_j A_j) \cdot t \quad (3.57)$$

3.2.4.4 Ventilation through the sunspace

About the sunspace, ANNEX E of the technical standard EN ISO 13790:2008 states that “*if there is a permanent opening between the conditioned space and the sunspace, it shall be considered as part of the conditioned space*”. Hence in a situation of constant mechanical air extraction in the internal rooms, with an air flow crossing the sunspace (see Figure 3.18), according to the annex, the sunspace should be considered part of the conditioned space. That is an approximation, particularly because the presence of ventilation in that direction increases the temperature difference between the sunspace and the internal environment. Therefore there is a paradox: in the calculation of the thermal losses, if there is not ventilation according to the technical standard we have to consider the temperature of the sunspace lower than the temperature of the internal environment, if there is ventilation we have to consider the sunspace as part of the internal environment, although the temperature of the sunspace becomes lower than in absence of ventilation.

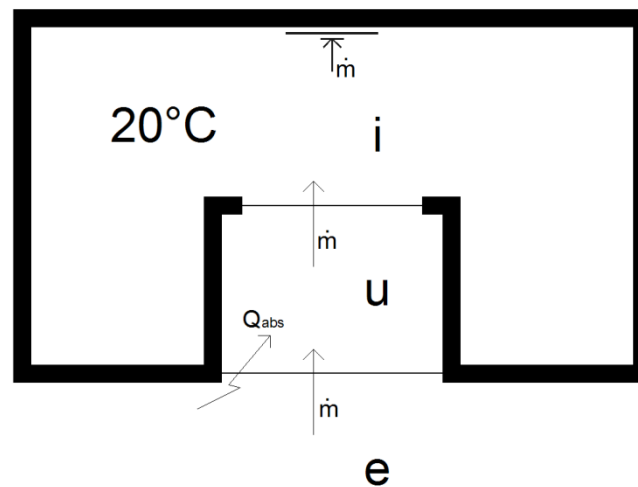


Figure 3.18 The air is extracted from the sunspace by a mechanical system, in order to preheat the ventilation air of the heated space

The problem is that a precise calculation of the ventilation losses in such a situation would need to consider how much heat the air flow adsorbs from the sunspace. The calculation, in order to be really accurate, needs to consider with precision the convective exchange coefficients, the air stratification, to consider the position of inlet and outlet... The only way to achieve this accuracy is probably the utilization of Computational Fluid Dynamic simulations. Therefore the technical standard is not utilizable to evaluate a situation with permanent ventilation through the sunspace. In a next study the supply air temperature in the heated space could be calculated through Computational Fluid Dynamic simulations for a great variety of situations, in order to give indications to the designers. For example, the technical standard with the output of CFD analysis could present graphs or tables which provide the supply air temperature in the heated space $T_{\text{sup,int}}$ as function of some variables and of some parameters:

$$T_{\text{sup,int}} = \text{funct}(\text{mean sunspace temperature; geometry; position of inlet and outlet; air flow...})$$

Otherwise, if the designer is interested in having a very high level of precision, the use of CFD software, in addition to three-dimensional dynamic models, is advisable.

The same reasoning could be applied to the preheating of the ventilation air through a normal unheated space, but generally the problem is more important in a sunspace because of the temperature differences among the different internal surfaces.

In the following part some considerations are developed with the hypothesis of uniformity of the air temperature inside the sunspace (“perfect mixing”), although in the real conditions the temperatures within the sunspace can vary a lot both in time and space.

The following definitions are considered:

Q_{abs} is the solar radiation which is absorbed by the sunspace and contributes to the

temperature increase

\dot{m} is the air flow from the external environment to the veranda and from the veranda to the internal space

T_u is the air temperature in the veranda

According to first law of thermodynamics in stationary conditions, with negligible variations of the kinetic energy and of the potential energy and in conditions of no useful work, the exchanged heat is equal to the change in enthalpy⁹.

$$\dot{Q}_{abs} + H_{i-u,tr} \cdot (T_i - T_u) + H_{u-e,tr} \cdot (T_e - T_u) = \dot{m}h_u - \dot{m}h_e \quad [W] \quad (3.58)$$

In the veranda the specific humidity does not change. If, as approximation, the air is considered dry, for perfect gas the following expression is valid:

$$h = c_a t \quad \left[\frac{J}{kg \cdot K} \right] \quad (3.59)$$

where c_a is the specific heat of the dry air. Equation (3.58) becomes:

$$\dot{Q}_{abs} + H_{i-u,tr} \cdot (T_i - T_u) + H_{u-e,tr} \cdot (T_e - T_u) = \dot{m}c_a T_u - \dot{m}c_a T_e \quad (3.60)$$

Therefore the mean temperature of the veranda is

$$T_u = \frac{\dot{Q}_{abs} + H_{i-u,tr} T_i + H_{u-e,tr} T_e + \dot{m}c_a T_e}{H_{i-u,tr} + H_{u-e,tr} + \dot{m}c_a} \quad (3.61)$$

It is possible to observe that $\dot{m}c_a$, which is relative to the ventilation flow, appears once in the numerator and once in the denominator.

The temperature increase due to solar radiation is

$$\Delta T_u = \frac{\dot{Q}_{abs}}{H_{i-u,tr} + H_{u-e,tr} + \dot{m}c_a} \quad (3.62)$$

The decrease of the heat conduction from the heated space to the veranda is

$$Q_{si,tr} = H_{i-u,tr} \cdot \Delta T_u \quad (3.63)$$

From the point of view of the heated space the decrease of the ventilation losses is

$$Q_{si,ve} = \dot{m}c \cdot \Delta T_u \quad (3.64)$$

The total indirect heat gain is therefore

⁹ Cavallini, A. and Mattarollo, L. (1992)

$$Q_{si} = (H_{i-u,tr} + \dot{m}c) \cdot \Delta T_u \quad (3.65)$$

which considering equation (3.62) can be expressed as

$$Q_{si} = (H_{i-u,tr} + \dot{m}c) \cdot \frac{\dot{Q}_{abs}}{H_{i-u,tr} + H_{u-e,tr} + \dot{m}c_a} \quad (3.66)$$

3.2.4.5 Solar heat dispersion through opaque surfaces

The technical standard in calculating the indirect gains considers that a part of the solar heat absorbed by the internal surfaces does not contribute to the temperature increase of the sunspace temperature, because it enters heated space directly through the opaque divisions. That part can be written as (see eq. (3.53)):

$$(1 - F_{F,e}) \cdot g_e \cdot \sum_k \left(F_{sh,p} \cdot \alpha_p A_p \frac{H_{p,tot}}{H_{p,e}} I_p \right)_k \cdot t \quad (3.67)$$

We have to consider that a part of the solar heat which is absorbed by the internal surfaces of the sunspace does not heat the sunspace air because it is dispersed directly towards the external environment. For example, a part of the solar heat which is absorbed by the floor is dispersed directly through the ground. The technical standard does not consider this dispersion (see Figure 3.17). In some cases, this approximation can be unacceptable, e.g. for sunspaces whose floor slab does not have insulating layers.

A model having an uninsulated floor slab ($U_g = 1,34 \text{ Wm}^{-2}\text{K}^{-1}$) and another model with the only difference that it has an insulating layer ($U_g = 0,32 \text{ Wm}^{-2}\text{K}^{-1}$) were simulated dynamically (also in this case with the test reference year of Bolzano). The thermal transmittances were calculated through COMSOL Multiphysics, a FEM software. The geometry of the model is presented in Figure 3.8 and in Figure 3.19.

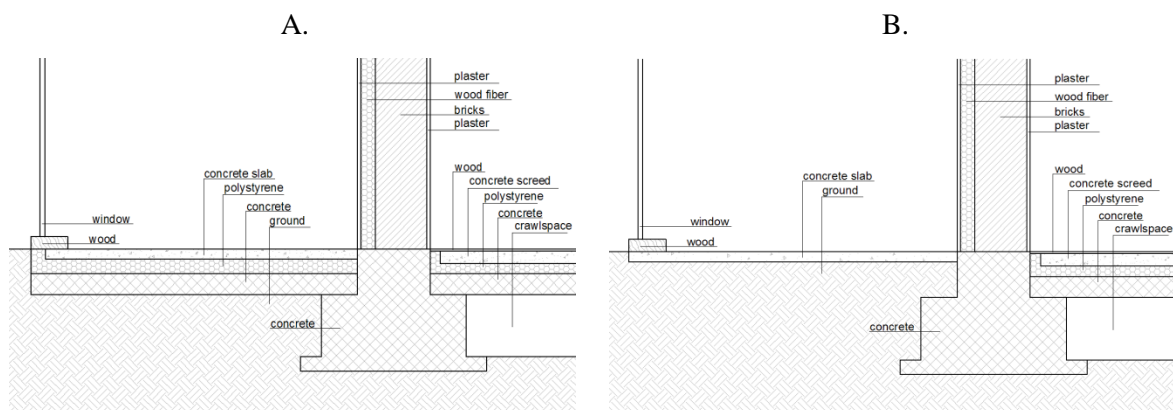


Figure 3.19 Geometry to calculate the thermal transmittance through the ground with FEM software A. with insulation B. without insulation

In Figure 3.20 the calculated increases in air temperatures due to solar radiation are presented.

The calculation was made through IDA-ICE. It is evident that if there is no heat insulation they are strongly lower. We can consider the dispersion of the heat having a solar origin through the ground subtracting from $Q_{abs,sur\neq p}$ the following term (compare with equation (3.53)):

$$F_{sh,ho} (1 - F_{F,e}) g_e \alpha_{ho} A_{ho} \frac{U_g}{h_{ho,int}} I_{ho} \tag{3.68}$$

where

$F_{sh,ho}$ is the shading factor from the point of view of the floor

α_{ho} is the absorption factor of the floor surface

$h_{ho,int}$ is the surface coefficient of heat transfer for internal horizontal surfaces

I_{ho} is the monthly solar radiation on horizontal surfaces

U_g is the thermal transmittance through the ground and it could be calculated through a FEM software or with the technical standard

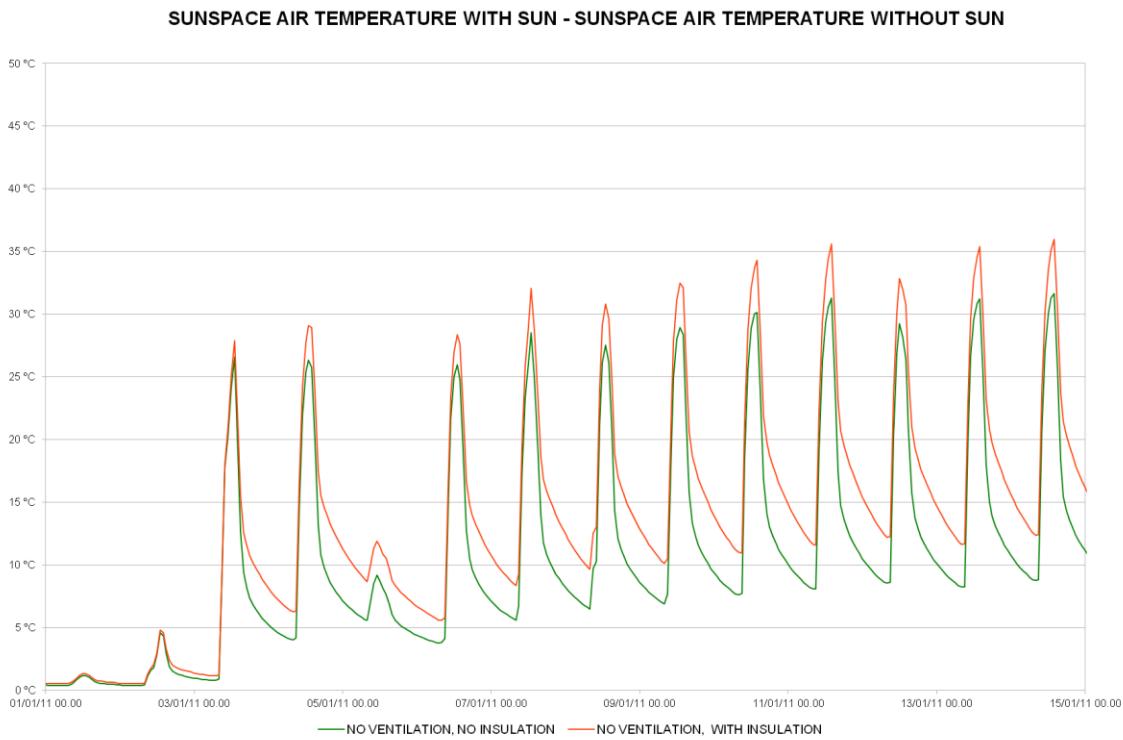


Figure 3.20 Temperature increase due to solar radiation in the case of insulated floor slab and in the case of uninsulated floor slab

3.2.4.6 Proposals of review of the technical standard: conclusions

Concluding, in a future revision of the ANNEX E of EN ISO 13790:2008 the following aspects should be considered:

1. For the radiation which enters heated space directly the global solar transmittance of the external envelope of the sunspace g_e is not involved. In fact, g_e considers also the convective exchange. The solar direct transmittance τ_e could be considered. A heat proportional to $(g_e - \tau_e)$ could be considered released by the external window of the sunspace to sunspace air as convective exchange. The relevance of this aspect should be better tested, considering a variety of situations.
2. Like in Oliveti, G. (2009), the suggested values of the correction factors F_w should be variable as function of the latitude, of the exposure direction and of the month (see paragraph 3.2.4.1 “Calculation of the solar heat entering the external windows”).
3. If a new version of the technical standard considered the reflections inside the sunspace, it should present graphs or tables to help the users to obtain the total absorbed heat, at least for the most common geometries. An approach similar to the Method 5000 (with the factors which correct the entering solar radiation in order to obtain the absorbed solar radiation; see Table 3.1) could be considered. It could take into account the studies of Wall, M. (1996) relative to the “solar collector property S” (see Chapter 2 “Literature overview”) and those ones of professor Oliveti.
4. A next version of the technical standard should consider the solar heat dispersions through opaque surfaces, in particular through the ground, which does not heat the sunspace air (see paragraph 3.2.4.5 “Solar heat dispersion through opaque surfaces”).

Before changing the technical standard a deeper analysis of benefits (typically greater precision) and costs (e.g. greater complexity for the users) of the proposals should be made, considering a great variety of cases.

3.3 Dynamic methods

The present research work does not have the aim to analyse deeply the dynamic models. Therefore the present paragraph provides only some information which can be useful in the context of the thesis.

For a really accurate design the use of dynamic models is advisable. In fact, they consider the thermal inertia effects (the materials adsorb and release heat and thus they change their temperature) in a much more realistic way than the “utilization factor”, which is used by the quasi-steady-methods. Moreover, generally the dynamic simulation programs use three-dimensional models, which allow a much more precise calculation of the radiative exchanges (shading effects, direct and diffuse radiation, I.R. exchanges...).

An overview of the features of a wide variety of building energy simulation programs is presented by Crawley, D.B., et al. (2008). Actually, keeping up with the different features characterizing new versions of simulation programs requires constant and demanding knowledge updates. In analysing glazed spaces we have to pay particular attention to how the

used calculation method models the solar radiation (distribution on external and internal surfaces, interaction with glazed surfaces), the surface convection, heat transmission through the ground, thermal bridges, air temperature, and ventilation.

For the development of some parts of the present work the software IDA – Indoor Climate and Energy (ICE) was used.

Björnsell, N. et al. (1999) states that for IDA-ICE:

“The mathematical models have been developed at the Royal Institute of Technology in Stockholm (KTH) and at Helsinki University of Technology within the framework of IEA SH&C Task 22”

and that:

“Most input parameters are grouped into objects, which in turn contain other objects”.

A Report of Task 22 Building Energy Analysis Tools (1999)¹⁰ observes that IDA-ICE *“treats the mathematical models as input data, thus allowing a user to simulate a wide range of system designs and configurations. Their main advantage is flexibility (...) One can build successively larger component model libraries”*. Generally, we can consider a model as an integration of many modules. For example, the model of a building is composed by zones, windows, air leakages, walls... For every type of “object” there is a specific model, whose parameters have to be fixed. In IDA-ICE the modules *“can be connected in arbitrary configurations and causality (what is calculated from what) is undetermined”*. The mathematical models are equation based.

Vuolle, M. (1999) observes that *“the equation-based tools are transparent; every variable, parameter and equation in the model is available for inspection. Every variable can be plotted”*. This is a very important feature for an accurate modeling and to analyse the involved physical quantities.

Figure 3.21 represents schematically the calculation of the solar radiation entering internal rooms in IDA-ICE. If the detailed model of the zones which is available in the library is used, the amount of solar radiation in internal rooms is calculated considering the geometry of the veranda, while the distribution of the solar radiation coming from verandas in internal rooms is simplified, because it is calculated by the module “Ray”, which does not consider the presence of the veranda.

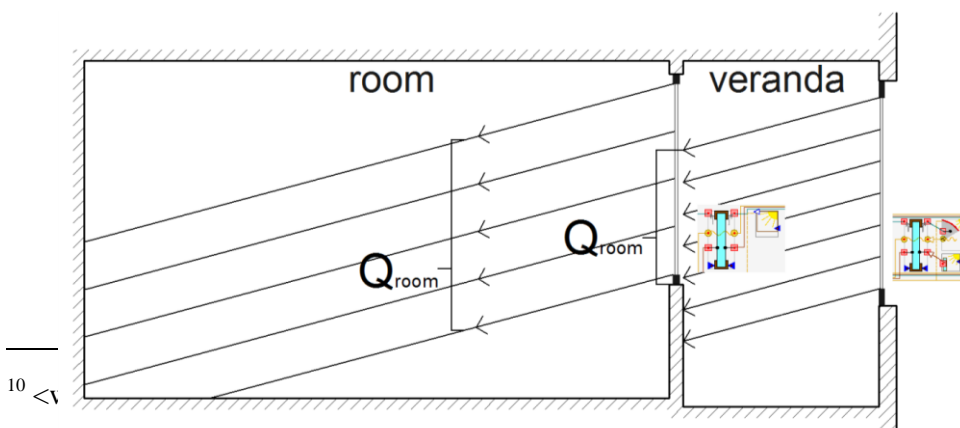


Figure 3.21 Scheme of the calculation of the solar radiation entering internal rooms in IDA-ICE

The radiation which is directly absorbed by the air is not considered. The heat balance of the air considers only the convective exchange with the surfaces which delimit the space. The radiation which is reflected by an internal surface is considered as diffuse radiation.

IDA-ICE calculates the convective exchange coefficients as a function of the slope of the surface temperature difference between the air and the surface and the, according to Brown and Isfält (1974). The function is graphically represented in the Figure 3.22.

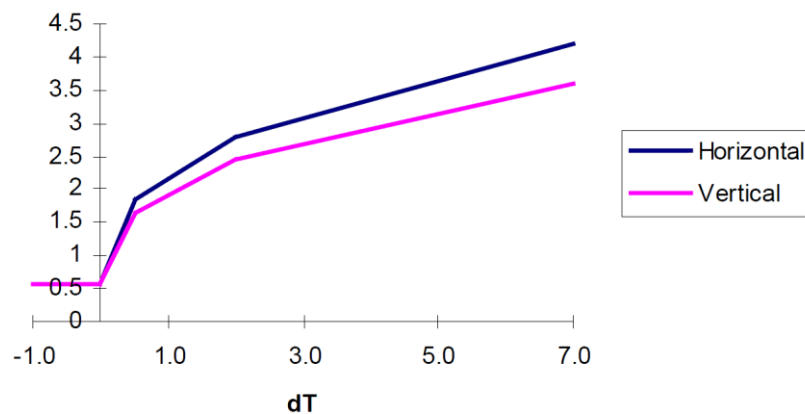


Figure 3.22 Convective exchange coefficients as function of the temperature difference between air and surface

IDA-ICE is not a Computational Fluid Dynamic software. Thanks to the available models library, it can handle well mixed air or a linear vertical gradient, which also is a simplification respect to the big variety of conditions which can occur. To estimate the air flows between zones IDA-ICE provides a fully integrated airflow network model which handles wind and buoyancy driven airflows through leaks and openings (see Kalamees, T. (2004)).

4. Scale models. An experimental case study in Trento (Italy)

4.1 Introduction to scale models

The goals of the work about scale models were:

- 1) To observe how the physical behaviour of sunspaces changes changing their dimensions. Understanding this issue could be useful to construct small sunspaces in order to forecast the behaviour of sunspaces having normal dimensions.
- 2) To achieve a deep comprehension of sunspaces through quantitative analyses of involved physical quantities.
- 3) To create dynamic models of sunspaces with an acceptable agreement with empirical data, in order to use the models to make new observations.



Figure 4.1 The two sunspaces during the construction phase

In 2010 a prototype and its scale model (halved linear geometrical dimensions) have been designed and constructed specifically for the present research work (see Figure 4.1). The frames were built in wood and double glazing windows were installed. The glazed part to total surface ratio is the same for both sunspaces. In order to permit the transverse ventilation, two windows for every sunspace, on the opposite short sides and at different heights, can be opened.

The smallest sunspace can be considered a reproduction of the biggest one from the geometrical point of view, but the involved physical phenomena change in different ways. The Table 4.1 reports how some important physical quantities change if the geometrical dimensions change.

Table 4.1 Relationships between geometrical dimensions and physical quantities

	small sunspace characteristic dimension L	big sunspace characteristic dimension $2L$
point thermal bridges	$k_{PTL} \Delta T$	$k_{PTL} \Delta T$
conduction through linear thermal bridges	$k_{TL} \Delta T L$	$k_{TL} \Delta T 2L$
heat conduction through surfaces	$k_{HC} \Delta T L^2$	$k_{HC} \Delta T 4L^2$
entering solar radiation	$k_{SR} I L^2$	$k_{SR} I 4L^2$
thermal inertia	air: $k_A L^3$ floor: $k_F L^2$	air: $k_A 8L^3$ floor: $k_F 4L^2$

It is approximately supposed that the linear thermal bridges do not change their values changing the linear dimensions. With the letter k are indicated physical quantities which are independent from the geometrical dimensions.

In addition to physical quantities reported in the Table 4.1, we should consider that changing the scale also the convective coefficients change, with laws depending on the type of convection (natural or forced), on the type of heat exchange (laminar, turbulent, intermediate), on the geometry and on the orientation of the surface. The resolution of such a problem is not easy and its generalization for different geometries and different properties seems impossible.

We can observe that the relative importance of thermal bridges, in comparison with other phenomena, is greater for the small sunspace than for the big one. For example, the ratio

between conduction through linear thermal bridges and the entering solar radiation is $\frac{k_{TL} \Delta T}{k_{SR} I L}$

for the small sunspace and $\frac{k_{TL} \Delta T}{2k_{SR} I L}$, i.e. the half, for the big one.

For the small sunspace the global heat transfer coefficient is calculated equal to 8,6 W/K and for the big one equal to 27,3 W/K. The ratio between them is 3,2.

In literature there are a lot of examples of scale models which were utilized to transfer the results of the scale model to an object having normal dimensions. Some examples are provided in paragraph 2.4 of the literature overview. Typically, the scale model is designed in order to obtain the thermal similarity with the model having normal dimensions. Among the found examples that one which is closest to the case of sunspaces is Grimmer, D.P. et al. (1979), but in that case

the thermal behaviour was easier than in the case studied in the present thesis, because the heat transfer was almost one-dimensional. Because of the complexity of the problem (dynamic and three-dimensional phenomena), achieving similarity for sunspaces seems impossible, at least when thermal bridges and three-dimensional phenomena have an important role. Nevertheless, a comparison between the small sunspace and the big one was possible, but without a generalisation valid for every case. The next paragraph shows the analysis of the monitored data while paragraph 4.3 shows the results of modelling activity.

4.2 Monitoring

A monitoring campaign started in January 2011 and finished in July 2011, in Trento. The sunspaces are oriented 27° west of due south.



Figure 4.2 The two sunspaces attached to the container and the measuring instruments

Sensors monitored:

- weather conditions (temperature, relative humidity, solar radiation, wind velocity and direction);
- temperatures of external surfaces;
- conditions of both sunspaces (air temperatures, which in both sunspaces have been monitored at two different heights, RH, surface temperatures, air velocity);

- container conditions (air temperature, surface temperatures, RH, heat fluxes from the external walls which separate the container from the sunspaces).

Positions of the sensors in the two sunspaces respect the proportionality factor, i.e. in the smaller sunspace the distances relative to the sensors are half the corresponding ones in the bigger sunspace (see Figure 4.3).

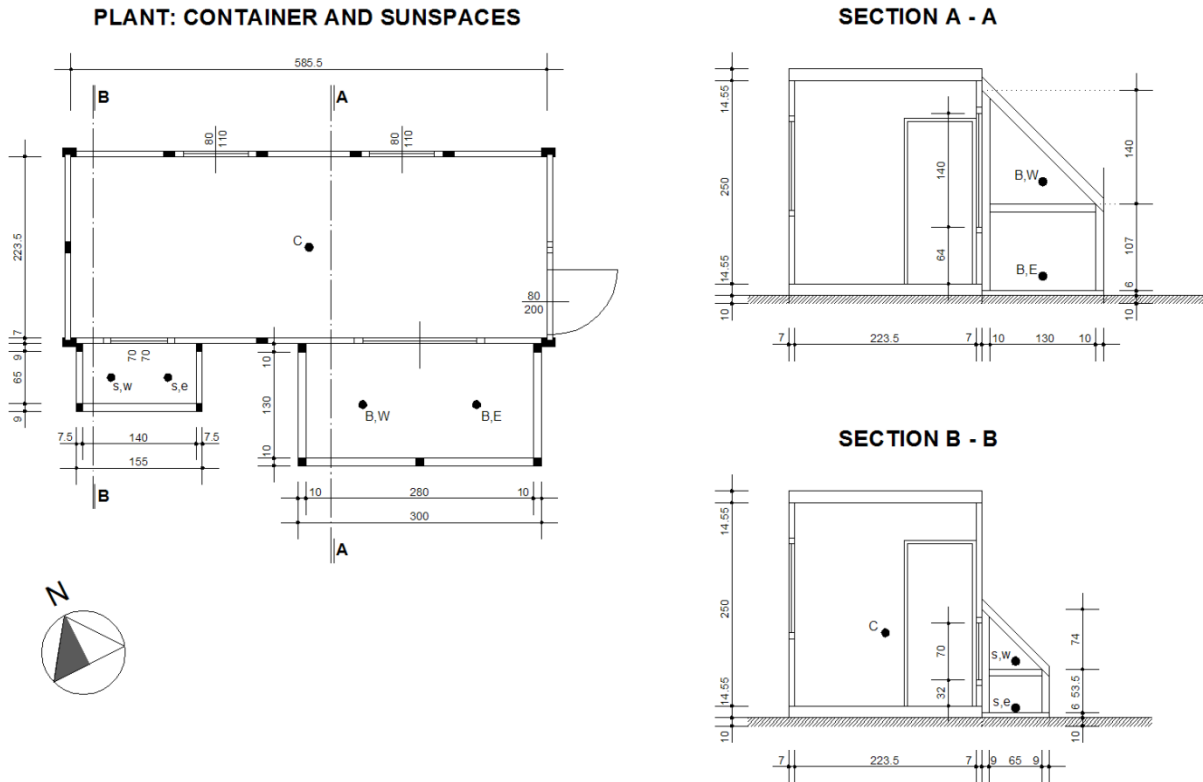


Figure 4.3 Position of the air temperature and relative humidity sensors.

B = bigger sunspace; s = smaller sunspace; w = west; e = east

The utilized measuring instruments are produced by the Laboratori di Strumentazione Industriale from Milan¹¹.

In the weather station the instruments are connected to an E-Log data-logger and they are:

- thermo-hygrometer DMA 527 with antiradiant shield DYA230 and natural ventilation

	Temperature	Rel. humidity
Range	-30÷70°C	0÷100%
Sensitive element	Pt100 1/3 DIN-B	Capacitive
Accuracy	±0,1°C (0°C)	1,5% (if 5÷95% and 23°C) 2% (if <5 or >95% and 23°C)
Response time (Sens. element)	10s	
Operating temperature	-40°÷95°C	

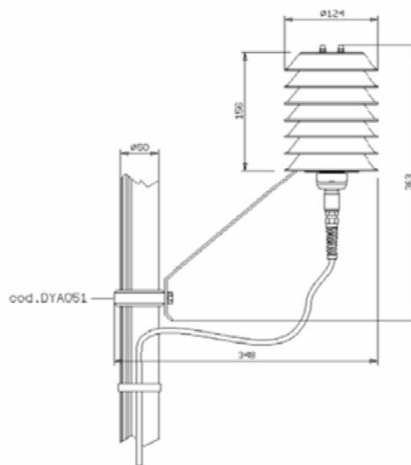


Figure 4.4 Thermo-hygrometer DMA 527

- global radiation sensor DPA047. It was installed horizontally

Sensitive element	Photodiode
Spectral range	300÷1100 nm
Range	<2000 W/m ²
Output (Sensitivity)	10 V/Wm ⁻²
Total achievable daily uncertainty	<10%
Response time (90%)	50 ms

¹¹ www.lsi-lastem.it

Temperature dependence of sensitivity	0,05% sensitivity/°C
Environmental limits	-40° ÷ 80°C

- CombiSD, combined wind speed-direction sensor DNA 021

Principle of operation	3 cups and vane anemometer
Speed sensor	Optoelectronic disk
Direction sensor	2000 Ohm wire potentiometer
Housing	Heavy gauge anodised aluminium
Damage threshold	>75 m/s
Operating temperature	-30 ÷ 70 °C
Speed	
Measurement range	0 ÷ 60 m/s
Threshold	0,38 m/s
Response time (63% at 5 m/s)	0,8 s
Resolution (integration time=1s)	0,05 m/s
Accuracy and linearity	0,1 m/s+1% VL (readout)
Direction	
Measurement range	0 ÷ 360°
Threshold	0,15 m/s
Response time (at 5 m/s)	0,26s
Damping coefficient (VDI 3786)	0,21
Overshoot ratio	0,25
Transfer function	Dir(°)= 355 x R(Ohm)/2000
Resolution	0,1°
Accuracy	1% FS (Full scale)

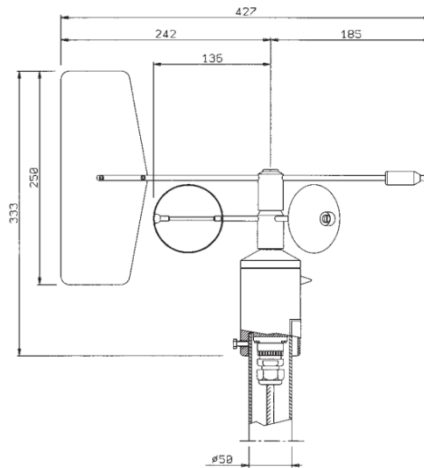


Figure 4.5 Combined wind speed-direction sensor DNA 021

In the sunspaces the data were stored in data-loggers BABUC/A.

The thermo-hygrometers were:

- BSU102 psychrometric probe with forced ventilation and distilled water tank (ISO 7726 standard) at the lower height

Temperature measurement range	-5 ÷ 60°C
Temperature accuracy	0,15°C (for 0°C)
Humidity measurement range	0÷100%
Humidity accuracy (T = 15÷45°C)	2%
Response time (T90)	1,5 minutes
Resolution	%Rel 0,1%
Sensitive element	2xPt100 1/3 DIN

- thermo-hygrometers BSU 104 at the higher height

Sensitive element	2 Pt100 1/3 DIN-B
Measure physical quantities	Dry-bulb temperature and dew-point temperature
Range	Temp. -50 ÷ +150°C, RH%: 0÷100%
Accuracy T	0,1 °C if T = 0°C (DIN-IEC751)
Accuracy RH	1,0 % if T=15÷25°C and RH = 70÷98 % 1,5 % if T=15÷25°C and RH = 40÷70 % 2,0 % if T=15÷25°C and RH = 15÷40 %
Resolution RH	0,1%
Response time (T90)	2 minutes
Forced ventilation	>3 m/s

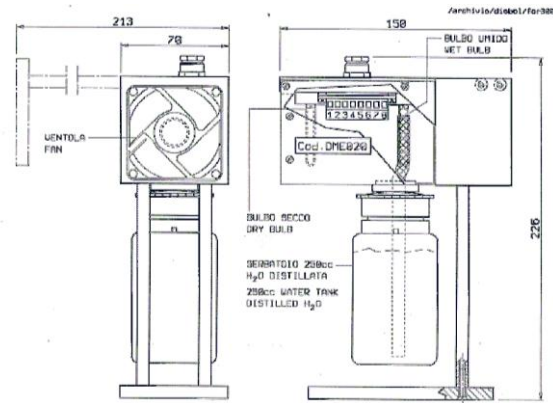


Figure 4.6 Thermo-hygrometer BSU 104

The main properties of the sensors for surface temperature are as in the following table.

range	max +80°C
accuracy	0,15°C (if T = 0°C)
sensitive element	Pt100 DIN-A



Figure 4.7 Inside the sunspaces the thermo-hygrometric conditions were measured at two different heights. The sensors were shaded in order to avoid the heating due to the incident solar radiation. Moreover, the air velocity and the surface temperatures of the glazed roof panel, of the floor and of the wall were monitored

The data stored during the monitoring campaign have been analysed.

The following pictures represent the air temperatures within the sunspaces and the surface temperatures of the three main elements (wall of the container, floor, windows) which delimit the sunspace. Those surface sensors are all on the inner side, from the point of view of the sunspaces. The “window temperatures” refer to the inner surfaces of the glazed roof panels.

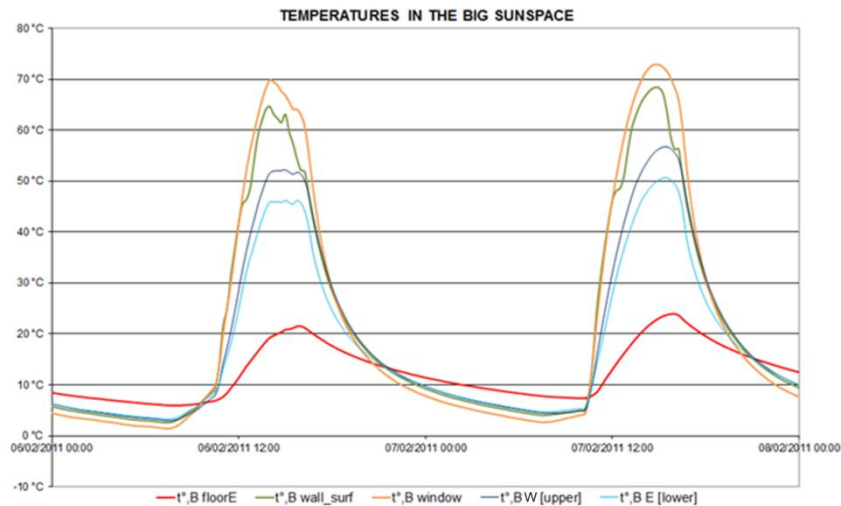


Figure 4.8 Temperatures monitored in the big sunspace: 3 are surface temperatures, 2 are air temperatures

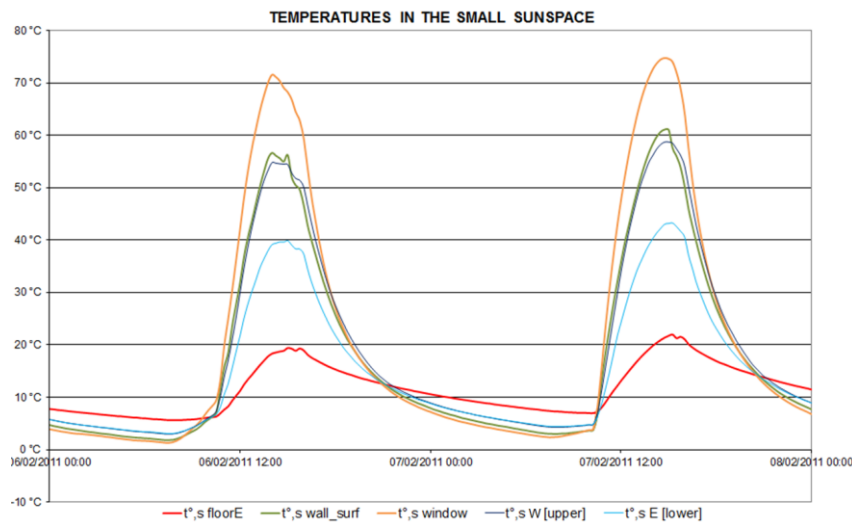


Figure 4.9 Temperatures monitored in the small sunspace: 3 are surface temperatures, 2 are air temperatures

It is possible to observe that, except for the floor, during the day/night cycle the temperature oscillations are very big. The floor temperatures are the lowest ones during the day and the highest ones during the night because of the thermal inertia of the ground.

The highest temperature values are in correspondence of the windows. In the smaller sunspace the temperature peaks of the floor and of the wall are lower than in the bigger one while it is

possible to observe that for the windows the difference between the big sunspace and the small one is small. Probably the reason is that the window is the surface which is less influenced by thermal bridges, which in comparison with the entering solar radiation are more important in the small sunspace than in the big one.

Considering the air temperatures, the temperatures of the lower sensor are closer to the floor temperature, obviously because of physical proximity.

During the night the window temperature and the wall surface temperature are similar. We have to consider that the container was not heated mechanically. If the container was heated, surely the wall temperature would become greater.

In some periods also the air velocity inside the sunspaces was measured.

Figure 4.10 shows that there are times when the temperatures of the different monitored points inside the sunspace are very similar: in those conditions, being the windows closed, the air velocity has its minimum values. The maximum velocities are in correspondence of the greatest differences among the internal surface temperatures.

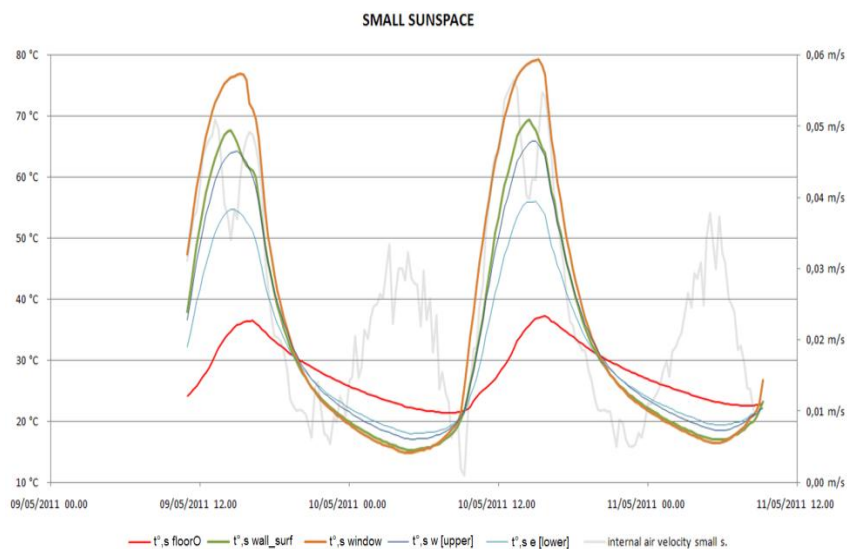


Figure 4.10 Surface temperatures and air velocity within the small sunspace

Because of the big differences among the temperatures of the different surfaces which define the sunspace envelope, within the sunspaces the monitored air temperatures vary a lot changing the position of the sensor. Approximately, the mean air temperature within the sunspaces can be considered as a weighted mean of the surface temperatures and the weights are the products between the surface heat transfer coefficients and the surface areas $h_i A_i$.

In some periods the windows between the sunspaces and the external environment were opened as hopper windows. An anemometer measured the internal air velocity. As the Figure 4.11

shows, the air velocity in the sunspace is obviously strongly influenced by the external wind velocity.

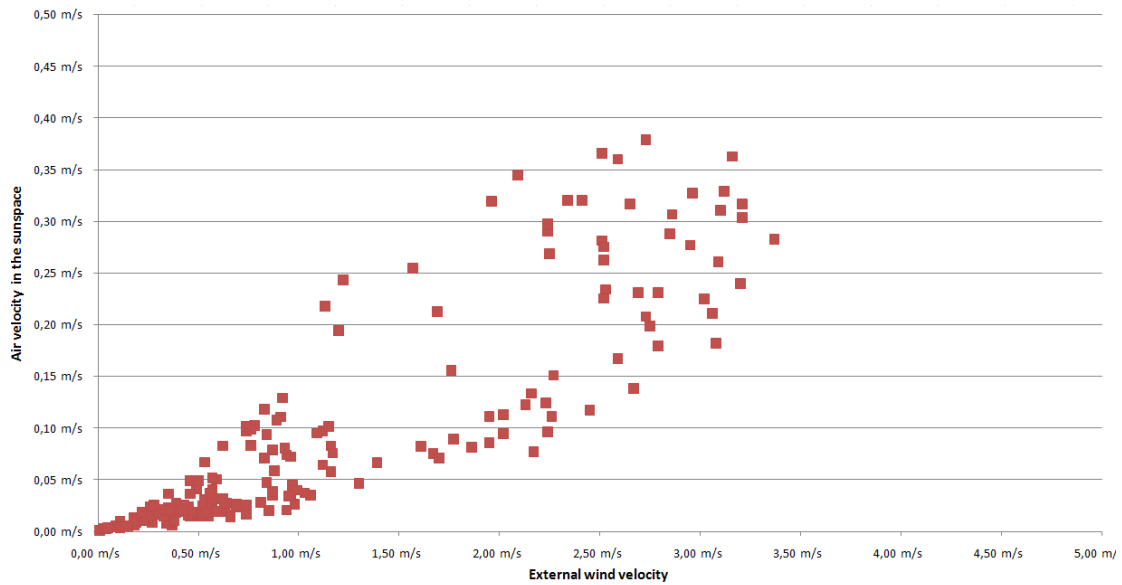


Figure 4.11 Relationship between external wind velocity and air velocity in the sunspace

Also the temperature difference between the sunspace and the external environment influences the internal air velocity: in fact for values of that difference greater than 35°C the air velocity was always greater than $0,2\text{ m/s}$ and for values of that difference smaller than 20°C the air velocity was always less than $0,15\text{ m/s}$ (Figure 4.12).

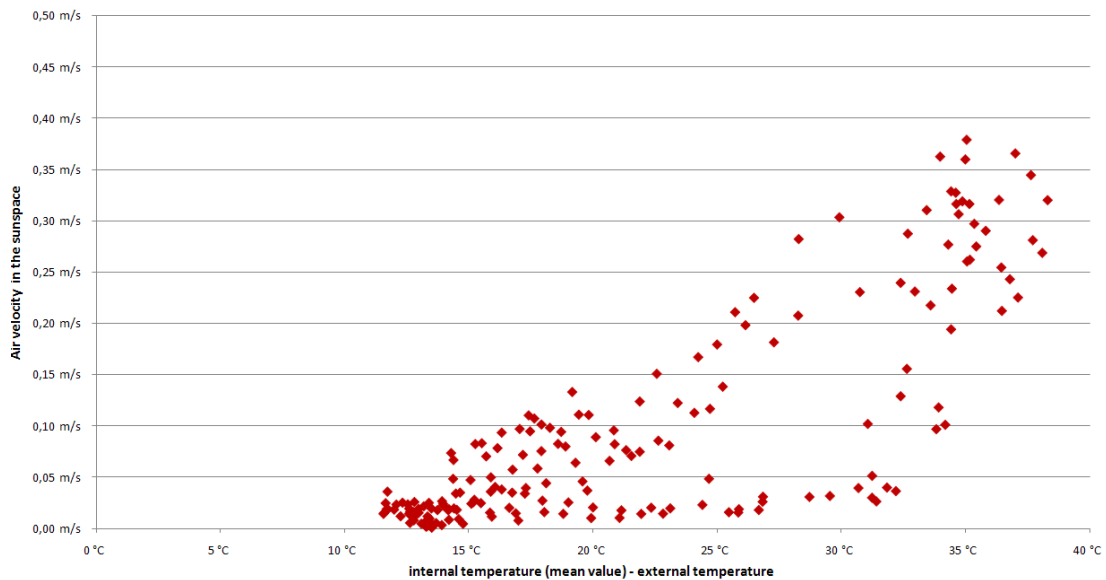


Figure 4.12 Influence of temperature difference between sunspace and external environment on the air velocity in the sunspace

In Figure 4.13 some temperature fluctuations outside container and sunspaces are plotted. Also

outside the sunspaces the ground temperature during the night remains higher than the air temperature and during the diurnal hours the wall surface becomes warmer than the ground surface.

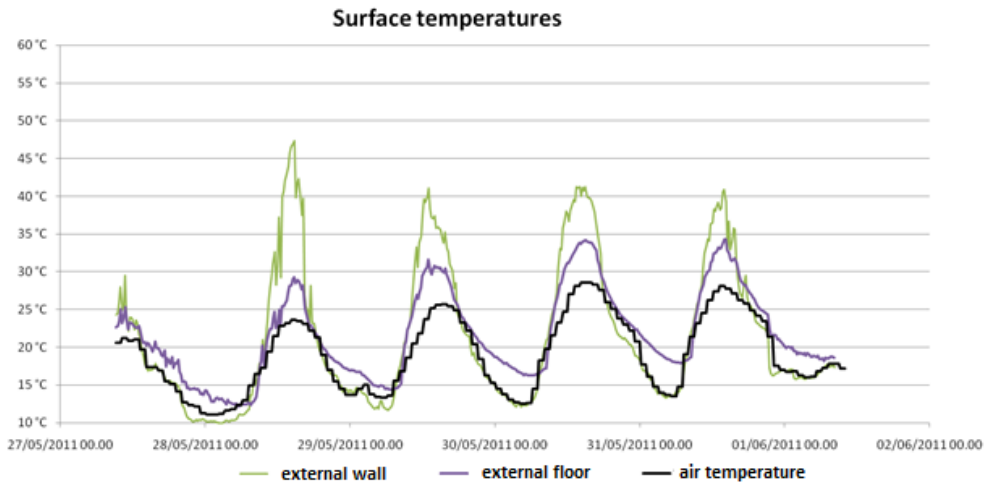


Figure 4.13 Temperatures outside container and sunspaces

During the night the external wall temperature is practically equal to the air temperature also because the container was not heated (anyway the Figure refers to May, therefore in that period heating would not have been necessary also in a real building).

In every sunspace two temperature sensors, in two different positions, monitored the floor surface temperature.

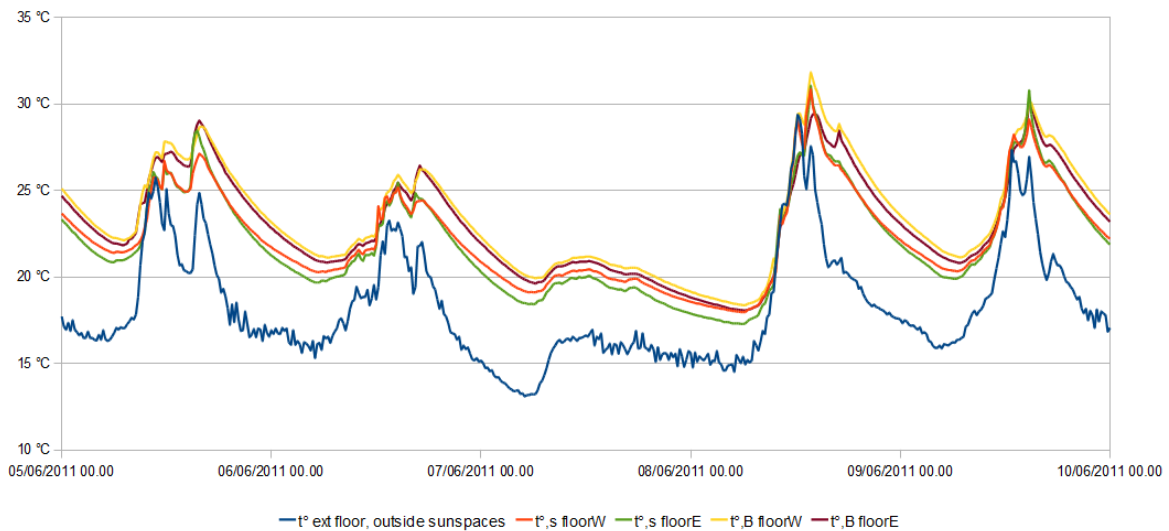


Figure 4.14 Temperatures of the floor inside sunspaces and outside them.

Figure 4.14 shows that changing the position of the sensor on the floor its temperature changes. The floor temperatures in the sunspaces are higher than the external floor temperatures even

during the night. The floor temperatures are lower in the small sunspace than in the big one because of thermal bridges.

5 litre water tanks were inserted in the small sunspace to see how their inertia influences the monitored data. Since the 13th March until the 22nd March two tanks were at the floor. On the 22nd March one was moved: from east to west and at a higher height. The Figure 4.15 shows the surface temperatures on the inner side of the external upper windows of the two sunspaces. Until 22nd March the peaks of the window temperature were higher for the smaller sunspace, after the water tank was moved they became very similar. It is a little example of the effect of the position of water on the inner temperatures. The closeness between the temperatures suggests that the shadow of the big sunspace has little effect on the small one.

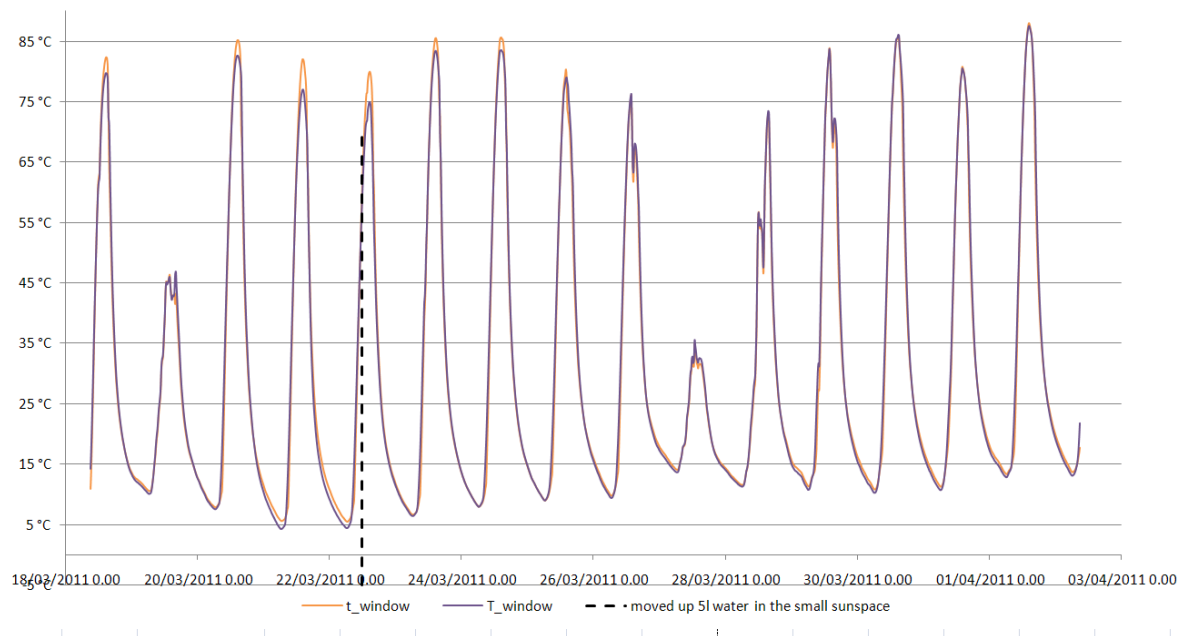


Figure 4.15 The temperatures on the inner side of the external tilted window for the two sunspaces. The time when the tank of water was moved is showed.

The effect is visible also considering the temperatures on the floor. In the smaller sunspace the movement of the water from east to west has as effect the increase of the peaks of the sensor placed towards the east.

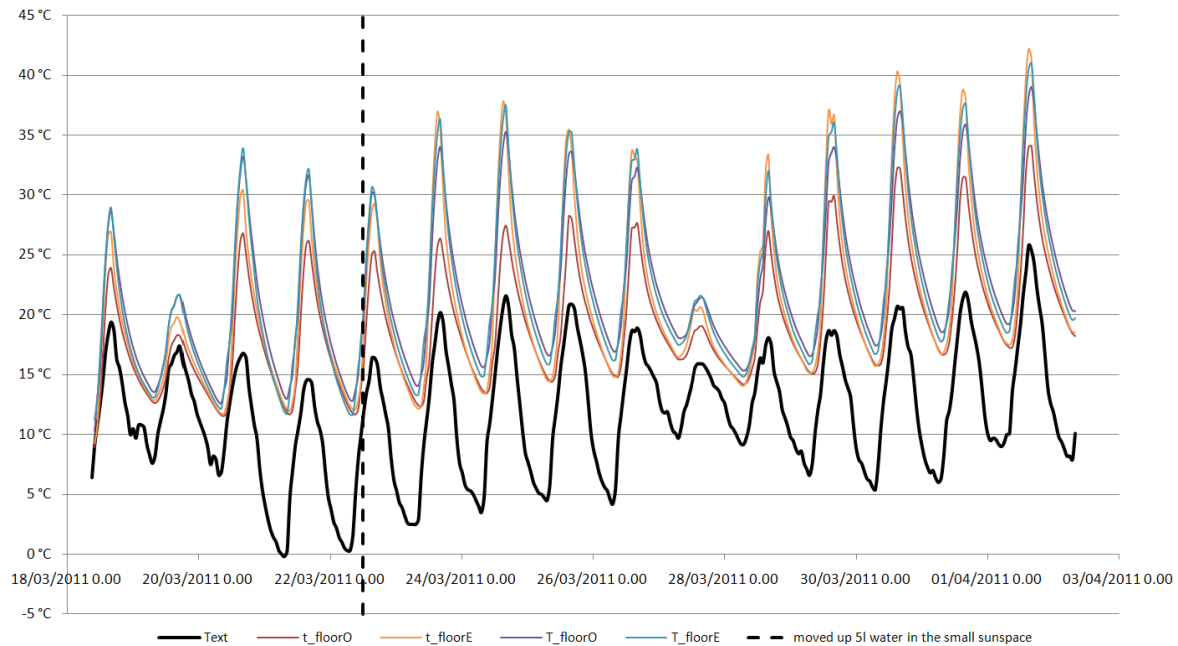


Figure 4.16 Temperatures on the floors of the two sunspace (2 sensors for every sunspace). The time when the tank of water was moved is showed.

4.3 Modelling

The two sunspaces have been modeled using the software for dynamic simulations IDA-ICE. In such a model the radiation which is directly absorbed by the air is neglected. The heat balance of the air considers only the convective exchange with the surfaces which delimit the space. The radiation which is reflected by an internal surface is considered as diffuse radiation. The main problematic aspects of modeling such sunspaces are:

1. The air temperature is not spatially uniform. The main reasons for the spatial non-uniformity are: the inner surfaces have very different temperatures, there is internal mass which is not equally distributed and the air is thermally stratified (the warmer air has a lower density). The non-uniformity of the air temperature was not considered, because IDA-ICE is not Computational Fluid Dynamics software and does not have the capability to model adequately the spatial variations in air temperature. Therefore the comparison between monitored data and simulation results was made considering the surface temperatures of floor, container wall and window. A study with a CFD could be useful also for a better estimation of the surface heat transfer coefficients. IDA-ICE calculates the convective exchange coefficients as a function of temperature difference between the air and the surface and the slope of the surface, according to Brown and Isfält (1974). The function is graphically represented in the Figure 3.22.
2. The heat dispersion through the floors is strongly tridimensional, also because the floors are not insulated and rather small. Kreider et al. (2002) states that: “*Ground thermal coupling*

calculations have probably been the least accurate of any in building thermal analysis. Fortunately for designers of commercial buildings, basement and slab heat losses are a small portion of the total heat load” (p. 35). Unfortunately, in the case of the studied sunspaces the slab heat losses are not a small portion.

The thermal bridges in sunspaces which have been installed directly on a concrete slab have a very important role. Simulation programs like IDA, which can model the heat conduction through opaque elements of the envelope with a network Resistances – Capacities or with the finite differences method, model the heat conduction in one-dimensional ways. Therefore to have a good evaluation of the heat transfer through the ground a finite element calculation of thermal bridges was made with the software COMSOL Multiphysics. In COMSOL the heat transmission through the ground was calculated three-dimensionally within a stationary model (see Figures 4.17 and 4.18). The results have been used inside the dynamic model of IDA-ICE.

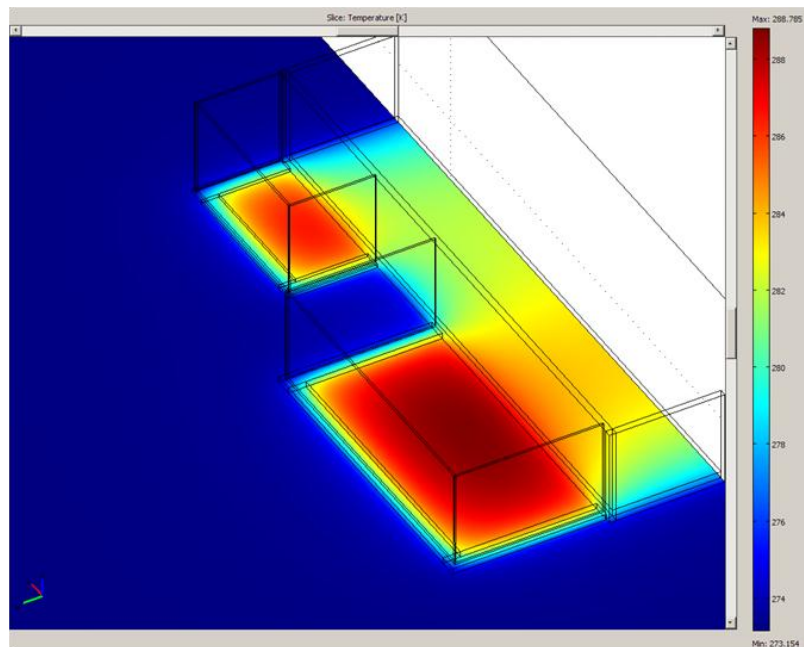


Figure 4.17 Horizontal section of the results of the finite-element calculation

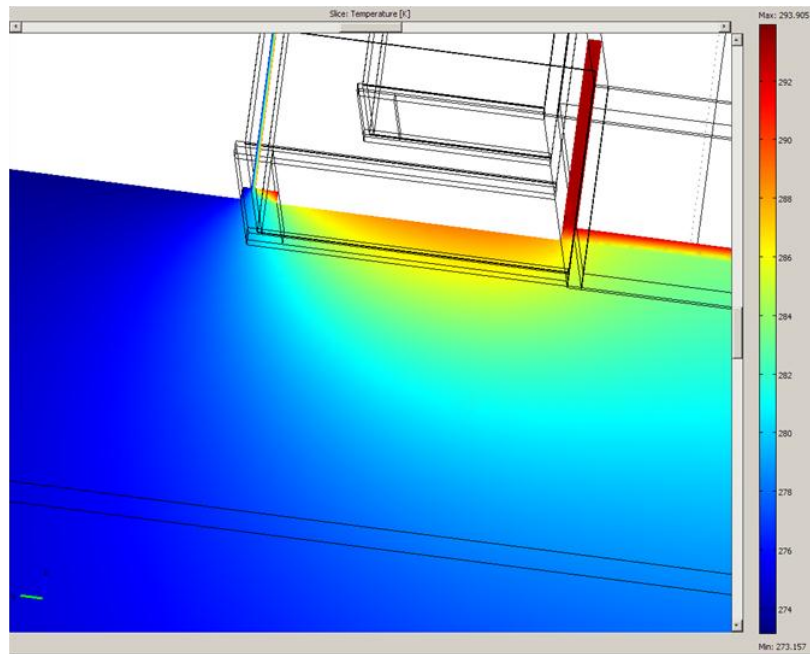


Figure 4.18 Vertical section of the results of the finite-element calculation. The floor of the container is insulated.

As boundary conditions, in the internal environments the temperature is imposed equal to 20°C and in the external one equal to 0°C. The thermal transmittance of the floors were calculated as the ratio between the total heat passing from the floors and the product of the corresponding floor area and the temperature difference between the internal and the external environment:

$$U_{\text{suns.floor}} = \frac{\Phi_{\text{suns.floor}}}{\Delta T \cdot A_{\text{suns.floor}}} \quad (4.1)$$

That thermal transmittance considers the heat passing through the sunspace frames and the thermal bridge effects between the ground and the wood frame as well.

The results were $U_{\text{suns.floor}} = 2,2 \text{ W} \cdot \text{m}^{-2} \text{K}^{-1}$ for the small sunspace and $U_{\text{suns.floor}} = 1,8 \text{ W} \cdot \text{m}^{-2} \text{K}^{-1}$ for the big one. The difference is due to the greater importance of thermal bridges for the small sunspace.

In the physical reality the heat flows from the sunspace floor both towards the external air than towards deeper layers of the soil. Therefore, the coupling of slab and ground can be considered as a division among three different environments: the sunspace, the external air and the deeper layers of the soil. The problematic issue is that in IDA the coupling slab-ground is modeled one-dimensionally and at the bottom side the temperature is considered constant. Generally, during the winter season the deeper layers of the soil are warmer than the external air, while during the summer season they are colder. The reason is the soil thermal inertia. The simulations were made on monthly basis, because having a constant temperature at the bottom side of the ground throughout the year would be a too rough approximation. During the winter the

temperature T_v at the bottom side was imposed equal to the average monthly external temperature while during the summer it was imposed equal to the estimated average ground temperature at a depth of 50cm.

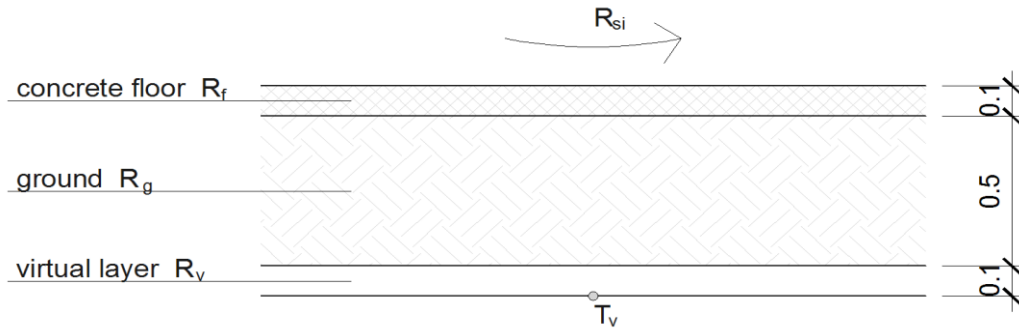


Figure 4.19 The modelled stratification of the coupling of concrete slab and ground

As the Figure 4.19 shows, the coupling of slab and ground was modeled with three layers. The lowest layer is a “virtual layer”, i.e. of a “virtual” material whose conductivity was imposed in order to obtain the thermal transmittance calculated through COMSOL. Therefore the conductivities of the virtual layers of the two sunspaces are different.

$$R_{tot} = R_{si} + R_f + R_g + R_v \quad (4.2)$$

where

R_{si} is the convective resistance between the floor and the air inside the sunspace

R_f is the resistance of floor slab, which is made by concrete

R_g is the resistance of the ground layer

R_v is the resistance of the virtual layer and it is calculated as following

$$R_v = R_{tot} - R_{si} - R_f - R_g = R_v = 1/U_{suns.floor} - R_{si} - R_f - R_g$$

The density of the virtual layers was imposed 1kg/m^3 and its thermal capacity $1\text{ J}/(\text{kg}\cdot\text{K})$

In order to estimate the emissivity and the solar absorptance of the external surfaces of the container and of the concrete slab, the temperatures of those surfaces were monitored also outside the sunspaces. In the model the values of emissivity and solar absorptance were adjusted in order to have a good agreement between the results of the simulation and the monitored data. The Figure 4.20 shows that with $\varepsilon = 0,85$ and solar absorptance $a = 0,3$ the agreement is generally acceptable (in some days good).

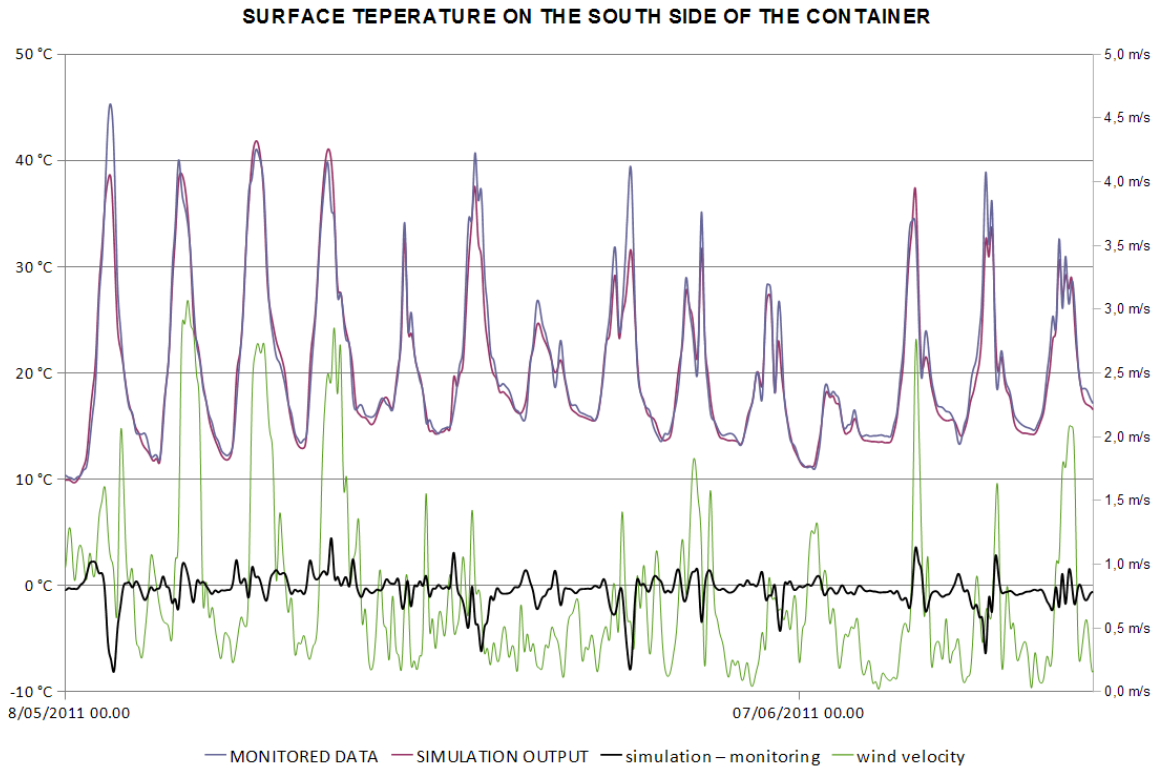


Figure 4.20 Comparison between the monitored temperatures of the container surface and the simulated temperatures with emissivity $\varepsilon = 0,85$ and solar absorptance $a = 0,3$

In the Figure also the wind velocity was plotted and so we can observe that the errors are independent on wind velocity, i.e. on the extent of the convective exchange. It was observed that they are independent also on solar radiation, i.e. on the extent of the radiative exchange.

In following pictures the comparison between the simulations and the monitored data in terms of temperatures of the surfaces inside the sunspaces is presented.

Because of the greater relative importance of the thermal bridges, the peaks are lower in the small sunspace.

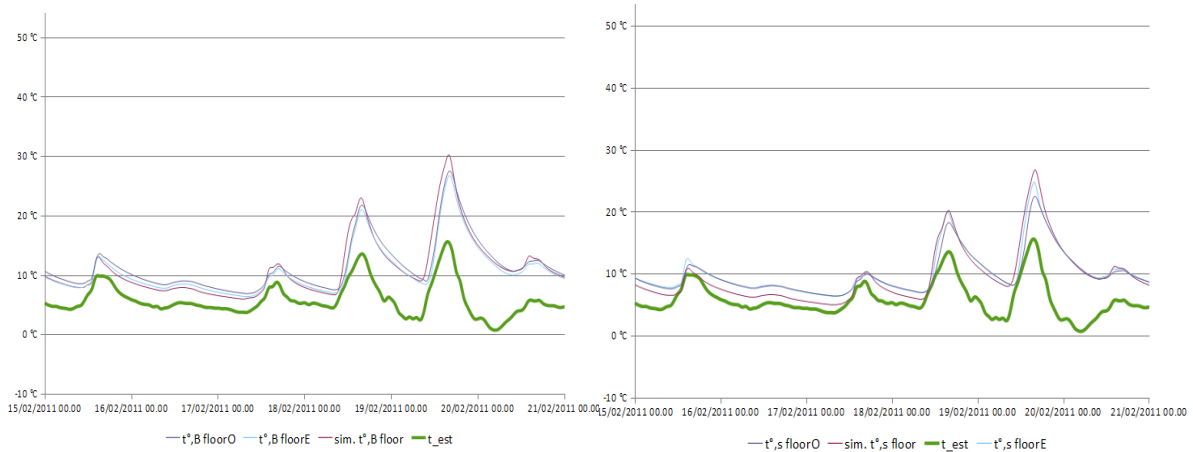


Figure 4.21 Simulated and monitored floor temperatures in February Left: big sunspace. Right: small sunspace

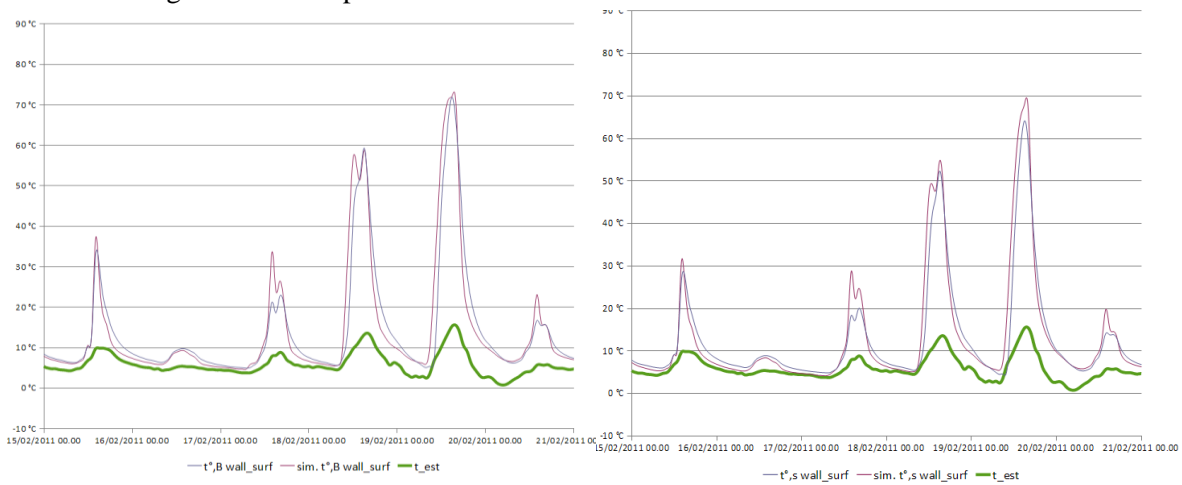


Figure 4.22 Simulated and monitored wall temperatures in February. Left: big sunspace. Right: small sunspace.

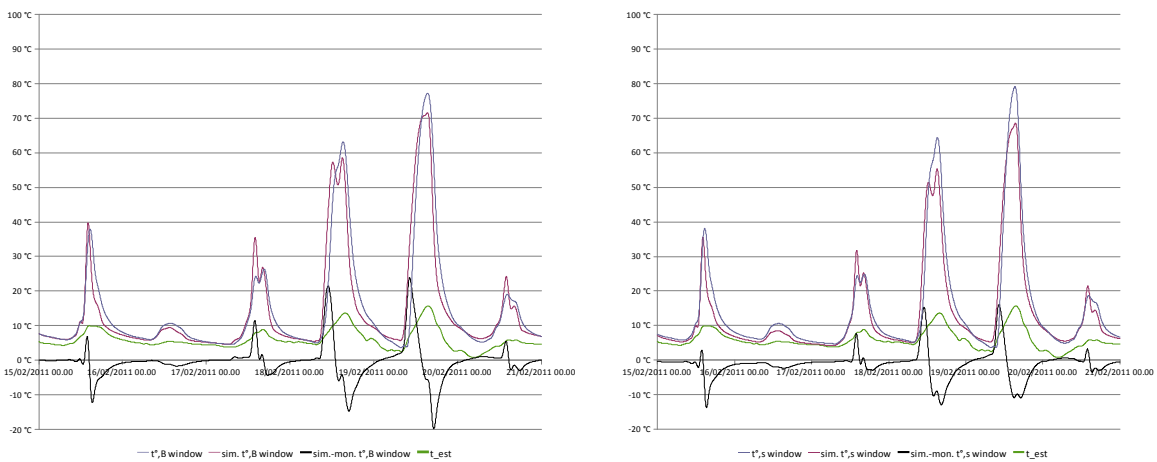


Figure 4.23 Simulated and monitored window temperatures in February. Left: big sunspace. Right: small sunspace.

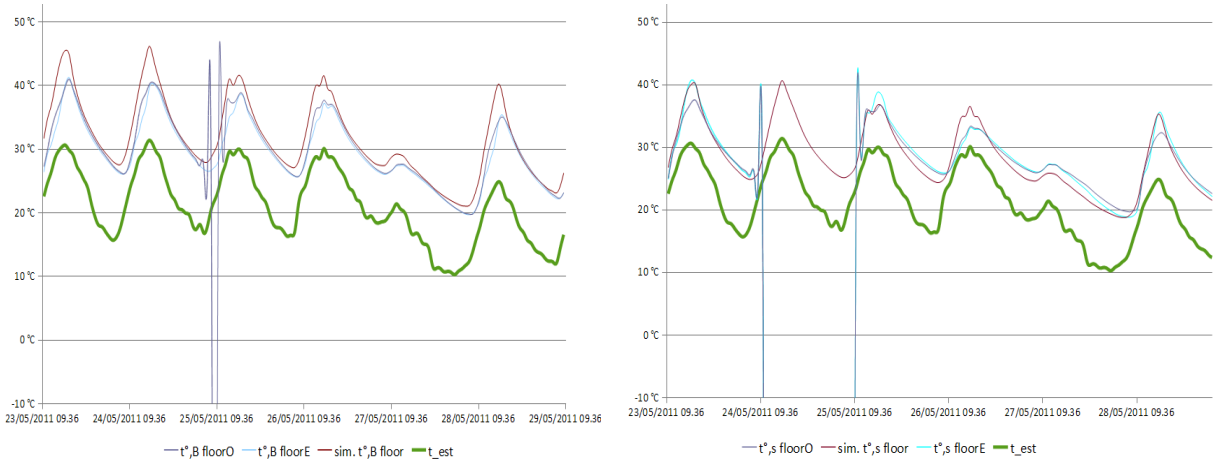


Figure 4.24 Simulated and monitored floor temperatures in May. Left: big sunspace. Right: small sunspace.

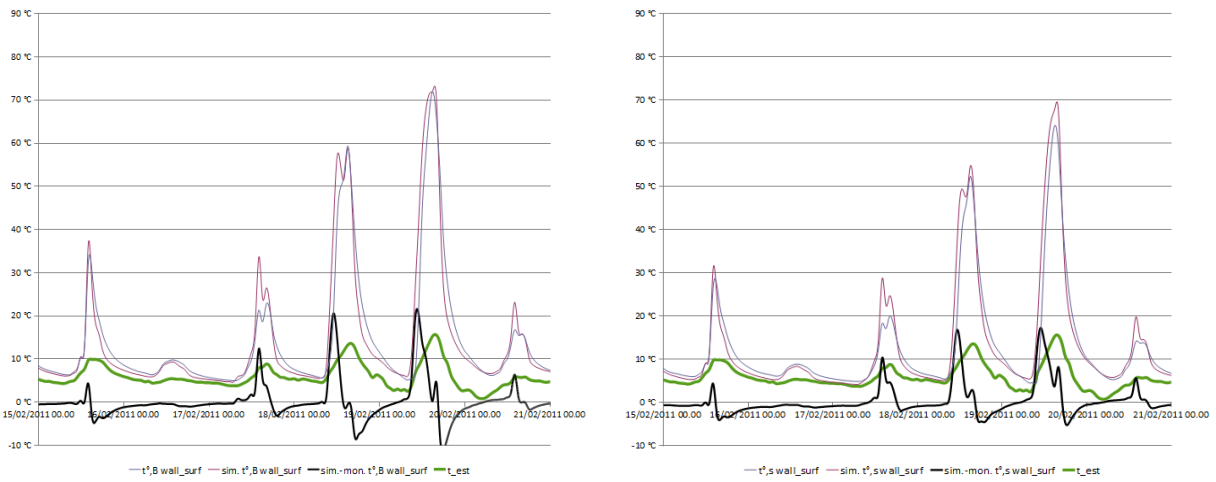


Figure 4.25 Simulated and monitored wall temperatures in May. Left: big sunspace. Right: small sunspace.

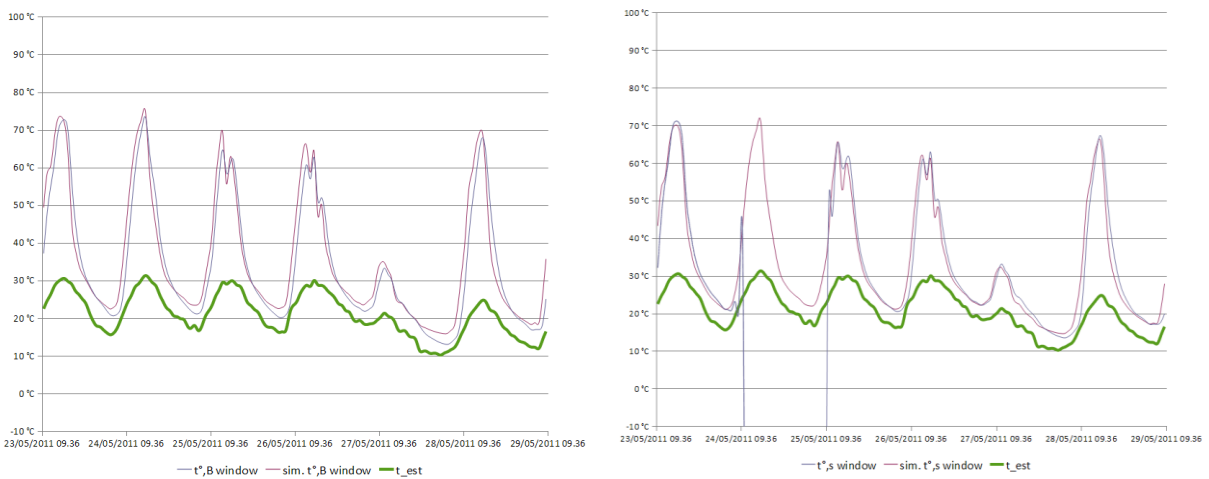
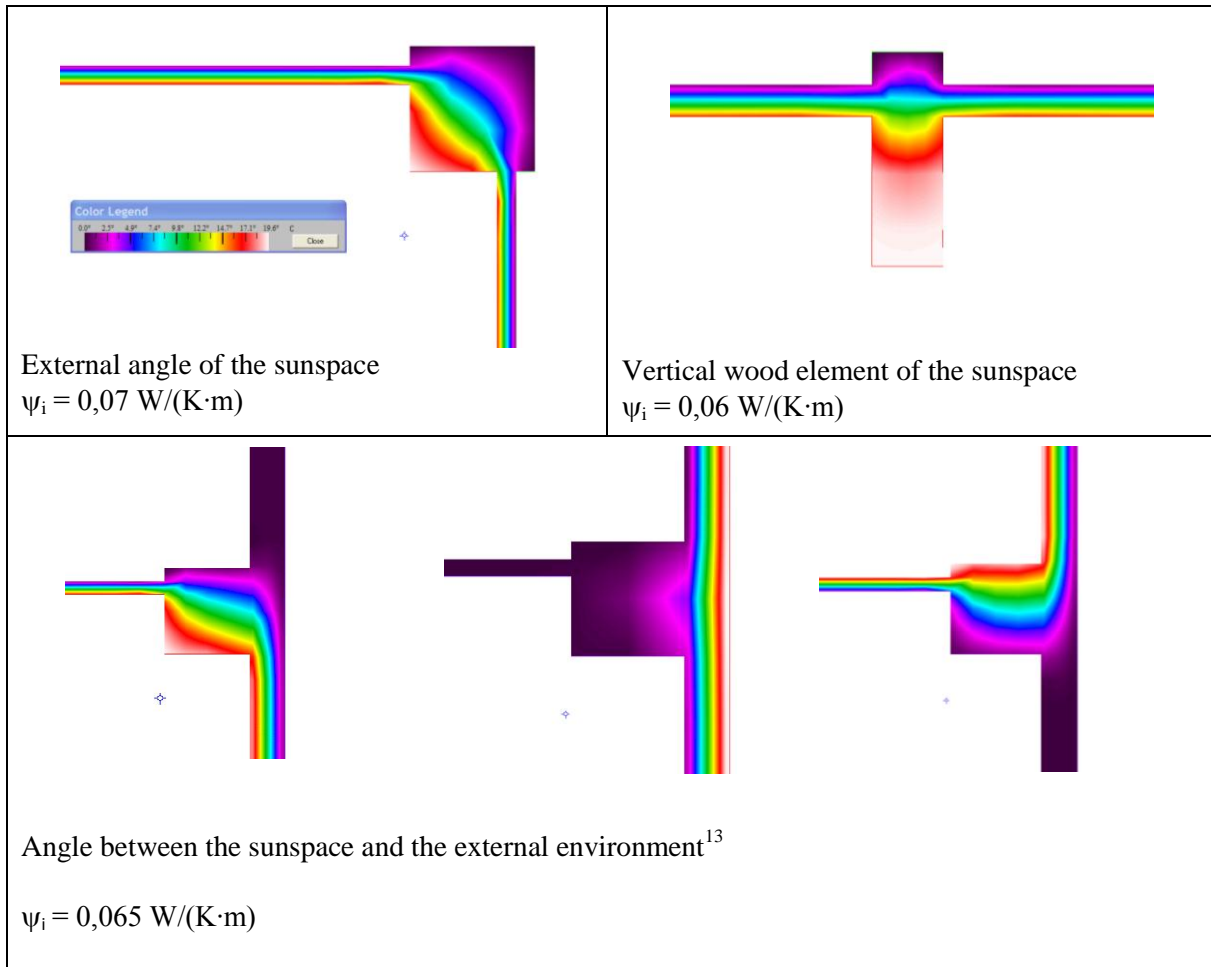


Figure 4.26 Simulated and monitored window temperatures in May. Left: big sunspace. Right: small sunspace

Other thermal bridges were calculated with the FEM software THERM¹².

Between the container and the sunspaces' frame in order to decrease the heat dispersion and to improve the adhesion polyurethane foam was inserted. That aspect was not modelled and in THERM a perfect adhesion between the wood frame and the external surface of the container was supposed. The results of the thermal bridges calculation is presented in the Table 4.2.

Table 4.2 Results of calculation of the thermal bridges between the sunspace and the external environment



A comparison of the values of the daily temperature peaks of the two sunspaces was made on the basis of the results of the dynamic simulations, which can be considered an acceptable approximation of the real data. In the following figures on the horizontal axis there is the global solar radiation when the daily peak is reached, on the vertical axis there is the difference of the temperature peaks between the two sunspaces (temperatures on the floor). The comparison was possible because the daily peaks in the two sunspaces occur practically at the same time (see e.g.

¹² <<http://windows.lbl.gov/software/therm/therm.html>>

¹³ Because three different environments (the external one, the container and the sunspace) are adjacent, to calculate the linear transmittance the calculation of the heat transfer has to be done with three different boundary conditions. See EN ISO 10211:2008

the Figures 4.8 and 4.9). Generally, with higher values of the solar radiation the difference between the peaks increases.

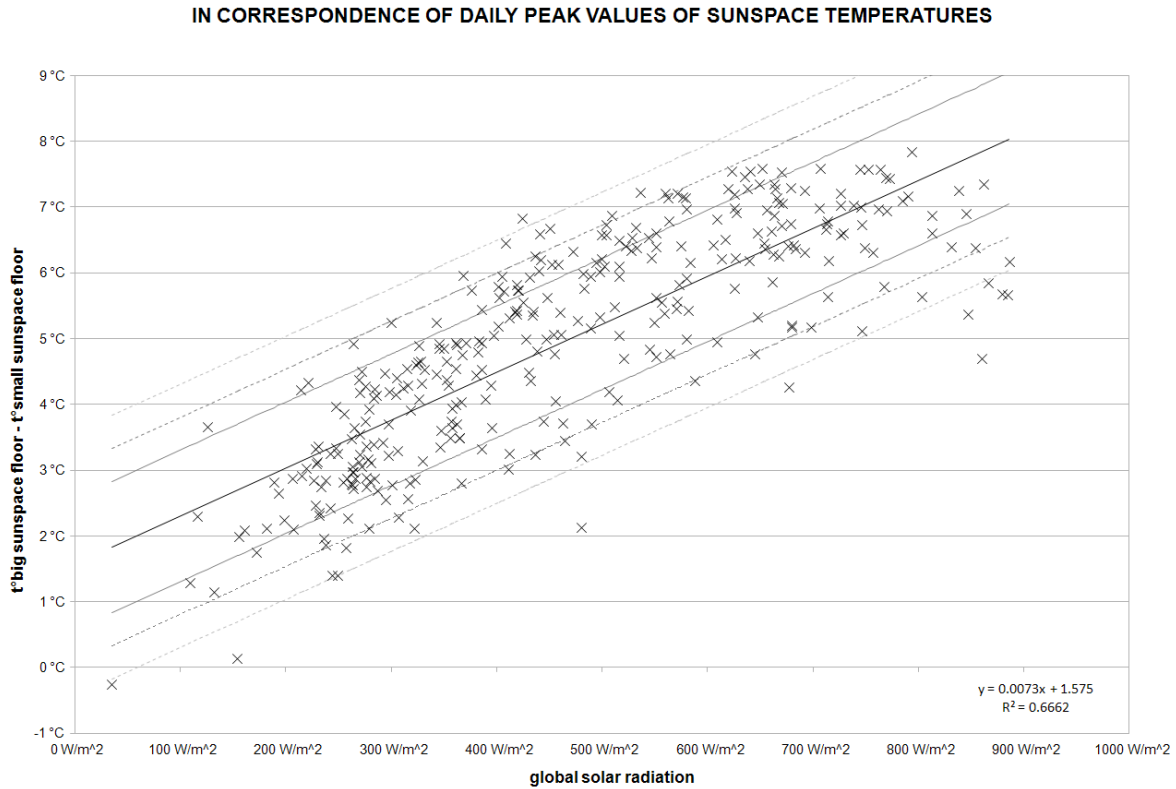


Figure 4.27 On the horizontal axis: global solar radiation. On the vertical axis: floor temperature difference between the big sunspace and the small one in correspondence of daily peak values of sunspace temperature

A linear regression has been performed but the obtained correlation coefficient R^2 of the points is low: 0,67. Lines parallel to the regression line have been plotted in order to create three ranges of distance of the points from the regression line .The results are available in Table 4.3.

Table 4.3 Distribution of the points in relationship with the ranges of Figure 4.27

Points belonging to the range:	
$\pm 1^\circ\text{C}$ respect to the regression line	68,7%
$\pm 1,5^\circ\text{C}$ respect to the regression line	90,7%
$\pm 2^\circ\text{C}$ respect to the regression line	97,0%

Very probably, the regression line is strongly dependent on the shape of the sunspaces. In IDA-ICE another sunspace model, having linear dimensions which are all two times the dimensions of the big sunspace and called “2 x big”, was created.

IN CORRESPONDENCE OF DAILY PEAK VALUES OF SUNSPACE TEMPERATURES

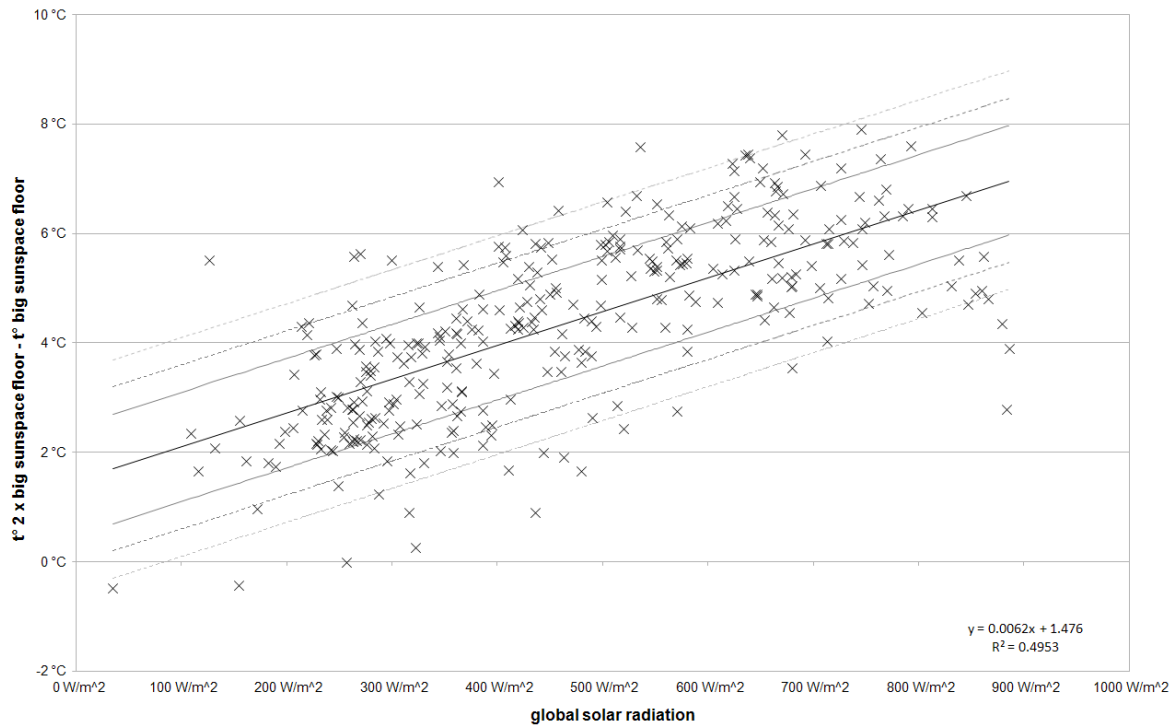


Figure 4.28 On the horizontal axis: global solar radiation. On the vertical axis: floor temperature difference between the sunspace having linear dimensions which are two times the dimension of the big one and the big one in correspondence of daily peak values of sunspace temperature

For the graph where the temperature difference regards “2 x big” and the big sunspace the obtained correlation coefficient R^2 of the points was lower: 0,495.

Table 4.4 Distribution of the points in relationship with the ranges of Figure 4.28

Points belonging to the range:	
$\pm 1^\circ\text{C}$ respect to the regression line	64,5%
$\pm 1,5^\circ\text{C}$ respect to the regression line	80,4%
$\pm 2^\circ\text{C}$ respect to the regression line	91,3%

Finally, the differences between the daily temperature peaks of the sunspace “2 x big” and of the small one have been plotted in Figure 4.29.

In that case the linear dimensional ratio between the compared sunspaces is no more 2, but 4. We can observe that the slope of the line is more or less twice than in the previous graphs: $13 \cdot 10^{-3}$ instead of $7 \cdot 10^{-3}$ and $6 \cdot 10^{-3}$. The same observation can be made for the constant term of the regression line equation: for the comparison between the sunspace “2 x big” and the small sunspace the constant term is 3, while in the previous cases it was about 1,5. Therefore for the

same level of solar radiation the temperature difference is for the last linear regression equation about twice those ones of the previous ones (e.g. for solar radiation equal to 500 W/m^2 with the first linear regression equation the temperature difference is $5,2^\circ\text{C}$, with the second one it is $4,6^\circ$ and with the last one it is $9,8^\circ\text{C}$).

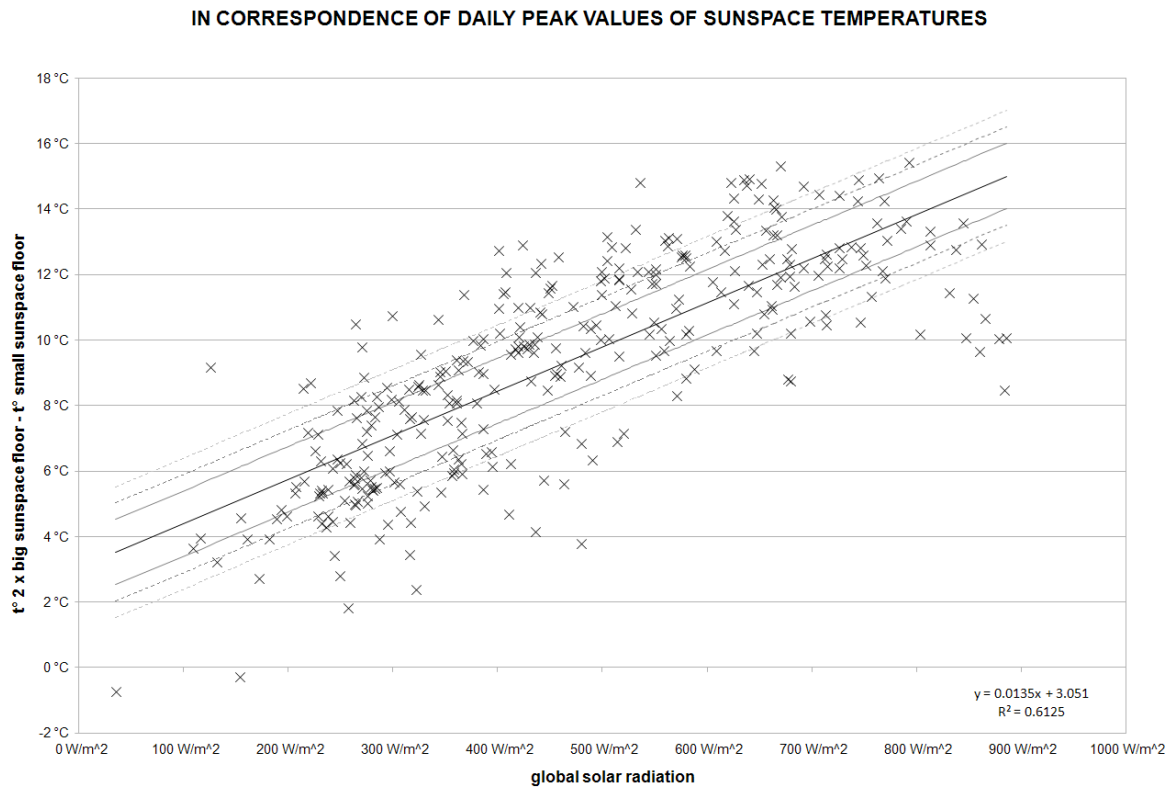


Figure 4.29 On the horizontal axis: global solar radiation. On the vertical axis: floor temperature difference between the sunspace having linear dimensions which are two times the dimension of the big one and the small one in correspondence of daily peak values of sunspace temperature

In that case the obtained correlation coefficient R^2 of the points was 0,61.

Table 4.5 Distribution of the points in relationship with the ranges of Figure 4.29.

Points belonging to the range:	
$\pm 1^{\circ}\text{C}$ respect to the regression line	36,4%
$\pm 1,5^{\circ}\text{C}$ respect to the regression line	52,7%
$\pm 2^{\circ}\text{C}$ respect to the regression line	70,5%

4.4 Conclusions

At the end of this chapter we can conclude that:

- Floor is fundamental for the inertia of a sunspace.
- The difference between sunspaces having different dimensions generally increases with the solar radiation. Through graphs and linear regressions a comparison of the peaks of sunspaces having different dimensions is presented. If the ratio between the linear dimensions is 4, the difference in peak temperatures is more or less twice the temperature difference with a ratio between the linear dimensions of 2. However, we have to consider that the regression is not good.
- A model having, from the point of view of the surface temperatures, a good agreement with the empirical data was created, both for the bigger sunspace than for the smaller one. That suggests that the method used for modeling is valid also if modeling some phenomena regarding the sunspaces is problematic.
- A future work could focus on the air temperature and on the convective heat exchange coefficients through a Computational Fluid Dynamic software.

5. Sunspaces to improve energy retrofitting in Freiburg (Germany)

5.1 Verandas as passive solar system

The 15th preamble of the European Directive 2010/31/EU notices that:

*“Buildings have an impact on long-term energy consumption. Given the long renovation cycle for existing buildings, (...) existing buildings that are subject to major renovation should therefore meet minimum energy performance requirements adapted to the local climate”*¹⁴.

The importance of refurbishments from the point of view of energy requirements is highlighted by the following observation of the *World Energy Outlook 2009*¹⁵:

“For OECD+¹⁶ countries, where new construction activity is estimated to be as low as 1% of the building stock per year and demolitions 0.3% to 0.5%, the biggest potential savings are in existing buildings.”

That was the reason because of which part of the research concerns the refurbishments of verandas which are closed with elements having a big glazed surface.

As part of refurbishments, constructing glazed verandas presents different advantages:

- a close space is added to the living space;
- an unheated space adjacent to the heated one has a temperature higher than the external environment and therefore the heat losses decrease (buffer effect);
- if the air is preheated in the veranda also the ventilation losses decrease;
- closing the veranda the thermal bridges can decrease.

The Figure 5.1 shows a calculation through the finite element software THERM¹⁷ of the reduction of heat transfer from the internal environment to the external one due to modifications of a veranda. Also the possibility to apply thermal insulation on the external side of the parapet was considered. The air is considered as a solid having equivalent thermal

¹⁴ According to the previous Directive 2002/91/EC: *“Major renovations are cases such as those where the total cost of the renovation related to the building shell and/or energy installations such as heating, hot water supply, air-conditioning, ventilation and lighting is higher than 25 % of the value of the building, excluding the value of the land upon which the building is situated, or those where more than 25% of the building shell undergoes renovation. (...) However, the improvement of the overall energy performance of an existing building does not necessarily mean a total renovation of the building but could be confined to those parts that are most relevant for the energy performance of the building and are cost-effective”*.

¹⁵ <www.iea.org/textbase/nppdf/free/2009/WEO2009.pdf> p. 252

¹⁶ OECD+ groups (Organization for Economic Co-operation and Development) accession countries and enhanced engagement countries for a total of 40 countries.

¹⁷ THERM is a state-of-the-art, Microsoft Windows™-based computer program developed at Lawrence Berkeley National Laboratory (LBNL) <<http://windows.lbl.gov/software/therm/therm.html>>

resistance. Therefore the results can give no indications about the temperature stratification inside the veranda. The calculated heat transmissions are:

- in the case of open balconies (A) $15,5 \frac{W}{m \cdot K}$
- in the case of glazing but without insulation (B) $9,0 \frac{W}{m \cdot K}$ (41,9% reduction compared to A)
- in the case of glazing and additional thermal insulation on the external side of the parapet, in order to reduce the heat transmission, (C) $8,2 \frac{W}{m \cdot K}$ (47,0% reduction compared to A).

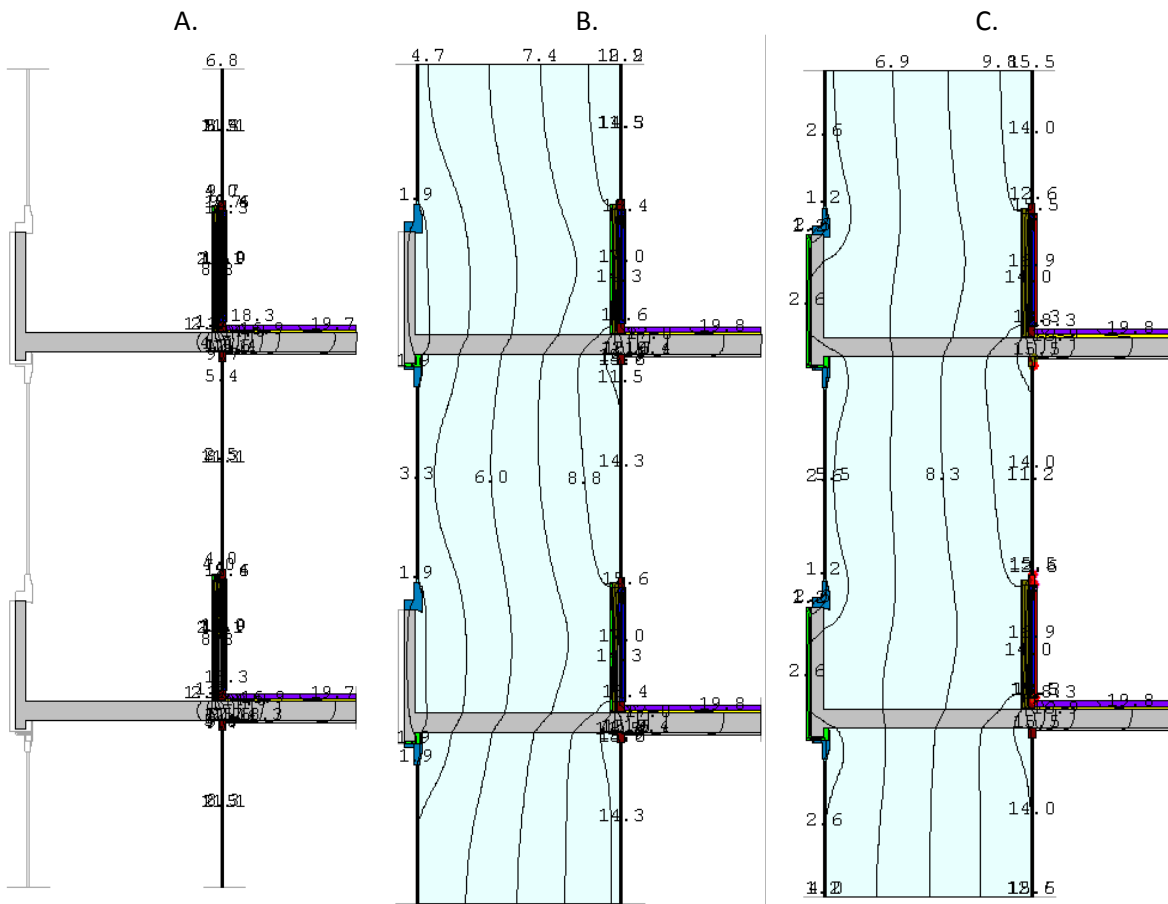


Figure 5.1 Output of THERM. A. open veranda B. close veranda C. close veranda with external application of thermal insulation

5.2 Analysis of a case study

5.2.1 The building

A social house building located in Freiburg was analysed. It was built in 1972 and it was refurbished between 1997 and 1999. The heated surface is 7300 m². It has 14 flats and 84 apartments. During the renovation works:

- the balconies were insulated and closed;
- the windows, except those ones towards the balconies, were changed, reducing the thermal transmittance;
- external insulation was applied;
- solar air collectors were applied to the parapets;
- a mechanical extraction system was installed, with the outlets in the WCs, and special openings were created between the verandas and the internal rooms.

The openings of the solar collector in the veranda remain always open, while the openings between the veranda and the internal rooms can be regulated by the inhabitants. Between the internal doors and the floor there is space (between 1,8 cm and 2,5 cm) through which the air can pass also if the doors are closed.

According to measurements relative to 1999, the heating requirements were reduced from 98 kWh/m² to 64 kWh/m² (34,7% reduction).



Figure 5.2 The refurbished building which was analysed.

The ventilation scheme was devised in order to preheat the ventilation air in the solar air collector and in the glazed verandas and to decrease ventilation losses.

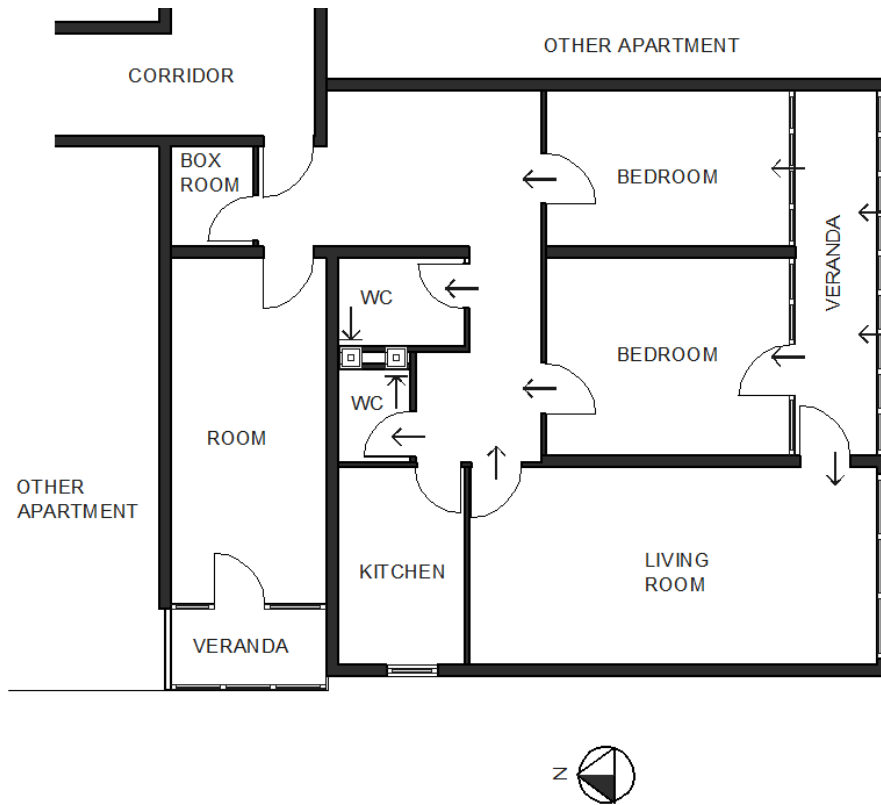


Figure 5.3 Plan of the apartment and ventilation scheme

The extractor fans were produced by Aldes¹⁸ and were installed on the flat roof (see Figure 5.4).



Figure 5.4 Extractor chimneys and extractor fans on the flat roof

¹⁸ <www.aldes.com>

5.2.2 Monitoring

The conditions in an apartment having the veranda facing south and the external weather conditions were monitored since 2nd February 2011 until 9th March 2011.

During the monitoring period the apartment was unoccupied. The windows, both between the veranda and the internal rooms and between the veranda and the external environment, were always close. The apartment is on the 13th floor. Since the height of the surrounding buildings is lower and the mountains are far away, there is no external shading on the veranda windows.

A portable anemometer Testo 410 measured that some air passes also through the door towards the corridor. It was evident that when there is strong wind coming from the south the air exits from the apartment towards the corridor, while in normal conditions because of the mechanical extraction system the pressure in the apartment is lower than in the corridor and the air flow enters apartment.



Figure 5.5 Weather station on the flat roof

Outside, the relative humidity, the global radiation on a horizontal surface, the direct radiation, the wind velocity (Figure 5.5) and the global radiation on a vertical surface (Figure 5.6) were monitored. In the veranda and in an internal room adjacent to the veranda, the air temperature, the global temperature, the air velocity, the relative humidity and the concentration of CO₂ were monitored.



Figure 5.6 Monitoring of the radiation on vertical surface facing south

A humidity and temperature instrument in shelter produced by Theodor Friedrichs¹⁹ was used to measure outside conditions. It uses a capacitive measuring element for the relative humidity and a Pt 100 for the measurement of the air temperature. Its properties are the following ones.

Humidity Sensor:

- measuring range: 0...100 % R.H.
- accuracy: ± 1 % R.H.

Temperature Sensor:

- Operating range: $-40...+85$ °C
- Pt 100, according to DIN 60751 B, 1/3 tolerance

A product by Theodor Friedrichs was used also to measure the wind velocity (series 4035):

- measuring range: $0\div 70$ m/s
- accuracy: 0,2 m/s;
- at $v > 15$ m/s 2% f. FS;
- threshold: $< 0,3$ m/s;
- survival speed: over 100 m/s.

To measure the solar radiation sensors produced by Indium Sensor were used²⁰.

On the horizontal plane a SDE 9.1. On the vertical plane a “head type 10.7”. For both the error can be $\pm 10\%$.

¹⁹ <www.th-friedrichs.de/en>

²⁰ <www.indiumsensor.de>



Figure 5.7 Monitoring of internal conditions

In the internal room and in the veranda the data-logger Testo 454 was used to store the data (Figure 5.7). The connected measurement instruments were produced by Testo AG²¹ as well and they have the following properties.

Humidity/temperature probes (0636.9740) were used:

- measurement range: RH 0 to 100 %
- accuracy: $\pm 2\%$ RH (2 to 98 % RH), $\pm 0.4^\circ\text{C}$ (0 to 50°C), $\pm 0.5^\circ\text{C}$ (rem. range)

The supply air velocity was measured with Testo (the supply air temperature was measured with a specific sensor Pt100):

- measurement ranges: 0 to +10 m/s -20 to +70 °C
- accuracy: $\pm(0.03 \text{ m/s} \pm 5\% \text{ of mv})$ (0 to +10 m/s)

The used CO₂ probe has the following properties:

- measurement range: 0 to 1 vol. % CO₂ (0 to 10000 ppm CO₂)
- accuracy: 50 ppm $\pm 2\%$ of m.v. (0 to 5000 ppm), 100 ppm $\pm 3\%$ of m.v. (rem. range)

The globe thermometer 0554.0670 (D = 150 mm) can measure radiation temperature in accordance with ISO 7243, ISO 7726, DIN EN 27726, DIN 33403:

- measurement range: 0÷120°C
- accuracy: $\pm 0.5^\circ\text{C}$ (0 to 50°C), $\pm 1^\circ\text{C}$ (50 to 120°C)

Surface temperatures both in the veranda and outside, on the building envelope, were measured

²¹ <www.testo-international.com>

through Pt100 sensors having measurement range $-50\div 180^{\circ}\text{C}$ (Figure 5.8).

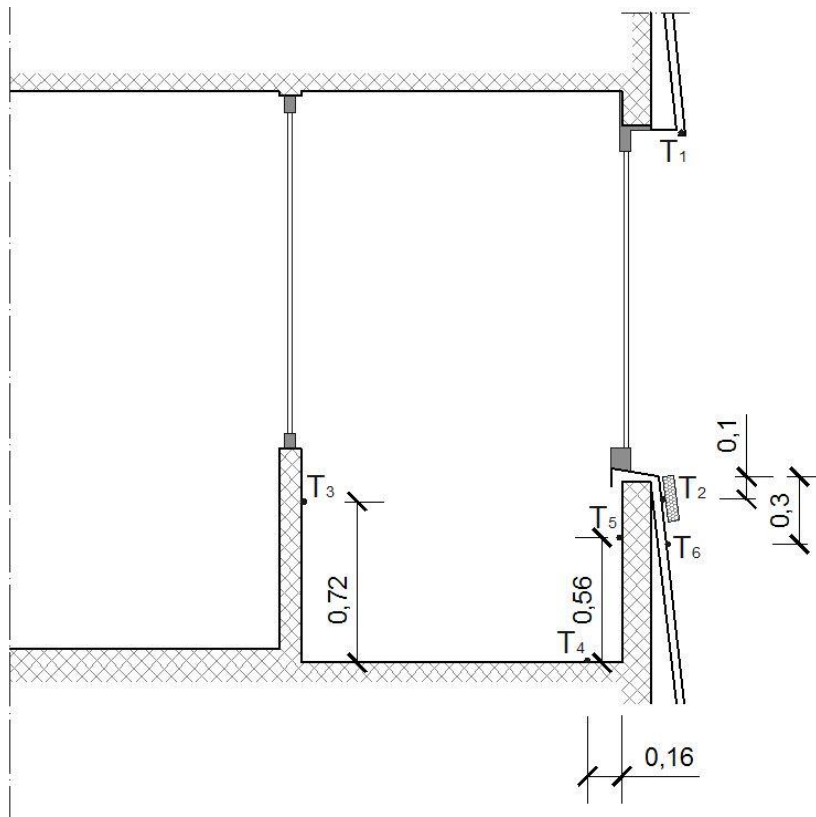


Figure 5.8 Positions of the surface temperature sensors

Particular attention was given to the preheating of the ventilation air, because it is a fundamental aspect of the refurbishment. The supply air velocity and air temperatures in the sunspace, entering through the solar air collector, and in the monitored room, entering through the specific openings, were monitored (Figure 5.9).

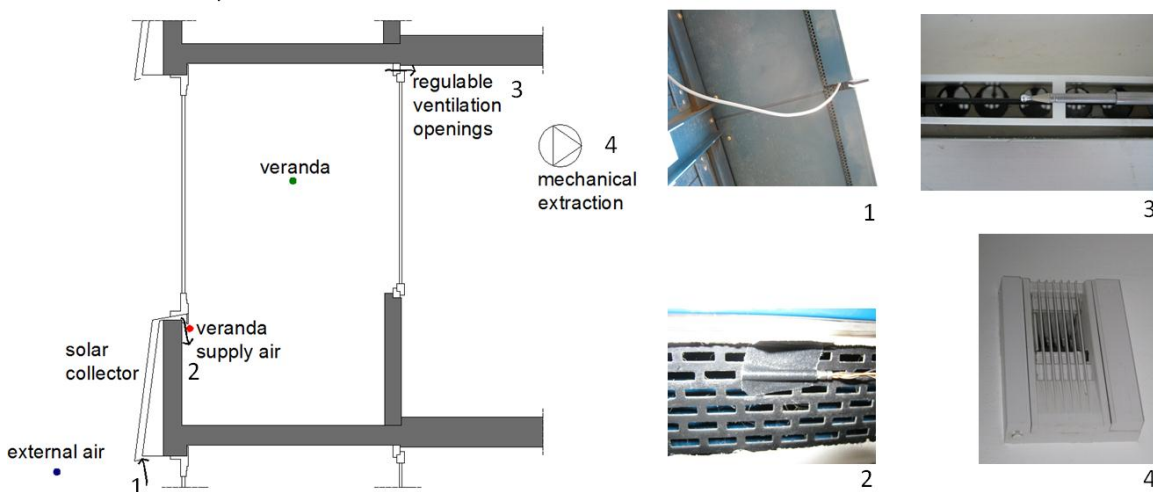


Figure 5.9 Sensors which monitor the preheating of ventilation air and the openings through which the ventilation air has to pass

5.2.3 Data analysis

The apartment was unheated, but, because it is adjacent to 4 heated apartments (2 at the same floor, one at the upper floor, one at the lower floor) the temperature during the monitoring period was around 20°C, with a mean value of 20,1°C). Figure 5.10 shows the temperatures in the veranda and in the internal room. Both are influenced by the external temperature, but the temperature of the internal room is much less variable. Every plotted point corresponds to a mean value relative to 30 minutes.

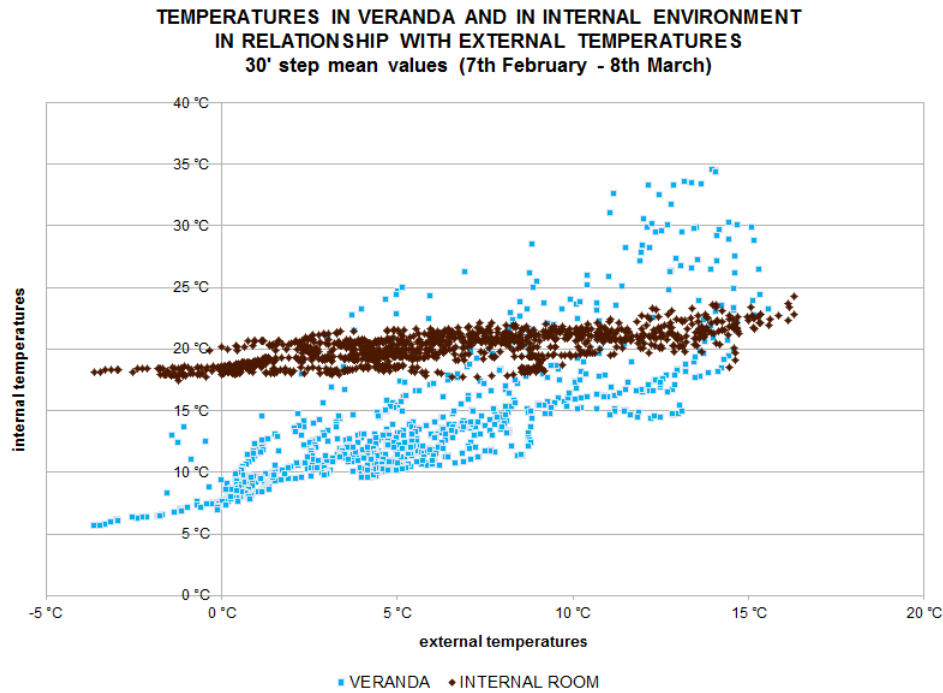


Figure 5.10 On the horizontal axis: air temperatures in the external environment. On the vertical axis: air temperatures in the veranda and in the internal room

In Figure 5.11 only the points relative to the veranda are reported. They are subdivided in three ranges of solar radiation. The range corresponding to the lowest level of solar radiation was divided in two parts, in order to consider the part of the day (0.00-12.00 or 12.00-24.00). In fact, during the evening hours, the temperature is influenced, because of the thermal inertia, by the temperatures reached during the sunny hours. Obviously, the highest temperatures are reached with the highest level of solar radiation on vertical surfaces facing south. The yellow line corresponds to conditions of veranda having the same temperature of the external environment. All the points are above that line.

The black line indicates theoretical stationary conditions, in absence of solar radiation and of ventilation and corresponds to the equation

$$(T_v)_{st,no_vent} = \frac{H_{iu}T_{int} + H_{ue}T_{out}}{H_{iu} + H_{ue}} \quad (5.1)$$

where

H_{iu} is the heat transfer coefficient, due to conduction, between apartment and veranda [W/K]

H_{ue} is the heat transfer coefficient, due to conduction, between veranda and external environment [W/K]

T_{int} is the air temperature in the internal environment and in this calculation it was supposed constant and equal to 20,1°C, the mean value in the considered period

T_{out} is the measured air temperature in the external environment

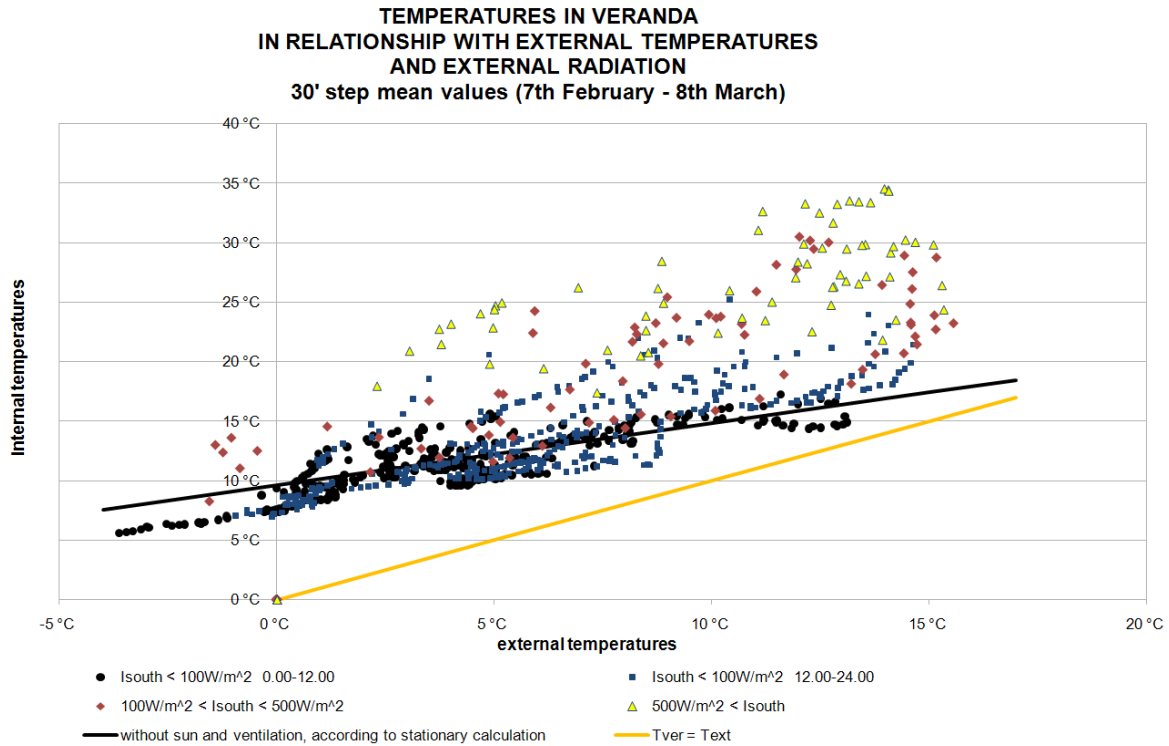


Figure 5.11 On the horizontal axis: air temperatures in the external environment. On the vertical axis: air temperatures in the veranda. They are divided according to three ranges of solar radiation on the vertical surface facing south. The range corresponding to the lowest level of solar radiation was divided in two parts, in order to consider the part of the day (0.00-12.00 or 12.00-24.00).

Figure 5.12 shows the preheating of the ventilation air due to the presence of the veranda and of the solar air collector.

Actually, if the air velocity is not particularly high the temperature measurements of the supply air in the veranda are not considered reliable, because the measure is taken on the internal side of the inlet and therefore it is influenced by the temperature of the environment where the sensor is. In fact, during the night the supply temperature in the veranda should be very close to the external temperature, because between the air cavity of the solar collector and the external environment there is only a metal sheet, while between the air cavity and the veranda there is an insulated parapet.

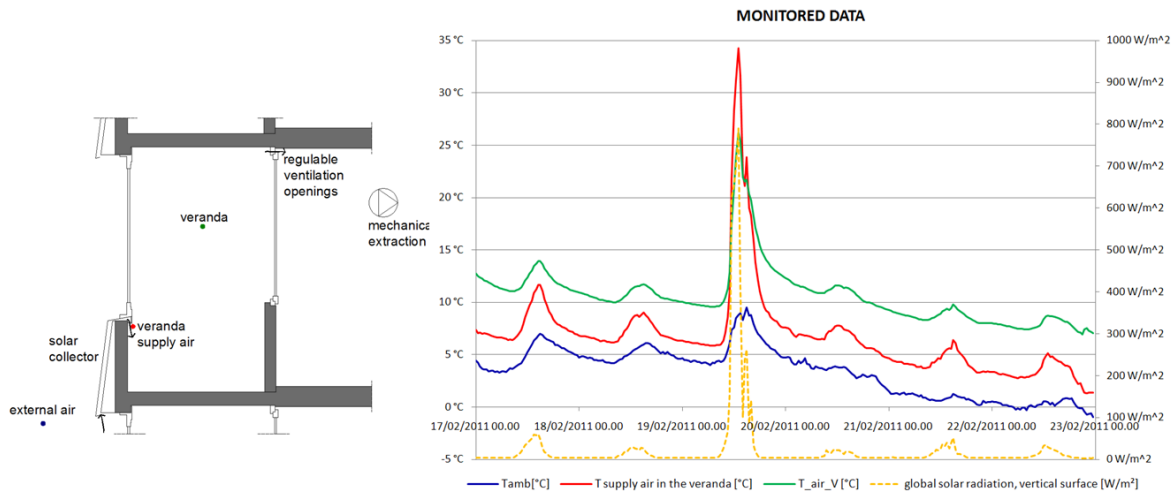


Figure 5.12 Air temperatures (external environment, supply air in the veranda, veranda) in relationship with the solar radiation on the vertical surface facing south

In Figure 5.13 on the secondary axis the wind velocity is plotted. It is possible to observe that the measured supply air temperature is close to the external temperature in the days when the wind velocity is higher.

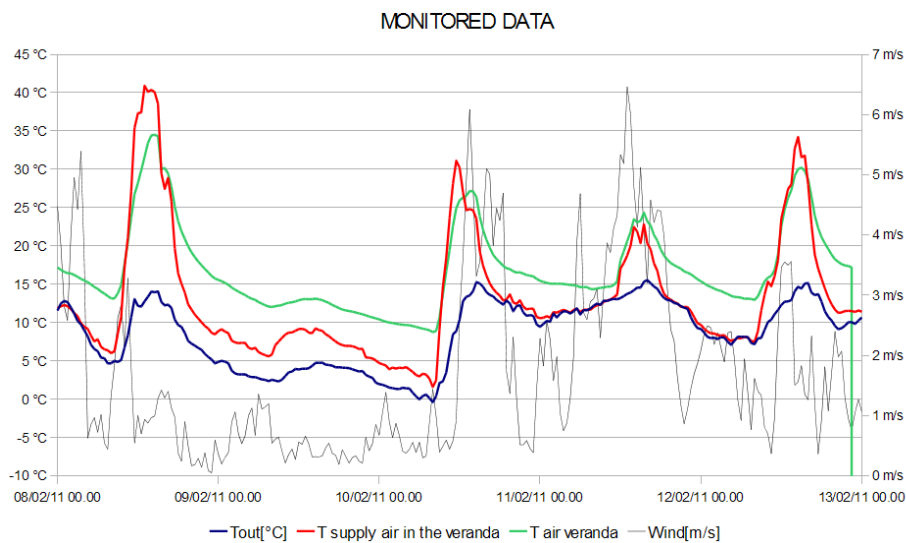


Figure 5.13 Monitored air temperatures in relationship with the wind velocity

This experience suggests that the empirical data must be considered critically, because the measured data do not always correspond to what we wanted to measure originally.

In order to estimate the air change ACH in the monitored room, on the 3rd February CO₂ was appositely released and diluted in the air. The level of CO₂ achieves a maximum value of about 3100 ppm.

To estimate the air change the following hypotheses are made (they are approximations):

- concentration of CO₂ in the internal environment C uniform;

- concentration of CO₂ in the external environment C_{ext} constant;
- air change pro hour ACH constant.

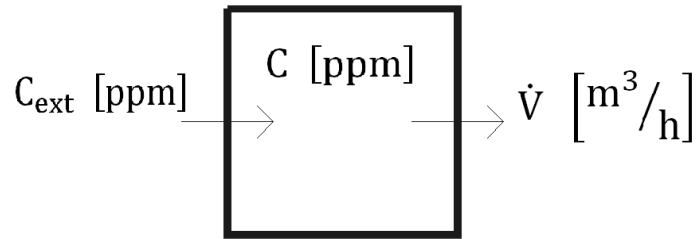


Figure 5.14 Scheme for the estimation of the air change

The definition of ACH is

$$\text{ACH} = \frac{\dot{V}}{V} \quad (5.2)$$

where V [m³] is the room volume and \dot{V} [m³/h] the air flow, relative to both entering and exiting air

The infinitesimal variation of the CO₂ concentration during the infinitesimal time step dt can be expressed by the following equation

$$-dC = \frac{C\dot{V} - C_{\text{ext}}\dot{V}}{V} dt = (C - C_{\text{ext}}) \cdot \text{ACH} dt$$

Integrating from the conditions at the initial time t_0 to the generic time t :

$$\int_{t_0}^t \frac{-dC}{C - C_{\text{ext}}} = \int_{t_0}^t \text{ACH} dt$$

$$\ln(C - C_{\text{ext}})|_{t_0}^t = -\text{ACH} \cdot (t - t_0)$$

Calling the concentration at the initial time $C(t_0) = C_0$

$$\ln\left(\frac{C - C_{\text{ext}}}{C_0 - C_{\text{ext}}}\right) = -\text{ACH} \cdot (t - t_0)$$

$$\frac{C - C_{\text{ext}}}{C_0 - C_{\text{ext}}} = e^{-\text{ACH} \cdot (t - t_0)}$$

$$C - C_{\text{ext}} = (C_0 - C_{\text{ext}}) \cdot e^{-ACH \cdot (t-t_0)}$$

The time can be defined in order to have $t_0 = 0$

$$C = C_{\text{ext}} + (C_0 - C_{\text{ext}}) \cdot e^{-ACH \cdot t} \quad (5.3)$$

Therefore the used fitting function for the empirical data has the form

$$y = a + b \cdot e^{-c \cdot x} \quad (5.4)$$

where a, b and c are considered constant values.

A specific sensor monitored CO₂ concentration with a time step of 5 minutes. In the Figures 5.15 and 5.16 the monitored values are plotted, considering $t_0 = 0$ the time correspondent to the maximum level of CO₂ concentration.

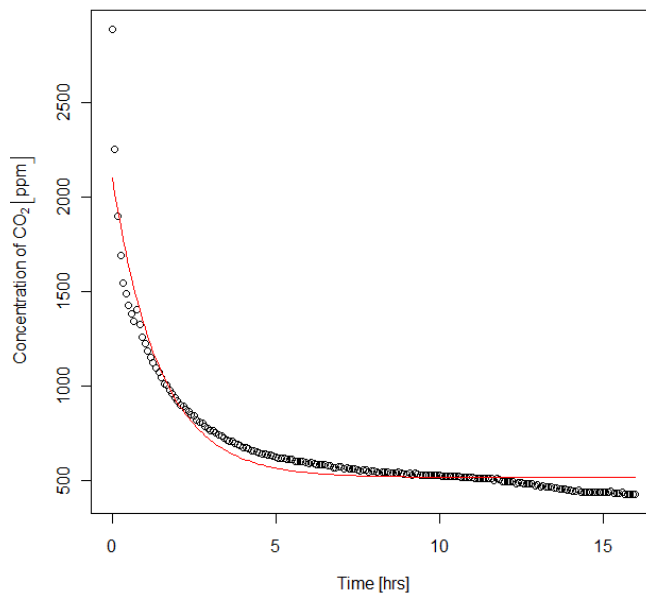


Figure 5.15 On the horizontal axis: time in hours. On the vertical axis: variation of CO₂ concentration. For the fitting the considered time interval is 0-16 [fitting and graphs produced by the software R v.2.12.2 <www.r-project.org>]

Considering the time step 0 - 16 (hours after the achievement of the maximum CO₂ concentration) the parameters which give the best fitting are:

$$a = 516,9 \text{ ppm}$$

$$b = 1588 \text{ ppm}$$

$$c = -0,6954 \text{ h}^{-1}$$

Therefore the estimated ACH would be 0,695. The coefficient of determination R^2 is 0,93. It is

possible to observe that the obtained curve does not fit well the first points and the last ones of the series. Probably during the first hour (or at least during the first minutes) the CO₂ was not well mixed in the internal environment. During the last ones high wind velocities were monitored and probably the air change was increased because of the wind. Then the fitting was made considering the time range 1 ÷ 11 hours after the maximum value of the CO₂ concentration.

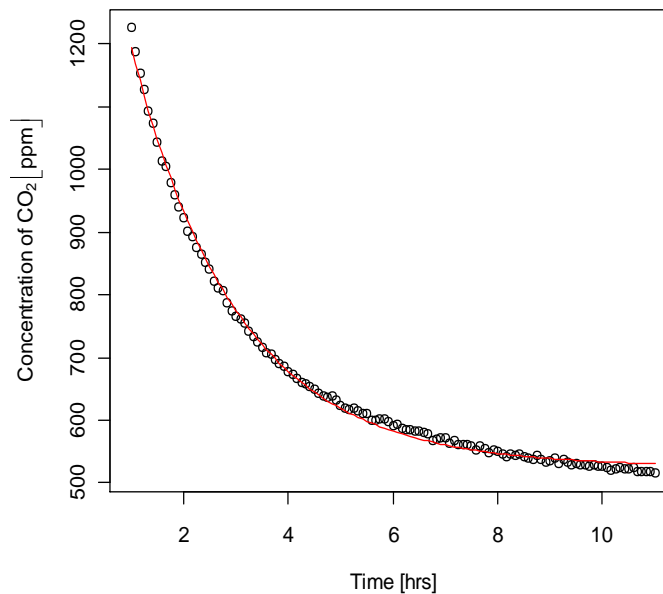


Figure 5.16 On the horizontal axis: time in hours. On the vertical axis: variation of CO₂ concentration. For the fitting the considered time interval is 1-11 [fitting and graphs produced by the software R v.2.12.2 <www.r-project.org>]

Considering the time step 1 - 11 (hours after the achievement of the maximum CO₂ concentration) the parameters which give the best fitting are:

$$a = 525,8 \text{ ppm}$$

$$b = 1096 \text{ ppm}$$

$$c = -0,4935 \text{ h}^{-1}$$

Therefore the estimated ACH would be 0,49. The coefficient of determination R^2 is 0,997 and the fitting is very good. The mechanical ventilation system was designed for 0,5 ACH, therefore a value close to the value estimated from the monitoring campaign.

5.2.4.2 Unknown physical quantities

$T(y)$ temperature in the air layer at the generic level y [K]

\dot{m} air mass flow within parapet [kg/s]

T_{sur} temperature of the metal surface [K]

T_{sup} supply air temperature [K]

h_{out} surface coefficient of heat transfer between the metal surface and the external environment [W/(m²K)]

h_{cav} surface coefficient of heat transfer between the metal surface and the air cavity [W/(m²K)]

5.2.4.3 Development of the model

From the energy balance of the metal surface at the generic level y :

$$\alpha I + h_{\text{out}} \cdot (T_{\text{out}} - T_{\text{sur}}) + h_{\text{cav}} \cdot (T - T_{\text{sur}}) = 0 \quad (5.5)$$

it is possible to obtain

$$T_{\text{sur}} = \frac{\alpha I + h_{\text{out}} T_{\text{out}} + h_{\text{cav}} T}{h_{\text{out}} + h_{\text{cav}}} \quad (5.6)$$

With this formulation if T increases when y increases (and, considering that the temperature of the veranda is higher than outer temperature, it is always so), T_{sur} increases as well.

During the night there is no solar radiation but there is heat exchange with the sky and therefore the surface temperature is lower than the air temperature. When $I=0\text{W/m}^2$ we can consider a negative heat exchange with the sky.

According to the empirical data, when $I=0\text{W/m}^2$ we can replace αI with -10W/m^2 , although more accurate models of the nocturnal exchange with the sky would be available in literature.

Energy balance of the generic infinitesimal portion of the air cavity:

$$h_{\text{cav}} L \cdot dy \cdot (T_{\text{sur}} - T) + UL \cdot dy \cdot (T_L - T) = \dot{m} c \cdot dT \quad (5.7)$$

The balance of the equation (5.7) is approximated, because, in contrast with the equation (5.6), it supposes that T_{sur} is constant in the infinitesimal portion dy . However, considering that the external surface of the solar collector is metallic and therefore with a high conductivity, the temperature differences within it should be very small and the error relative to the approximation should be negligible.

The equation (5.7) can be integrated:

$$\int_0^h dy = \frac{\dot{m}c}{L} \cdot \int_{T_{out}}^{T_{sup}} \frac{dT}{h_{cav} \cdot (T_{sur} - T) + U \cdot (T_L - T)} \quad (5.8)$$

Inserting equation (5.6) in equation (5.8):

$$\int_0^h dy = \frac{\dot{m}c}{L} \cdot \int_{T_{out}}^{T_{sup}} \frac{dT}{h_{cav} \cdot \left(\frac{\alpha I + h_{out} T_{out} + h_{cav} T}{h_{out} + h_{cav}} - T \right) + U \cdot (T_L - T)} \quad (5.9)$$

$$\int_0^h dy = \frac{\dot{m}c}{L} \cdot \int_{T_{out}}^{T_{sup}} \frac{dT}{h_{cav} \cdot \frac{\alpha I + h_{out} T_{out}}{h_{out} + h_{cav}} + UT_L - T \cdot \left(h_{cav} + U - \frac{h_{cav}^2}{h_{out} + h_{cav}} \right)}$$

Solving the integral:

$$\frac{hL}{\dot{m}c} = \frac{\ln \left(h_{cav} \cdot \frac{\alpha I + h_{out} T_{out}}{h_{out} + h_{cav}} + UT_L - T \cdot \left(h_{cav} + U - \frac{h_{cav}^2}{h_{out} + h_{cav}} \right) \right) \Big|_{T_{out}}^{T_{sup}}}{-\left(h_{cav} + U - \frac{h_{cav}^2}{h_{out} + h_{cav}} \right)}$$

$$-\frac{hL}{\dot{m}c} \cdot \left(h_{cav} + U - \frac{h_{cav}^2}{h_{out} + h_{cav}} \right) = \ln \left(\frac{h_{cav} \cdot \frac{\alpha I + h_{out} T_{out}}{h_{out} + h_{cav}} + UT_L - T_{sup} \cdot \left(h_{cav} + U - \frac{h_{cav}^2}{h_{out} + h_{cav}} \right)}{h_{cav} \cdot \frac{\alpha I + h_{out} T_{out}}{h_{out} + h_{cav}} + UT_L - T_{out} \cdot \left(h_{cav} + U - \frac{h_{cav}^2}{h_{out} + h_{cav}} \right)} \right)$$

$$\frac{h_{cav} \cdot \frac{\alpha I + h_{out} T_{out}}{h_{out} + h_{cav}} + UT_L - T_{sup} \cdot \left(h_{cav} + U - \frac{h_{cav}^2}{h_{out} + h_{cav}} \right)}{h_{cav} \cdot \frac{\alpha I + h_{out} T_{out}}{h_{out} + h_{cav}} + UT_L - T_{out} \cdot \left(h_{cav} + U - \frac{h_{cav}^2}{h_{out} + h_{cav}} \right)} = \exp \left[-\frac{hL}{\dot{m}c} \cdot \left(h_{cav} + U - \frac{h_{cav}^2}{h_{out} + h_{cav}} \right) \right]$$

$$h_{cav} \cdot \frac{\alpha I + h_{out} T_{out}}{h_{out} + h_{cav}} + UT_L - T_{sup} \cdot \left(h_{cav} + U - \frac{h_{cav}^2}{h_{out} + h_{cav}} \right) =$$

$$= \left[h_{cav} \cdot \frac{\alpha I + h_{out} T_{out}}{h_{out} + h_{cav}} + UT_L - T_{out} \cdot \left(h_{cav} + U - \frac{h_{cav}^2}{h_{out} + h_{cav}} \right) \right] \cdot \exp \left[-\frac{hL}{\dot{m}c} \cdot \left(h_{cav} + U - \frac{h_{cav}^2}{h_{out} + h_{cav}} \right) \right]$$

$$T_{sup} = \frac{h_{cav} \cdot \frac{\alpha I + h_{out} T_{out}}{h_{out} + h_{cav}} + UT_L - \left[h_{cav} \cdot \frac{\alpha I + h_{out} T_{out}}{h_{out} + h_{cav}} + UT_L - T_{out} \cdot \left(h_{cav} + U - \frac{h_{cav}^2}{h_{out} + h_{cav}} \right) \right] \cdot \exp \left[-\frac{hL}{\dot{m}c} \cdot \left(h_{cav} + U - \frac{h_{cav}^2}{h_{out} + h_{cav}} \right) \right]}{h_{cav} + U - \frac{h_{cav}^2}{h_{out} + h_{cav}}}$$

The following expressions are defined

$$k_1 = h_{\text{cav}} \cdot \frac{\alpha I + h_{\text{out}} T_{\text{out}}}{h_{\text{out}} + h_{\text{cav}}} + UT_L \quad (5.10)$$

$$k_2 = h_{\text{cav}} + U - \frac{h_{\text{cav}}^2}{h_{\text{out}} + h_{\text{cav}}} \quad (5.11)$$

in order to obtain T_{sup} in the following form:

$$T_{\text{sup}} = \frac{k_1 - (k_1 - T_{\text{out}} \cdot k_2) \cdot \exp\left(-\frac{hL}{\dot{m}c} \cdot k_2\right)}{k_2} \quad (5.12)$$

What happens at the limit conditions?

1. If $I = 0$ and $\dot{m} \rightarrow 0$

$$\exp\left[-\frac{hL}{\dot{m}c} \cdot \left(h_{cav} + U - \frac{h_{cav}^2}{h_{out} + h_{cav}}\right)\right] \rightarrow 0$$

$$T_{sup} \rightarrow \frac{k_1}{k_2} = \frac{h_{cav} \cdot \frac{h_{out} T_{out}}{h_{out} + h_{cav}} + UT_L}{h_{cav} + U - \frac{h_{cav}^2}{h_{out} + h_{cav}}} = \frac{\frac{h_{cav} h_{out}}{h_{out} + h_{cav}} \cdot T_{out} + UT_L}{\frac{h_{cav} h_{out}}{h_{out} + h_{cav}} + U}$$

$\frac{h_{cav} h_{out}}{h_{out} + h_{cav}}$ is the inverse of the thermal resistance between the air cavity and the outer environment (the thermal resistance of the metal sheet is neglected).

Therefore T_{sup} tends to be the weighted average between T_{out} and T_L with the thermal transmittances between the external environment and the air cavity and that one between the veranda and the air cavity as relative weights.

2. If $\dot{m} \rightarrow \infty$

$$\exp\left[-\frac{hL}{\dot{m}c} \cdot \left(h_{cav} + U - \frac{h_{cav}^2}{h_{out} + h_{cav}}\right)\right] \rightarrow 1$$

$$T_{sup} \rightarrow T_{out}$$

3. If $I \rightarrow \infty$

$$k_1 \rightarrow \infty$$

$$T_{sup} = \frac{k_1 \cdot \left(1 - \exp\left(-\frac{hL}{\dot{m}c} \cdot k_2\right)\right) + T_{out} k_2 \exp\left(-\frac{hL}{\dot{m}c} \cdot k_2\right)}{k_2} \rightarrow \infty$$

It is possible to conclude that the mathematical solutions of the obtained equation are reasonable from the physical point of view.

5.2.4.4 Estimation of the external surface heat transfer coefficient

h_{out} is the external surface heat transfer coefficient and it can be considered due to both natural convection and forced convection (if wind is present).

Palyvos, J.A. (2008) presents a critical discussion of the models of external convection coefficients due to the wind. For smooth surfaces McAdams proposed the equation:

$$h_{out} = 3.8 \cdot V_w + 5.78 \quad (5.13)$$

It is proposed the following equation in order to consider the effects of forced convection and of

the natural convection together (e.g. to consider the increase of convection in presence of solar radiation):

$$h_{\text{out}} = 3.8 \cdot V_w + 3 + h_{\text{out,nat_conv}} \quad (5.14)$$

In the McAdams equation the constant value is different because the contribution of natural convection is considered as well.

In literature for the natural convection on a vertical surface the following equations are presented²²:

$$h_{\text{out,nat_conv}} = \frac{\text{Nu} \cdot \lambda}{h} \quad (5.15)$$

$$\text{Nu} = \text{Nu}(\text{Ra}; \text{Gr}; \text{Pr}) \quad (5.16)$$

where

Nu is the Nusselt number

Ra = Gr·Pr is the Rayleigh number

Gr = $\frac{h^3 \rho^2 \cdot (1/T) \cdot g \cdot \Delta T}{\mu^2}$ is the Grashof number

Pr = $\frac{c_p \mu}{\lambda}$ is the Prandtl number

ΔT is also dependent on the convective exchange. It can be estimated as

$$\Delta T = T_{\text{sur},0} - T_{\text{out}} = \frac{h_{\text{out},0} \cdot T_{\text{out}} + \frac{1}{\frac{1}{U} + \frac{1}{h_{\text{cav},0}}} \cdot T_L + \alpha I}{h_{\text{out},0} + \frac{1}{\frac{1}{U} + \frac{1}{h_{\text{cav},0}}}} - T_{\text{out}}$$

where $h_{\text{out},0}$ and $h_{\text{cav},0}$ are first attempt values.

5.2.4.5 Estimation of the internal surface heat transfer coefficient h_{cav}

h_{cav} is the internal surface heat transfer coefficient and it is due both to forced convection (the air moves because of external causes: mechanical extraction and wind) and to natural

²² Bonacina, C. et al. (1992) *Trasmissione del calore*, Padova, CLEUP editore, pp. 294-298

convection (there is temperature difference between the metal sheet and the air cavity). According to Çengel, Y.A. (2007) when the natural convection and the forced convection are combined for vertical surfaces the following equation can be used:

$$Nu_{\text{combined}} = (Nu_{\text{forced}}^3 \pm Nu_{\text{natural}}^3)^{1/3} \quad (5.17)$$

where

+ is for the case of natural convection helping the forced convection

– is for the case of natural convection hurting the forced convection

The previous equation makes sense only if the Nu_{forced} and Nu_{natural} are calculated for the same geometrical length (otherwise Nu_{combined} would have no sense).

Therefore considering the equation (5.15) we can express the equation (5.17) as

$$h_{\text{combined}} = (h_{\text{forced}}^3 \pm h_{\text{natural}}^3)^{1/3} \quad (5.18)$$

where there are not geometrical dimensions

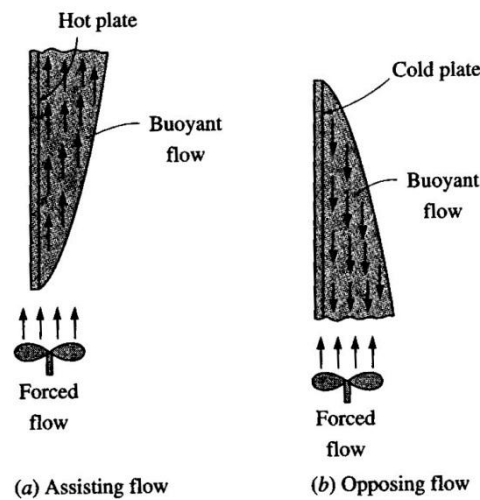


Figure 5.18 Examples of combination between forced and natural convection

Source: Çengel, Y.A. (2007)

In the present case, it is possible consider + when the metal sheet temperature is higher than the air temperature and – when it is colder.

In literature, to estimate the internal surface heat transfer coefficient due to forced ventilation in cavities, the following kind of functions is proposed:

$$Nu = Nu (Re; Pr; \text{geometry}; \text{viscosity} \dots) \quad (5.19)$$

where $Re = \frac{\rho UL}{\mu}$ is the Reynolds number

To estimate the internal surface heat transfer coefficient due to natural ventilation the estimation of the temperature difference between the metal sheet and the air cavity is necessary:

$$\Delta T = T_{sur,0} - T_0 = \frac{h_{out,0} T_{out} + \frac{1}{\bar{U} + \frac{1}{h_{cav,0}}} \cdot T_L + \alpha I}{h_{out,0} + \frac{1}{\bar{U} + \frac{1}{h_{cav,0}}}} - \frac{h_{cav,0} \cdot \left(\frac{h_{out,0} T_{out} + \frac{1}{\bar{U} + \frac{1}{h_{cav,0}}} \cdot T_L + \alpha I}{h_{out,0} + \frac{1}{\bar{U} + \frac{1}{h_{cav,0}}}} \right) + U T_L + \dot{m} c T_{out}}{h_{cav,0} + U + \dot{m} c}$$

where $h_{out,0}$ and $h_{cav,0}$ are first attempt values.

5.2.4.6 Validation with empirical values

In the previous discussion the supply air velocity was considered as a known quantity, but in the considered case study it was not. It was strongly influenced by air flow extracted by the mechanical extraction system, which can be considered as constant, but also by variable environmental conditions, in particular, by the wind velocity and direction and by the temperature field.

A formulation of the supply air velocity with a constant value, due to the mechanical extraction, and a linear dependence on the solar radiation and on the wind velocity is proposed (unfortunately the wind direction was not object of the monitoring campaign).

$$v = c_0 + c_I I + c_v V_w \quad (5.20)$$

The results of that formulation have achieved a reasonable agreement (see Figure 5.19) imposing the following values:

$$c_0 = 0,7 \text{ m/s}$$

$$c_I = 5 \cdot 10^{-4} \frac{\text{m/s}}{\text{W/m}^2}$$

$$c_v = 0,08$$

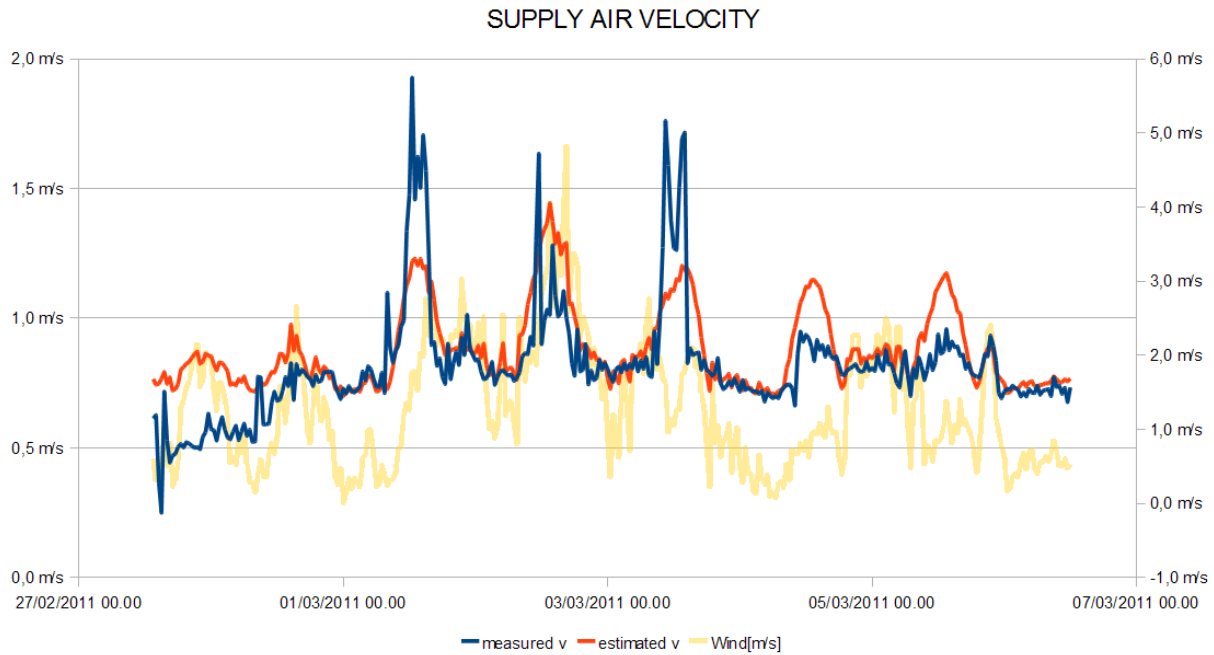


Figure 5.19 Comparison between the measured and the calculated supply air velocity. On 1st March and on 3rd March high supply air velocity peaks were measured but they were not due to a particularly high wind velocity. Probably the wind direction, which was not measured, influences strongly the supply air velocity.

The agreement between the calculated supply air temperature and the monitored data is good (Figure 5.20). The measured temperatures are higher during the nights in which the wind is not strong, probably because in that case the temperature measured by the sensor, which was situated on the inner end of the air collector, was strongly influenced by the veranda temperature. Supposing that the supply air temperature during the night, i.e. in absence of solar radiation, is close to the temperature of the external air is reasonable, because the parapet between the veranda and the cavity of solar collector is insulated and the air cavity is separated from the external environment only by a metal sheet.

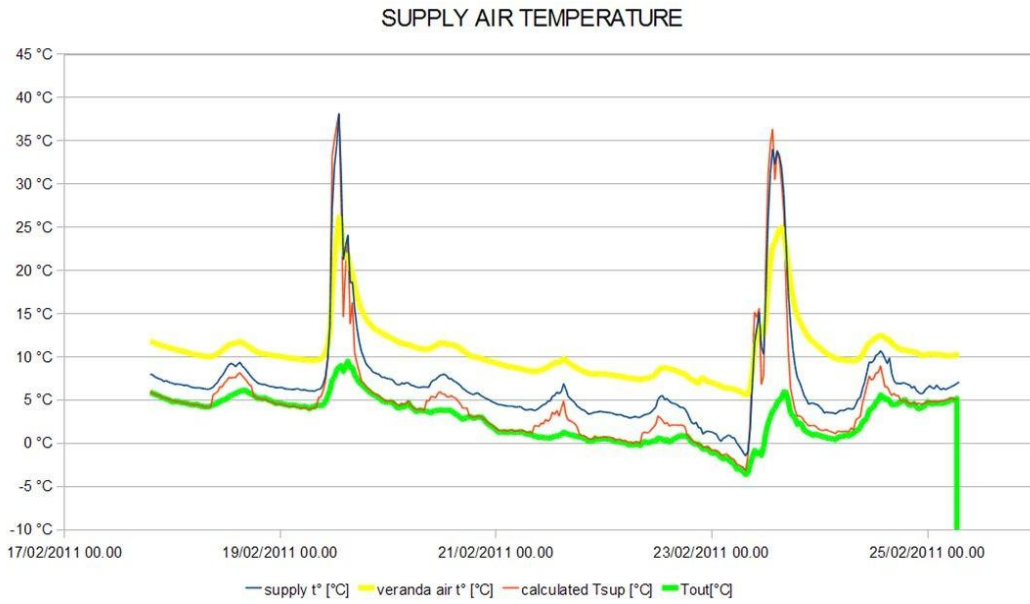


Figure 5.20 Comparison between the measured and the calculated supply air temperature

In conditions of high wind velocity the measured air temperature and the calculated air temperature were similar also during the night (see in Figure 5.21 11th February and 12th February).

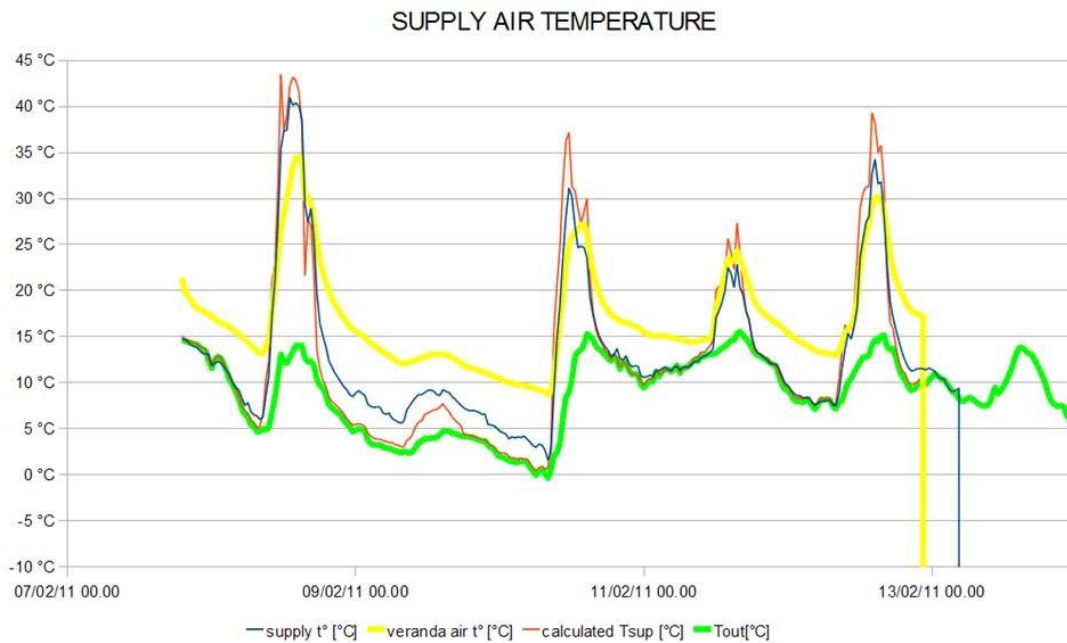


Figure 5.21 Comparison between the measured and the calculated supply air temperature for the period 8th- 13th February. On 10th and 11th February the wind velocity was, considering 30 minutes average values, even more than 6m/s

The model of the solar collector could be used in a next study in an analysis of costs/benefits of the convenience of this technology. Such an analysis should consider different climatic

conditions.

5.3 Design proposals

5.3.1 Introduction to the design proposals

Paragraph 5.2 shows an example of refurbishment of a social house in Freiburg. The municipality of Freiburg is going to refurbish similar buildings; e.g., the area of Weingarten West is object of a specific plan called "Weingarten 2020"²³.

The goal of the calculations which are presented in this paragraph is the comparison between an existing very poor insulated situation, a refurbishment only with the addition of a thick layer of insulation (20 cm) and different solutions in which the veranda is closed with a partly glazed vertical surface, giving attention both to the envelope and to the ventilation system. The analysis of a closed veranda was started with three versions: the version *V1* has the insulation -from the internal environment to the external one, passing through the veranda- in particular between the internal environment and the veranda, the version *V2* in particular between the veranda and the external environment, in the version *V3* the levels of insulation are between those ones of the previous versions. In modified versions of those basic solutions the possibility to separate the veranda from the external environment with completed transparent element, i.e. without opaque parapet, in order to maximize the solar gains, was considered and indicated with *mod_wp*. The possibility to utilize different ventilation systems was considered as well. The exposure was considered to south direction, because for passive solar systems it is the best one (see Chapter 1 "Passive solar systems").

5.3.2 Introduction to calculations

The calculation was made through the method Passive House Planning Package (PHPP)²⁴, which is available in excel worksheets and which is in accordance with the European technical standard EN ISO 13790:2008, and adding a part concerning the buffer effect, including the preheating of the ventilation air (with the hypothesis of perfect mixing, see paragraph 3.2.4.4 "Ventilation through the sunspace"), and the solar gains relative to the glazed veranda, in accordance with ANNEX E "Heat transfer and solar heat gains of special elements" of EN ISO 13790:2008.

As Chapter 3 explains in detail, ANNEX E divides solar heat gains relative to the presence of a glazed sunspace in:

²³ The developers of the project are the municipality of Freiburg, the local energy company badenova and Fraunhofer-ISE

<<http://www.eneff-stadt.info/en/news/news/details/new-pilot-project-weingarten-2020-begins/>>

²⁴ The Passive House Planning Package (PHPP) is the design tool produced by the Passivhaus Institut to model the performance of a proposed Passivhaus building. <www.passivhaus.org.uk/page.jsp?id=25>

- direct heat gains, i.e. the gains entering heated environment directly through the division between the heated environment and the sunspace (considering both the glazed part and the opaque one);
- indirect heat gains, i.e. the decrease of heat dispersions through the veranda (considering ventilation as well) due to the increase of the veranda temperature caused by the solar radiation.

The primary energy is calculated as sum of the boiler energy requirements (according to the PHPP method, through the German standard DIN V 4701-10) and of the requirements of the mechanical ventilation system, if it is present. It is considered a conversion factor of 1,1 for the thermal energy and of 2,7 for the electrical energy. According to the indication of PHPP worksheet, the ventilation was considered 77m³/h and generally it was supposed that its half passes through the veranda, except when another hypothesis is specified. The electrical requirements due to the exhaust ventilation were supposed 0,15 Wh/m³ in the cases with mechanical extraction of the air, 0,30 Wh/m³ in the cases with a fan also for the air introduction. The heat recovery efficiency was supposed 75%.

Because those calculations could be useful for the refurbishments of social dwellings in Freiburg im Breisgau the climate data of PHPP relative to that locality were considered.

Generally the shape of the veranda was considered as enclosed in the building, i.e. the verandas are not particularly big, their lateral walls divide them from the heated space and there are walls which divide the internal environment directly from the external one. In fact the buildings of Weingarten West, the area which is interested by the renovation, are in this way (see Figures 5.22 and 5.23). However, an example of “long veranda”, i.e. there is no direct contact between the heated space and the external environment because the heat space borders only with the veranda, is proposed. In fact, this report does not want to be limited to a specific case, but to be a more general reference.

In calculating indirect heat gains ANNEX E does not consider heat absorbed by the sunspace after multiple reflections. In that way it underestimates the absorbed heat. In the case in which there is the presence of a parapet the heat absorbed after reflections is not negligible and therefore it was considered and estimated as:

$$Q_{\text{abs,ar}} = \frac{h_{\text{par}}}{h_{\text{tot}}} \cdot (Q_{\text{rad,ent}} - Q_{\text{abs,dir}}) \quad (5.21)$$

where

h_{par} is the height of the opaque parapet

h_{tot} is the total net height of the veranda

$Q_{\text{rad,ent}}$ is the total solar radiation entering the veranda and which does not pass to the heated environment directly through the glass $Q_{\text{rad,ent}} = F_{\text{sh}} \cdot (1 - F_{\text{F,e}}) \cdot g_e A_e I_p - Q_{\text{sd,gl}}$

Where $Q_{\text{sd,gl}}$ is the radiation which enters heated space directly through the windows:

$$Q_{sd,gl} = (1 - F_{F,e}) \cdot g_e \cdot \sum_j (F_{sh,w} \cdot (1 - F_w) g_w A_w)_j$$

$Q_{abs,dir}$ is the total solar radiation absorbed directly by the veranda, calculated according to equation (E.3) in annex E and subtracting the heat entering the heated space through the opaque surfaces (which is considered among direct heat gains):

$$Q_{abs,dir} = (1 - F_{F,e}) \cdot g_e \cdot \sum_j (F_{sh,j} I_j a_j A_j) - Q_{sd,op} \quad (5.22)$$

Therefore also with the utilized modify the solar radiation absorbed by the veranda after multiple reflections is calculated as zero if there is no opaque parapet. It is an underestimation of the thermal contribution of the veranda.

The total radiation absorbed by the veranda is

$$Q_{abs} = Q_{abs,dir} + Q_{abs,amr} \quad (5.23)$$

It was imposed the physically obvious condition

$$(1 - F_{F,e}) \cdot g_e \cdot \sum_j (F_{sh,j} I_j a_j A_j) < Q_{rad,ent} \quad (5.24)$$

i.e. the solar radiation adsorbed by the internal surface cannot be greater than the solar radiation entering veranda. It can be considered as a check of the calculation, in particular of the shading factors. For every internal surface the shading factors were estimated, according to the method PHPP or to the German technical standard DIN V 18599:2007 (ANNEX A). The PHPP method use calculation algorithms, with trigonometric functions, which “*derive from building simulation. The calculated shading factors depend upon the window geometry, shading elements, the orientation of the window and the time of the year*” (see Passive Haus Intitut (2007)). DIN V 18599-2:2007 presents tables where the shading factors are presented as functions of the kind of obstacle (frontal, vertical, horizontal), exposure, shading angle, and season. No dispersions to unheated spaces or towards the ground are considered, because the verandas are adjacent only to the external environment (through one surface) and to the heated space (through 5 surfaces).



Figure 5.22 External facade of an apartment block of Weingarten West (Freiburg im Breisgau, Germany) which is going to be refurbished

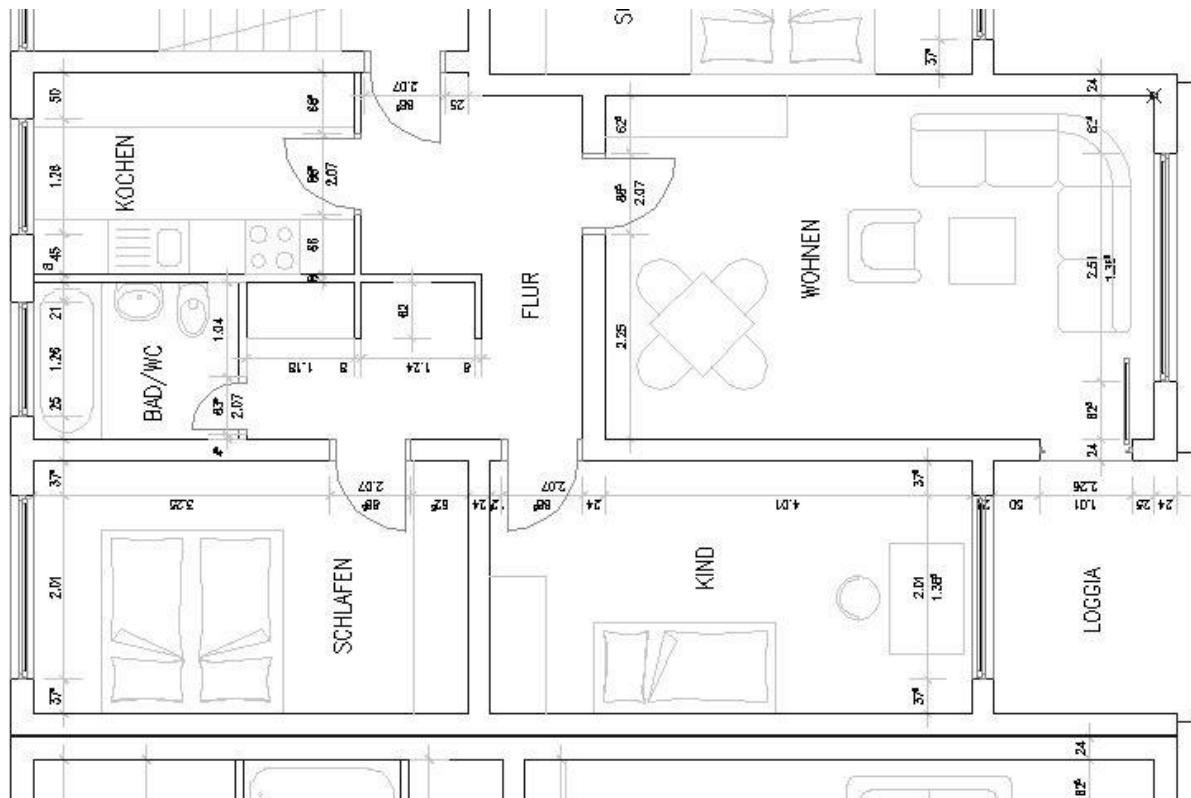


Figure 5.23 An example of apartment of Weingarten West (Freiburg im Breisgau, Germany)

5.3.3 Thermal properties of the considered elements

Original wall, without insulation $U = 3,15 \frac{W}{m^2K}$

Wall with 5 cm external insulation $U = 0,57 \frac{W}{m^2K}$

Wall with 20 cm external insulation $U = 0,17 \frac{W}{m^2K}$

Original windows (all the windows of the models A and B and in the other cases the two windows which are not connected with the veranda) $U = 2,8 \frac{W}{m^2K}$ $g = 0,77$

Simple glazed window $U = 5,8 \frac{W}{m^2K}$ $g = 0,87$

Double glazed window $U = 1,30 \frac{W}{m^2K}$ $g = 0,64$

Triple glazed window $U = 0,66 \frac{W}{m^2K}$ $g = 0,47$

For different solutions relative values of the thermal bridges were supposed, according to technical standard EN ISO 14683:2008 “Thermal bridges in building construction - Linear thermal transmittance - Simplified methods and default values” and to FEM calculation of thermal bridges, according to EN ISO 10211:2008 “Thermal bridges in building construction - Heat flows and surface temperatures - Detailed calculations”. The FEM calculation, using the software THERM, was particularly important to calculate the heat dispersion through the corners which divide the internal environment both from the external one and the veranda. In fact the heat leaving the heated environment and entering the veranda contributes to the buffer effect, while the heat exiting directly to the external one does not, therefore they must be calculated separately (for calculations of thermal bridges concerning three different environments having three different temperatures the normative reference is the ANNEX C in the technical standard EN ISO 10211). For the solutions without an opaque parapet and with a big window it was supposed that the thermal bridges do not change, therefore the calculation supposes that the extremity of the veranda slab is well insulated also in those cases.

5.3.4 Outputs

The outputs are presented in this way:

$$H_{i-e, tr} \quad [W/K]$$

$$H_{i-e, ve} \quad [W/K]$$

$$H_{i-e} \quad [W/K]$$

f	
Sp.H.D. $\left[\frac{kWh}{m^2y} \right]$	H.D. $\left[\frac{kWh}{y} \right]$
Sp.Pr.En.H.V. $\left[\frac{kWh}{m^2y} \right]$	Pr.En.H.V $\left[\frac{kWh}{y} \right]$

where

$H_{i-e, tr} \quad [W/K]$ is the transmission heat transfer coefficient between the internal environment and the external one

$H_{i-e, ve} \quad [W/K]$ is the ventilation heat transfer coefficient between the internal environment and the external one

$H_{i-e} \quad [W/K]$ is the heat transfer coefficient between the internal environment and the external one $H_{i-e} = H_{i-e, tr} + H_{i-e, ve}$

f is the factor for transmission through the veranda

Sp.H.D. $\left[\frac{kWh}{m^2y} \right]$ is the specific heat demand

H.D. $\left[\frac{kWh}{y} \right]$ is the heat demand

Sp.Pr.En.H.V. $\left[\frac{kWh}{m^2y} \right]$ is the specific primary energy for heating and mechanical ventilation

Pr.En.H.V $\left[\frac{kWh}{y} \right]$ is the primary energy for heating and mechanical ventilation

An indication of the dispersions is given by the heat transfer coefficients between the internal environment and the external one: the transmission heat transfer coefficient $H_{i-e, tr}$, the ventilation heat transfer coefficient $H_{i-e, ve}$ and their sum. It is important to remember that the transmission heat transfer coefficient considers the heat transfer through unconditioned spaces as well (see EN ISO 13790:2008 and EN ISO 13789:2007). Therefore it is influenced by the factor of transmission through the veranda f, which is the ratio between the temperature

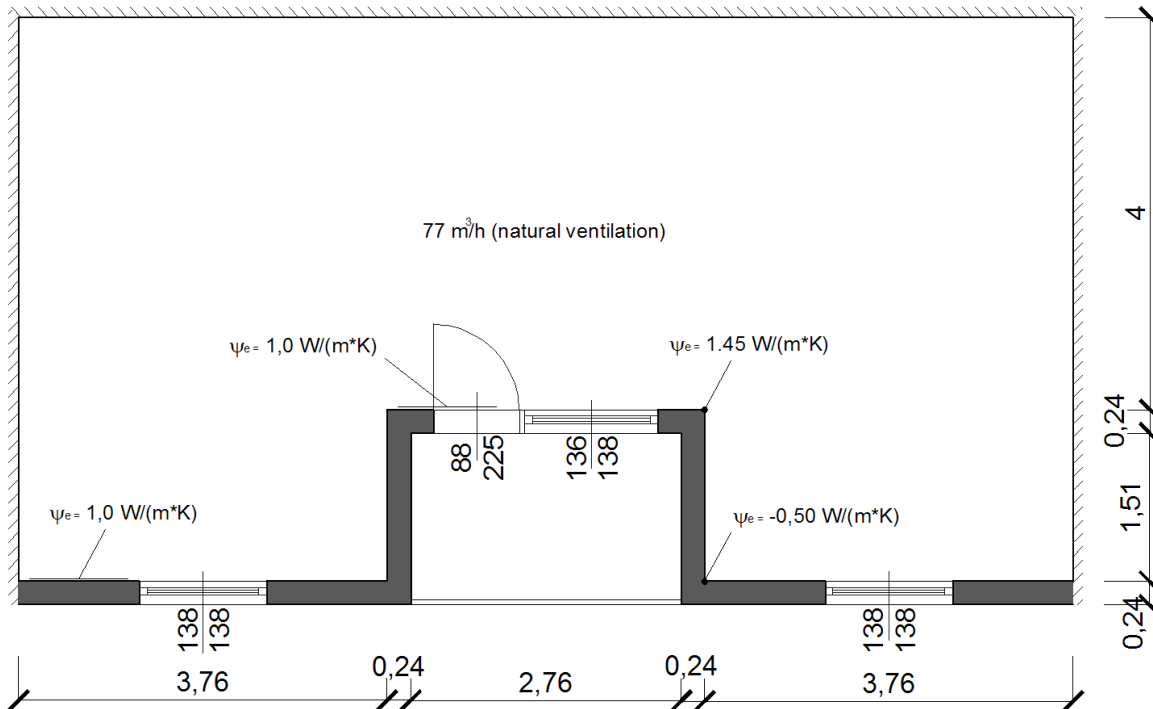
difference between the heated environment and the veranda and the temperature difference between the heated environment and the external one:

$$f = \frac{T_i - T_u}{T_i - T_e} \quad (5.25)$$

Since the factor of transmission through the veranda is influenced by the ventilation flow which passes through it, also the transmission heat transfer coefficient is partially influenced by the ventilation. As indication of the heating requirements the heat demand and the primary energy for heating and for the mechanical ventilation (if it is present) are reported. Both absolute values and specific values, i.e. dividing by the treated floor area, are reported in order to facilitate the comparison among cases having different floor areas.

5.3.5 Results

A) without insulation and without external glazing



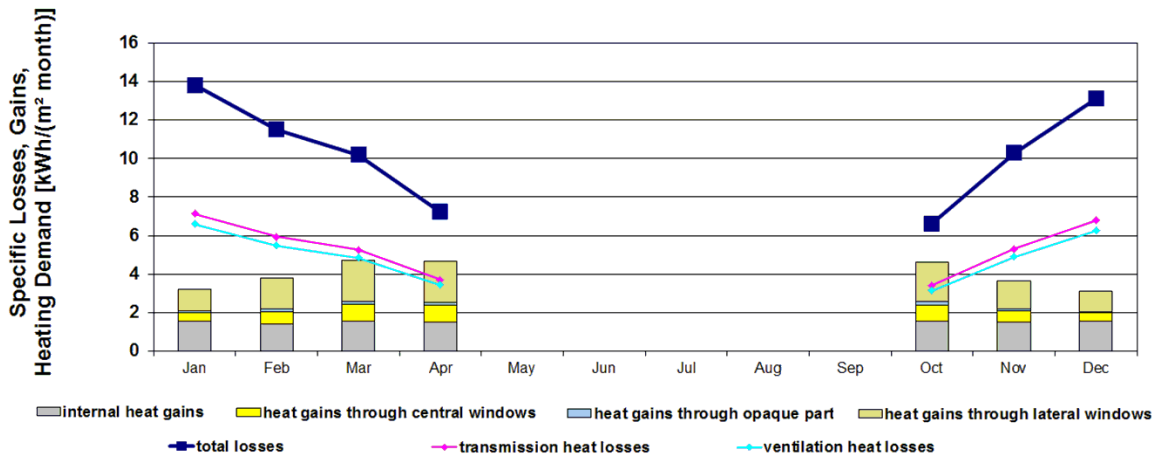
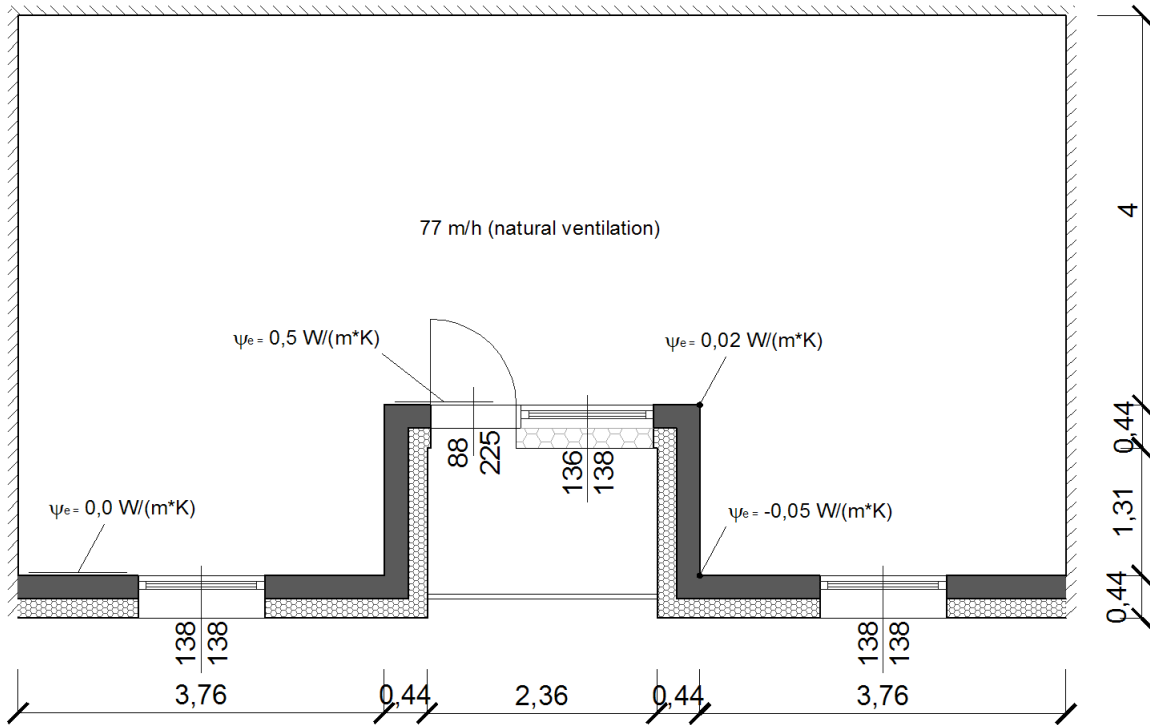
$$H_{i-e, tr} = 134,1 \text{ W/K}$$

$$H_{i-e, ve} = 27,3 \text{ W/K}$$

$$H_{i-e} = 161,7 \text{ W/K}$$

Sp.H.D. = $169,5 \frac{\text{kWh}}{\text{m}^2\text{y}}$	H.D. = $9523,4 \frac{\text{kWh}}{\text{y}}$
Sp.Pr.En.H.V. = $204,2 \frac{\text{kWh}}{\text{m}^2\text{y}}$	Pr.En.H.V = $11478,5 \frac{\text{kWh}}{\text{y}}$

B) with insulation and without external glazing



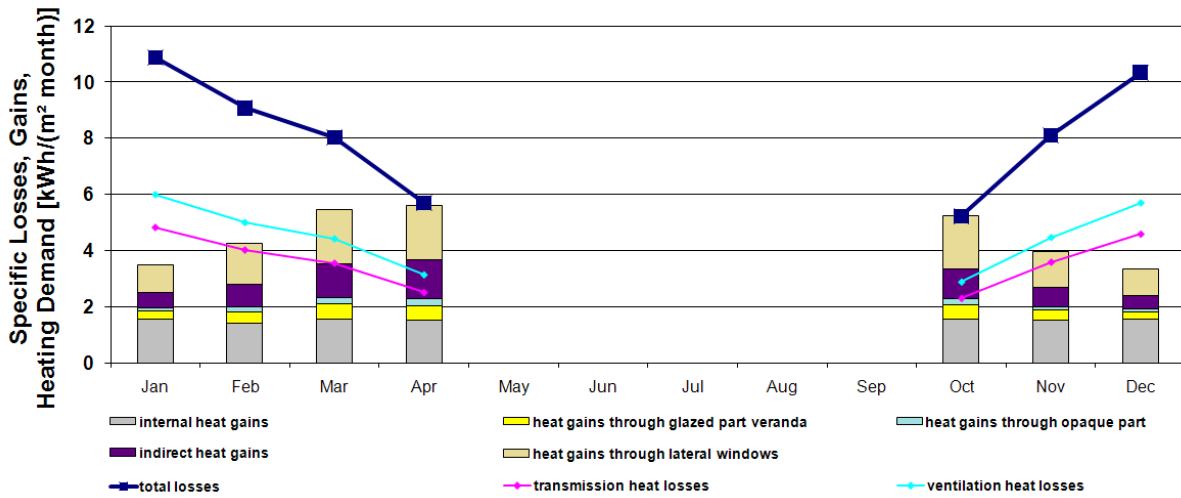
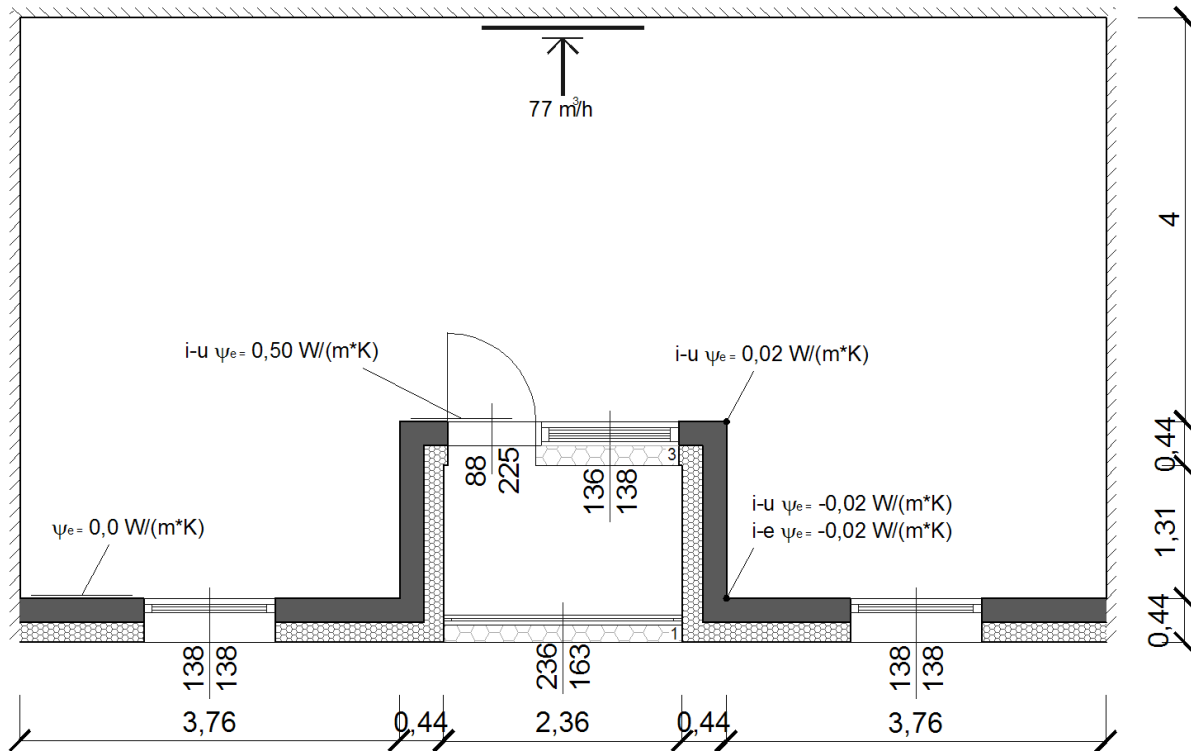
$$H_{i-e, tr} = 29,6 \text{ W/K}$$

$$H_{i-e, ve} = 27,3 \text{ W/K}$$

$$H_{i-e} = 57,0 \text{ W/K}$$

Sp.H.D. = $45,3 \frac{\text{kWh}}{\text{m}^2\text{y}}$	H.D. = $2547,0 \frac{\text{kWh}}{\text{y}}$
Sp.Pr.En.H.V. = $59,1 \frac{\text{kWh}}{\text{m}^2\text{y}}$	Pr.En.H.V. = $3319,4 \frac{\text{kWh}}{\text{y}}$

V1



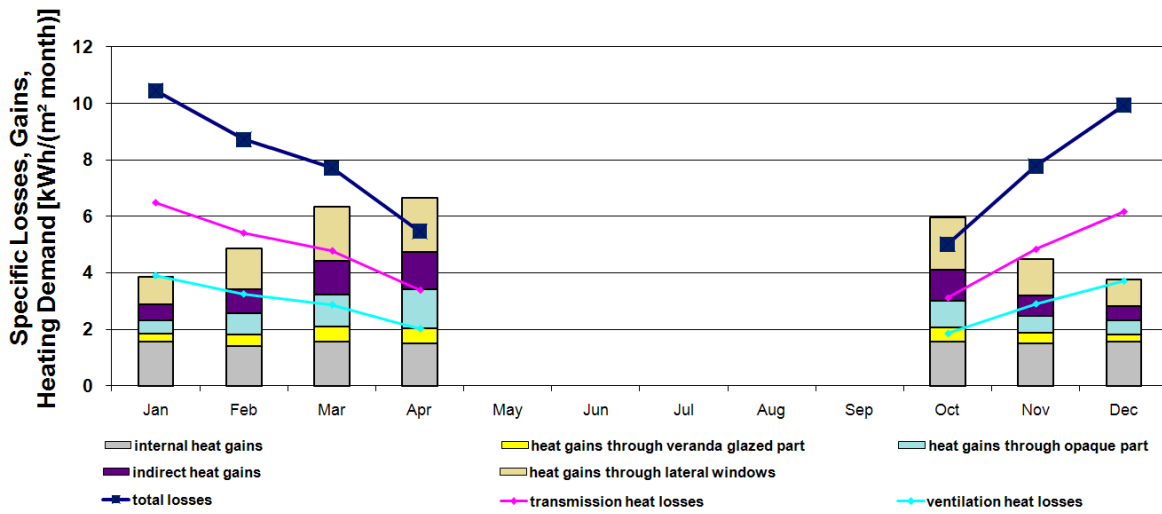
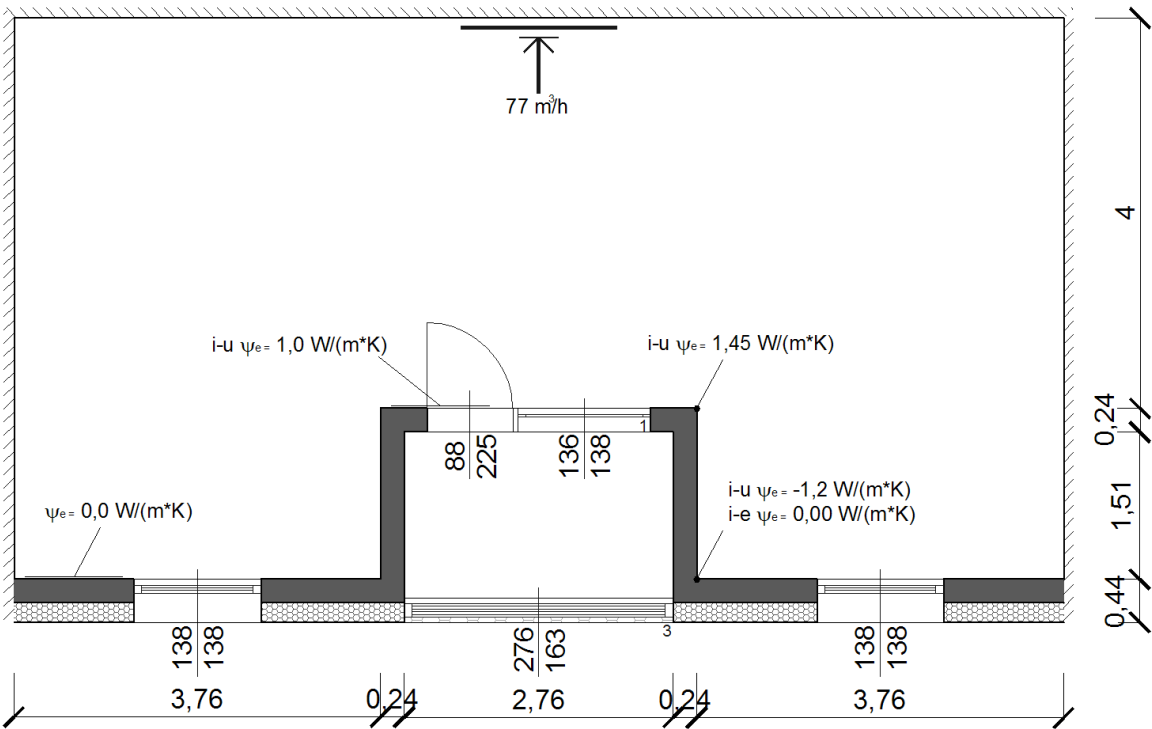
$$H_{i-e,tr} = 20,0 \text{ W/K}$$

$$H_{i-e,ve} = 24,9 \text{ W/K}$$

$$H_{i-e} = 44,9 \text{ W/K}$$

f = 82,1%	
Sp.H.D. = $25,6 \frac{\text{kWh}}{\text{m}^2\text{y}}$	H.D. = $1437,1 \frac{\text{kWh}}{\text{y}}$
Sp.Pr.En.H.V. = $36,7 \frac{\text{kWh}}{\text{m}^2\text{y}}$	Pr.En.H.V. = $2062,6 \frac{\text{kWh}}{\text{y}}$

V2



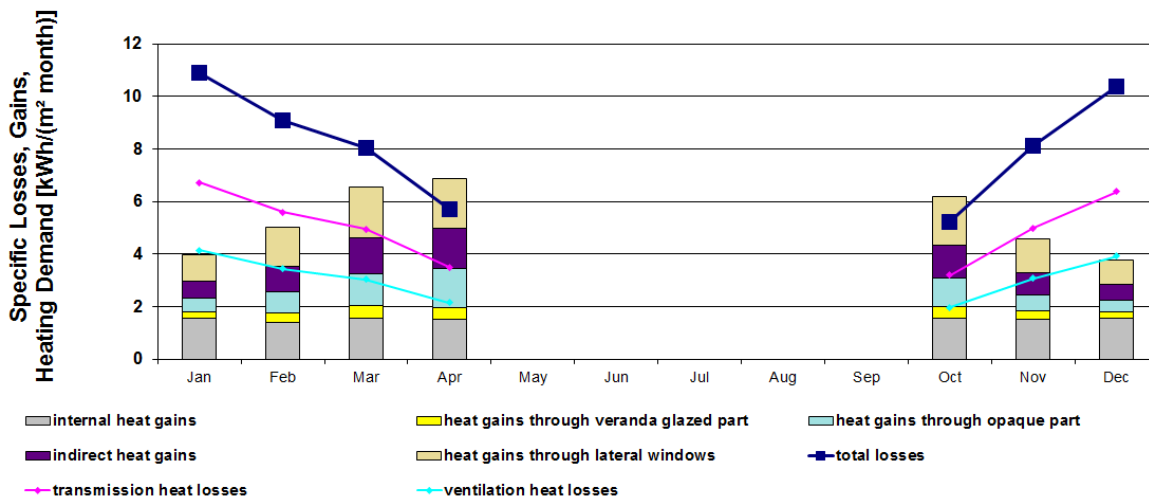
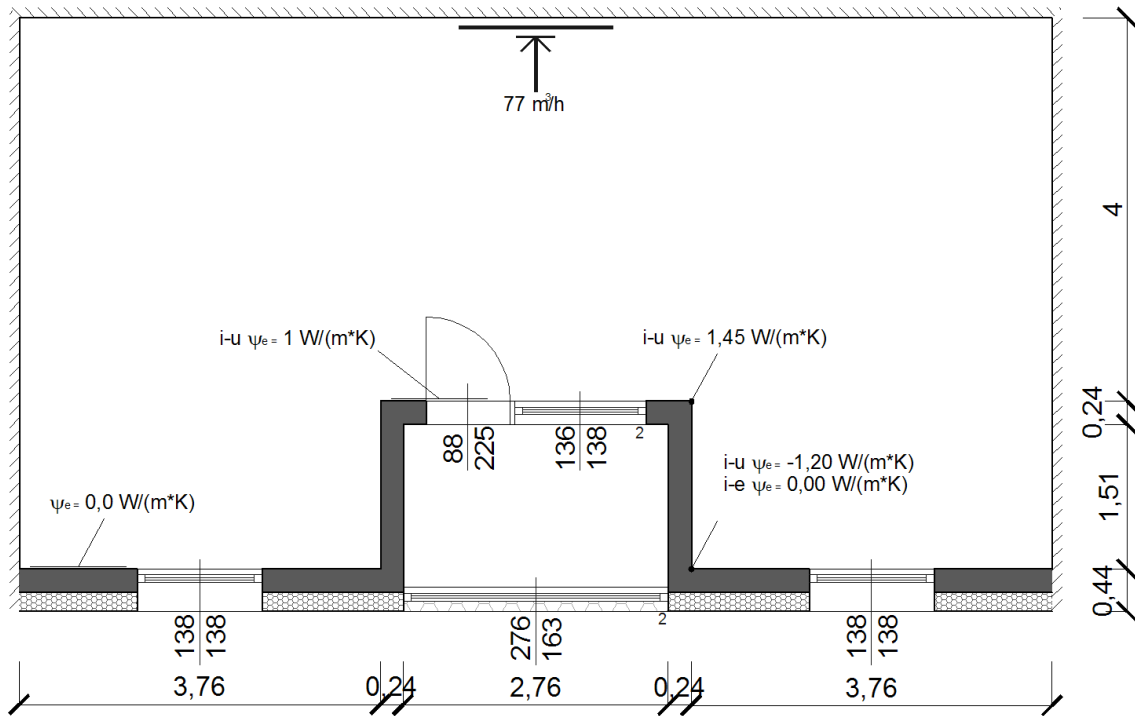
$$H_{i-e, tr} = 26,9 \text{ W/K}$$

$$H_{i-e, ve} = 16,2 \text{ W/K}$$

$$H_{i-e} = 43,1 \text{ W/K}$$

f = 18,3%	
Sp.H.D. = $22,3 \frac{\text{kWh}}{\text{m}^2\text{y}}$	H.D. = $1250,8 \frac{\text{kWh}}{\text{y}}$
Sp.Pr.En.H.V. = $31,8 \frac{\text{kWh}}{\text{m}^2\text{y}}$	Pr.En.H.V. = $1785,3 \frac{\text{kWh}}{\text{y}}$

V3



$$H_{i-e, tr} = 27,9 \text{ W/K}$$

$$H_{i-e, ve} = 17,2 \text{ W/K}$$

$$H_{i-e} = 45,1 \text{ W/K}$$

$$f = 25,7\%$$

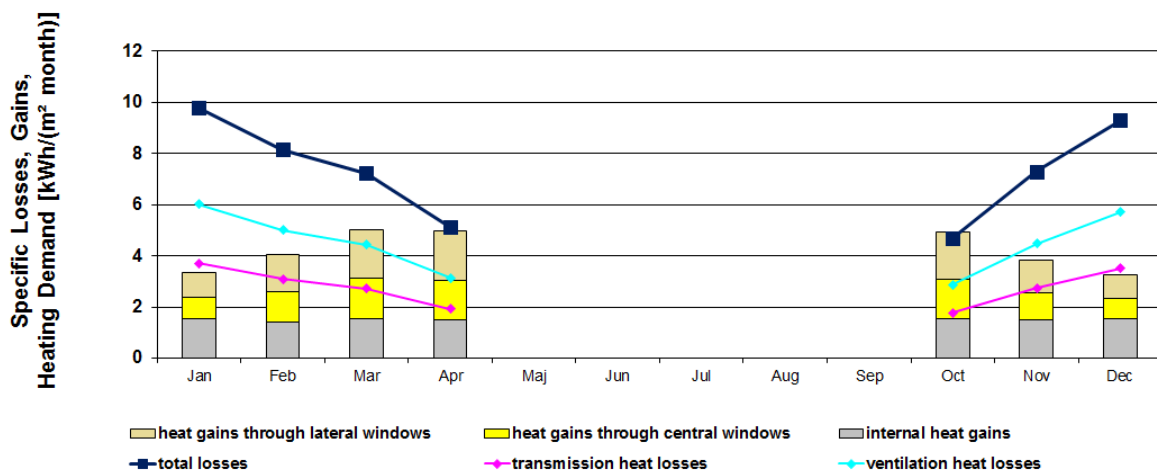
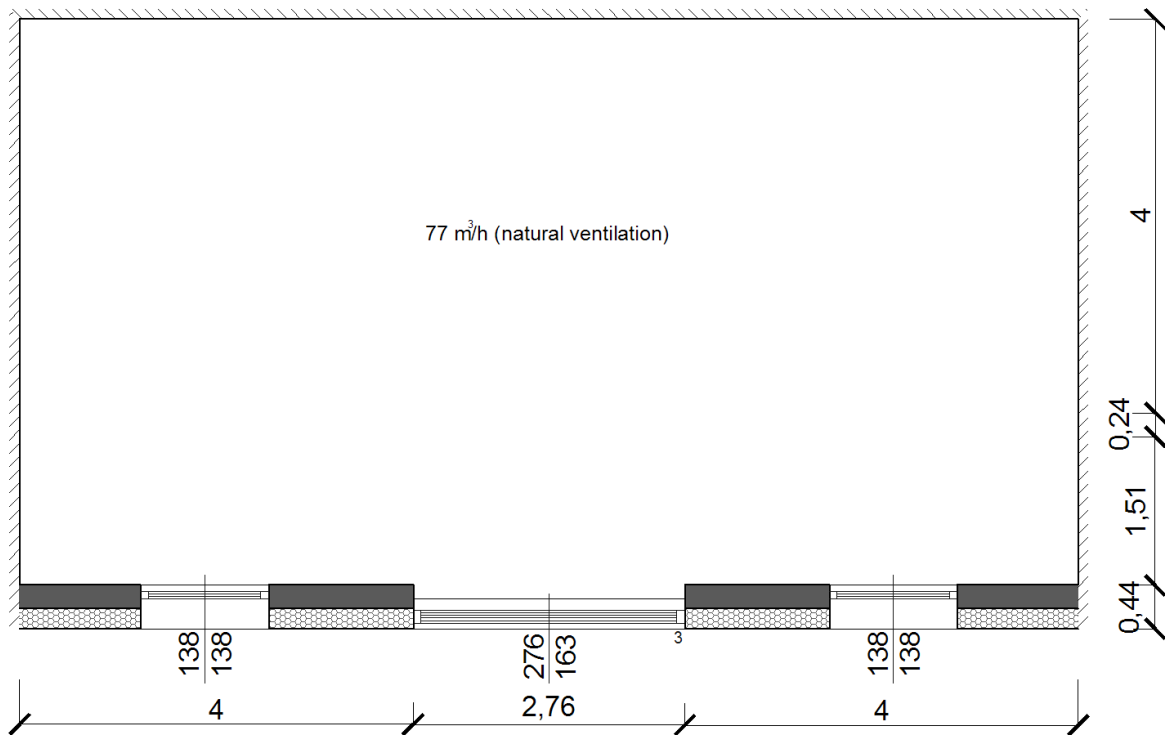
$$\text{Sp.H.D.} = 22,0 \frac{\text{kWh}}{\text{m}^2\text{y}}$$

$$\text{H.D.} = 1234,5 \frac{\text{kWh}}{\text{y}}$$

$$\text{Sp.Pr.En.H.V.} = 31,3 \frac{\text{kWh}}{\text{m}^2\text{y}}$$

$$\text{Pr.En.H.V.} = 1760,7 \frac{\text{kWh}}{\text{y}}$$

no_veranda



In the present solution there is no more the veranda, having included the relative space in the heated space. Reading in the graph the specific gains and losses it must be considered that the heated floor surface in that case is greater than in the cases having a veranda.

$$H_{i-e, tr} = 16,9 \text{ W/K}$$

$$H_{i-e, ve} = 27,5 \text{ W/K}$$

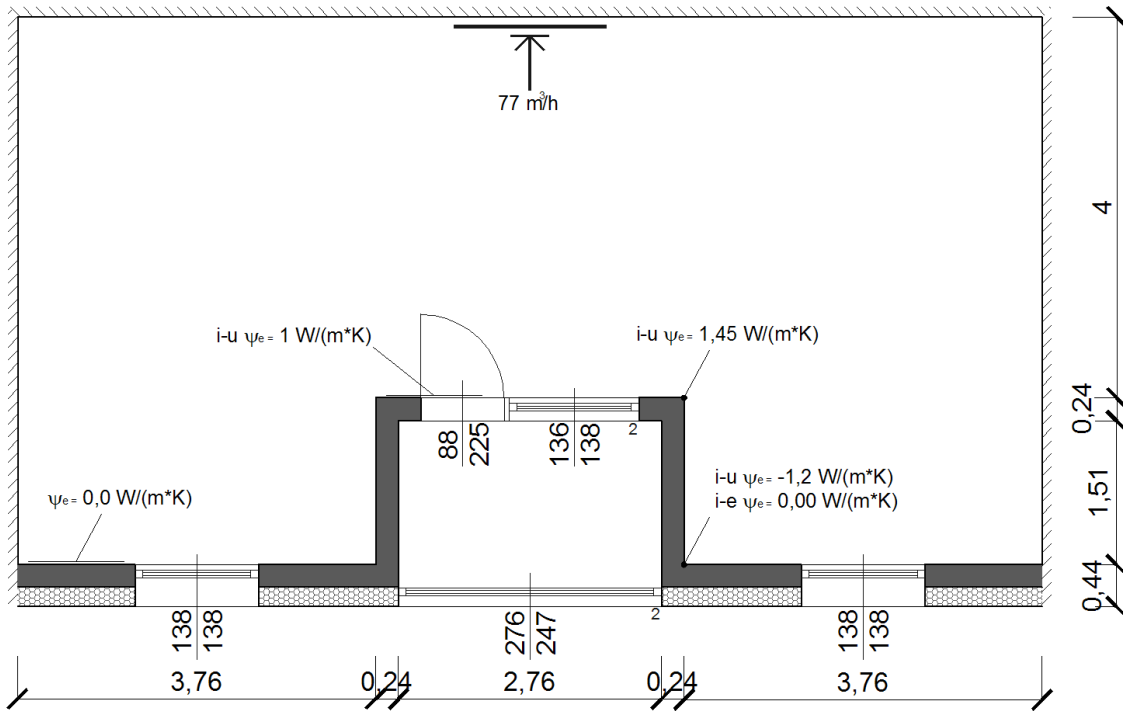
$$H_{i-e} = 44,5 \text{ W/K}$$

Sp.H.D. = $22,1 \frac{\text{kWh}}{\text{m}^2\text{y}}$	H.D. = $1368,7 \frac{\text{kWh}}{\text{y}}$
Sp.Pr.En.H.V. = $30,1 \frac{\text{kWh}}{\text{m}^2\text{y}}$	Pr.En.H.V. = $1862,6 \frac{\text{kWh}}{\text{y}}$

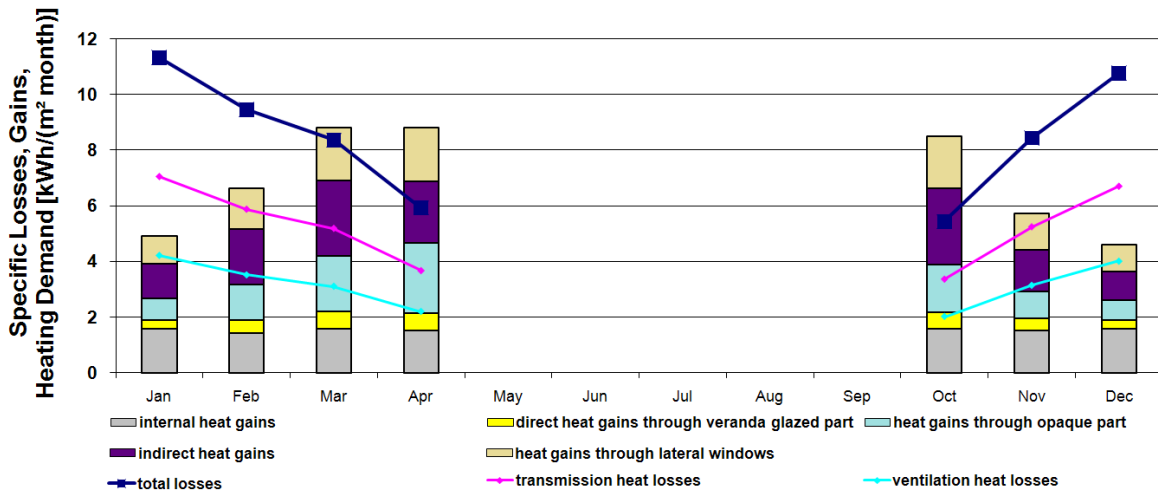
Considering the heat transfer coefficient of cases *V2* and *no_veranda* we can do some interesting observations: if there was no ventilation through the veranda the heat transfer coefficient by transmission $H_{i-e, tr}$ would be surely lower in the case of presence of a veranda (*V2*), because the separation between the veranda and the internal space increases the thermal resistance. But in the case of ventilation passing through the veranda there is a decrease of the veranda temperature and therefore the heat dispersion from the heated ambient to the veranda increases. That one is the reason because of which $H_{i-e, tr}$ is greater for *V2* than for *no_veranda*. However, the passage of the supply air through the veranda causes the decrease of the ventilation losses and the total heat transfer coefficient H_{i-e} is lower for *V2*.

In refurbishments of buildings having originally a veranda, like the social houses of Weingarten West, we have to observe that for the elimination of the veranda an important work in the internal environment would be needed; on the contrary the work in Weingarten West should be little intrusive, because the inhabitants will remain inside the apartments all the time.

V3 mod_wp



This solution is without opaque parapet: the external window of the veranda is enlarged.



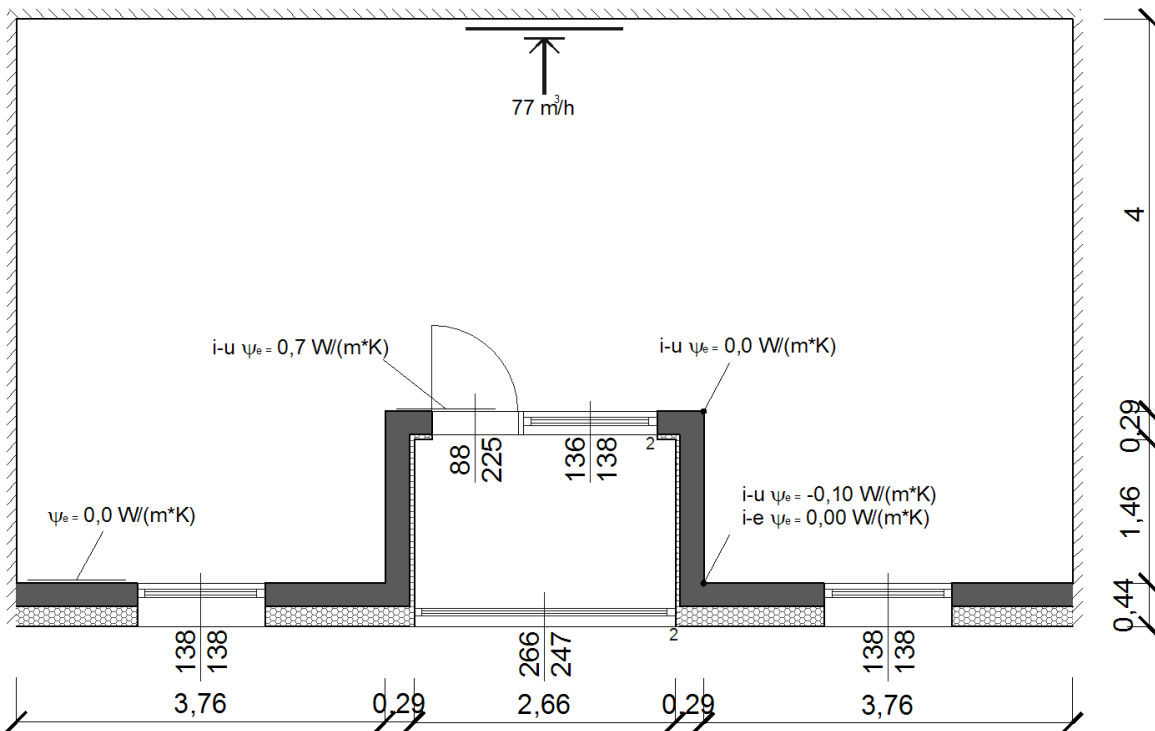
$$H_{i-e, tr} = 29,3 \text{ W/K}$$

$$H_{i-e, ve} = 17,5 \text{ W/K}$$

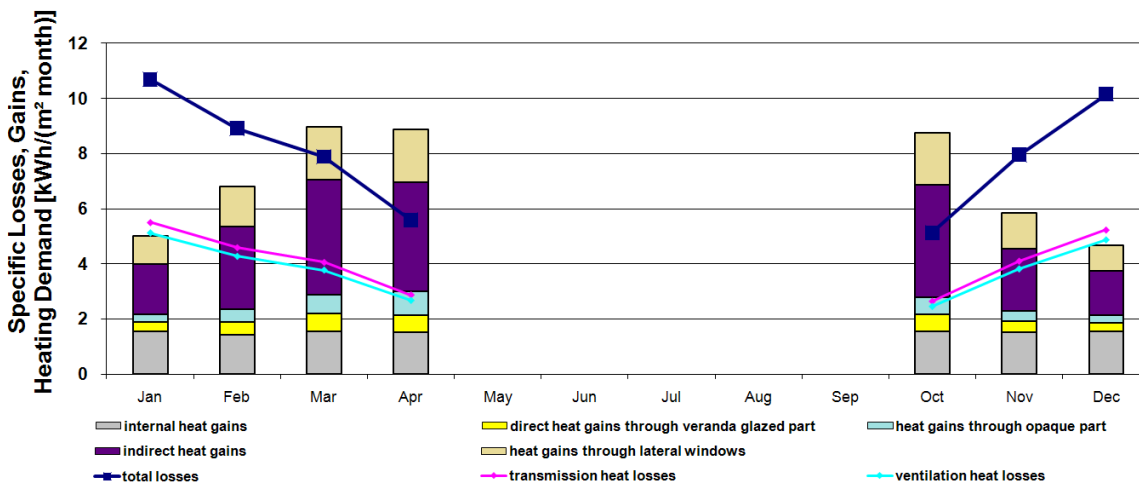
$$H_{i-e} = 46,8 \text{ W/K}$$

f = 28,2%	
Sp.H.D. = 18,9 $\frac{\text{kWh}}{\text{m}^2\text{y}}$	H.D. = 1060,0 $\frac{\text{kWh}}{\text{y}}$
Sp.Pr.En.H.V. = 27,2 $\frac{\text{kWh}}{\text{m}^2\text{y}}$	Pr.En.H.V. = 1529,4 $\frac{\text{kWh}}{\text{y}}$

V3 mod_wp + mod_ins



On the external side of the wall between the internal environment and the veranda there is 5 cm insulation.



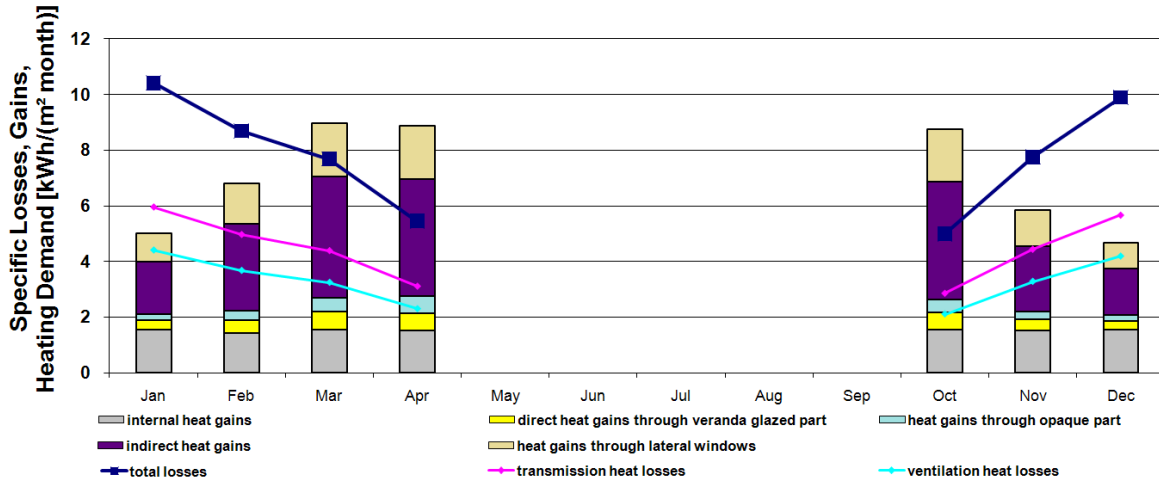
$$H_{i-e, tr} = 22,9 \text{ W/K}$$

$$H_{i-e, ve} = 21,3 \text{ W/K}$$

$$H_{i-e} = 44,1 \text{ W/K}$$

f = 55,6%	
Sp.H.D. = $17,7 \frac{\text{kWh}}{\text{m}^2\text{y}}$	H.D. = $995,4 \frac{\text{kWh}}{\text{y}}$
Sp.Pr.En.H.V. = $26,1 \frac{\text{kWh}}{\text{m}^2\text{y}}$	Pr.En.H.V. = $1465,0 \frac{\text{kWh}}{\text{y}}$

Generally, the presented calculations consider that half ventilation crosses the veranda and that the other half enters through the lateral windows. With all the ventilation through the veranda the result is the following one (no ventilation is considered through the lateral windows; the ventilation can be completely through the veranda imposing a given air flow through the mechanical air extraction and facilitating for the air the passage through the veranda, e.g. through apposite holes, like in the example presented in paragraph 5.2):



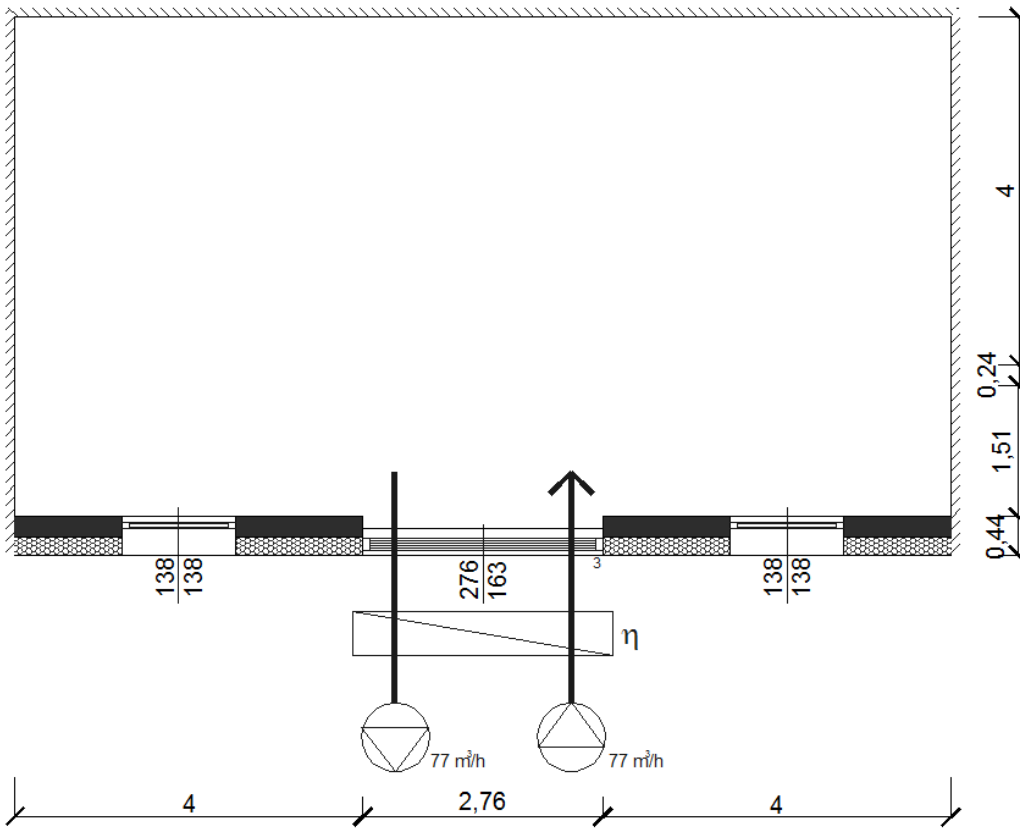
$$H_{i-e,tr} = 24,8 \text{ W/K}$$

$$H_{i-e,ve} = 18,8 \text{ W/K}$$

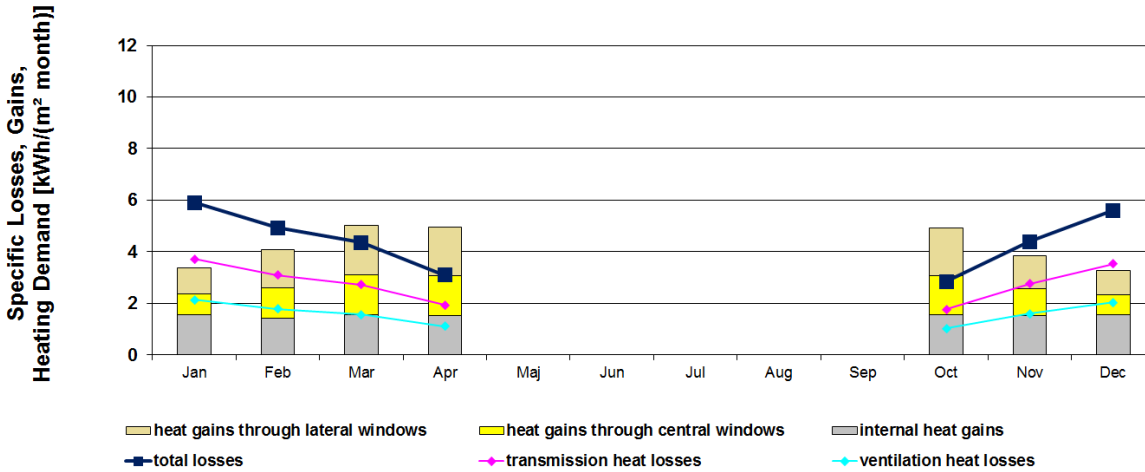
$$H_{i-e} = 43,6 \text{ W/K}$$

f = 67,5%	
Sp.H.D. = $14,8 \frac{\text{kWh}}{\text{m}^2\text{y}}$	H.D. = $830,9 \frac{\text{kWh}}{\text{y}}$
Sp.Pr.En.H.V. = $22,1 \frac{\text{kWh}}{\text{m}^2\text{y}}$	Pr.En.H.V. = $1243,0 \frac{\text{kWh}}{\text{y}}$

no_veranda + heat exchanger



It was considered $\eta = 75\%$ in this case as well.



$$H_{i-e, tr} = 16,9 \text{ W/K}$$

$$H_{i-e, ve} = 9,8 \text{ W/K}$$

$$H_{i-e} = 26,7 \text{ W/K}$$

Sp.H.D. = $5,0 \frac{\text{kWh}}{\text{m}^2\text{y}}$	H.D. = $310,0 \frac{\text{kWh}}{\text{y}}$
Sp.Pr.En.H.V. = $12,9 \frac{\text{kWh}}{\text{m}^2\text{y}}$	Pr.En.H.V. = $793,7 \frac{\text{kWh}}{\text{y}}$

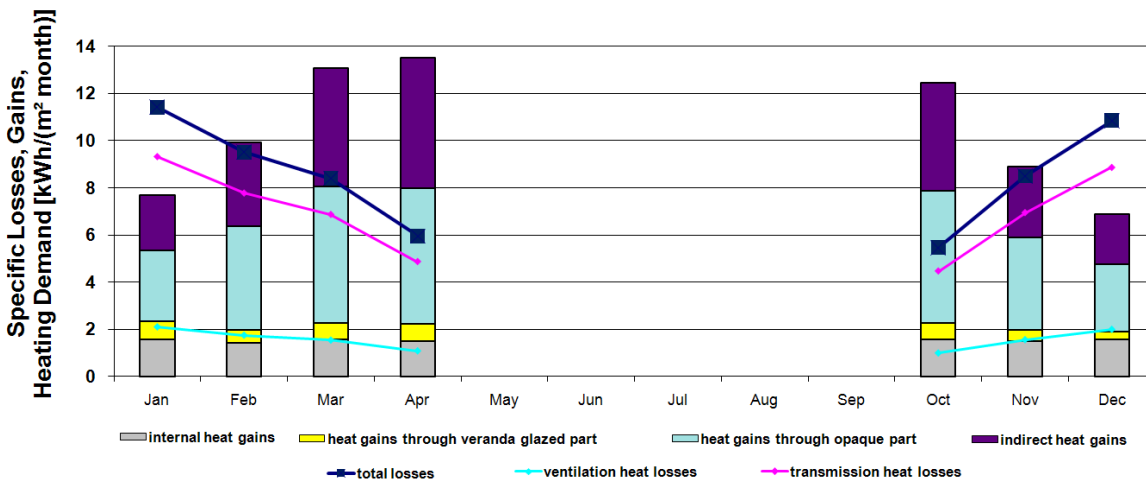
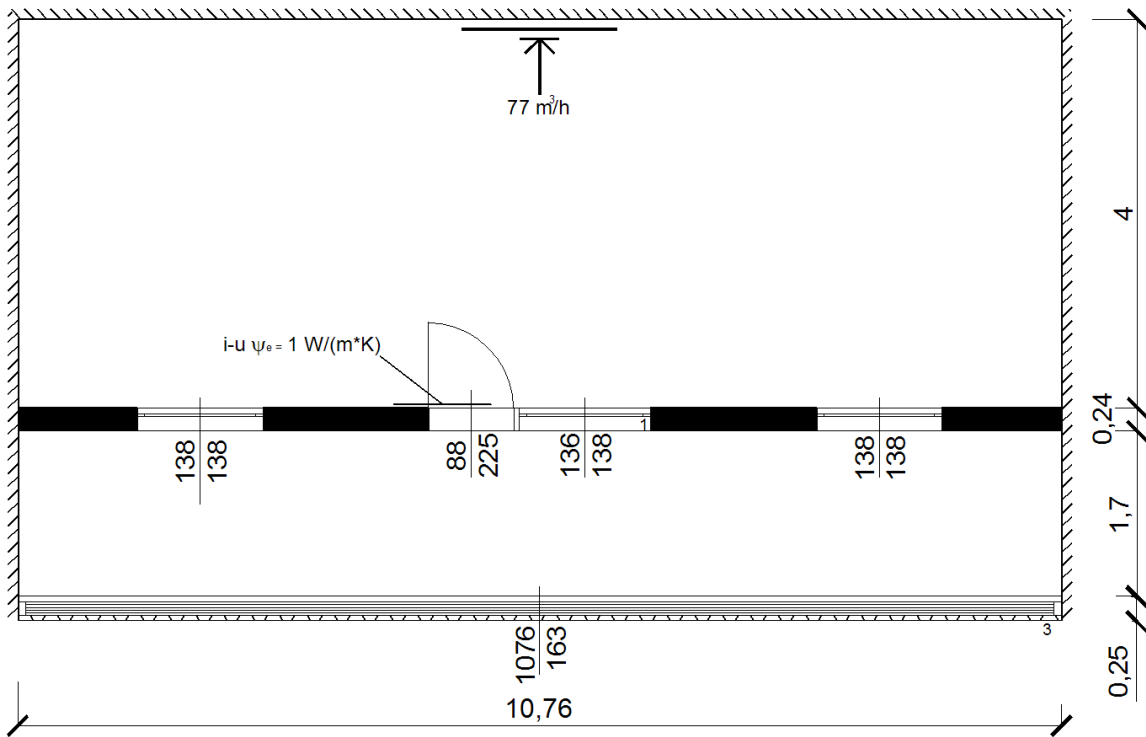
$$H_{i-e, tr} = 20,7 \text{ W/K}$$

$$H_{i-e, ve} = 25,4 \text{ W/K}$$

$$H_{i-e} = 46,1 \text{ W/K}$$

f = 42,8%	
Sp.H.D. = $22,4 \frac{\text{kWh}}{\text{m}^2\text{y}}$	H.D. = $1257,0 \frac{\text{kWh}}{\text{y}}$
Sp.Pr.En.H.V. = $29,1 \frac{\text{kWh}}{\text{m}^2\text{y}}$	Pr.En.H.V. = $1633,2 \frac{\text{kWh}}{\text{y}}$

V2 long veranda



$$H_{i-e, tr} = 29,6 \text{ W/K}$$

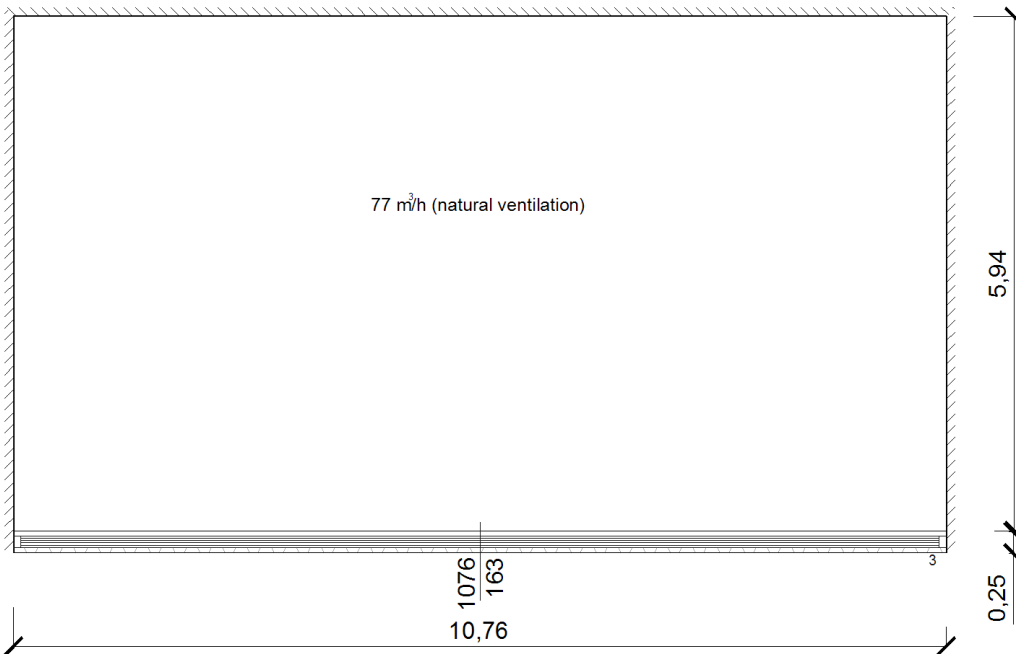
$$H_{i-e, ve} = 6,6 \text{ W/K}$$

$$H_{i-e} = 36,2 \text{ W/K}$$

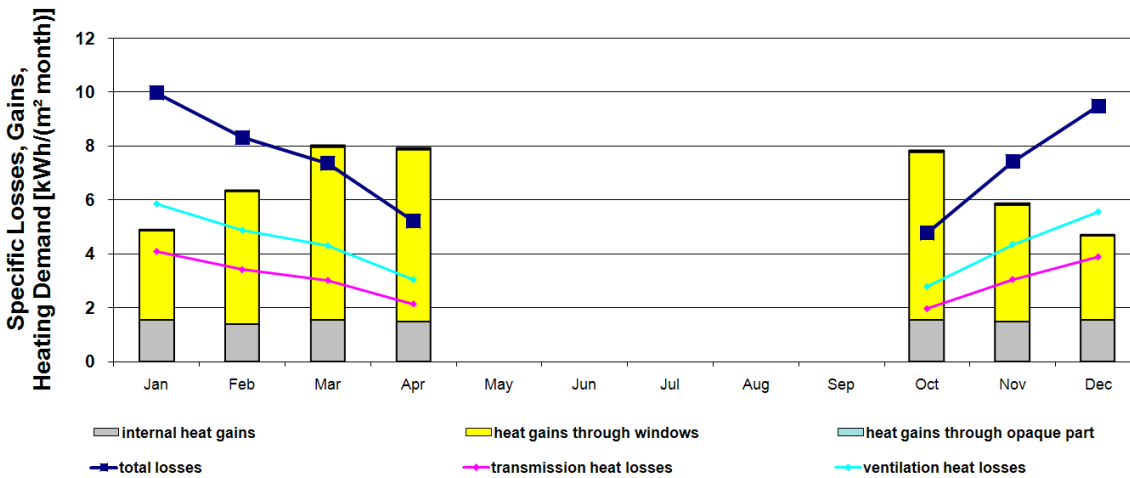
f = 24,7%	
Sp.H.D. = $11,4 \frac{\text{kWh}}{\text{m}^2\text{y}}$	H.D. = $490,7 \frac{\text{kWh}}{\text{y}}$
Sp.Pr.En.H.V. = $18,2 \frac{\text{kWh}}{\text{m}^2\text{y}}$	Pr.En.H.V. = $785,3 \frac{\text{kWh}}{\text{y}}$

The transmission heat transfer coefficient is higher in the present case than in the case V2 because all the ventilation air passes through the veranda, cooling it, while in the case V2 half ventilation was supposed to pass through the lateral windows.

no veranda, long window



In absence of a very careful shading this solution could carry problems of overheating.



$$H_{i-e,tr} = 19,4 \text{ W/K}$$

$$H_{i-e,ve} = 27,6 \text{ W/K}$$

$$H_{i-e} = 47,0 \text{ W/K}$$

Sp.H.D. = $13,6 \frac{\text{kWh}}{\text{m}^2\text{y}}$	H.D. = $866,5 \frac{\text{kWh}}{\text{y}}$
Sp.Pr.En.H.V. = $18,8 \frac{\text{kWh}}{\text{m}^2\text{y}}$	Pr.En.H.V. = $1202,2 \frac{\text{kWh}}{\text{y}}$

5.3.6 Conclusions

This paragraph presents some considerations about the obtained results.

The calculations highlight that just adding the external insulation layer (from possibility A to possibility B) the heat demand becomes less than 30% of the initial one and closing the veranda with a single glass and with an insulated parapet (*V1*) the heat demand becomes about 18% of the initial one. A limitation of solutions, like *V2* and *V3*, having no insulation on the wall between the internal space and the veranda is the difficulty in managing it, in particular during intermediate seasons, because to avoid overheating the external windows could be opened, but then there would be very little thermal resistance between internal and external environment and it could be a problem when later, e.g. during the evening, the external temperature and the external radiation decrease.

Ordering the most interesting considered solutions from that one with the lowest level of heating requirement to that one with the greatest level we have the results presented in Table 5.1. In Table 5.2 a long veranda is compared with a long window.

Among the cases *V1*, *V2* and *V3*, *V1* utilizes the greatest quantity of insulation, because all the divisions between veranda and internal environment are insulated but nevertheless it has the worst performance. From the point of view of the ventilation the best solutions are those ones which have a low factor of the transmission through the veranda, i.e. the solutions in which the veranda temperature is closest to the temperature of the internal environment. The relative importance of the ventilation in comparison with the transmission depends on the total air change rate and on the air fraction passing through the veranda. The solutions which exploit the veranda to preheat the ventilation air could be evaluated better through CFD simulations.

With the climate data of Freiburg, the solutions in which the division between the veranda and the external environment is completely glazed give better values than the solutions with opaque parapet (*V3 mod_wp* needs about 15% less primary energy than *V3*). They have more losses but at the same time higher solar gains.

The version *V3 mod_wp + mod_ins*, with completely glazed vertical surface between veranda and external environment and with 5 cm insulation on the wall between the internal environment and the veranda, has good energetic performance (it is the best one without heat recovery) and if the external glazed surfaces are opened there is, however, a good thermal insulation.

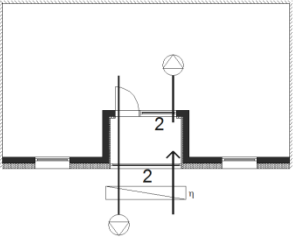
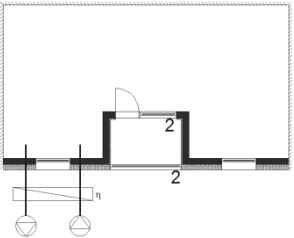
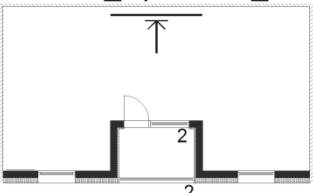
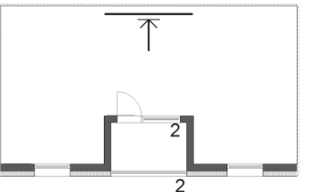
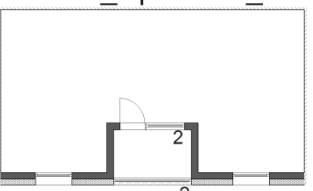
Generally speaking, the advantage of the solutions with veranda is the increase of the thermal resistance and of the preheating, the advantage of the solution without veranda is that the solar radiation enters directly in the heated space (but it could become a problem if we consider the overheating). Considering the results, the solutions with the removal of the veranda are not particularly good from the energetic point of view (*no_veranda* needs more than 5% energy than *V3*) and, in addition, in the context of refurbishments they need more work. They could be a solution if bigger internal rooms are desired, but the presence of a veranda is generally

appreciated by the people. The difference of the performances could be better analysed through a dynamic calculation. The presented semi-stationary calculations considered that the solutions with a veranda have a greater thermal inertia and that has influence on the utilization factor.

With 20 cm insulation the transmission by conduction through the envelope is low, therefore in order to decrease further, in a significant way, the heat demand a heat exchanger can be very useful, but it is a more expansive solution and if the ventilation passes through the veranda a wrong management can waste the usefulness of the system (e.g. if the windows between the veranda and the external environment are open the work of the heat recovery system is wasted). That management problem could be avoided bypassing the veranda: the theoretical increase in energy demand is about 7% (see $V3 \text{ mod_wp} + \text{mod_ins} + \text{heat recovery}$ and $V3 \text{ mod_wp} + \text{mod_ins} + \text{heat recovery bypassing the veranda}$) but the real energy requirement, with a non-perfect windows management, could be greater with the air ventilation passing through the veranda.

The presence of an air extraction system is estimated corresponding to an energy demand reduction of the 26% (from the comparison between $V3 \text{ mod_wp} + \text{mod_ins}$ and $V3 \text{ mod_wp} + \text{mod_ins nat. vent.}$).

Table 5.1 Design proposals - Summary of the most important calculation results

<p>V3 mod_wp + mod_ins + heat recovery</p> 	$\text{Pr.En.H.V.} = 595,4 \frac{\text{kWh}}{\text{y}}$
<p>V3 mod_wp + mod_ins + heat recovery bypassing the veranda</p> 	$\text{Pr.En.H.V.} = 635,0 \frac{\text{kWh}}{\text{y}}$
<p>V3 mod_wp + mod_ins</p> 	$\text{Pr.En.H.V.} = 1465,0 \frac{\text{kWh}}{\text{y}}$ <p>With all the ventilation through the veranda</p> $\text{Pr.En.H.V.} = 1243,0 \frac{\text{kWh}}{\text{y}}$
<p>V3 mod_wp</p> 	$\text{Pr.En.H.V.} = 1529,4 \frac{\text{kWh}}{\text{y}}$
<p>V3 mod_wp + mod_ins nat. vent.</p> 	$\text{Pr.En.H.V.} = 1633,2 \frac{\text{kWh}}{\text{y}}$

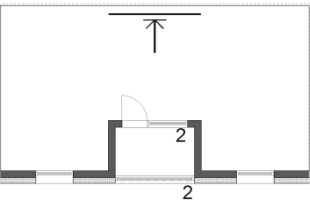
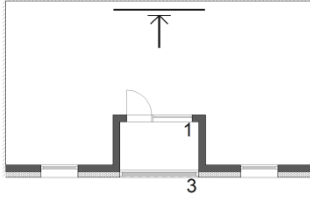
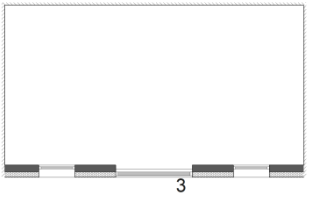
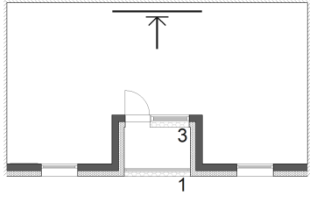
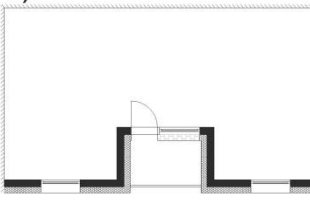
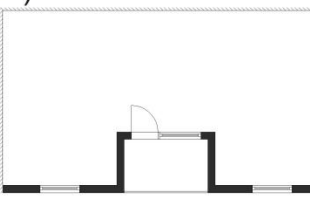
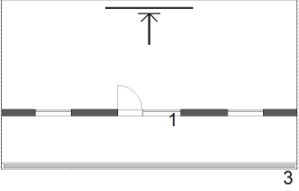
<p>V3</p> 	$\text{Pr.En.H.V.} = 1760,7 \frac{\text{kWh}}{y}$
<p>V2</p> 	$\text{Pr.En.H.V.} = 1785,3 \frac{\text{kWh}}{y}$
<p>no_veranda</p> 	$\text{Pr.En.H.V.} = 1862,6 \frac{\text{kWh}}{y}$
<p>V1</p> 	$\text{Pr.En.H.V.} = 2062,6 \frac{\text{kWh}}{y}$
<p>B)</p> 	$\text{Pr.En.H.V.} = 3319,4 \frac{\text{kWh}}{y}$
<p>A)</p> 	$\text{Pr.En.H.V.} = 11'478,5 \frac{\text{kWh}}{y}$

Table 5.2 Results for a longer shape of the veranda

<p>V2 long veranda</p> 	$\text{Pr.En.H.V.} = 785,3 \frac{\text{kWh}}{\text{y}}$
	$\text{Sp.Pr.En.H.V.} = 18,2 \frac{\text{kWh}}{\text{m}^2\text{y}}$
<p>no veranda, long window</p> 	$\text{Pr.En.H.V.} = 1202,2 \frac{\text{kWh}}{\text{y}}$
	$\text{Sp.Pr.En.H.V.} = 18,8 \frac{\text{kWh}}{\text{m}^2\text{y}}$

6. Guided procedure to the proper design of sunspaces

The present chapter describes what should be considered in order to design sunspaces properly. If the designer is interested in “rule of thumb” for the preliminary design, the “patterns” of Mazria, E. (1979) are advisable (each pattern contains a rule of thumb and further information about a particular aspect of bioclimatic design).

6.1 New construction

6.1.1 Clarifying the goals of bioclimatic design

The general principles a designer follows in order to create his design are obviously also valid for the design of sunspaces. In particular, as preliminary, in accordance with the client, step he has to clarify:

- the architectural value of the sunspace in the context of the building;
- how the sunspace will be used (e.g. relaxation area, or winter garden, or transition space) and the frequency of its use;
- the expected level of comfort in the sunspace;
- whether a decrease in energy requirements is expected and in what amount;
- how much comfort he is willing to compromise in order to improve energy performance.

Communication with the client, in order to understand his expectations and views as to how he will use the sunspace, is therefore fundamental.

Moreover, the designer must be conscious that a sunspace cannot be highly comfortable throughout the year. In fact, it is not mechanically heated or cooled; because of the glazed envelope it is subject to high heat exchanges with the external environment and the heat exchanges of a person present in a sunspace are generally strongly asymmetric. Furthermore, during the winter uncomfortable overheating in the sunspace can be acceptable because it causes a decrease in the heating requirements of the heated area.

6.1.2 Analysing the local climate

In passive design a preliminary knowledge of the local climate is fundamental. In fact, a bioclimatic building is integrated in the environmental context in order to exploit natural resources in a sustainable way. The design of passive solar systems has to consider the local availability of solar radiation. Therefore historical data of solar radiation has to be analysed and local obstacles have to be identified and plotted on a sun chart. If the design includes natural ventilation, the data of wind direction and wind velocity have to be analysed. Data obtained by

statistical procedures, in order to consider the long-term properties of the climate, should be used. In conclusion, the analysis of the local climate is fundamental to estimate the potential of bioclimatic strategies and to design them properly.

6.1.3 Defining position and shape of the sunspace

In order to define the position and the shape of a new sunspace, the sunspace's compactness, its exposure to solar radiation, the inclination of the opaque and glazed surfaces must be considered. From this point of view the contents of paragraph 1.2 "Shape, solar gains and heating requirements" of the present thesis could be useful. Obviously, the designer has to consider that bioclimatic goals are the maximum exploitation of solar energy, the reduction of loss during the heating season and avoiding overheating during the rest of the year.

Natural and artificial obstacles which create shade must be identified (e.g. other buildings, trees, mountains...). Occasional and seasonal obstacles must be considered in a different way to permanent ones. For such work the creation of solar charts can be very useful. In a more advanced phase of the design, a three-dimensional virtual model of the shading effects can be created.

Generally, in the boreal hemisphere the best direction is towards south. An easterly direction is more preferable to a westerly, because passive heating can be more useful during the morning, when external temperatures are colder. On the other hand, heat gains from the west can be particularly undesirable during the warmer season.

If the sunspace is used to preheat the ventilation air, the shape can favour the stratification effect in order to supply air as warm as possible to the internal environment.

6.1.4 Defining the insulation levels

The definition of the insulation levels depends overall on the comfort level that the designer wants to achieve within the sunspace. If thermal conditions similar to the internal ones are desired avoiding temperatures which are too low, the thermal resistance between the sunspace and the external environment must be much higher than that between the sunspace and the internal environment. Otherwise in choosing insulation levels, energy saving considerations have to be taken into account. If the sunspace is used as an area where the external air is preheated before supplying the heated space, the insulation between the sunspace and the external environment becomes a fundamental element in order to avoid temperatures of the entering air being too low and therefore to decrease the ventilation loss. The possibility of using nocturnal insulation, e.g. using insulated window shutters, should also be considered. Nocturnal insulation is useful also for avoiding frost forming on the external surface of the window. If there is frost on the window in the morning solar radiation does not enter the sunspace, but it becomes latent heat for the frost. Moreover, the designer has to pay particular attention to

thermal bridges, which change the heat transmission properties of the sunspace envelope.

6.1.5 Providing thermal inertia

The thermal inertia of the sunspace causes a decrease in temperature fluctuation, which in a sunspace is much higher than in a normal room. The thermal inertia depends on the extension and on the exposure of the surfaces and on the properties of the utilized materials. The interaction of surfaces with the surrounding environment also depends on the colour and surface finish. To have an inertial effect on the sunspace climate, it is better if such elements are not in shaded zones. Thermal inertia has more effect if the surfaces of bodies having a high inertia are directly exposed to solar radiation, which is then absorbed by them and is released when the sunspace air becomes colder than the surface. An element having an important thermal inertia which is practically always present is the floor slab. If the floor slab is insulated the heat which it absorbs is released towards the air to a larger extent than in the case of uninsulated slab. In fact, without insulation more heat is dispersed towards the ground. For thermal inertia Mazria, E. (1979) advises adobe, soil-cement, brick, stone, concrete and water in containers. Thermal inertia can be provided also by other opaque elements, like lateral walls or even the furniture (e.g. water tanks which have also another function can be a solution).

6.1.6 Defining ventilation strategies

It is well-known that ventilation is a fundamental aspect in a building's energy behaviour. Moreover, it is fundamental for the internal comfort, for the quality of the internal environment and to decrease the risk of mould. The sunspace can be integrated with ventilation strategies and the ventilation system. The presence of a sunspace can be exploited to decrease ventilation losses through preheating of the entering air. The designer has to establish if natural or mechanical ventilation is preferable. There is the possibility of using mechanical extraction in order to create a depression in the internal rooms and a constant air flow from the external environment to the internal one crossing the sunspace.

Combination with heat recovery can be taken into consideration, but because of passive preheating due to the sunspace, the cost of an additional heat recovery equipment can be not advantageous.

The sunspace can be placed adjacent to an opening (window or door) which is often opened, in order to decrease the ventilation loss through it.

Natural ventilation can be determined by the shape and the openings of the sunspace. During the warm season the sunspace could become, in fact, a solar chimney or a wind tower for night cooling.

6.1.7 Avoiding overheating during intermediate seasons and during summer

Sunspace exploits solar radiation through the increase in its temperature. Such a system can be counter-productive when heating is not required. The designer must therefore define proper strategies to avoid overheating when it is harmful. He has to consider the possibility of activating ventilation from the external environment, of finding technical solutions in order to remove the complete sunspace, or at least the glazed parts, during the summer, and to providing shade. The best solutions are those ones which stop most of the entering solar radiation while they guarantee the necessary natural lighting for visual comfort.

6.1.8 Dealing with a possible automation system

The conditions inside a sunspace are strongly influenced by the night/day cycle and by the changeable weather conditions and they can vary very quickly. Because of that, correct management can be difficult and it can require commitment by the building occupants. The solution could be the use of an automation (domotic) system which manages the sunspace configuration (in particular, openings and shading) on the basis of algorithms which consider external and internal conditions and whose goal is the increase in energy saving and of thermal comfort. If a domotic system is evaluated as not necessary, however the building occupants should be instructed in the correct management of the sunspace.

6.1.9 Calculations

The designer should think what kinds of calculation could be useful in order to verify the design hypotheses, to improve the design and to propose management strategies. Hopefully, Chapter 3. “Calculation methods” of the present thesis can be useful from this point of view.

6.2 Refurbishment

In the case of refurbishment the designer’s choices are generally more constrained.

In the context of refurbishment we can distinguish two cases:

- creation of a new sunspace, e.g. through the closure of a veranda with a glazed surface;
- refurbishment of an existing sunspace.

In the first case, Chapter 5. “Sunspaces to improve energy retrofitting in Freiburg (Germany)” could be useful, in particular in the context of social housing.

In this field, providing general advice is not easy, because real situations differ greatly.

6.2.1 Clarifying the goals of bioclimatic design

The same considerations which were made for new constructions are also valid here. Generally,

refurbishing provides the opportunity to significantly improve the energetic performance of old buildings. The European Directive 2010/31/EU on the energy performance of buildings states that:

“Given the long renovation cycle for existing buildings, new, and existing buildings that are subject to major renovation, should therefore meet minimum energy performance requirements adapted to the local climate”

and that

“Member States shall (...) develop policies and take measures such as the setting of targets in order to stimulate the transformation of buildings that are refurbished into nearly zero-energy buildings”.

6.2.2 Analysing the local climate

The same considerations which were made for new constructions are also valid here.

6.2.3 Defining insulation levels

The same considerations which were made for new constructions are also valid here. In the context of refurbishment there is the possibility to increase insulation levels, particularly by decreasing the thermal bridges. In fact in the past decades little attention has been paid to avoiding thermal bridges.

6.2.4 Providing thermal inertia

Providing thermal inertia is generally more complicated when refurbishing than for new constructions. In fact, in some cases the only solution to adding inertia could be demolition and rebuilding. Adding a layer to the floor slab could be possible, but only if the height of the room remains acceptable. Moreover, any modification to the mass has to be compatible with structural safety. In all probability and generally speaking, decreasing thermal loss when refurbishing is easier and more important than adding new thermal inertia.

6.2.5 Defining ventilation strategies

Inserting new ventilation systems into old buildings is not so easy as thinking and designing ventilation systems in new constructions. If there are ventilation chimneys, e.g. to extract used air in bathrooms or kitchens, they could be used to create lower pressure in the internal rooms and, as a consequence, an air flow which is preheated by the passage through the sunspace (see Figure 5.4 and 5.12). New openings between the different rooms could be necessary to permit the passage of air.

6.2.6 Avoiding overheating during intermediate seasons and during summer

The same considerations which were made for new constructions are also valid here. The installation of new systems could be complicated (e.g. finding the proper space for shading systems could be difficult). If new windows are installed, the possibility of a complete opening has to be provided.

6.2.7 Dealing with a possible automation system

The installation of an automation system should be subject to a costs/benefits analysis.

6.2.8 Calculations

The same considerations which were made for new constructions are also valid here.

7. Conclusions

The conclusions summarize what the previous chapters present, highlighting in particular the innovative aspects, and provide some advice for future developments of researches about the subjects which the present work deals with.

The present thesis deals with a subject which is a part of the more general subject of the improvement of the energy performance of buildings, to which legislation and market are paying more and more attention. To reduce energy requirements the designers have to pay attention not only to the HVAC plants, but also to the architectural design (building shape, thermal properties of the building, construction techniques...). Buildings have a long-term impact (generally the “life” of a building is longer than the one of a HVAC system) and the margin for improvement is considerable.

The subject of passive solar systems is introduced in Chapter 1 (“Passive solar systems”), which provides definitions and classifications, explains the functioning of different types of systems, presents and discusses calculations regarding the relationship between shape and heating requirements. The chapter highlights that building shape is important not only from the point of view of compactness, but also from the point of view of the exposure to solar radiation and of the ability to exploit it. It provides indications both qualitatively and quantitatively. In particular, it indicates how much a greater exposure to south can balance a decrease of compactness in different Italian localities and what slopes of the window maximize the entering solar radiation during the heating season in two locations having different climates (Bologna, in Italy, and Cordova, in Alaska). The importance of the local conditions for the bioclimatic design is highlighted. Moreover, some considerations are made about the influence of the ground albedo and of the diffuse radiation model.

The main subject of the thesis is the sunspace, a particular passive solar system. The technology to build a sunspace is simple, but a rigorous study of its behaviour is complex. In fact, thermal and fluid-dynamic phenomena interact dynamically in a three-dimensional space and the radiative exchanges play a fundamental role. The literature overview highlights that the sunspaces have relevant impacts on the energy performance of buildings. Sunspaces have been already investigated from a lot of points of view, but a deep investigation of their physical behaviour and a critical analysis of the quasi-steady-state methods, which are the easiest ones and the most utilized by the designers, is necessary. Hopefully, the present thesis is a contribution to the achievement of that goal.

Chapter 3 (“Calculation methods”) analyses the calculation methods paying particular attention to the quasi-steady-state methods. Proposals of improvement of the method of the European technical standard EN ISO 13790:2008, which has an official value and is easily utilizable, are

presented. The proposals regard the correction factor of the solar transmission of windows, shading factors (the technical standard considers a unique value for all the internal surfaces), formulation of the indirect gain, heat dispersion of the solar gain through the ground, air ventilation passing through the sunspace. Nevertheless, the proposals are not immediately applicable. They should be further analysed and validated, particularly quantitatively. The validations should consider a representative variety of situations (from the point of view of geometry, properties, climatic context...).

The European technical standard EN ISO 13790:2008 excludes situations with a constant ventilation through the sunspace. The reasoning about the ventilation presented in Chapter 3 is based on the “perfect mixing” hypothesis (i.e. inside the sunspace the air temperature is considered uniform). Since the temperatures inside sunspaces change a lot both in time and space (see Chapter 4), the calculation of the ventilation air preheating, in order to be really accurate, needs Computational Fluid Dynamic simulations. In a next study the preheating effect due to sunspaces could be calculated for a great variety of situations, in order to give designers precise indications. Attention should be paid to the aspects which influence the supply air temperature, such as:

- geometry of the sunspace;
- air velocity;
- characteristics of inlets and outlets (positions, geometry, dimensions, the direction toward which the air is introduced in the environment...).

The CFD simulation could be validated through comparison with empirical data. Through CFD simulations also the surface coefficients of heat transfer could be investigated, because they determine the conditions inside the sunspace.

Future works should also consider the possibility to estimate better, also through quasi-steady-state methods, the solar radiation which contributes to an increase in the sunspace temperature. In fact, the present version of the technical standard considers only the radiation which is adsorbed directly by the internal surfaces of sunspaces and it neglects the absorption after reflections. An approach similar to the Method 5000 (with specific factors, see Table 3.1), maybe taking in account the study of Wall, M. (1996) relative to the “solar collector property S” (see Chapter 2 “Literature overview”), could be considered also by the technical standard.

The presented proposals of modification of the sunspace calculation partially complicate the calculation. Before their effective implementation, the advantages and disadvantages, also in term of loss of ease and quickness of the quasi-steady-state method for the customers, should be better investigated.

Chapter 4 (“Scale models - An experimental case study in Trento (Italy)”) deals with construction, monitoring, and analysis of two sunspaces created specifically for the present research. The linear dimensions of the smaller sunspace are half those of the larger one. In such a way, observing how the physical quantities change by adjusting the scale was possible. This

chapter analyses through measurements and calculations the physical quantities involved in sunspace functioning, with their local variations, in a more exhaustive manner than is generally done. Since the sunspaces were placed directly on a concrete slab, without insulation, the thermal transmission through the ground has a high relevance and Kreider et al. (2002) states that: “*Ground thermal coupling calculations have probably been the least accurate of any in building thermal analysis*”. The conclusions of this part of the research are:

- Floor is fundamental for the inertia of a sunspace.
- The difference between sunspaces having different dimensions generally increases with the solar radiation. Through graphs and linear regressions a comparison of the peaks of sunspaces having different dimensions is presented.
- A dynamic model having, from the point of view of the surface temperatures, a good agreement with the empirical data was created, both for the bigger sunspace than for the smaller one. That suggests that the method used for modelling is valid although modelling some phenomena regarding the sunspaces is problematic.
- A future work could focus on the air temperature and on the convective heat exchange coefficients through the comparison of experimental data with results of CFD software.

Chapter 5 (“Sunspaces to improve energy retrofitting in Freiburg (Germany)”) focuses on refurbishments, which have a fundamental importance for the energy savings but they are not dealt with often. An apartment, which is part of a building which was refurbished between 1997 and 1999, was studied through monitoring and data analysis. The veranda was closed with windows and a mechanical air extraction system was installed in order to preheat the air in the veranda, also through a solar air collector. A model of the solar collector was proposed and compared with empirical data. Then quasi-steady-state calculations were applied to different refurbishment possibilities in other buildings having verandas. Attention was paid both to the envelope and to integration with the ventilation system (mechanical air extraction system, heat exchanger, natural ventilation). The differences among the different possibilities were analysed, both quantitatively and qualitatively.

In Chapter 6, a guided procedure for the proper design and management of sunspaces is defined. Hopefully, such a guide can be useful for designers. In fact, its goal is to present clearly and with a logical sequence what aspects the designers have to take into account to build sunspaces properly.

A future study could regard the utilization of automation systems to optimize the management of passive solar systems from the point of view of energy requirements and comfort. In an automation system devices are managed by actuators, connected into a network where sensors also are present. For a sunspace sensors could monitor the presence of people (in case of presence, strategies to improve the comfort level would be activated), the solar radiation, temperatures in the sunspace, in the internal rooms and in the external environment while actuators could control HVAC plants, opening, shading, and so on.

Bibliography

- VV.AA. (1992-1995) *Manuale di progettazione edilizia – Fondamenti, strumenti, norme*, vol. 2: criteri ambientali e impianti, Milano: Hoepli
- VV.AA. *TRNSYS 16 a TRaNsient SYstem Simulation program*, Vol. 5 Mathematical Reference
- ASHRAE (1997) *Handbook of Fundamentals*. Atlanta
- Athienitis, A.K. and Santamouris, M. (2002), *Thermal analysis and design of passive solar buildings*. London: James & James science
- Bakos, G.C. and Tsagas, N.F. (2000), “Technology, thermal analysis and economic evaluation of a sunspace located in northern Greece”, *Energy and Buildings*, Amsterdam, Elsevier Science Ltd., vol. 31, Issues 3, April 2000, pp. 261-266
- Bataineh, K.M. and Fayez, N. (2011) “Analysis of thermal performance of building attached sunspace”, *Energy and Buildings*, Amsterdam, Elsevier Science Ltd., vol. 43, pp. 1863-1868
- Björnsell, N. et al. (1999) “IDA indoor climate and energy”, *Proceedings of Building Simulation '99*, Kyoto, Japan, September 1999. IBPSA
- Bonacina, C. et al. (1992) *Trasmissione del calore*. Padova: CLEUP editore
- Cardinale, N. and Ruggiero, F. (2000), “Energetic aspects of bioclimatic buildings in the Mediterranean area: a comparison between two different computation methods”, *Energy and Buildings*, Amsterdam, Elsevier Science Ltd., vol. 31, pp. 55-63
- Cavallini, A. and Mattarollo, L. (1992) *Termodinamica applicata*. Padova: CLEUP editore
- Çengel, Y.A. (2007), *Heat and mass transfer: a practical approach*. Boston: McGraw-Hill
- Colombo, R. et al. (1994), *Passive solar architecture for Mediterranean*. Joint Research Center – Commission of the European Communities
- Crawley, D.B. et al. (2008), “Contrasting the capabilities of building energy performance simulation programs”, *Building and Environment*, Amsterdam, Elsevier Science Ltd., Volume 43, Issue 4, April 2008, Pages 661-673
- Depecker, P. et al. (2001) “Design of buildings shape and energetic consumption”, *Building and Environment*, Amsterdam, Elsevier Science Ltd., Volume 36, Issue 5, pp. 627-635
- Duffie, J. A. and Beckman, W.A. (1980), *Solar engineering of thermal processes*. New York: Wiley
- Fredlund, B. (1989), *Blocks of flats with glazed verandas, Taberg – Analysis of energy and internal climate*. Stockholm: Swedish Council for Building Research
- Grimmer, D.P. (1979) “Theoretical considerations in the use of small passive-solar test-boxes to model the thermal performance of passively solar-heated building designs”, *Solar Energy*, Amsterdam, Elsevier Science Ltd., Volume 22, pp. 343-350

- Grimmer, D.P. et al. (1979) “Initial experimental tests on the use of small passive-solar test-boxes to model the thermal performance of passively solar-heated building designs”, *Solar Energy*, Amsterdam, Elsevier Science Ltd., Volume 22, pp. 351-354
- Gueymard, C.A. (2009) “Direct and indirect uncertainties in the prediction of tilted irradiance for solar engineering applications”, *Solar Energy*, Amsterdam, Elsevier Science Ltd., Vol. 83, Issue: 3, pp. 432-444
- Hestnes, A.G. et al. (2003), *Solar energy houses: strategies, technologies, examples*. International Energy Agency
- Kalamees, T. (2004), “IDA ICE: the simulation tool for making the whole building energy- and HAM analysis”, *IEA-Annex 41 MOIST-ENG*, Working meeting: Zürich, Switzerland, 12-14 May 2004
- Karlsson, J. and Roos, A. (2000) “Modelling the angular behaviour of the total solar energy transmittance of windows”, *Solar Energy*, Amsterdam, Elsevier Science Ltd., Volume 69, No. 4, pp. 321-329
- Kreider, J.F. et al. (2002) *Heating and cooling of buildings: design for efficiency*. New York: McGraw-Hill
- Kunz, M. (1990), *Zwei Solarhäuser unter der Lupe*. Zürich: SIA
- Mazria, E. (1979), *The passive solar energy book*. Emmaus: Rodale Press
- Meroni, I. et al. (1991), “Experimental analysis of the energy performance of a passive attached sunspace”, *Solar Energy*, Amsterdam, Elsevier Science Ltd., Volume 47, n. 5, pp. 329-332
- Mottard, J.M. and Fissore, A. (2007), “Thermal simulation of an attached sunspace and its experimental validation”, *Solar Energy*, Amsterdam, Elsevier Science Ltd., Volume 81, Issue 3, March 2007, pp. 305-315
- Oliveti, G. et al. (2008), “Evaluation of the absorption coefficient for solar radiation in sunspaces and windowed rooms”, *Solar Energy*, Amsterdam, Elsevier Science Ltd., vol. 82, Issue 3, March 2008, pp. 212-219
- Oliveti, G. et al. (2009), *Valutazione del coefficiente correttivo F_w della trasmittanza solare totale delle superfici vetrate*, III Congresso Nazionale AIGE, Parma 4th-5th June 2009
- Oliveti, G. et al. (2011), “An accurate calculation model of solar heat gain through glazed surfaces”, *Energy and Buildings*, Amsterdam, Elsevier Science Ltd., vol. 43, pp. 269-274
- Palyvos, J.A. (2008), “A survey of wind convection coefficient correlations for building envelope energy systems’ modeling”, *Applied thermal engineering*, Amsterdam, Elsevier Science Ltd., vol. 28, pp. 801-808
- Passive Haus Intitut (2007), *Passive House Planning Package 2007*. Darmstadt: Passive Haus Intitut – Dr. Wolfgang Feist
- Perez, R. et al. (1990), “Modelling daylight availability and irradiance components from direct and global irradiance”, *Solar Energy*, Amsterdam, Elsevier Science Ltd.,

- Volume: 44, n. 5, pp. 271-289
- Pfrommer, P. (1995), *Thermal modelling of highly glazed spaces*. Leicester: De Montfort University
- Reindl, D.T. et al. (1990) “Diffuse fraction correlations”, *Solar Energy*, Amsterdam, Elsevier Science Ltd., Volume: 45, n. 1, pp. 1-7
- Simpson, J.R. and McPherson, E.G. (1997), “The effects of roof albedo modification on cooling loads of scale model residences in Tucson, Arizona”, *Energy and Buildings*, Amsterdam, Elsevier Science Ltd., Volume 25, Issue 2, pp. 127-137
- Sodha, M.S. et al. (1986), *Solar passive building: science and design*. Oxford: Pergamon
- Sommereux, I. (1985), *A design method for passive sunspace systems*. University of Wisconsin-Madison
- Spitters, C.J.T. et al. (1990), “Separating the diffuse and direct component of global radiation and its implications for modeling canopy photosynthesis Part I. Components of incoming radiation”, *Agricultural and Forest Meteorology*, Amsterdam, Elsevier Science Ltd., Volume 38, Issues 1-3, ottobre 1986, pp. 217-229
- Steven Winter Associates (1998), *The passive solar design and construction handbook* edited by M.J. Crosbie. New York: Wiley
- Thevenard, D. and Haddad, K. (2006), “Ground reflectivity in the context of building energy simulation”, *Energy and Buildings*, Amsterdam, Elsevier Science Ltd., vol. 38, Issue: 8, pp. 972-980
- Turns, S.R. (2006), *Thermal-fluid sciences: an integrated approach*. Cambridge: Cambridge university press
- Voeltzel, A. et al. (2001), “Thermal and ventilation modelling of large highly-glazed spaces”, *Energy and Buildings*, Amsterdam, Elsevier Science Ltd., vol. 33, Issue: 2, January 2001, pp. 121-132
- Vuolle, M. (1999), “An NMF based model library for building thermal simulation”, *Proceedings of Building Simulation '99*, Kyoto, Japan, September 1999. IBPSA.
- Wall, M. (1996), *Climate and energy use in glazed spaces*. Lund: Building Science
- Zappone, C. (2005) *La serra solare*. Napoli: Sistemi editoriali

Technical standards

- DIN V 18599-2:2007 *Energy efficiency of buildings — Calculation of the energy needs, delivered energy and primary energy for heating, cooling, ventilation, domestic hot water and lighting — Part 2: Energy needs for heating and cooling of building zones*
- EN 410:2011 *Glass in buildings – Determination of luminous and solar characteristics of glazing*
- EN ISO 10077-1:2007 *Thermal performance of windows, doors and shutters - Calculation of thermal transmittance - Part 1: General*
- EN ISO 10211:2007 *Thermal bridges in building construction - Heat flows and surface temperatures - Detailed calculations*

EN ISO 13790:2008 *Energy performance of buildings - Calculation of energy use for space heating and cooling*

UNI 10349:1994 *Riscaldamento e raffrescamento degli edifici. Dati climatici*

UNI/TS 11300-1:2008 *Prestazioni energetiche degli edifici - Parte 1: Determinazione del fabbisogno di energia termica dell'edificio per la climatizzazione estiva ed invernale*

Online resources

A Report of Task 22 Building Energy Analysis Tools (1999) Models for Building Indoor Climate and Energy Simulation <www.iea-shc.org/task22/publications/t22brep.pdf>

Comitato Termotecnico Italiano <www.cti2000.it>

COMSOL Multiphysics <www.comsol.com/>

Directives of the European Union <<http://eur-lex.europa.eu/en/index.htm>>

International Energy Agency, *World Energy Outlook 2009*

<www.iea.org/textbase/nppdf/free/2009/weo2009.pdf>

THERM <<http://windows.lbl.gov/software/therm/therm.html>>

Appendix

Bioclimatic design of buildings considering heating requirements in Italian climatic conditions. A simplified approach

The Appendix is reprinted from Building and Environment, Vol. 46, Authors: Albatici, Rossano; Passerini, Francesco, Bioclimatic design of building considering heating requirements in Italian climatic conditions. A simplified approach, Pages 1624 - 1631, Copyright (2011), with permission from Elsevier < <http://www.elsevier.com>>